12-2017

The Biochemical Characterization of the Phosphatidylserine Synthase from *Candida albicans* as a Drug Target

Chelsi Danielle Cassilly
University of Tennessee, ccassill@vols.utk.edu

To the Graduate Council:

I am submitting herewith a dissertation written by Chelsi Danielle Cassilly entitled "The Biochemical Characterization of the Phosphatidylserine Synthase from *Candida albicans* as a Drug Target." I have examined the final electronic copy of this dissertation for form and content and recommend that it be accepted in partial fulfillment of the requirements for the degree of Doctor of Philosophy, with a major in Microbiology.

Todd B. Reynolds, Major Professor

We have read this dissertation and recommend its acceptance:

Jeffrey M. Becker, Shawn R. Campagna, Elizabeth M. Fozo, Richard E. Lee

Accepted for the Council:
Carolyn R. Hodges

Vice Provost and Dean of the Graduate School

(Original signatures are on file with official student records.)

The Biochemical Characterization of the Phosphatidylserine Synthase from *Candida albicans* as a Drug Target

A Dissertation Presented for the

Doctor of Philosophy

Degree

The University of Tennessee, Knoxville

Chelsi Danielle Cassilly

December 2017

DEDICATION

This dissertation is dedicated to Dr. Joan Patricia Cassilly. You did it first; thanks for showing me the way. (Farthing and Cassilly 1976)

ACKNOWLEDGEMENTS

First and foremost, I thank God for giving me the fortitude, courage, and strength to finish my Ph.D.

I must next thank my mentor Dr. Todd Reynolds. I have never met a more patient and approachable individual. I owe my doctorate to him. Thank you to my dissertation committee—Dr. Elizabeth Fozo, Dr. Jeff Becker, Dr. Shawn Campagna, Dr. Richard Lee—I am more confident and curious because of the influence each of you has had in my career. Thank you to my collaborators for teaching me how to work in various disciplines and alongside so many people of different backgrounds.

Next I want to thank Mom, Dad, Summer, Kortney, Wesley, Grandma, and Grandpa who supported me, encouraged me, and propagated the idea that I would be the one to cure cancer.

Thank you to my best friends in and out of Knoxville who always reminded me of just how long I had been in graduate school. Three special friends helped me through some of the most difficult times in Knoxville: Thomas Brandenburg, Trina Hughes, and Dr. Joel Cullen Bucci. It is rare to find even one supportive and dedicated friend—I am fortunate to have found three. I'd like to thank the Laurel Church of Christ, and in particular Mike and Regina Buckley, for providing me with a loving community. Thank you to previous teachers and professors who helped in their own ways to get me to this point.

Thank you to the Reynolds Lab members both present and past—Joseph Chen, Sarah Davis, Bob Tams, Tian Chen, Kyle Bonifer, Dr. Sahar Hasim, Dr. Billy Carver, Miranda Crouch, Rebecca Fong, Sabrina Williamson, Ethan Burks, Elizabeth Emanuel, and Madison Steiner—who helped me with my science, kept me on my toes, and dubbed me: Chelsius Cassillius Maximus Decimus Meridius Aruleus IX, Queen of the Lipids. This title will sound all the better with a “doctor” in front.

Thank you to the Fozo Lab for the friendship, the excellent hallway conversations, and the steady exchange of materials and ideas. Thank you to Josh Stough, Joseph Jackson, Andrew Stafford, Holly Saito, and Jenny Onley who helped strengthen by faith in a season riddled with doubts. Thank you to Elizabeth McPherson who not only was a fantastic teaching mentor, but also became my friend. Thank you to the Microbiology Department faculty, staff, and especially students who were a unique support system that provided solidarity and understanding during the many failures and successes of graduate school.

“Science is made up of so many things that appear obvious after they are explained.”

-Frank Herbert; *Dune*

ABSTRACT

Treatments for *Candida albicans* systemic infections are limited to three classes of antifungals, some of which have harmful side effects or increasing instances of antifungal resistance. These shortcomings illustrate a need for new antifungals. The phosphatidylserine (PS) synthase, Cho1p, represents a potential drug target that can address this need. Cho1p is involved in a major phospholipid biosynthesis pathway and represents a novel drug target for three key reasons: 1) It is required for virulence, indicating that inhibitors of Cho1p would render the organism incapable of causing infection; 2) it is absent in mammals, so inhibitors potentially have no toxic side effects; and 3) the enzyme appears to be well conserved across fungi, indicating that inhibitors could be broadly effective against many fungal pathogens. In order to take full advantage of Cho1p as a drug target, we performed several screens of small molecules for ones that inhibit Cho1p. In one screen we identified SB-224289 that seems to act by inducing large scale endocytosis. A second screen identified the compound Lee-3664 which demonstrates selective toxicity against *C. albicans*. Further, we performed a detailed biochemical characterization of Cho1p where we identified substrate binding sites as well as the K_m [subscript M] and apparent V_{max} [subscript max] for each substrate. Computational modeling has produced a useful model of what Cho1p might look like and has further increased interest in crystallizing the protein in future work. The results of this dissertation will lead to more direct approaches for finding Cho1p inhibitors, leading ultimately to more

effective antifungals, as well as a greater understanding of enzymes involved in phospholipid biosynthesis, which is necessary for virulence in this pathogen.

TABLE OF CONTENTS

LIST OF TABLES

LIST OF FIGURES

INTRODUCTION

Understanding the roles for lipids in the virulence of microbial pathogens has long been an area of interest. Virulence is a broad area of study, encompassing both host and microbe factors, however, within the last decade the role of microbial physiology in virulence has become more appreciated. Many microbes have complex life cycles or reside in a variety of locations and must sense their environment in order to survive and reproduce. This adjustment to environmental stimuli (e.g. nutrient availability, temperature, pH) plays a large role in the metabolism and virulence of microbes (Finlay and Falkow 1989, Finlay and Falkow 1997, Mahan, *et al.* 2000).

Lipids are one of the four main macromolecules (along with nucleic acids, proteins, and carbohydrates) essential for cells to function. Depending on their properties, lipids can have many roles in the cell including control of membrane structure and fluidity (Cronan 2003, Dowhan 1997), signaling (Shea and Del Poeta 2006), facilitating membrane-associated functions (Bogdanov and Dowhan 1999, Cronan 2003), virulence (Bhatt, *et al.* 2007, Jain, *et al.* 2007, Mirucki, *et al.* 2014, Upreti, *et al.* 1984, Wessel, *et al.* 2006) and drug resistance (Anderes, *et al.* 1971, Cronan 2003, Rakotomanga, *et al.* 2005). A great deal of research has been conducted to help better understand the role that lipids play in virulence across species, and even within strains of the same species (Cox and Best 1972, Disalvo and Denton 1963, Nielsen 1965). Some of the first studies into the importance of lipids within fungal pathogens compared lipid composition of different strains of *Blastomyces dermatitidis* (Disalvo and Denton 1963).

Differences in total lipid content were observed, revealing that the more virulent strains had higher levels of total lipids. However, no correlation was seen between virulence and increased phospholipids in particular. In contrast, a similar study on *Histoplasma capsulatum* revealed no direct correlation between virulence and lipid content (Nielsen 1965). A later study on the impact of lipid composition on virulence in *Cryptococcus neoformans* found that lower virulence correlated with decreased levels of total lipids and phospholipids, but no major association between virulence and specific lipids was identified (Upreti, *et al.* 1984). Over the past few decades, a great deal of research has led to a deeper understanding of lipids and their roles in virulence.

Within the broad category of lipids are many different subtypes, including sphingolipids, phospholipids, and sterols. Nearly all of these have been implicated in virulence across a wide range of pathogens (Davis, *et al*. 2014a, Geiger 2010, Goren, *et al*. 1974, Rella, *et al*. 2016, Tilney, *et al*. 2001, Wessel, *et al*. 2006). Furthermore, some microbes have been shown to have the ability to take up host fatty acids which alters the microbe's membrane, allowing them to resist antibiotics and other stressors (Giles, *et al.* 2011, Harp, *et al.* 2016, Saito, *et al.* 2014, Yao and Rock 2017). While there are many reviews describing the general role of lipids in microbial pathogenesis (Geiger 2010, Mishra, *et al.* 1992, Ramakrishnan, *et al.* 2013, Rella, *et al.* 2016, Sant, *et al.* 2016), this review will focus on a specific subset of aminophospholipids, phosphatidylserine (PS) and phosphatidylethanolamine (PE), and their role in microbial pathogenesis. PS and

PE have been subject to fewer studies than some other classes regarding their roles in virulence, but a number of more recent reports reveal interesting roles for PS and PE in a variety of fungal, protozoan, and prokaryotic pathogens, indicating that these phospholipids and their biosynthetic enzymes should be considered more carefully. This introduction will briefly review PS and PE synthesis, and then cover the role of PS and PE in particular cellular pathogens as regulators of virulence and the role of host PS/PE as facilitators of virulence.

Phosphatidylserine and phosphatidylethanolamine synthesis in microbes

Phosphatidylserine

PS is a negatively charged phospholipid with a glycerol backbone and two fatty acid tails (Fig. I.1A). In bacteria and fungi, PS is produced from two substrates: cytidine diphosphate diacylglycerol (CDP-DAG) and serine (Fig. I.2). Although the enzymes responsible for this reaction can differ greatly in sequence between fungi and many prokaryotic microbes (excepting some bacteria like *B. subtillis* or *Sinorhizobium meliloti* whose PS synthase is similar to *S. cerevisiae*) the mechanism by which they produce PS is similar (Carman and Han 2011, Carman and Zeimetz 1996, Cronan 2003, Henry, *et al*. 2012, Raetz and Dowhan 1990, Sohlenkamp, *et al*. 2004, Vance 2015, Vance and Steenbergen 2005a). In mammals and many parasites like *Trypanosoma brucei*, PS is produced through a base-exchange reaction. In mammals, head groups of existing phosphatidylcholine (PC) and PE are cleaved off by two different enzymes, PSS2

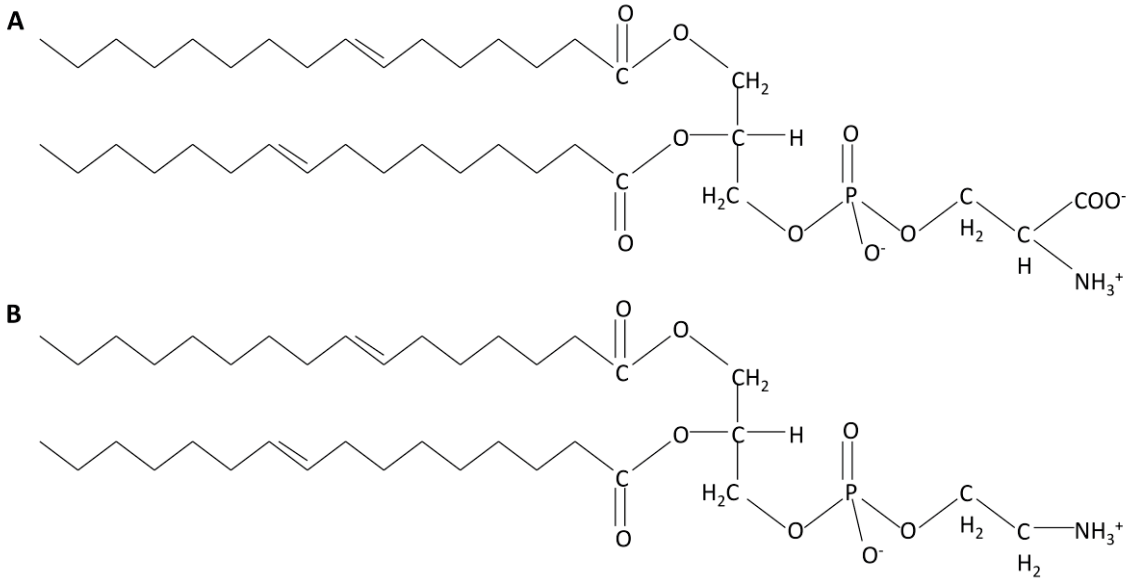

Figure I. 1 The Structure of Two Amino Phospholipids

(A) phosphatidylserine and (B) phosphatidylethanolamine

and PSS1 respectively, and replaced with serine to produce PS (Kuge and Nishijima 1997, Signorell, *et al.* 2008, Tasseva, *et al.* 2013, Vance 2015) (Fig. I.3).

Phosphatidylethanolamine

Phosphatidylethanolamine (PE) is considered a major phospholipid in many eukaryotic organisms and some prokaryotes. It is an uncharged, non-bilayer forming phospholipid due to its small head group, which causes a cone-like shape for its structure (Fig. I.1B). In eukaryotes and most prokaryotes that contain it, PE is produced by the decarboxylation of PS (Carman and Han 2011, Cassilly, *et al.* 2017, Cronan 2003, Dowhan 1997, Kanfer and Kennedy 1964). However, in many eukaryotes PE can alternatively be made from ethanolamine *via* a scavenging pathway known as the Kennedy Pathway (Fig. I.2 and I.3) (Kennedy and Weiss 1956). In the Kennedy pathway, ethanolamine is taken up by the cells and phosphorylated to produce phosphoethanolamine, which is then condensed with CTP to produce CDP-ethanolamine. The third and final step is condensation of CDP-ethanolamine with diacylglycerol (DAG) to generate PE and CMP (Gibellini and Smith 2010).

Although the CDP-DAG and Kennedy pathways are the most common methods employed to generate PE in mammals and fungi, there are alternative mechanisms that produce PE or its precursors in other microbes. In the bacterial plant pathogen *Xanthomonas campestris*, a bifunctional cardiolipin/PE synthase

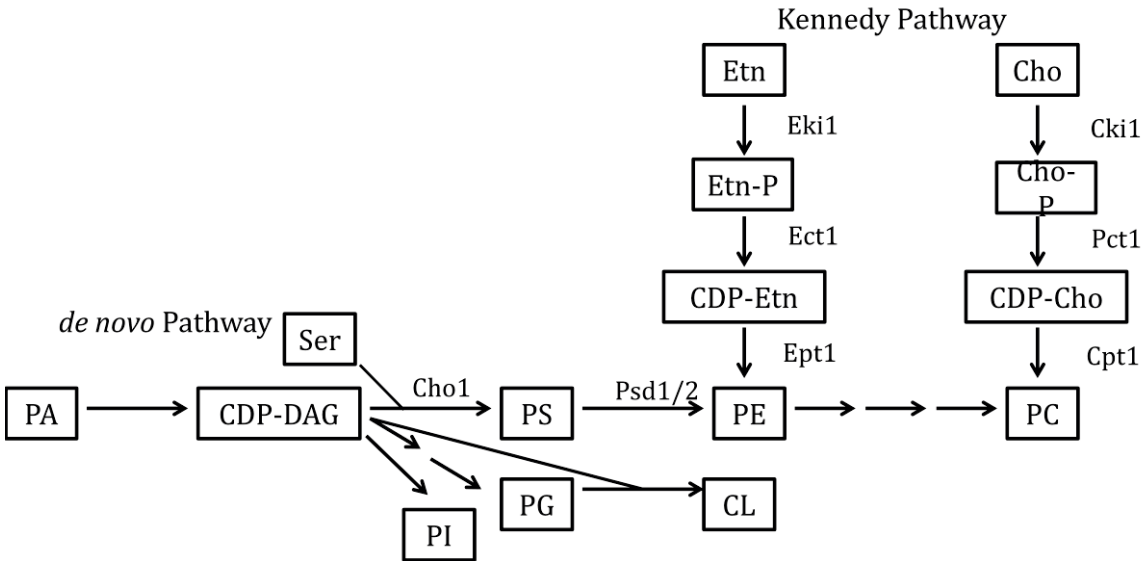

Figure I. 2 Phospholipid Biosynthesis Pathways in *C. albicans*

C. albicans acquires phospholipids via both an endogenous pathway, the *de novo* pathway, and an exogenous pathway, the Kennedy pathway. The precursors for producing the most common phospholipids are PA and CDP-DAG. CDP-DAG is then converted to PI, PS, or PG. The endogenously produced PS can be decarboxylated into PE and then further methylated into PC. In the Kennedy pathway, exogenous ethanolamine (Etn) and/or choline (Cho) are brought into the cell and converted into PE and PC. Abbreviations: PA – phosphatidic acid; CDP-DAG – cytidine diphosphate diacylglycerol; PI – phosphatidylinositol; PS – phosphatidylserine; PG – phosphatidylglycerol; PE – phosphatidylethanolamine; CL – cardiolipin; PC – phosphatidylcholine; Etn – ethanolamine; Cho – choline, Etn-P-phosphoethanolamine, Cho-P-phosphocholine, CDP-Etn-cytidyldiphosphate-ethanolamine, CDP-Cho-cytidyldiphosphate-choline, Ser-serine

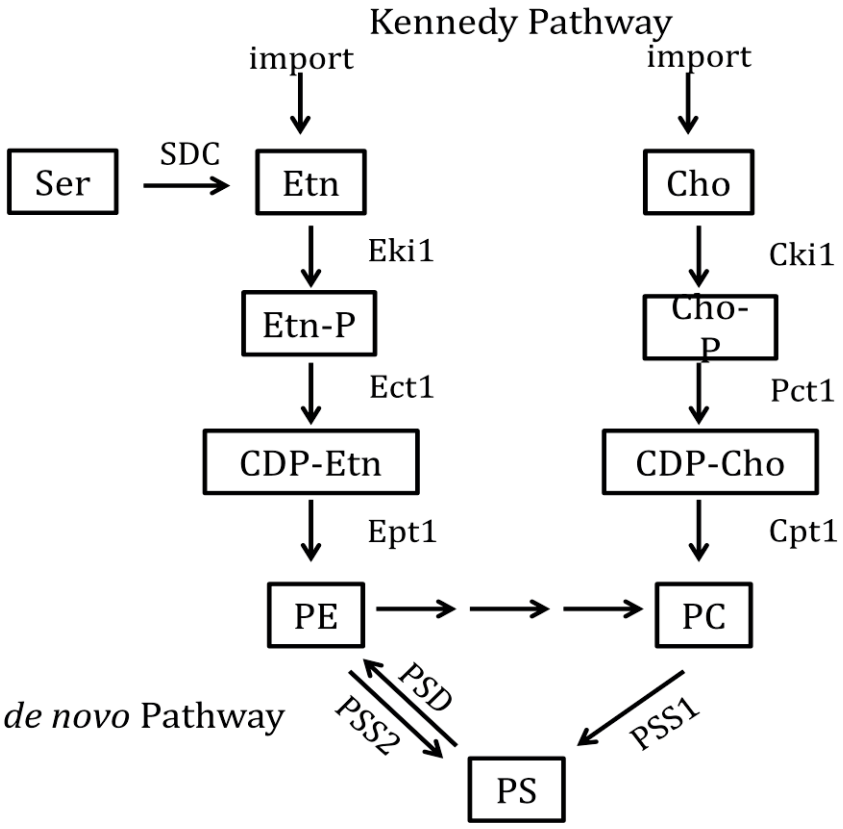

Figure I. 3 Phospholipid Biosynthesis Pathways in Mammals and Parasites

Mammals acquire phospholipids via both an endogenous pathway, the *de novo* pathway, and a scavenging pathway, the Kennedy pathway. Headgroups of existing PE and PC can be cleaved and replaced with serine to produce PS. PS can be decarboxylated to produce PE. PE can then be methylated three times to produce PC. In the Kennedy pathway, exogenous ethanolamine (Etn) and/or choline (Cho) are brought into the cell and converted into PE and PC. Abbreviations: PS – phosphatidylserine; PE – phosphatidylethanolamine; PC – phosphatidylcholine; Etn – ethanolamine; Cho – choline (Figure adapted from Chen *et al.*, 2010)

was identified. *X. campestris* produces PE by the decarboxylation of PS; however, upon the deletion of PS decarboxylase, growth of the organism was partially restored when exogenous ethanolamine was supplemented. Researchers identified a putative cardiolipin synthase gene that, in addition to making CL from CDP-DAG and phosphatidylglycerol-phosphate, could produce PE from CDP-DAG and ethanolamine. This process, which may be important in certain conditions, seems to be restricted to *Xanthomonadales* and *Pseudomonadales* orders based on phylogenetic analysis (Moser, *et al.* 2014).

In the kinetoplast parasites such as Trypanomes and *Leishmania*, the Kennedy pathway appears to be the key method of synthesizing PE. In *Trypanosoma brucei*, PE is maintained within the cell in two distinct pools (Signorell, *et al.* 2008). For *Leishmania* most of the ethanolamine used to produce PE is not taken up from the environment, but rather produced within the organism by cleaving sphingosine-1-phosphate to form long chain fatty aldehydes and phosphoethanolamine. The phosphoethanolamine can be funneled directly into the second step of the Kennedy pathway where phosphoethanolamine is converted to CDP-ethanolamine which leads in another step to PE (Fig. I.3) (Pulido, *et al.* 2017, Zhang, *et al.* 2007). This cleavage is carried out by the enzyme sphinosine-1-phosphate lyase, which is also found in other microbes such as *S. cerevisiae* (Dpl1). In yeast, Dpl1 can support growth of yeast in the absence of PS decarboxylase (*psd1*Δ *psd2*Δ) and exogenous ethanolamine, indicating that it can support PE synthesis by the Kennedy

pathway in yeast as well. However, under normal conditions, Dpl1 is not a major source for PE synthesis in this organism (Birner, *et al.* 2001, Mao, *et al.* 1997, Saba, *et al.* 1997). Yeast also have the ability to take up and acylate lyso-PE to produce PE or remodel existing PE species (Burgermeister, *et al.* 2004, Deng, *et al.* 2010, Flis and Daum 2013, Riekhof and Voelker 2006, Riekhof, *et al.* 2007a, Riekhof, *et al.* 2007b).

The apicomplexan parasites also have unusual characteristics regarding PS and PE. The malaria parasite *Plasmodium falciparum* can acquire ethanolamine for the Kennedy pathway by directly decarboxylating serine into ethanolamine, by means of the serine decarboxylase (SDC) enzyme, an enzymatic activity shared with plants but not animals or fungi (Fig 3) (Elabbadi, *et al.* 1997).

Toxoplasma gondii is an intracellular apicomplexan parasite that reproduces within a parasitophorous vacuole. In *T. gondii*, PE is produced via the Kennedy pathway and via the decarboxylation of PS in the mitochondria (Hartmann, *et al.* 2014) as is seen in fungi or mammals. However, *T. gondii* also has unusual versions of the canonical base-exchanging PS synthase and PS decarboxylase enzymes. First, in addition to an internal, membrane-bound PS decarboxylase, it has a second, soluble PS decarboxylase enzyme (*Tg*PSD1) that is secreted extracellularly from *T. gondii* cells and appears to decarboxylate PS to PE in the parasitophorous vacuole (Hartmann, *et al.* 2014). This is highly unusual because both PS decarboxylase and PS synthase are typically

membrane bound enzymes with multiple transmembrane domains. There have been other reports of hyperexpressed PS decarboxylase enzymes dissociating from the cytoplasmic membrane in bacteria (Tyhach, *et al.* 1979) and in *Plasmodium falciparum* (Baunaure, *et al.* 2004, Choi, *et al.* 2016), but *Tg*PSD1 is the first example of a secreted PS decarboxylase with the enzymatic ability to convert PS to PE. *Tg*PSD1 has also been detected within the parasitophorous vacuole. Although its function within this compartment is not entirely clear, it could potentially help damage the host cell membrane to allow *T. gondii* to escape the parasitophorous vacuole when it lyses the cell. Furthermore, the secreted enzyme may bind liposomes and host membranes to allow for membrane biogenesis and parasite replication. Thirdly, the secreted enzyme may suppress PS exposure on the apoptotic host cell, thereby avoiding phagocytosis, and allowing the parasite to replicate and avoid the immune system. While these possibilities are likely, the exact reasons for its unique function still remain to be elucidated (Gupta, *et al.* 2012). *T. gondii* also appears to have the ability to take up host PE (possibly via a permease) when production of PE is inhibited intracellularly, further increasing the survival and fitness of this organism (Hartmann, *et al.* 2014).

In addition to an unusual PS decarboxylase that could affect host PE, *T. gondii* also been shown to make an unusual phospholipid that is closely related to PS called phosphatidylthreonine (PT). PT is found in small amounts in mammals and some bacteria (Heikinheimo and Somerharju 2002, Ivanova, *et al.*

2010, Mitoma, *et al.* 1998, Muller, *et al.* 2011), but in *T. gondii* PT is found in more substantial amounts than PS. PT is synthesized in *T. gondii* by an enzyme with close homology to the mammalian PSS base-exchange enzymes (Fig 3), but it exchanges threonine or serine instead of serine alone (Arroyo-Olarte, *et al.* 2015, Arroyo-Olarte and Gupta 2016). The PT synthase is predicted to be found in a few other protozoa including *Neospora, Eimeria, Phytophtora,* and *Perkinsus* (Arroyo-Olarte, *et al.* 2015, Arroyo-Olarte and Gupta 2016).

PS and PE as Modulators of Virulence

Candida albicans

Candida albicans is a commensal fungus that normally inhabits the gut and skin of healthy people. However, immunocompromised individuals are at a high risk of developing bloodstream infections where *C. albicans* can infect the deep organs leading to sepsis. *C. albicans* is known to produce several virulence factors including hyphae, adhesins, lipases, proteases, and the more recently described *Candida*lysin (Moyes, *et al.* 2016). It is also able to hide itself to a limited extent from the innate immune system by a process called masking. Yeast cell walls contain four main components: chitin, mannosylated proteins (mannan), β(1-6)-glucan and β(1-3)-glucan. Mannan makes up the majority of the surface layer of the cell wall, while β-glucans, and chitin are “hidden” beneath. β-(1,3)-glucan is a pathogen associate molecular pattern (PAMP) that can be detected by the innate immune receptor Dectin-1 as a signal that the host is infected by a fungal pathogen (Brown and Gordon 2001) . Dectin-1 is found on macrophages,

dendritic cells, neutrophils, and some other immune cells. The proposed layered topology, where mannan masks the immunogenic molecule β(1-3)-glucan is a method of innate immune system evasion by this yeast (Davis, *et al*. 2014a). Disruption of this layering (*i.e.* unmasking) makes it easier for the host to detect the fungus (Hasim, *et al.* 2017, Wheeler and Fink 2006, Wheeler, *et al.* 2008).

It has been shown that the fungal phosphatidylserine (PS) synthase, Cho1p, is absolutely required for virulence of *C. albicans*. In a mouse model of systemic infection, the *cho1*ΔΔ deletion mutant was unable to cause infection, while mice infected with wild-type or *cho1*Δ/Δ*::CHO1* reintegrant strains died within two weeks (Chen, *et al.* 2010). In addition, *cho1*ΔΔ shows significant reduction in kidney colonization and is completely cleared from the mice, even when they are made neutropenic with cyclophosphamide (Y. L. Chen and T. B. Reynolds, unpublished data). In contrast, mice infected with wild-type *C. albicans* showed high kidney burden before succumbing to infection (Chen, *et al.* 2010).

In addition to a complete loss of PS, the *cho1*ΔΔ mutation also causes a loss of PE synthesized from PS (Fig 2) (Cassilly, *et al.* 2017). This suggested that the avirulence could be caused by loss of PE as well as PS. A *psd1*ΔΔ *psd2*ΔΔ double mutation, which eliminates all PS decarboxylase activity, also causes severe avirulence; however, there is a significantly greater loss of *C. albicans* colonization from the kidneys in *cho1*ΔΔ than in *psd1*ΔΔ *psd2*ΔΔ (Davis, *et al.*, data unpublished). The major difference between *cho1*ΔΔ and *psd1*ΔΔ *psd2*ΔΔ is that only *cho1*ΔΔ has increased β(1-3)-glucan unmasking in its cell

wall, increasing host immune recognition of this microbe (Davis, *et al*. 2014a). Thus, other underlying factors related to loss of PE play a role in the loss of virulence, but cell wall unmasking driven by the loss of PS correlates with even faster clearance. The mechanism responsible for cell wall unmasking in the *cho1*ΔΔ mutant are currently under investigation.

These defects in virulence in the *cho1*ΔΔ and *psd1*ΔΔ *psd2*ΔΔ mutants are manifest despite the presence of an alternative Kennedy pathway for PE synthesis (Fig. 2). This brings up questions as to whether Kennedy pathway synthesized PE is able to compensate for PS-derived PE or if cells are unable to make sufficient PE by the Kennedy pathway. Furthermore, this also opens the question of how much of a role the loss of PS alone plays in virulence, in addition to its effects on cell wall unmasking.

Due to these virulence defects, Cho1p represents a good drug target in *C. albicans* (Cassilly, *et al.* 2016, Chen, *et al.* 2010). First, as loss of Cho1p renders *C. albicans* avirulent, inhibition of Cho1p should render *C. albicans* nonpathogenic to the host. Secondly, since the mammalian PS synthase enzymes are not orthologous with the fungal PS synthase, an inhibitor of Cho1p should be very specific for fungi without affecting mammalian Pss1p and Pss2p (Compare Figs I.2 and I.3). Identification of small molecule inhibitors of Cho1p as potential therapeutics is a priority (Cassilly, *et al.* 2016). Finally, Cho1p is conserved throughout pathogenic fungi, so an inhibitor could be broad spectrum (Braun, *et al.* 2005).

Brucella abortus

Brucella abortus is the causative agent of brucellosis which can be a severe and chronic infection within humans. This organism is a facultative, intracellular pathogen that typically resides within a specific compartment in the host cell called the *Brucella*-containing vacuole (BCV). From this location, *B. abortus* can control the host cell machinery and replicate. Several factors contribute to *B. abortus* virulence including immune modulators, smooth lipopolysaccharide (LPS), and cyclic β-glucans. However, recent studies have shown that the membrane phospholipid composition is crucial for interaction of the microbe with the host cells (Bukata, *et al.* 2008, Comerci, *et al.* 2006). For example, phosphatidylcholine (PC)—one of the main phospholipids produced in this microbe—is necessary for the organism to set up a chronic infection in a murine model (Comerci, *et al.* 2006, Conde-Alvarez, *et al.* 2006). Further studies showed that PS and PE play significant roles in virulence. A mutant of the phosphatidylserine synthase (*pssA*), was produced. PS is not considered a major phospholipid within *B. abortus*, but this enzyme is crucial for production of PE (Fig 2) (Bukata, *et al.* 2008, Thiele and Kehr 1969). The *pssA* mutant had a loss of PE and showed increased sensitivity to membrane-perturbing agents like SDS. The *pssA* mutant also showed decreased survival intracellularly in tissue culture cells and showed a marked decrease in maturation of the BCV that protects the bacteria intracellularly. Finally, a marked decrease in virulence was found in the *pssA* mutant as compared to the wild-type within a mouse model of

infection (Bukata, *et al.* 2008). Although the exact impact on virulence is not known, it is thought that PE contributes to BCV formation and thus is necessary for virulence. Further, by disrupting the structure of the membrane, it is possible that important protein complexes or virulence determinants are also disrupted which negatively affects the organism's ability to survive within host cells.

The *pssA* gene is important for growth in *Escherichia coli*, but it has only been examined for its role in growth in non-pathogenic laboratory strains. As in *B. abortus* deletion of *pssA* causes not only a decrease in PS and PE, but it also causes a growth defect unless the media is supplemented with divalent cations like Ca^{2+} or Mn^{2+} (Nakajima, *et al.* 1991). Further investigations into the role for PS/PE synthesis in the pathogenesis of Gram negative organisms is warranted as it may be important for virulence in a variety of these often-drug-resistant pathogens.

Plasmodium

Plasmodium parasites are the causative agents of malaria, which is one of the most important health problems in the developing world. Finding new treatments with novel modes of actions to better combat this pathogen is a major area of current research because of the rising resistance to existing anti-malarial therapies. Enzymes involved in the production of important malarial lipids, like the PS decarboxylase (PSD) enzyme, have been suggested as a drug target since PE is an essential phospholipid within *Plasmodium* membranes. Indeed,

inhibition of PSD results in growth arrest of the parasite (Ben Mamoun, *et al.* 2010, Choi, *et al.* 2016, Serran-Aguilera, *et al.* 2016). Recent findings have shown that the PSD enzyme from *Plasmodium falciparum*, though both soluble and membrane-bound in this organism, can complement yeast *psd* mutants (Choi, *et al.* 2016). Furthermore, screening a library of known malaria inhibitors identified a particular compound, 7-chloro-N-(4-ethoxyphenyl)-4-quinolinamine (MMV007285), with potent activity against *Plasmodium*, and the ability to inhibit the catalytic function of PSD (Choi, *et al.* 2016).

In addition to PSD, the choline kinase (CK) is crucial for PE synthesis in *Plasmodium*, and has been suggested as another drug target (Serran-Aguilera, *et al.* 2016). This enzyme is involved in the Kennedy Pathway where choline and ethanolamine are taken up from the environment and used to produce PC and PE, respectively (Fig 3). Recent work has found that known anti-cancer compounds BR23 and BR25 that inhibit human choline kinase cause a dramatic drop in the levels of PE within *P. falciparum* but not PC, as these compounds influence PE synthesis more than PC synthesis in this parasite (Serran-Aguilera, *et al.* 2016). The CK of *P. falciparum* is involved in both choline and ethanolamine phosphorylation, but the drugs seem to primarily impact ethanolamine phosphorylation, rather than choline phosphorylation, explaining the differential effects on PE and PC synthesis. Treatment with either drug led to arrested development of the parasite, likely as a result of the loss of membrane PE, and ultimately were lethal (Serran-Aguilera, *et al.* 2016). These findings

demonstrate the importance of PE biosynthesis in survival and pathogenicity of microbes, and are some of the first studies where small molecule inhibition of an ethanolamine kinase in a pathogen has led to promising lead inhibitory compounds.

Finally, although *P. falciparum* has two different pathways to make PE, (both CDP-DAG and Kennedy, Fig 2-3), loss of either pathway appears to be sufficient to compromise its growth. This is surprising, and indicates several possible explanations: 1) the molecular species of PE made from the two pathway differ and each is crucial for virulence, 2) localization of PE synthesis for each pathway differs (PSD is in the mitochondria while the Kennedy pathway synthesizes PE in the ER) and PE made in one location is not sufficient to make up for the other, 3) the volume of PE made by either pathway alone is not sufficient to support virulence (Choi, *et al.* 2016, Serran-Aguilera, *et al.* 2016).

Trypanosomes

Trypanosoma brucei is a neglected tropical pathogen that affects both humans and livestock within specific regions of Africa. Current therapies are inadequate due to rising drug resistance and high toxicity, creating a need for new drugs. Like in *Plasmodium*, phospholipid biosynthetic pathways have been suggested as excellent targets for therapy in *T. brucei*. PE represents a good target for several reasons including its importance in providing the phophoethanolamine moiety that links GPI anchors to membrane proteins, including variant surface

glycoprotein (VSG) (Menon, *et al.* 1993, Menon and Stevens 1992). VSG is a crucial aspect of *T. brucei* virulence as it is key in allowing the organism to evade the immune system and set up chronic infections within the host. Thus, disruption of proper VSG production and localization represents an excellent drug target in this organism. Indeed, a conditional knockout of the ethanolamine-phosphate cytidyltransferase (EPT) in *T. brucei* revealed that this gene is essential for growth and crucial in the synthesis of both PE and GPI-anchors (Gibellini, *et al.* 2009). In addition, ethanolamine analogues are being explored as inhibitors of the ethanolamine kinase enzyme (Gibellini, *et al.* 2008).

Toxoplasma gondii

Phosphatidylthreonine (PT) has been shown to be naturally abundant in *T. gondii* and play a role in virulences. In a *Δtgpts* PT synthase mutant, replication of the parasite was normal, but a marked decrease in plaques and plaque size was seen upon infection, when compared with a wild-type control. Further, the *Δtgpts* mutant showed a decrease in motility, which is a major contributor to virulence within this organism. As expected, the *Δtgpts* mutant demonstrated decreased virulence in a mouse model of infection. These findings implicate PT in the lysis of host cells, as well as possible egression into new host cells for propagation of infection, indicating that the parasite has evolved PT specifically for use in its lytic cycle of infection. Although the exact mechanism of PT in disease is still unknown, it is likely that PT may affect calcium flux at the plasma membrane and

calcium homeostasis, which could in turn control motility (Arroyo-Olarte, *et al.* 2015, Arroyo-Olarte and Gupta 2016).

Host PS and PE are utilized by pathogens for virulence

Host membranes serve as a barrier to microbes, either by preventing entry into tissues or limiting access to necessary nutrients. It is a common trait for microbes to manipulate and alter host membranes in order to establish infection and persist within the host (Ham, *et al.* 2011, Sarantis and Grinstein 2012). PS is an important phospholipid in a variety of processes. In mammalian systems, redistribution of PS is a key indicator that a cell is undergoing apoptosis. Cells typically maintain an asymmetrical distribution of PS in the plasma membrane, where most PS faces the cytoplasm (localized to the inner leaflet of the membrane). Upon receipt of "death signals" for apoptosis from the cell, PS is flipped to the outer leaflet as a signal to macrophages that a cell is dying. Macrophages use PS as the "eat me" signal to then engulf the apoptotic cells. Exposed PS (or even PE) on the host cell, either naturally or as a result of promoted PS externalization *via* activity of the microbe (Fujimoto, *et al.* 1998, Gao and Abu Kwaik 1999, Goth and Stephens 2001, Murata-Kamiya, *et al.* 2010, Semiramoth, *et al.* 2010, Wandler, *et al.* 2010), can be recognized and exploited by microbes. Some microbes, like *Chlamydia trachomatis* or the influenza virus enter cells and promote PS-externalization and apoptosis, likely to ensure exit from the infected cell and further dissemination (Fujimoto, *et al.* 1998, Goth and

Stephens 2001). In *Helicobacter pylori*, the virulence determinant CagA was shown to bind tightly to PS exposed on host cells via a specific motif. Once bound, CagA is thought to promote its own uptake into the host cell where it remains tethered to the membrane *via* PS and modulates several signaling pathways (Backert, *et al.* 2011, Murata-Kamiya, *et al.* 2010, Wandler, *et al.* 2010).

In addition, enterohemorrhagic *Escherichia coli* (EHEC) has been shown to induce apoptosis and expose both PS and PE on host cell surfaces. EHEC can then bind to the exposed PE, establishing a tight connection with the host, followed by subsequent internalization of the microbe, nutrient acquisition, or delivery of toxins deep into host tissues (Barnett Foster, *et al.* 2000, Barnett Foster, *et al.* 1999). Exposed host PS can also be used as a tool for microbial dissemination.

Listeria monocytogenes exploits efferocytosis, or the removal of dead cells and debris via phagocytosis, to facilitate spread from cell to cell. These bacteria are phagocytosed, but can escape from the phagosome through the activity of their pore-forming toxin listeriolysin O (LLO). LLO then can promote the release of bacteria-containing vesicles with exposed PS on the surface which are then phagocytosed by macrophages, continuing the cycle of dissemination (Czuczman, *et al.* 2014).

Similarly, *Mycobacterium tuberculosis* also has the ability to escape the phagosome and can produce the secreted protein EspB which, when processed,

has been shown to bind phosphatidic acid (PA) and PS. Although the exact function of this binding is still unknown, it is hypothesized that EspB may interfere with PA- and PS-mediated signaling in the host (Chen, *et al.* 2013, Korotkova, *et al.* 2015). Based on these examples, it is clear that interaction with host phospholipids is crucial in many aspects of infection. However, in addition to this face of virulence, *microbial* phospholipids have also been shown to be important in virulence.

PS-Exposure and Apoptotic Mimicry

Many obligate- or facultative-intracellular pathogens employ various methods of invading host cells. In addition to other various surface determinants, like sugars (van Zandbergen, *et al.* 2007), the lipid composition in the microbe's plasma membrane can play a role in promoting their uptake by host cells (e.g. phagocytosis by host macrophages). Phospholipids like PS can play a major role in this process.

Leishmania

L. braziliensis is known to have multiple virulence factors associated with its disease and includes cell surface molecules like lipophosphoglycan (LPG) and carbohydrates. In addition, PS also serves as a ligand for mononuclear macrophages. *L. tropica* promastigote forms expose higher levels of PS on their surface during the infective growth phases (Tripathi and Gupta 2003). Furthermore, amastigotes of *L. amazonensis* with higher levels of PS on the cell

surface had increased infectivity *in vivo* and *in vitro* (Wanderley, *et al.* 2006). These findings indicate that a higher concentration of PS on the surface of these organisms increases the chances of being internalized by the host macrophages (Wanderley, *et al.* 2006).

The PS exposed on the membrane of the parasite is thought to play a role in apoptotic mimicry, allowing *L. brasiliensis* to establish an infection within the host (de Freitas Balanco, *et al.* 2001, van Zandbergen, *et al.* 2007). When PS exposed on the surface of *L. brasiliensis*, *L. tropica* or *L. amazonensis* is blocked with annexin V, the infectivity of the parasite in murine peritoneal macrophages is decreased (de Freitas Balanco, *et al.* 2001, Farias, *et al.* 2013, Tripathi and Gupta 2003, Wanderley, *et al.* 2006, Wanderley, *et al.* 2009).

Interestingly, PS exposure seems to have importance even beyond the initial entry into host macrophages. *L. amazonensis* and *L. major*, subpopulations of PS-positive and PS-negative promastigotes cooperate to produce a sustained and successful infection of host macrophages (van Zandbergen, *et al.* 2006, Wanderley, *et al.* 2009). *L. amazonensis* amastigotes with high levels of PS exposed on their cell surfaces are able to induce cytokine production as well as inhibit NO production (Wanderley, *et al.* 2006). These findings implicate PS production and exposure as an excellent drug target within *Leishmania*.

Similar instances of apoptotic mimicry have also been reported for *Trypanosoma cruzi* (Damatta, *et al.* 2007, Freire-de-Lima, *et al.* 2000),

Toxoplasma gondii (Seabra, *et al.* 2004), and even enveloped viruses (Jemielity, *et al.* 2013, Moller-Tank, *et al.* 2013, Soares, *et al.* 2008, Vanlandschoot and Leroux-Roels 2003), demonstrating the prevalence of PS exposure in regulating infection. Targeting proteins responsible for this PS exposure (Araujo-Santos, *et al.* 2003, dos Santos, *et al.* 2013) or enzymes involved in PS synthesis, could be a viable option for future therapies across a wide variety of pathogens.

Cryptococcus neoformans

Cryptococcus neoformans is a facultative intracellular fungal pathogen. Recent studies have demonstrated that beyond secreted virulence factors, there are also other important proteins within the organism that play a role in virulence. One such example is Cdc50, which is a lipid flippase responsible for maintaining asymmetry in the phospholipid bilayer (Huang, *et al.* 2016). Upon deletion of Cdc50, *C. neoformans* becomes more sensitive to fluconazole, caspofungin, and SDS likely due to a change in membrane integrity. In mice, the *cdc50*Δ mutant was unable to cause a robust infection and was cleared from the lungs, further implicating this protein as a virulence factor. Though the exact mechanism behind this loss of virulence is currently still under scrutiny, the *cdc50*Δ mutant had increased levels of PS exposed to the outer membrane, further supporting the importance of proper PS localization and membrane integrity for the virulence of this fungus. These results indicate that loss of Cdc50, and likely a change in PS localization, can massively disrupt virulence, and fitness of the organism, thus

representing a drug target within *Cryptococcus*. In addition, since the *cdc50*Δ mutant showed greater susceptibility to caspofungin, a common antifungal drug that *Cryptococcus* is naturally resistant to, further exploration of phospholipid flippases or membrane symmetry could improve the effectiveness of echinocandins against the fungus.

PS and PE in Extracellular Vesicles

A potential contributor to virulence in microbes is the use of extracellular vesicles as delivery systems for virulence factors. This characteristic can be found in *C. albicans*, *Candida parapsilosis*, *Sporothrix schenckii*, *Saccharomyces cerevisiae* (Albuquerque, *et al.* 2008), *Cryptococcus neoformans* (Oliveira, *et al.* 2010, Rodrigues, *et al.* 2008), and *Paracoccidioides brasiliensis* (Manocha, *et al.* 1980), and even Gram negative bacteria like *E. coli* (Hoekstra, *et al.* 1976, Horstman and Kuehn 2000), *Pseudomonas aeurginosa* (Tashiro, *et al.* 2011), *Legionella pneumophila* (Fernandez-Moreira, *et al.* 2006, Wessel, *et al.* 2006) and *Haemophilus influenzae* (Kulkarni and Jagannadham 2014, Kulp and Kuehn 2010, Roier, *et al.* 2015, Sharpe, *et al.* 2011).

A recent study found that the *cho1*ΔΔ mutant of *C. albicans* displayed decreased ability to secrete proteases and phospholipases via extracellular vesicles (Wolf, *et al.* 2015), indicating the importance of proper phospholipid balance in this process.

Lipid profiles from 4 different strains of *P. brasiliensis* (Manocha, *et al.* 1980) revealed that the concentration of PC was higher in virulent strains than in the avirulent strain. Further studies into the lipid composition of fungal extracellular vesicles, known to harbor various virulence factors, showed some differences in the lipid composition, which is theorized to play a role in the virulence of different strains of *P. brasiliensis* (Vallejo, *et al.* 2012).

Histoplasma capsulatum is a pathogenic fungus that can cause life-threatening systemic disease. This organism has many different characteristics that allow it to grow well within the host environment, including survival in a wide pH range and nutrient starvation. *H. capsulatum* also produces various virulence factors like heat-shock proteins and the cell wall protein YPS3p. Analysis of the composition of extracellular vesicles reveals that the vesicles were made up of common plasma membrane phospholipids including PE, PS, and PC (Albuquerque, *et al.* 2008). This composition is similar to what is found in mammalian exosomes which are known to transport important molecules like bioactive lipids and lipid-degrading enzymes. The biogenesis of exosomes in mammals is a specific process that requires certain lipids with a characteristic membrane organization (Laulagnier, *et al.* 2004, Subra, *et al.* 2007). Although the importance of this phospholipid composition has not been studied in *H. capsulatum*, it is likely that the specific phospholipids making up the extracellular vesicles are important in virulence and proper function.

Significance

Because of this clear significance of aminophospholipids within microbial virulence, we were interested in focusing on PS synthesis in *Candida albicans* as a possible drug target. *C. albicans* is an opportunistic fungal pathogen that, along with several other species in the *Candida* genus, represents the most common fungal pathogen of humans and has even been shown to cause problems to astronauts on the international space station (Crabbe, *et al*. 2013). In most people, this organism occupies the skin, gut, and vagina as a commensal (Hube 2004); however, it can be a severe threat to immunocompromised individuals (rendered so by HIV-AIDS, chemotherapy, etc.). In these patients, *C. albicans* causes oral thrush, infects skin wounds, and causes life-threatening invasive bloodstream infections and fungal endocarditis (FE) (Mishra, *et al.* 2007, Pierrotti and Baddour 2002). Invasive bloodstream infections and FE—which can arise from implanted medical devices like long-dwelling intravascular catheters or prosthetic heart valves (Mishra, *et al.* 2007, Sun, *et al.* 2013)—have high mortality rates, around 30% and 50%, respectively (Baddley, *et al.* 2008, Maccallum, *et al.* 2013, Pierrotti and Baddour 2002). There are three main classes of antifungals used to treat *C. albicans* invasive bloodstream infections: azoles (i.e. fluconazole, itraconazole) which inhibit ergosterol synthesis; polyenes (i.e. amphotericin B) which target existing ergosterol in the plasma membrane (Anderson, *et al.* 2014, Ghannoum and Rice 1999); and echinocandins (i.e. caspofungin) which target the fungal cell wall (Alem and Douglas 2004,

Bachmann, *et al.* 2002, Baddley, *et al.* 2008, Lyons and White 2000). However, because of rising drug resistance (azoles, echinocandins), high toxicity (amphotericin B), and poor oral availability (polyenes, echinocandins) of these drugs, they are not always effective at safely eliminating the infection (Anderson 2005, Ghannoum and Rice 1999). Lack of effective treatment contributes to high mortality in individuals with FE or invasive bloodstream infections (Sun, *et al.* 2013), which creates the need for novel drug targets in the organism as well as new antifungal compounds (Maccallum, *et al.* 2013).

Despite this pressing need, little progress has been made in recent decades to identify new antifungal compounds. The process of drug development is notoriously slow, but rendered slower in fungi. One main reason for this delay is the amount of similarity between fungi and humans. *Saccharomyces cerevisiae* has long been used as a model organism for understanding eukaryotic organisms and mammalian processes. Because of this, finding drugs that are selectively toxic to fungi, while having no side effects on mammalian host cells, is a monumental hurdle. Even the currently used Amphotericin B suffers from toxic side effects due to the similarities between fungal ergosterol and mammalian cholesterol. Thus, it is of utmost importance to identify new or better targets for antifungal therapies.

Several recent reviews have highlighted the potential of the fungal cell membrane as an excellent drug target (Rella, *et al.* 2016, Sant, *et al.* 2016). While those reviews aim to provide a general overview of fungal membranes and

lipids as antifungal targets, the aim of this work was to fully understand PS synthesis as a drug target within *C. albicans*.

Screening Approaches for Identifying PS Synthase Inhibitors

Because of the promise of using Cho1p as a drug target, we developed several approaches for identifying small molecule inhibitors. These approaches largely hinge on using phenotypic traits of *cho1*ΔΔ as indicators that Cho1p is being inhibited. Our first method, described in Chapter 2 was based on the anti-fungal activity of a marine depsipeptide Papuamide A (Pap-A). This compound has been shown to bind specifically to PS in membranes of liposomes (Andjelic, *et al.* 2008). Although the exact mechanism of action has not been demonstrated, it is thought that Pap-A binds PS by inserting a lipophilic tail into cell membranes, causing a disruption in membrane integrity and subsequent lysis. Indeed, the *cho1*ΔΔ mutant is completely resistant to Pap-A (Cassilly, *et al.* 2016, Chen, *et al.* 2010). As a result, we used Pap-A as an indicator of functional PS synthesis, hypothesizing that if a small molecule inhibited Cho1p, it would cause the organism to become resistant to Pap-A. The screening approach and results from this study can be found in Chapters 2 and 3 and Appendix 3.

A second phenotypic trait that we wished to exploit for our screening was ethanolamine auxotrophy. Because phosphatidylethanolamine is an essential phospholipid, the *cho1*ΔΔ cannot survive without ethanolamine provided in the growth medium. This exogenous ethanolamine can be taken up by the cells and

used in the Kennedy pathway to circumvent the organism's requirement for PS (as a precursor for PE). Thus, *cho1*ΔΔ has a very distinct characteristic of growth inhibition in minimal medium deplete of ethanolamine, but showing a return of growth when ethanolamine is supplemented back into the medium. We hypothesized that small molecules that inhibit Cho1p would cause ethanolamine auxotrophy in wild-type *C. albicans* that we could detect based on a lack of growth in minimal medium. The screening approach and results from this study can be found in Appendix 1.

Characterization of PS Synthase and PS Trafficking

Although our screening approaches have been beneficial in certain ways, they have not yet yielded PS synthase inhibitors as we expected. Thus, in addition to our screening, we were also interested in characterizing the PS synthase enzyme to provide information that could aid in a more rational drug design approach. We hypothesized that identifying specific regions on Cho1p that were crucial for enzyme function could help provide a framework by which we could design inhibitors to competitively or allosterically inhibit the enzyme. In order to perform these studies, we began by characterizing Cho1p both *in vivo* and *in vitro*. The results of these studies are described in Chapter 1. Further, we began biochemical characterization where we mapped the substrate binding sites in Cho1p. This study is described in Chapter 4.

In addition to these biochemical characterizations, we were interested in describing PS dynamics within yeast. Although we wished to perform these studies in *C. albicans*, the model yeast *S. cerevisiae* was more amendable to use of genetic tools and thus characterization of PS trafficking and dynamics at the membrane was performed in yeast. The findings from this study can be found in Appendix 2.

Last, we wished to complete our biochemical characterization by solving the 3D crystal structure of Cho1p. Although we were unable to complete this project due to time constraints, we developed several strains of *S. cerevisiae* containing Cho1p tagged with 3X FLAG and 6X His which will ultimately allow purification of the protein via affinity chromatography. These strains will be useful in future studies to determine the structure of Cho1p. These preliminary experiments can be found in Appendix 4.

References

Albuquerque PC, Nakayasu ES, Rodrigues ML *et al.* Vesicular transport in *Histoplasma capsulatum*: an effective mechanism for trans-cell wall transfer of proteins and lipids in ascomycetes. *Cell Microbiol* 2008;**10**: 1695-710.

Alem MA, Douglas LJ. Effects of aspirin and other nonsteroidal anti-inflammatory drugs on biofilms and planktonic cells of *Candida albicans*. *Antimicrob Agents Chemother* 2004;**48**: 41-7.

Anderes EA, Sandine WE, Elliker PR. Lipids of antibiotic-sensitive and -resistant strains of Pseudomonas aeruginosa. *Can J Microbiol* 1971;**17**: 1357-65.

Anderson JB. Evolution of antifungal-drug resistance: mechanisms and pathogen fitness. *Nat Rev Microbiol* 2005;**3**: 547-56.

Anderson TM, Clay MC, Cioffi AG *et al.* Amphotericin forms an extramembranous and fungicidal sterol sponge. *Nat Chem Biol* 2014;**10**: 400-6.

Andjelic CD, Planelles V, Barrows LR. Characterizing the anti-HIV activity of papuamide A. *Mar Drugs* 2008;**6**: 528-49.

Araujo-Santos JM, Gamarro F, Castanys S *et al.* Rapid transport of phospholipids across the plasma membrane of *Leishmania* infantum. *Biochem Biophys Res Commun* 2003;**306**: 250-5.

Arroyo-Olarte RD, Brouwers JF, Kuchipudi A *et al.* Phosphatidylthreonine and Lipid-Mediated Control of Parasite Virulence. *PLoS Biol* 2015;**13**: e1002288.

Arroyo-Olarte RD, Gupta N. Phosphatidylthreonine: An exclusive phospholipid regulating calcium homeostasis and virulence in a parasitic protest. *Microb Cell* 2016;**3**: 189-90.

Bachmann SP, VandeWalle K, Ramage G *et al. In vitro* activity of caspofungin against *Candida albicans* biofilms. *Antimicrob Agents Chemother* 2002;**46**: 3591-6.

Backert S, Clyne M, Tegtmeyer N. Molecular mechanisms of gastric epithelial cell adhesion and injection of CagA by *Helicobacter pylori*. *Cell Commun Signal* 2011;**9**: 28.

Baddley JW, Benjamin DK, Jr., Patel M *et al. Candida* infective endocarditis. *Eur J Clin Microbiol Infect Dis* 2008;**27**: 519-29.

Barnett Foster D, Abul-Milh M, Huesca M *et al.* Enterohemorrhagic *Escherichia coli* induces apoptosis which augments bacterial binding and phosphatidylethanolamine exposure on the plasma membrane outer leaflet. *Infect Immun* 2000;**68**: 3108-15.

Barnett Foster D, Philpott D, Abul-Milh M *et al.* Phosphatidylethanolamine recognition promotes enteropathogenic *E. coli* and enterohemorrhagic *E. coli* host cell attachment. *Microb Pathog* 1999;**27**: 289-301.

Baunaure F, Eldin P, Cathiard AM *et al.* Characterization of a non-mitochondrial type I phosphatidylserine decarboxylase in *Plasmodium falciparum*. *Mol Microbiol* 2004;**51**: 33-46.

Ben Mamoun C, Prigge ST, Vial H. Targeting the Lipid Metabolic Pathways for the Treatment of Malaria. *Drug Dev Res* 2010;**71**: 44-55.

Bhatt A, Molle V, Besra GS *et al.* The *Mycobacterium tuberculosis* FAS-II condensing enzymes: their role in mycolic acid biosynthesis, acid-fastness, pathogenesis and in future drug development. *Mol Microbiol* 2007;**64**: 1442-54.

Birner R, Burgermeister M, Schneiter R *et al.* Roles of phosphatidylethanolamine and of its several biosynthetic pathways in *Saccharomyces cerevisiae*. *Mol Biol Cell* 2001;**12**: 997-1007.

Bogdanov M, Dowhan W. Lipid-assisted protein folding. *J Biol Chem* 1999;**274**: 36827-30.

Braun BR, van Het Hoog M, d'Enfert C *et al.* A human-curated annotation of the *Candida albicans* genome. *PLoS Genet* 2005;**1**: 36-57.

Brown GD, Gordon S. Immune recognition. A new receptor for beta-glucans. *Nature* 2001;**413**: 36-7.

Bukata L, Altabe S, de Mendoza D *et al.* Phosphatidylethanolamine synthesis is required for optimal virulence of *Brucella abortus*. *J Bacteriol* 2008;**190**: 8197-203.

Burgermeister M, Birner-Grunberger R, Nebauer R *et al.* Contribution of different pathways to the supply of phosphatidylethanolamine and phosphatidylcholine to mitochondrial membranes of the yeast *Saccharomyces cerevisiae*. *Biochim Biophys Acta* 2004;**1686**: 161-8.

Carman GM, Han GS. Regulation of phospholipid synthesis in the yeast *Saccharomyces cerevisiae*. *Annu Rev Biochem* 2011;**80**: 859-83.

Carman GM, Zeimetz GM. Regulation of phospholipid biosynthesis in the yeast *Saccharomyces cerevisiae*. *J Biol Chem* 1996;**271**: 13293-6.

Cassilly CD, Farmer AT, Montedonico AE *et al.* Role of phosphatidylserine synthase in shaping the phospholipidome of *Candida albicans*. *FEMS Yeast Res* 2017;**17**.

Cassilly CD, Maddox MM, Cherian PT *et al.* SB-224289 Antagonizes the Antifungal Mechanism of the Marine Depsipeptide Papuamide A. *PLoS One* 2016;**11**: e0154932.

Chen JM, Zhang M, Rybniker J *et al. Mycobacterium tuberculosis* EspB binds phospholipids and mediates EsxA-independent virulence. *Mol Microbiol* 2013;**89**: 1154-66.

Chen YL, Montedonico AE, Kauffman S *et al.* Phosphatidylserine synthase and phosphatidylserine decarboxylase are essential for cell wall integrity and virulence in *Candida albicans*. *Mol Microbiol* 2010;**75**: 1112-32.

Choi JY, Kumar V, Pachikara N *et al.* Characterization of *Plasmodium* phosphatidylserine decarboxylase expressed in yeast and application for inhibitor screening. *Mol Microbiol* 2016;**99**: 999-1014.

Comerci DJ, Altabe S, de Mendoza D *et al. Brucella abortus* synthesizes phosphatidylcholine from choline provided by the host. *J Bacteriol* 2006;**188**: 1929-34.

Conde-Alvarez R, Grillo MJ, Salcedo SP *et al.* Synthesis of phosphatidylcholine, a typical eukaryotic phospholipid, is necessary for full virulence of the intracellular bacterial parasite *Brucella abortus*. *Cell Microbiol* 2006;**8**: 1322-35.

Cox RA, Best GK. Cell wall composition of two strains of *Blastomyces dermatitidis* exhibiting differences in virulence for mice. *Infect Immun* 1972;**5**: 449-53.

Crabbe A, Nielsen-Preiss SM, Woolley CM *et al.* Spaceflight enhances cell aggregation and random budding in *Candida albicans*. *PLoS One* 2013;**8**: e80677.

Cronan JE. Bacterial membrane lipids: where do we stand? *Annu Rev Microbiol* 2003;**57**: 203-24.

Czuczman MA, Fattouh R, van Rijn JM *et al. Listeria monocytogenes* exploits efferocytosis to promote cell-to-cell spread. *Nature* 2014;**509**: 230-4.

Damatta RA, Seabra SH, Deolindo P *et al. Trypanosoma cruzi* exposes phosphatidylserine as an evasion mechanism. *FEMS Microbiol Lett* 2007;**266**: 29-33.

Davis SE, Hopke A, Minkin SC, Jr. *et al.* Masking of beta(1-3)-glucan in the cell wall of *Candida albicans* from detection by innate immune cells depends on phosphatidylserine. *Infect Immun* 2014;**82**: 4405-13.

de Freitas Balanco JM, Moreira ME, Bonomo A *et al.* Apoptotic mimicry by an obligate intracellular parasite downregulates macrophage microbicidal activity. *Curr Biol* 2001;**11**: 1870-3.

Deng L, Fukuda R, Kakihara T *et al.* Incorporation and remodeling of phosphatidylethanolamine containing short acyl residues in yeast. *Biochim Biophys Acta* 2010;**1801**: 635-45.

Disalvo AF, Denton JF. Lipid Content of Four Strains of *Blastomyces dermatitidis* of Different Mouse Virulence. *J Bacteriol* 1963;**85**: 927-31.

dos Santos MG, Muxel SM, Zampieri RA *et al.* Transbilayer dynamics of phospholipids in the plasma membrane of the *Leishmania* genus. *PLoS One* 2013;**8**: e55604.

Dowhan W. Molecular basis for membrane phospholipid diversity: why are there so many lipids? *Annu Rev Biochem* 1997;**66**: 199-232.

Elabbadi N, Ancelin ML, Vial HJ. Phospholipid metabolism of serine in *Plasmodium*-infected erythrocytes involves phosphatidylserine and direct serine decarboxylation. *Biochem J* 1997;**324 (Pt 2)**: 435-45.

Farias LH, Rodrigues AP, Silveira FT *et al.* Phosphatidylserine exposure and surface sugars in two *Leishmania* (Viannia) *braziliensis* strains involved in cutaneous and mucocutaneous *Leishmania*sis. *J Infect Dis* 2013;**207**: 537-43.

Farthing MA, Cassilly JP. Acceptability of three convenience chicken products. *J Am Diet Assoc* 1976;**68**: 148-51.

Fernandez-Moreira E, Helbig JH, Swanson MS. Membrane vesicles shed by *Legionella pneumophila* inhibit fusion of phagosomes with lysosomes. *Infect Immun* 2006;**74**: 3285-95.

Finlay BB, Falkow S. Common themes in microbial pathogenicity. *Microbiol Rev* 1989;**53**: 210-30.

Finlay BB, Falkow S. Common themes in microbial pathogenicity revisited. *Microbiol Mol Biol Rev* 1997;**61**: 136-69.

Flis VV, Daum G. Lipid transport between the endoplasmic reticulum and mitochondria. *Cold Spring Harb Perspect Biol* 2013;**5**.

Freire-de-Lima CG, Nascimento DO, Soares MB *et al.* Uptake of apoptotic cells drives the growth of a pathogenic trypanosome in macrophages. *Nature* 2000;**403**: 199-203.

Fujimoto I, Takizawa T, Ohba Y *et al.* Co-expression of Fas and Fas-ligand on the surface of influenza virus-infected cells. *Cell Death Differ* 1998;**5**: 426-31.

Gao LY, Abu Kwaik Y. Apoptosis in macrophages and alveolar epithelial cells during early stages of infection by *Legionella pneumophila* and its role in cytopathogenicity. *Infect Immun* 1999;**67**: 862-70.

Geiger O. Lipids and Legionella Virulence. In: Timmis KN (ed.) *Handbook of Hydrocarbon and Lipid Microbiology*. Berlin, Heidelberg: Springer Berlin Heidelberg, 2010, 3195-202.

Ghannoum MA, Rice LB. Antifungal agents: mode of action, mechanisms of resistance, and correlation of these mechanisms with bacterial resistance. *Clin Microbiol Rev* 1999;**12**: 501-17.

Gibellini F, Hunter WN, Smith TK. Biochemical characterization of the initial steps of the Kennedy pathway in *Trypanosoma brucei*: the ethanolamine and choline kinases. *Biochem J* 2008;**415**: 135-44.

Gibellini F, Hunter WN, Smith TK. The ethanolamine branch of the Kennedy pathway is essential in the bloodstream form of *Trypanosoma brucei*. *Mol Microbiol* 2009;**73**: 826-43.

Gibellini F, Smith TK. The Kennedy pathway--De novo synthesis of phosphatidylethanolamine and phosphatidylcholine. *IUBMB Life* 2010;**62**: 414-28.

Giles DK, Hankins JV, Guan Z *et al.* Remodelling of the *Vibrio cholerae* membrane by incorporation of exogenous fatty acids from host and aquatic environments. *Mol Microbiol* 2011;**79**: 716-28.

Goren MB, Brokl O, Schaefer WB. Lipids of putative relevance to virulence in *Mycobacterium tuberculosis*: correlation of virulence with elaboration of sulfatides and strongly acidic lipids. *Infect Immun* 1974;**9**: 142-9.

Goth SR, Stephens RS. Rapid, transient phosphatidylserine externalization induced in host cells by infection with *Chlamydia* spp. *Infect Immun* 2001;**69**: 1109-19.

Gupta N, Hartmann A, Lucius R *et al.* The obligate intracellular parasite *Toxoplasma gondii* secretes a soluble phosphatidylserine decarboxylase. *J Biol Chem* 2012;**287**: 22938-47.

Ham H, Sreelatha A, Orth K. Manipulation of host membranes by bacterial effectors. *Nat Rev Microbiol* 2011;**9**: 635-46.

Harp JR, Saito HE, Bourdon AK *et al.* Exogenous Fatty Acids Protect *Enterococcus faecalis* from Daptomycin-Induced Membrane Stress Independently of the Response Regulator LiaR. *Appl Environ Microbiol* 2016;**82**: 4410-20.

Hartmann A, Hellmund M, Lucius R *et al.* Phosphatidylethanolamine synthesis in the parasite mitochondrion is required for efficient growth but dispensable for survival of *Toxoplasma gondii*. *J Biol Chem* 2014;**289**: 6809-24.

Hasim S, Allison DP, Retterer ST *et al.* beta-(1,3)-Glucan Unmasking in Some *Candida albicans* Mutants Correlates with Increases in Cell Wall Surface Roughness and Decreases in Cell Wall Elasticity. *Infect Immun* 2017;**85**.

Heikinheimo L, Somerharju P. Translocation of phosphatidylthreonine and -serine to mitochondria diminishes exponentially with increasing molecular hydrophobicity. *Traffic* 2002;**3**: 367-77.

Henry SA, Kohlwein SD, Carman GM. Metabolism and regulation of glycerolipids in the yeast *Saccharomyces cerevisiae*. *Genetics* 2012;**190**: 317-49.

Hoekstra D, van der Laan JW, de Leij L *et al.* Release of outer membrane fragments from normally growing *Escherichia coli*. *Biochim Biophys Acta* 1976;**455**: 889-99.

Horstman AL, Kuehn MJ. Enterotoxigenic *Escherichia coli* secretes active heat-labile enterotoxin via outer membrane vesicles. *J Biol Chem* 2000;**275**: 12489-96.

Huang W, Liao G, Baker GM *et al.* Lipid Flippase Subunit Cdc50 Mediates Drug Resistance and Virulence in Cryptococcus neoformans. *MBio* 2016;**7**.

Hube B. From commensal to pathogen: stage- and tissue-specific gene expression of *Candida albicans*. *Curr Opin Microbiol* 2004;**7**: 336-41.

Ivanova PT, Milne SB, Brown HA. Identification of atypical ether-linked glycerophospholipid species in macrophages by mass spectrometry. *J Lipid Res* 2010;**51**: 1581-90.

Jain M, Petzold CJ, Schelle MW *et al.* Lipidomics reveals control of *Mycobacterium tuberculosis* virulence lipids via metabolic coupling. *Proc Natl Acad Sci U S A* 2007;**104**: 5133-8.

Jemielity S, Wang JJ, Chan YK *et al.* TIM-family proteins promote infection of multiple enveloped viruses through virion-associated phosphatidylserine. *PLoS Pathog* 2013;**9**: e1003232.

Kanfer J, Kennedy EP. Metabolism and Function of Bacterial Lipids. Ii. Biosynthesis of Phospholipids in *Escherichia coli*. *J Biol Chem* 1964;**239**: 1720-6.

Kennedy EP, Weiss SB. The function of cytidine coenzymes in the biosynthesis of phospholipides. *J Biol Chem* 1956;**222**: 193-214.

Korotkova N, Piton J, Wagner JM *et al.* Structure of EspB, a secreted substrate of the ESX-1 secretion system of *Mycobacterium tuberculosis*. *J Struct Biol* 2015;**191**: 236-44.

Kuge O, Nishijima M. Phosphatidylserine synthase I and II of mammalian cells. *Biochim Biophys Acta* 1997;**1348**: 151-6.

Kulkarni HM, Jagannadham MV. Biogenesis and multifaceted roles of outer membrane vesicles from Gram-negative bacteria. *Microbiology* 2014;**160**: 2109-21.

Kulp A, Kuehn MJ. Biological functions and biogenesis of secreted bacterial outer membrane vesicles. *Annu Rev Microbiol* 2010;**64**: 163-84.

Laulagnier K, Motta C, Hamdi S *et al.* Mast cell- and dendritic cell-derived exosomes display a specific lipid composition and an unusual membrane organization. *Biochem J* 2004;**380**: 161-71.

Lyons CN, White TC. Transcriptional analyses of antifungal drug resistance in *Candida albicans*. *Antimicrob Agents Chemother* 2000;**44**: 2296-303.

Maccallum DM, Desbois AP, Coote PJ. Enhanced efficacy of synergistic combinations of antimicrobial peptides with caspofungin versus *Candida albicans* in insect and murine models of systemic infection. *Eur J Clin Microbiol Infect Dis* 2013.

Mahan MJ, Heithoff DM, Sinsheimer RL *et al.* Assessment of bacterial pathogenesis by analysis of gene expression in the host. *Annu Rev Genet* 2000;**34**: 139-64.

Manocha MS, San-Blas G, Centeno S. Lipid composition of *Paracoccidioides brasiliensis*: possible correlation with virulence of different strains. *J Gen Microbiol* 1980;**117**: 147-54.

Mao C, Wadleigh M, Jenkins GM *et al.* Identification and characterization of *Saccharomyces cerevisiae* dihydrosphingosine-1-phosphate phosphatase. *J Biol Chem* 1997;**272**: 28690-4.

Menon AK, Eppinger M, Mayor S *et al.* Phosphatidylethanolamine is the donor of the terminal phosphoethanolamine group in trypanosome glycosylphosphatidylinositols. *Embo J* 1993;**12**: 1907-14.

Menon AK, Stevens VL. Phosphatidylethanolamine is the donor of the ethanolamine residue linking a glycosylphosphatidylinositol anchor to protein. *J Biol Chem* 1992;**267**: 15277-80.

Mirucki CS, Abedi M, Jiang J *et al.* Biologic activity of porphyromonas endodontalis complex lipids. *J Endod* 2014;**40**: 1342-8.

Mishra NN, Prasad T, Sharma N *et al.* Pathogenicity and drug resistance in *Candida albicans* and other yeast species. A review. *Acta Microbiol Immunol Hung* 2007;**54**: 201-35.

Mishra P, Bolard J, Prasad R. Emerging role of lipids of *Candida albicans*, a pathogenic dimorphic yeast. *Biochim Biophys Acta* 1992;**1127**: 1-14.

Mitoma J, Kasama T, Furuya S *et al.* Occurrence of an unusual phospholipid, phosphatidyl-L-threonine, in cultured hippocampal neurons. Exogenous L-serine is required for the synthesis of neuronal phosphatidyl-L-serine and sphingolipids. *J Biol Chem* 1998;**273**: 19363-6.

Moller-Tank S, Kondratowicz AS, Davey RA *et al.* Role of the phosphatidylserine receptor TIM-1 in enveloped-virus entry. *J Virol* 2013;**87**: 8327-41.

Moser R, Aktas M, Fritz C *et al.* Discovery of a bifunctional cardiolipin/phosphatidylethanolamine synthase in bacteria. *Mol Microbiol* 2014;**92**: 959-72.

Moyes DL, Wilson D, Richardson JP *et al. Candida*lysin is a fungal peptide toxin critical for mucosal infection. *Nature* 2016;**532**: 64-8.

Muller FD, Beck S, Strauch E *et al.* Bacterial predators possess unique membrane lipid structures. *Lipids* 2011;**46**: 1129-40.

Murata-Kamiya N, Kikuchi K, Hayashi T *et al. Helicobacter pylori* exploits host membrane phosphatidylserine for delivery, localization, and

pathophysiological action of the CagA oncoprotein. *Cell Host Microbe* 2010;**7**: 399-411.

Nakajima M, DeChavigny A, Johnson CE *et al.* Suramin. A potent inhibitor of melanoma heparanase and invasion. *J Biol Chem* 1991;**266**: 9661-6.

Nielsen HS. Variation in Lipid Content of Strains of *Histoplasma capsulatum* Exhibiting Different Virulence Properties for Mice. *J Bacteriol* 1965;**91**: 273 - 7.

Oliveira DL, Freire-de-Lima CG, Nosanchuk JD *et al.* Extracellular vesicles from Cryptococcus neoformans modulate macrophage functions. *Infect Immun* 2010;**78**: 1601-9.

Pierrotti LC, Baddour LM. Fungal endocarditis, 1995-2000. *Chest* 2002;**122**: 302-10.

Pulido SA, Nguyen VH, Alzate JF *et al.* Insights into the phosphatidylcholine and phosphatidylethanolamine biosynthetic pathways in *Leishmania* parasites and characterization of a choline kinase from *Leishmania* infantum. *Comp Biochem Physiol B Biochem Mol Biol* 2017;**213**: 45-54.

Raetz CR, Dowhan W. Biosynthesis and function of phospholipids in *Escherichia coli*. *J Biol Chem* 1990;**265**: 1235-8.

Rakotomanga M, Saint-Pierre-Chazalet M, Loiseau PM. Alteration of fatty acid and sterol metabolism in miltefosine-resistant *Leishmania donovani* promastigotes and consequences for drug-membrane interactions. *Antimicrob Agents Chemother* 2005;**49**: 2677-86.

Ramakrishnan S, Serricchio M, Striepen B *et al.* Lipid synthesis in protozoan parasites: a comparison between kinetoplastids and apicomplexans. *Prog Lipid Res* 2013;**52**: 488-512.

Rella A, Farnoud AM, Del Poeta M. Plasma membrane lipids and their role in fungal virulence. *Prog Lipid Res* 2016;**61**: 63-72.

Riekhof WR, Voelker DR. Uptake and utilization of lyso-phosphatidylethanolamine by *Saccharomyces cerevisiae*. *J Biol Chem* 2006;**281**: 36588-96.

Riekhof WR, Wu J, Gijon MA *et al.* Lysophosphatidylcholine metabolism in *Saccharomyces cerevisiae*: the role of P-type ATPases in transport and a broad specificity acyltransferase in acylation. *J Biol Chem* 2007a;**282**: 36853-61.

Riekhof WR, Wu J, Jones JL *et al.* Identification and characterization of the major lysophosphatidylethanolamine acyltransferase in *Saccharomyces cerevisiae*. *J Biol Chem* 2007b;**282**: 28344-52.

Rodrigues ML, Nakayasu ES, Oliveira DL *et al.* Extracellular vesicles produced by Cryptococcus neoformans contain protein components associated with virulence. *Eukaryot Cell* 2008;**7**: 58-67.

Roier S, Blume T, Klug L *et al.* A basis for vaccine development: Comparative characterization of *Haemophilus influenzae* outer membrane vesicles. *Int J Med Microbiol* 2015;**305**: 298-309.

Saba JD, Nara F, Bielawska A *et al.* The BST1 gene of *Saccharomyces cerevisiae* is the sphingosine-1-phosphate lyase. *J Biol Chem* 1997;**272**: 26087-90.

Saito HE, Harp JR, Fozo EM. Incorporation of exogenous fatty acids protects *Enterococcus faecalis* from membrane-damaging agents. *Appl Environ Microbiol* 2014;**80**: 6527-38.

Sant DG, Tupe SG, Ramana CV *et al.* Fungal cell membrane-promising drug target for antifungal therapy. *J Appl Microbiol* 2016;**121**: 1498-510.

Sarantis H, Grinstein S. Subversion of phagocytosis for pathogen survival. *Cell Host Microbe* 2012;**12**: 419-31.

Seabra SH, de Souza W, Damatta RA. *Toxoplasma gondii* exposes phosphatidylserine inducing a TGF-beta1 autocrine effect orchestrating macrophage evasion. *Biochem Biophys Res Commun* 2004;**324**: 744-52.

Semiramoth N, Gleizes A, Turbica I *et al.* Afa/Dr-expressing, diffusely adhering *Escherichia coli* strain C1845 triggers F1845 fimbria-dependent phosphatidylserine externalization on neutrophil-like differentiated PLB-985 cells through an apoptosis-independent mechanism. *Infect Immun* 2010;**78**: 2974-83.

Serran-Aguilera L, Denton H, Rubio-Ruiz B *et al. Plasmodium falciparum* Choline Kinase Inhibition Leads to a Major Decrease in Phosphatidylethanolamine Causing Parasite Death. *Sci Rep* 2016;**6**: 33189.

Sharpe SW, Kuehn MJ, Mason KM. Elicitation of epithelial cell-derived immune effectors by outer membrane vesicles of nontypeable *Haemophilus influenzae*. *Infect Immun* 2011;**79**: 4361-9.

Shea JM, Del Poeta M. Lipid signaling in pathogenic fungi. *Curr Opin Microbiol* 2006;**9**: 352-8.

Signorell A, Rauch M, Jelk J *et al.* Phosphatidylethanolamine in *Trypanosoma brucei* is organized in two separate pools and is synthesized exclusively by the Kennedy pathway. *J Biol Chem* 2008;**283**: 23636-44.

Soares MM, King SW, Thorpe PE. Targeting inside-out phosphatidylserine as a therapeutic strategy for viral diseases. *Nat Med* 2008;**14**: 1357-62.

Sohlenkamp C, de Rudder KE, Geiger O. Phosphatidylethanolamine is not essential for growth of *Sinorhizobium meliloti* on complex culture media. *J Bacteriol* 2004;**186**: 1667-77.

Spore P. One Thousand Magical Herbs and Fungi. 1408.

Subra C, Laulagnier K, Perret B *et al.* Exosome lipidomics unravels lipid sorting at the level of multivesicular bodies. *Biochimie* 2007;**89**: 205-12.

Sun XL, Zhang J, Wang GG *et al.* Comparison of Characteristics and Short-Term Outcome From Fungal Infective Endocarditis in Prosthetic Valve Endocarditis Versus Native Valve Endocarditis. *Am J Cardiol* 2013.

Tashiro Y, Inagaki A, Shimizu M *et al.* Characterization of phospholipids in membrane vesicles derived from Pseudomonas aeruginosa. *Biosci Biotechnol Biochem* 2011;**75**: 605-7.

Tasseva G, Bai HD, Davidescu M *et al.* Phosphatidylethanolamine deficiency in Mammalian mitochondria impairs oxidative phosphorylation and alters mitochondrial morphology. *J Biol Chem* 2013;**288**: 4158-73.

Thiele OW, Kehr W. [The "free" lipids of *Brucella abortus* Bang. Concerning the neutral lipids]. *Eur J Biochem* 1969;**9**: 167-75.

Tilney LG, Harb OS, Connelly PS *et al.* How the parasitic bacterium *Legionella pneumophila* modifies its phagosome and transforms it into rough ER: implications for conversion of plasma membrane to the ER membrane. *J Cell Sci* 2001;**114**: 4637-50.

Tripathi A, Gupta CM. Transbilayer translocation of membrane phosphatidylserine and its role in macrophage invasion in *Leishmania* promastigotes. *Mol Biochem Parasitol* 2003;**128**: 1-9.

Tyhach RJ, Hawrot E, Satre M *et al.* Increased synthesis of phosphatidylserine decarboxylase in a strain of *Escherichia coli* bearing a hybrid plasmid. Altered association of enzyme with the membrane. *J Biol Chem* 1979;**254**: 627-33.

Upreti HB, Rawat DS, Das SK. Virulence, capsule size and lipid composition interrelation of Cryptococcus neoformans. *Microbiologica* 1984;**7**: 371-4.

Vallejo MC, Nakayasu ES, Longo LV *et al.* Lipidomic analysis of extracellular vesicles from the pathogenic phase of *Paracoccidioides brasiliensis*. *PLoS One* 2012;**7**: e39463.

van Zandbergen G, Bollinger A, Wenzel A *et al. Leishmania* disease development depends on the presence of apoptotic promastigotes in the virulent inoculum. *Proc Natl Acad Sci U S A* 2006;**103**: 13837-42.

van Zandbergen G, Solbach W, Laskay T. Apoptosis driven infection. *Autoimmunity* 2007;**40**: 349-52.

Vance JE. Phospholipid synthesis and transport in mammalian cells. *Traffic* 2015;**16**: 1-18.

Vance JE, Steenbergen R. Metabolism and functions of phosphatidylserine. *Prog Lipid Res* 2005;**44**: 207-34.

Vanlandschoot P, Leroux-Roels G. Viral apoptotic mimicry: an immune evasion strategy developed by the hepatitis B virus? *Trends Immunol* 2003;**24**: 144-7.

Wanderley JL, Moreira ME, Benjamin A *et al.* Mimicry of apoptotic cells by exposing phosphatidylserine participates in the establishment of amastigotes of *Leishmania* (L) amazonensis in mammalian hosts. *J Immunol* 2006;**176**: 1834-9.

Wanderley JL, Pinto da Silva LH, Deolindo P *et al.* Cooperation between apoptotic and viable metacyclics enhances the pathogenesis of *Leishmania*sis. *PLoS One* 2009;**4**: e5733.

Wandler AM, Parthasarathy R, Guillemin K. A greasy foothold for *Helicobacter pylori*. *Cell Host Microbe* 2010;**7**: 338-9.

Wessel M, Klusener S, Godeke J *et al.* Virulence of Agrobacterium tumefaciens requires phosphatidylcholine in the bacterial membrane. *Mol Microbiol* 2006;**62**: 906-15.

Wheeler RT, Fink GR. A drug-sensitive genetic network masks fungi from the immune system. *PLoS Pathog* 2006;**2**: e35.

Wheeler RT, Kombe D, Agarwala SD *et al.* Dynamic, morphotype-specific *Candida albicans* beta-glucan exposure during infection and drug treatment. *PLoS Pathog* 2008;**4**: e1000227.

Wolf JM, Espadas J, Luque-Garcia J *et al.* Lipid Biosynthetic Genes Affect *Candida albicans* Extracellular Vesicle Morphology, Cargo, and Immunostimulatory Properties. *Eukaryot Cell* 2015;**14**: 745-54.

Yao J, Rock CO. Exogenous fatty acid metabolism in bacteria. *Biochimie* 2017.

Zhang K, Pompey JM, Hsu FF *et al.* Redirection of sphingolipid metabolism toward de novo synthesis of ethanolamine in *Leishmania*. *Embo J* 2007;**26**: 1094-104.

CHAPTER I

ROLE OF PHOSPHATIDYLSERINE SYNTHASE IN SHAPING THE PHOSPHOLIPIDOME OF *CANDIDA ALBICANS*

A version of this chapter was originally published by Chelsi D. Cassilly, Abigail T. Farmer, Anthony E. Montedonico, Terry K. Smith, Shawn R. Campagna, and Todd B. Reynolds.

Chelsi D. Cassilly, Abigail T. Farmer, Anthony E. Montedonico, Terry K. Smith, Shawn R. Campagna, Todd B. Reynolds “Role of Phosphatidylserine synthase in shaping the phospholipidome of *Candida albicans*.” *FEMS Yeast Research* 17 (2017).

This article was not revised for inclusion in the present dissertation. The author contributions are as follows: Conceived and designed the experiments: CDC TBR SRC. Performed the experiments: CDC ATF AEM TKS. Analyzed the data: CDC TBR TKS ATF SRC. Contributed reagents/materials/analysis tools: TBR SRC TKS. Wrote the paper: TBR CDC ATF TKS SRC.

Abstract

Phosphatidylserine (PS) synthase (Cho1p) and the PS decarboxylase enzymes (Psd1p and Psd2p), which synthesize PS and phosphatidylethanolamine (PE), respectively, are crucial for *Candida albicans* virulence. Mutations that disrupt these enzymes, which are part of the cytidyldiphosphate-diacylglycerol (CDP-DAG) pathway (i.e. de novo pathway), utilized for phospholipid synthesis, compromise virulence. Understanding how losses of PS and/or PE synthesis

pathways affect the phospholipidome of *Candida* is important for fully understanding how these enzymes impact virulence. The *cho1Δ/Δ* and psd1Δ/Δ *psd2Δ/Δ* mutations cause similar changes in levels of phosphatidic acid (PA), phosphatidylglycerol (PG), phosphatidylinositol (PI), and PS. However, only slight changes were seen in PE and phosphatidylcholine (PC). This finding suggests that the alternative mechanism for making PE and PC, the Kennedy Pathway, can compensate for loss of the de novo synthesis pathway. *C. albicans* Cho1p, the lipid biosynthetic enzyme with the most potential as a drug target, has been biochemically characterized, and analysis of its substrate specificity and kinetics reveal that these are similar to those previously published for *Saccharomyces cerevisiae* Cho1p.

Introduction

Fungi of the genus *Candida* are opportunistic pathogens known to cause vulvovaginal, oral, and invasive bloodstream infections in humans. Invasive infections are the most serious, with a mortality rate around 30% (Morrell, *et al*. 2005, Wisplinghoff, *et al*. 2004). Currently, there are three main antifungal classes used to treat bloodstream infections of *C. albicans*, the species that causes the majority of these infections (Pfaller, *et al*. 2012). These therapies include azoles (e.g. fluconazole), echinocandins (e.g. caspofungin), and polyenes (amphotericin B). Unfortunately, these drugs have limited effectiveness due to documented cases of azole and echinocandin resistance (Mishra, *et al*.

2007), the nephrotoxicity of amphotericin B (Ghannoum and Rice 1999, Holeman and Einstein 1963), and the requirement for intravenous administration of both amphotericin B and caspofungin. Furthermore, the recent rise in patients that are immunocompromised puts more people at risk every year (Low and Rotstein 2011), while also dramatically increasing healthcare costs (Mishra, *et al*. 2007). As a result, it is of utmost importance to find novel antifungals to treat *C. albicans* potently and effectively.

Phospholipids are crucial components of biological membranes in both prokaryotes and eukaryotes. The phospholipidome of *C. albicans* is made up mostly of phosphatidylcholine (PC), phosphatidylethanolamine (PE), phosphatidylserine (PS), phosphatidylinositol (PI), phosphatidylglycerol (PG), and cardiolipin (CL) (Singh, *et al*. 2012). *C. albicans* has a *de novo* method for producing phospholipids, which involves the conversion of cytidine diphosphate-diacylglycerol (CDP-DAG) into PI, PG, and PS (Fig. 1.1). Although PI, PG, and PS can be end products; PG and PS can be further modified to form CL and PE, respectively, and PE can subsequently be methylated to produce PC. *C. albicans* also utilizes exogenously provided ethanolamine and choline to produce PE and PC via the Kennedy pathway (Chen, *et al*. 2010, Gibellini and Smith 2010, Henry, *et al*. 2012).

Previous studies have identified the PS synthase (Cho1p) as a potential drug target in *Candida albicans* (Braun, *et al*. 2005, Chen, *et al*. 2010). Studies have been done on the enzymology and lipid profiles associated with PS

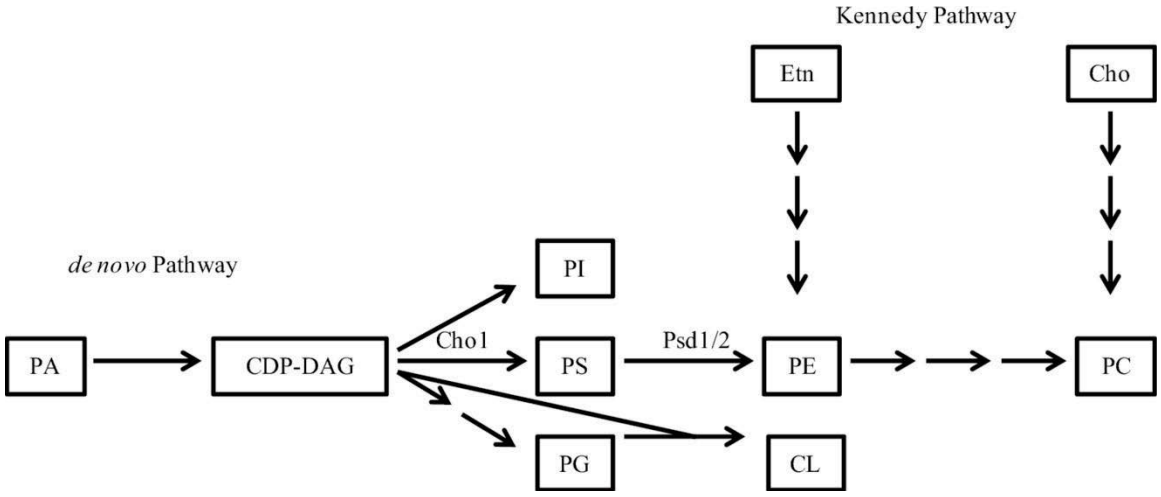

Figure 1. 1 Phospholipid Biosynthesis Pathways in *C. albicans.*
Canidida albicans phospholipid biosynthesis occurs via both an endogenous pathway, the de novo pathway and an exogenous pathway, the Kennedy pathway. The precursors for producing the most common phospholipids are PA and CDP-DAG. CDP-DAG is then converted into PI, PS or PG. The endogenously produced PS can then be decarboxylated via Psd1 or Psd2 (Psd1/2) into PE and then further methylated into PC. In the Kennedy pathway, exogenous ethanolamine (Etn) and/or choline (Cho) are brought into the cell and converted into PE and PC. PG and CDP-DAG can be combined to generate CL. Abbreviations: PA, phosphatidic acid; CDP-DAG, cytidine diphosphate-diacylglycerol; PI, phosphatidylinositol; PS, phosphatidylserine; PG, phosphatidylglycerol; PE, phosphatidylethanolamine; CL, cardiolipin; PC, phosphatidylcholine.

synthase in *S. cerevisiae* (Bae-Lee and Carman 1984), but little characterization of the orthologous enzyme or its effects on lipid profiles in *C. albicans* has been performed. Here we report the phospholipidome of the *Candida albicans cho1Δ/Δ* and *psd1Δ/Δ psd2Δ/Δ* strains, as well as the enzyme kinetics of *C. albicans* Cho1p, finding both the K_m and V_{max} to be in close agreement with those values reported for *S. cerevisiae* Cho1p (Bae-Lee and Carman 1984). The studies described in this report set the stage for further characterization of these enzymes as drug targets.

Materials and Methods

Strains used

The SC5314 (wild-type) strain of *C. albicans* and mutants used in this study have been previously described in (Chen, *et al*. 2010). These include *cho1Δ/Δ* (YLC337), *cho1Δ/Δ::CHO1* (YLC344), *psd1Δ/Δ* (YLC280), *psd1Δ/Δ::PSD1* (YLC294), *psd2Δ/Δ* (YLC271), *psd2Δ/Δ::PSD2* (YLC290), *psd1Δ/Δ psd2Δ/Δ* (YLC375). The media used to culture strains was YPD (1% yeast extract, 2% peptone, and 2% dextrose).

Lipid Isolation for Mass Spectrometry Analysis

Lipid isolations were adapted from the protocol of (Singh, *et al*. 2010). Cultures were grown overnight, shaking at 30° C in 5 mL of YPD. Cultures were then diluted to 0.4 OD_{600} in 25 mL of YPD and grown for 6 hours, shaking at 30° C.

After the 6 hours, cultures were pelleted and washed twice with PBS. The final pellets were incubated for at least 1 hour at -80° C, then lyophilized overnight. Dry mass was then recorded for normalization and pellets were suspended in 500 µL to 1 mL of PBS. The resulting thick suspension was then transferred to Teflon-capped glass tubes (Pyrex) and 1.5 mL of methanol was added. Two scoops of 150-212 µm sized glass beads (Sigma-Aldrich, St. Louis, MO) were added to each tube. Cells were lysed by vigorous vortexing for 30 seconds punctuated by 30 second incubations on ice. 3 mL of chloroform was added and the solution was vortexed briefly before being transferred to 15 mL glass funnel filtration system (Millipore, Billerica, MA, USA) with 24 mm glass microfibre filters (Whatman). Liquid collected was then poured into a separating funnel and washed with 900 µL of sterile 0.9% NaCl. The mixture was allowed to sit and separate for at least 5 minutes, or until adequate separation of the organic and aqueous layers was observed. The lower organic layer only was collected carefully into fresh Teflon-capped glass tubes. The organic layer was then dried under nitrogen gas until completely dry and stored at -20°C. Immediately before mass spectrometric analysis, the lipid extracts were resuspended in 300uL of 9:1 methanol:chloroform (v/v).

Mass Spectrometry Lipidomics

Lipid extracts were separated on a Kinetex HILIC column (150 mm x 2.1 mm, 2.6 µm: (Phenomenex, Torrance, CA, USA) connected to a Ultimate 3000 UltraHigh

Performance Liquid Chromatograph (UHPLC) with autosampler and an Exactive benchtop Orbitrap mass spectrometer (MS) (Thermo Fisher Scientific, San Jose, CA) equipped with a electrospray ionization (ESI) probe. The column oven temperature was maintained at 25°C, and the temperature of the autosampler was set to 4°C. For each analysis, 10 μL was injected onto the column. Separations ran for 35 minutes at a UHPLC flow rate of 0.2 mL/min with mobile phase A and B consisting of 10 mM aqueous ammonium formate pH 3 and 10 mM ammonium formate pH 3 in 93% ACN (v/v), respectively. The gradient started at 100% B and was altered based on the following profile: *t* = 0 minutes, 100% B; *t* = 1 minute, 100% B; *t* = 15 minutes, 81% B, 29% A; *t* = 15.1 minutes, 48% B, 52% A; *t* = 25 in, 48% B, 52% A; *t* = 25.1 minutes, 100% B, *t* = 35 minutes, 100% B. The same LC conditions and buffers were used for all MS experiments described below.

The MS spray voltage was set to 4 kV, and the heated capillary temperature was set at 350°C. The sheath and auxiliary gas flow rates were set to 25 units and 10 units, respectively. These conditions were held constant for both positive and negative ionization mode acquisitions, which were both performed for every sample. External mass calibration was accomplished using the standard calibration mixture and protocol from the manufacturer approximately every 2 days. For full scan profiling experiments, the MS was run with resolution of 140,000 with a scan range of 113-1700 *m/z*. For lipid identification studies, HCD fragmentation experiments were run. These

experiments were performed by alternating between full scan acquisitions and all ion fragmentation HCD scans. Samples were analyzed in both positive and negative mode, and full scan settings were the same as listed above. For the all ion fragmentation scans, the resolution was 140,000 with a scan range of 113-1700 *m/z*. The normalized collision energy was 30eV, and a stepped collision energy algorithm of 50% was used. Full scan MS data was evaluated using Maven software (Melamud, *et al*. 2010), and lipid classes were identified by their fragments using the Xcalibur software package (Thermo Fisher Scientific, San Jose, CA) and information from the LIPID MAPS initiative (Fahy, *et al*. 2007).

Lipid species were verified using retention times, high mass accuracy, and fragmentation data. Internal standards were not used in this study; therefore, the relative amounts of each phospholipid species are presented. Inter-class comparisons are possible, although some approximation of the relative intensities is inherent due to differing ionization efficiencies among lipids with different acyl chain lengths. Adequate separation of phospholipids was seen (data not shown) (Cassilly *et al*., 2017).

Phosphatidylserine Synthase Assay

This procedure was done as previously described with minor alterations (Bae-Lee and Carman 1984, Cassilly, *et al*. 2016, Matsuo, *et al*. 2007). Cultures were grown over night and then diluted into 1 L YPD, to approximately 0.1 OD_{600}/mL. These cultures were shaken at 30°C for 6 to 10 hours. Cells were then

harvested by centrifugation at 6,000 xg for 20 minutes. Pellets were then transferred to 50 mL conical tubes and washed with water and re-pelleted. Supernatant was removed and the wet weight of the samples was taken. Cell pellets were stored overnight in -80°C. The following day, a cold mixture of 0.1 M Tris-Cl pH 7.5, 5 mM β-mercaptoethanol (BME), 10% glycerol, and protease inhibitors (phenylmethylsuphonylfluoride (PMSF), leupeptin, and pepstatin) was added to the frozen pellets (1mL/g [wet weight]) and allowed to thaw on ice. Cells were lysed using a either a French Press (three passes at approximately 13,000 lb/in^2) or using osmotic lysis (Graham, *et al*. 1994). The homogenate was centrifuged at 4°C for 5 minutes at 3,000 rpm to clear unbroken cells and heavy material. Supernatant was then spun again at 27,000 g for 10 minutes at 4°C. For some experiments, the resulting supernatant was then spun at 100,000 g to collect the lower density membranes. Pellets were resuspended in 500 µL to 1 mL of 0.1 M Tris-Cl pH 7.5, 5 mM β-mercaptoethanol (BME), 10% glycerol, and protease inhibitors. This mixture was aliquoted into microcentrifuge tubes and homogenized to break apart clumps, keeping on ice as much as possible. Total crude protein concentration was determined using a Bradford Assay. The optimal assay mixture contained 50 mM Tris-HCl pH 7.5, 0.1% Triton X-100, 0.5 mM $MnCl_2$, 0.1 mM CDP-DAG (Avanti Polar Lipids, Alabaster, AL) added as a suspension in 1% to 20% Triton X-100 and 0.4-0.5 mg protein in a total volume of 0.1 mL. The PS synthase assay was performed by monitoring the incorporation of 0.5 mM L-serine spiked with 5% by volume [^{3}H]-L-serine (~20

Ci/mmol) into the chloroform-soluble product at 37°C for a predetermined amount of time. The reaction was terminated by the addition of 1 mL chloroform: methanol (2:1). Following a low-speed spin, 800 to 1000 µL of the supernatant was removed to a fresh tube and washed with 200 µL 0.9% NaCl. Following a second low-speed spin, 400-500 µL of the chloroform phase was removed to a new tube and washed with 500 µL of chloroform: methanol: 0.9% NaCl (3:48:47). Following a third low-speed spin, 200-300 µL was transferred into scintillation vials (Thermo Fisher Scientific, San Jose, CA). Tubes were left open in the hood until dried fully. The next day, 2.5 mL scintillation fluid was added to each tube and run through the scintillation counter.

Statistical analysis

Graphs were made using GraphPad Prism version 6.04. Unpaired t-tests were used to determine significance between results. The lipidomics data were normalized by dry weight prior to statistical analyses.

Results

Phospholipids synthesized in the de novo pathway are dominated by 34:n species

Phospholipid profiles have previously been generated for the *cho1Δ/Δ, psd1Δ/Δ*, and *psd1Δ/Δ psd2Δ/Δ* mutants using [^{32}P]-labeled phospholipids and thin layer chromatography (TLC) (Chen, *et al*. 2010). However, TLC only reveals levels of

different lipid classes (polar head groups). We wanted to also determine the differences among the individual species (fatty acid composition) within each class. Thus, profiles of the major phospholipid classes were generated via lipidomics from lipids extracted from wild-type, *cho1Δ/Δ*, *cho1Δ/Δ::CHO1*, *psd1Δ/Δ*, *psd1Δ/Δ::PSD1*, *psd2Δ/Δ*, *psd2Δ/Δ::PSD2*, *psd1Δ/Δ psd2Δ/Δ* strains of *C. albicans*. The lipids were analyzed by UHPLC-ESI-MS using the protocol described in methods and materials and adequate separation of standard phospholipids was seen (data not shown). Profiles of PA, CDP-DAG, PI, PG, CL, PS, PE, and PC from three biological replicates were generated and are shown in Figure 1.2. Statistically significant differences for particular species within each class compared to wild-type were seen (data not shown).

In the *cho1Δ/Δ* mutant, which lacks PS synthase (the initial step in the *de novo* pathway, Fig. 1), PS is essentially absent, as expected (Fig. 1.2). The *cho1Δ/Δ::CHO1* reintegrant strain exhibited a modest return of PS levels as compared with the *cho1Δ/Δ* and wild-type strains. The reintegrant strain has only one copy of *CHO1*, so haploinsufficiency is a possible explanation of this result. However, since the level of PS in the reintegrant is only about 37% of the wildtype, one allele may be dominant over the other. *C. albicans* has well-documented heterozygosity, which could account for this result (Eckert and Muhlschlegel 2009).

The distribution of PS species in the wild-type consists predominantly of 34:n species, with 34:2 being the most prevalent (Fig. 1.2). The *psd1Δ/Δ* mutant,

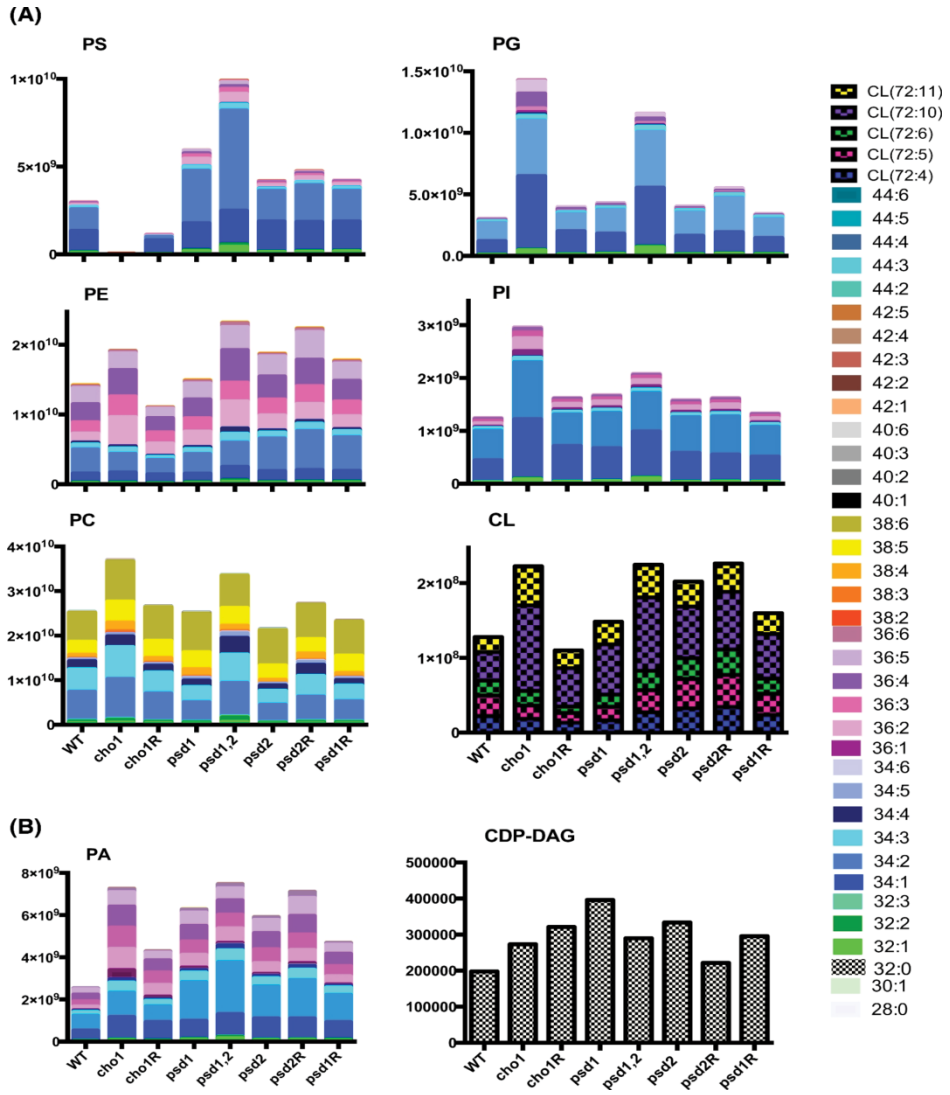

Figure 1. 2. The Phospholipid Species Profiles for the Major Classes of Phospholipids in *C. albicans* Phospholipid Synthesis Mutants

(A) The phospholipid species profiles are shown for the major phospholipid classes of phosphatidylserine (PS), phosphatidylethanolamine (PE), phosphatidylcholine (PC), phosphatidylglycerol (PG), phosphatidylinositol (PI) and cardiolipin (CL). (B) The species profiles detected are shown for the precursor lipids phosphatidic acid (PA) and cytidyldiphosphate-diacylglycerol (CDP-DAG). For each lipid class, a stacked bar graph is used and the species associated with each color is shown in the legend based on the combined carbon content and number of unsaturated bonds within the fatty acid component of the phospholipid. The Y-axis of the graph is the area under the peak for each species based on spectral profiles. The X-axis is the strains, which are as follows: wild-type (WT), cho1 (*cho1Δ/Δ*), psd1 (*psd1Δ/Δ*), psd1, 2 (*psd1Δ/Δ psd2Δ/Δ*), psd2 (*psd2Δ/Δ*), psd2R (*psd2Δ/Δ::PSD2*), psd1R (*psd1Δ/Δ::PSD1*).

which lacks the dominant PS decarboxylase (predicted to be localized to the mitochondria) that converts PS to PE, exhibits an overall increase in PS, but especially of the 34:2 species. A slight increase in PS is seen in the *psd2Δ/Δ* mutant, which lacks the alternative PS decarboxylase (predicted to localize to the Golgi/endosome). The reintegrant strains *psd1Δ/Δ::PSD1* and *psd2Δ/Δ::PSD2* also show slight increases in levels of PS. The *psd1Δ/Δ psd2Δ/Δ* mutant, which lacks all PS decarboxylase activity, has over a 3-fold increase in PS species overall, but individual species are over-represented by 2 to 5 fold. The 34:n species, which were the most abundant in wild-type, are also the most abundant in *psd1Δ/Δ psd2Δ/Δ* and are over-represented by ~5 fold compared to wild-type. However, it appears that all species are decarboxylated to some extent, given that they build up as well.

PE is the direct downstream product of PS decarboxylation (Fig. 1), and loss of PS was expected to result in a sizeable decrease in PE, but surprisingly we saw increases in PE levels in most of our mutants (Fig. 1.2). Most of these changes are not statistically significant in the majority of mutants, including *cho1Δ/Δ* (data not shown), although they are for *psd1Δ/Δ psd2Δ/Δ*. The maintenance of PE levels by the *cho1Δ/Δ* and *psd1Δ/Δ psd2Δ/Δ* mutants is likely due to growing these cultures in YPD, a rich medium containing ethanolamine and choline. Since the *cho1Δ/Δ* and *psd1Δ/Δ psd2Δ/Δ* mutants have no production of PE via the CDP-DAG pathway, it is likely that these mutants compensate through activity from the Kennedy Pathway in order to synthesize

PE. The *psd1Δ/Δ* mutant, which is missing the mitochondrial PS decarboxylase activity, showed wild-type levels of PE, suggesting that the loss of Psd1p was rescued by the redundant function of Psd2p. The *psd2Δ/Δ* strain exhibited an increase in PE, but this was again not statistically significant. The *psd2Δ/Δ::PSD2* strain did have significant increases in many phospholipids, which was unexpected. The *psd1Δ/Δ::PSD1* did not show many significant differences from wild-type. Overall, the majority of PE species in wild-type are of 36:n or 34:n, and even in the *psd1Δ/Δ psd2Δ/Δ* where the changes were significant, this only shifted slightly compared to wild-type.

Since the majority of PS is 34:n in wild-type cells, the Kennedy pathway may account for half of the PE population (34:n) or significant acyl remodeling of PS-derived PE is used to create other species after, or just prior to, decarboxylation. However, since a similar distribution of PE is found in wild-type, *cho1Δ/Δ* (totally lacks PS), and *psd1Δ/Δ psd2Δ/Δ* strains (cannot convert PS to PE), this suggests that most of the 36:n PE is derived from the Kennedy pathway, and the Kennedy pathway also synthesizes 34:n PE efficiently or converts 36:n by acyl remodeling.

Previous studies with *S. cerevisiae* showed an accumulation of PC in the *Sccho1*Δ mutant based upon TLC analysis (Atkinson, *et al*. 1980b). Indeed, our data show an approximately 1.5 fold increase in the level of PC in both the *cho1Δ/Δ* and *psd1Δ/Δ psd2Δ/Δ* mutants when compared to the wild-type (Fig 1.2). The most obvious common relationship between *cho1Δ/Δ* and

psd1Δ/Δ psd2Δ/Δ is that both have a complete loss of *de novo* PE synthesis, which may indicate that this metabolic alteration causes an increase in PC synthesis via the Kennedy pathway. In the *psd1Δ/Δ psd2Δ/Δ* or *cho1Δ/Δ* mutants, PC can be synthesized directly from choline and DAG via the Kennedy pathway or by methylation of Kennedy-pathway-derived PE via the *de novo* pathway (Fig. 1.1). However, from this data it is not possible to determine the level of PC coming directly from Kennedy pathway versus the methylation of Kennedy pathway derived PE to PC. Interestingly, the *cho1Δ/Δ::CHO1* strain, which has only one allele of *CHO1*, has wild-type levels of PC. Loss of PS decarboxylase activity in *psd1Δ/Δ* or *psd2Δ/Δ* mutants also has little effect on PC levels when compared with that of wild-type. Although there is a slight decrease in PC in the *psd2Δ/Δ* mutant, it does not appear to be statistically significant. These findings suggest that the organism strictly controls the production of PC to at least maintain wild-type levels. The majority of PC species are 36:n and 38:n. It is possible that the 36:n PC is formed through the *de novo* methylation of 36:n PE. The 38:n species are probably produced from the importation of exogenous choline. However, there are no striking changes within lipid species across mutant strains to confirm or deny these hypotheses.

Increases in other CDP-DAG derived phospholipids may be caused by an abundance of substrate in the PS synthase and PS decarboxylase mutants

Phosphatidic acid (PA) is the precursor for CDP-DAG (Gibellini, *et al.,* 2010) that is used to produce PS, PG, and PI (Fig. 1.1). The *cho1Δ/Δ* mutant showed a

nearly 3 fold increase in PA levels when compared to wild-type (Fig 1.2). These results were expected because the loss of PS synthesis causes a major blockage in *de novo* phospholipid synthesis, which would in turn lead to a build-up of the precursor molecule PA (substrate for CDP-DAG). This is further supported by the intermediate level of PA in *cho1Δ/Δ::CHO1*, which correlates with the partial return of PS production, and thus increased usage of PA. Varying increases are shown in PA levels within *psd1Δ/Δ* and *psd2Δ/Δ* mutants and their reintegrant strains, again potentially relating back to the build-up of PS in these strains, which translates into a build-up of PA. This is supported by the large increase in PA seen in *psd1Δ/Δ psd2Δ/Δ*, which has no *de novo* PE production, and thus represents a blockage in this biosynthetic pathway.

We also aimed to analyze the levels of CDP-DAG within our mutants and found that we could only detect 32:0 species and that the overall levels of this precursor lipid were extremely low (Fig. 1.2B). This suggests that there is a high turnover of CDP-DAG and that it is rapidly used to produce PS, PI, or PG. Although there was some variability within the CDP-DAG levels, including increases in most of the mutants tested, none of these changes were statistically significant when compared to wild-type. However, the change in CDP-DAG levels within our mutants again could easily be attributed to a back up in the *de novo* synthesis (either a halt of PS production or usage) which causes increases in CDP-DAG levels.

In addition to the precursors, we also looked at the levels of the other two phospholipids produced from CDP-DAG, PI and PG, as well as CL, which is produced from PG (Gibellini, *et al.,* 2010). Both the *cho1Δ/Δ* and the *psd1Δ/Δ psd2Δ/Δ* mutants show increases in PI and PG levels. Where the *cho1Δ/Δ* PI levels increase by around 2.5 fold, the *psd1Δ/Δ psd2Δ/Δ* increase is more modest. For PG we see an increase in both *cho1Δ/Δ* and *psd1Δ/Δpsd2Δ/Δ*, at approximately 5-fold and 4-fold, respectively. These findings could be a result of more CDP-DAG being available for the production of PI and PG due to a blockage of PS synthesis (*cho1Δ/Δ*) or a build-up in PS (*psd1Δ/Δ psd2Δ/Δ*). PI and PG seem to be tightly controlled, however, because in all other mutant and reintegrant strains, the levels return to wild-type. Finally, levels of CL correspond well with the changes in PG within our mutant strains. This indicates that some of the excess PG produced can be further modified to produce CL. These findings correlate well with studies in *S. cerevisiae* and confirm our previous results with TLC (Atkinson, *et al*. 1980b, Chen, *et al*. 2010). Interestingly, as with PS, the most abundant species of PI and PG appear to be 34:n, thus it is possible that most CDP-DAG destined for PS synthesis is 34:n, but our lipidomics yields of CDP-DAG were too low to verify this, and it may be 34:n CDP-DAG is so rapidly processed into other lipids that it is hard to detect at steady-state.

Phosphatidylserine Synthesis in PS synthase and PS decarboxylase mutants

The *psd1Δ/Δ psd2Δ/Δ* mutant exhibits a large increase in PS levels (Fig. 1.2), which is presumed to be caused by decreased decarboxylation of PS to PE. However, it is possible that this is due to increased PS synthase activity instead. This seemed doubtful, but to test this, an *in vitro* PS synthase assay was performed on cellular membranes, which were isolated from cell lysates via a 27,000xg centrifugation step. Additional low density membranes were isolated via a 100,000xg centrifugation step. However, as highly variable results were found in the 100,000xg membrane prep, data was generated from the 27,000xg membranes which provided more consistent results. The assay was used to compare the incorporation of [^{3}H]-serine into membranes upon the addition of CDP-DAG between wild-type, *cho1Δ/Δ*, *cho1Δ/Δ::CHO1*, *psd1Δ/Δ*, *psd1Δ/Δ psd2Δ/Δ*, and *psd1Δ/Δ::PSD1* strains. Wild-type levels of PS synthase activity were seen in the *psd1Δ/Δ* and *psd1Δ/Δ psd2Δ/Δ* strains, indicating that these strains have similar enzyme activities as the wild-type organism (Fig. 1.3). Thus, the excess PS in the *psd1Δ/Δ psd2Δ/Δ* mutant is likely a product of the loss of PS decarboxylase activity and build-up of substrate.

As expected from this assay, the *cho1Δ/Δ* mutant exhibited no PS synthase activity. However, the *cho1Δ/Δ::CHO1* reintegrant strain had only about 10% of the activity of the wild-type. This compares with the decreased PS

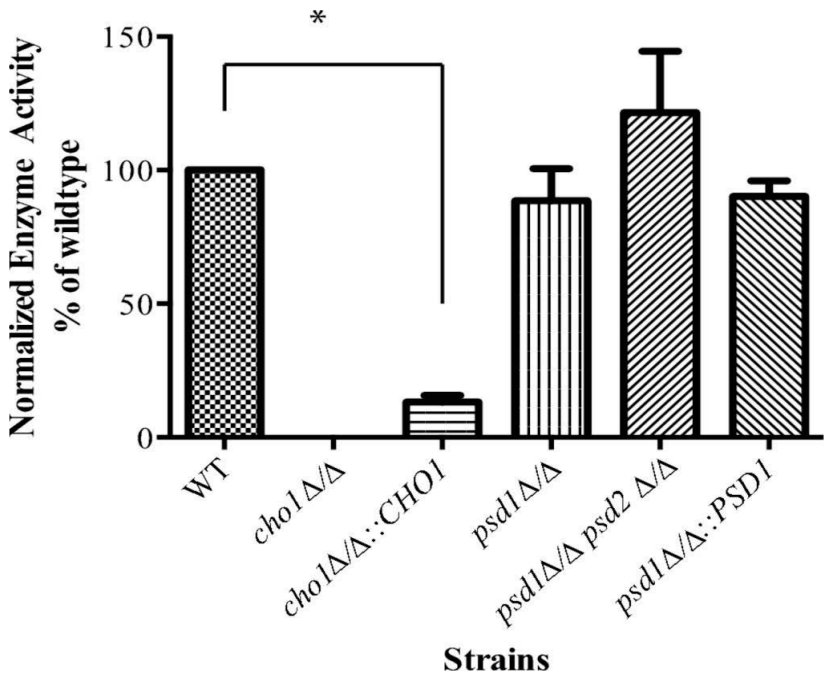

Figure 1. 3. PS Synthase Activity Across Strains
Cho1p activity within different mutant strains of *C. albicans*. Cellular membranes containing Cho1p were isolated and treated with CDP-DAG and [^{3}H]-serine. Activity is measured as counts per minute per milligram of protein. Values are shown as an average of three experiments averaged and normalized to the wild-type (WT) control. $P < 0.0001$.

levels in the reintegrant as measured by lipidomics (Fig. 1.2). Haploinsufficiency may account for this lower activity.

C. albicans Cho1p enzyme kinetics are similar to those reported for *S. cerevisiae*

The wild-type and other strains seemed to have similar PS synthase activity levels, but it was of interest to know more about the enzyme kinetics of *C. albicans* Cho1p, if it is to be considered for potential use as a drug target. The K_m and apparent V_{max} of this enzyme was calculated for both serine and CDP-DAG (Fig. 4). L-serine, where the CDP-DAG was held constant at 0.1 mM, yielded a K_m of 1.2±0.57 mM and an apparent V_{max} of 0.15±0.02 nmole/minute/mg of protein (Fig. 1.4A). For CDP-DAG, where the serine was held constant at 2.5 mM, a K_m of 43.17±19.18 μM and an apparent V_{max} of 0.19±0.023 nmole/minute/mg of protein (Fig. 1.4B) was obtained. Interestingly, the intracellular concentration of serine in *S. cerevisiae* has been estimated to be around 2 mM on average (Hans, *et al*. 2003), which fits well with the K_m for serine. These assays were performed on the crude 27,000xg membranes in order to determine their kinetics within native membranes. These compare relatively closely with what has been reported for *S. cerevisiae* (Bae-Lee and Carman 1984).

To control for the possibility that any similar substrate molecules to serine might give a similar activity, which could cast doubt on the accuracy of the assay,

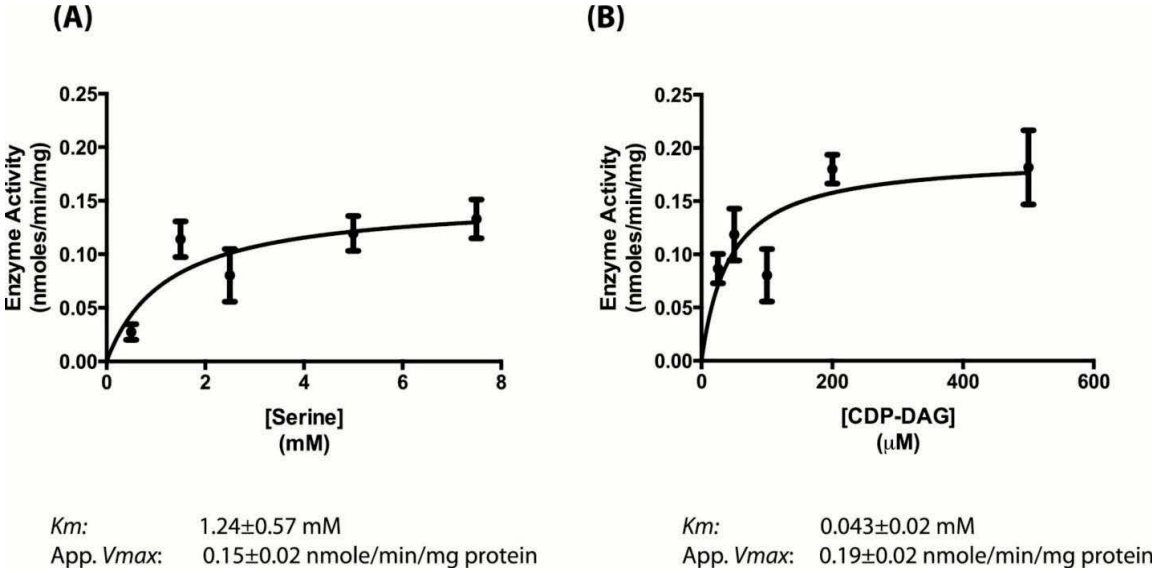

Figure 1. 4. Enzyme Kinetics for Cho1p

The PS synthase assay was performed with varying concentrations of substrate over time courses to generate enzyme kinetics for both substrates. (A) The Michaelis-Menton curve for the l-serine substrate shows a K_m of 1.243 ± 0.5715 mM and an apparent V_{max} of 0.1514 ± 0.02059 nmole/min/mg of protein. (B) The Michaelis-Menton curve for the CDP-DAG substrate shows a K_m of 43.17 ± 19.18 μM and an apparent V_{max} of 0.1919 ± 0.02361 nmole/min/mg of protein.

we determined whether increasing concentrations of cold D-serine or threonine (similar amino acid) could compete with [^{3}H]-L-serine for incorporation into [^{3}H]-PS. Only at the highest concentration of 200 mM (400x) did the cold D-serine show any competition with L-serine (Fig. 1.5). Threonine showed no statistically significant competition with L-serine, even at 200 mM (400x). As a control, cold L-serine eliminated incorporation of [^{3}H]-L-serine at a 10x concentration (5 mM). Thus, this assay would not yield a product with these two similar molecules (D-serine or threonine), thus suggesting that the assay is specifically measuring activity against L-serine.

Discussion

The loss of *de novo* PE synthesis and/or PS synthesis has striking effects on the phospholipidome, which are consistent with what we know from fungal phospholipid metabolism. In particular, the loss of the *de novo* pathway for PS and/or PE synthesis appears to increase the synthesis of other CDP-DAG-dependent phospholipids like PI and PG (Fig. 1.2). Surprisingly, PE and PC levels appear to be buffered against change, presumably by the activity of the Kennedy pathway. The 34:n species are the most prominent forms of PS, and 34:2 in particular is the most actively used substrate by PS decarboxylase enzymes to synthesize PE, and the 34:2 species is also what builds up in PI and PG, which may suggest that either Cho1p preferentially uses 34:2 CDP-DAG, or 34:2 CDP-DAG is what it encounters in its subdomains in the ER.

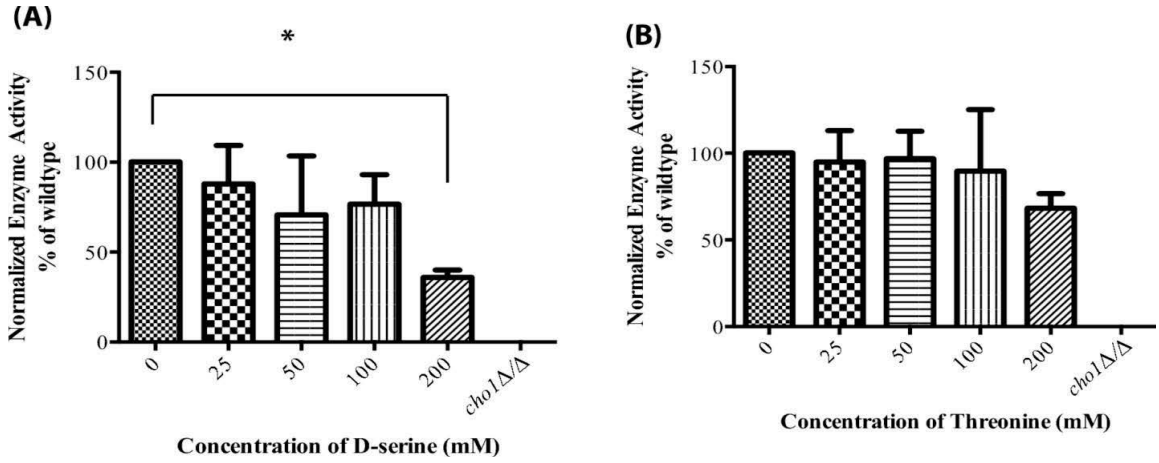

Figure 1. 5. Cho1p Specificity for L-serine.
The PS synthase assay was performed with 0.5 mM [^{3}H]-serine and 0.1 mM CDP-DAG. An excess of d-serine (A) or L-threonine (B) was added at varying concentrations. Only D-serine or L-threonine at concentrations 400-fold that of L-serine show any inhibition in [^{3}H]-PS production. Values are shown as an average of three experiments averaged and normalized to the wild-type control. P = 0.0361.

Finally, our analysis of the enzymology of Cho1p from *C. albicans* reveals it is very similar to *S. cerevisiae*, and that changes in the enzyme activity, for example in the *CHO1* compared to *cho1Δ/Δ::CHO1* strains, seem to correlate with one another rather closely. These analyses set the stage for better understanding how strategies to inhibit *de novo* PS or PE synthesis, which are required for virulence of *C. albicans*, may impact overall lipid profiles and ability to cause disease.

References

Atkinson K, Fogel S, Henry SA. Yeast mutant defective in phosphatidylserine synthesis. *J Biol Chem* 1980;**255**: 6653-61.

Bae-Lee MS, Carman GM. Phosphatidylserine synthesis in *Saccharomyces cerevisiae*. Purification and characterization of membrane-associated phosphatidylserine synthase. *J Biol Chem* 1984;**259**: 10857-62.

Braun BR, van Het Hoog M, d'Enfert C *et al.,* A human-curated annotation of the *Candida albicans* genome. *PLoS Genet* 2005;**1**: 36-57.

Cassilly CD, Maddox MM, Cherian PT *et al.,* SB-224289 Antagonizes the Antifungal Mechanism of the Marine Depsipeptide Papuamide A. *PLoS One* 2016;**11**: e0154932.

Chen YL, Montedonico AE, Kauffman S *et al.,* Phosphatidylserine synthase and phosphatidylserine decarboxylase are essential for cell wall integrity and virulence in *Candida albicans*. *Mol Microbiol* 2010;**75**: 1112-32.

Eckert SE, Muhlschlegel FA. Promoter regulation in *Candida albicans* and related species. *FEMS Yeast Res* 2009;**9**: 2-15.

Fahy E, Sud M, Cotter D *et al.,* LIPID MAPS online tools for lipid research. *Nucleic Acids Res* 2007;**35**: W606-12.

Ghannoum MA, Rice LB. Antifungal agents: mode of action, mechanisms of resistance, and correlation of these mechanisms with bacterial resistance. *Clin Microbiol Rev* 1999;**12**: 501-17.

Gibellini F, Smith TK. The Kennedy pathway--De novo synthesis of phosphatidylethanolamine and phosphatidylcholine. *IUBMB Life* 2010;**62**: 414-28.

Graham TR, Seeger M, Payne GS *et al.,* Clathrin-dependent localization of alpha 1,3 mannosyltransferase to the Golgi complex of *Saccharomyces cerevisiae*. *J Cell Biol* 1994;**127**: 667-78.

Hans MA, Heinzle E, Wittmann C. Free intracellular amino acid pools during autonomous oscillations in *Saccharomyces cerevisiae*. *Biotechnol Bioeng* 2003;**82**: 143-51.

Henry SA, Kohlwein SD, Carman GM. Metabolism and regulation of glycerolipids in the yeast *Saccharomyces cerevisiae*. *Genetics* 2012;**190**: 317-49.

Holeman CW, Jr., Einstein H. The toxic effects of amphotericin B in man. *Calif Med* 1963;**99**: 90-3.

Low CY, Rotstein C. Emerging fungal infections in immunocompromised patients. *F1000 Med Rep* 2011;**3**: 14.

Matsuo Y, Fisher E, Patton-Vogt J *et al.,* Functional characterization of the fission yeast phosphatidylserine synthase gene, pps1, reveals novel cellular functions for phosphatidylserine. *Eukaryot Cell* 2007;**6**: 2092-101.

Melamud E, Vastag L, Rabinowitz JD. Metabolomic analysis and visualization engine for LC-MS data. *Anal Chem* 2010;**82**: 9818-26.

Mishra NN, Prasad T, Sharma N *et al.,* Pathogenicity and drug resistance in *Candida albicans* and other yeast species. A review. *Acta Microbiol Immunol Hung* 2007;**54**: 201-35.

Morrell M, Fraser VJ, Kollef MH. Delaying the empiric treatment of *Candida* bloodstream infection until positive blood culture results are obtained: a potential risk factor for hospital mortality. *Antimicrob Agents Chemother* 2005;**49**: 3640-5.

Pfaller M, Neofytos D, Diekema D *et al.,* Epidemiology and outcomes of candidemia in 3648 patients: data from the Prospective Antifungal Therapy (PATH Alliance(R)) registry, 2004-2008. *Diagn Microbiol Infect Dis* 2012;**74**: 323-31.

Singh A, Prasad T, Kapoor K *et al.,* Phospholipidome of *Candida*: Each Species of *Candida* Has Distinctive Phospholipid Molecular Species. *Omics* 2010;**14**: 665-77.

Singh A, Yadav V, Prasad R. Comparative lipidomics in clinical isolates of *Candida albicans* reveal crosstalk between mitochondria, cell wall integrity and azole resistance. *PLoS One* 2012;**7**: e39812.

Wisplinghoff H, Bischoff T, Tallent SM *et al.,* Nosocomial bloodstream infections in US hospitals: analysis of 24,179 cases from a prospective nationwide surveillance study. *Clin Infect Dis* 2004;**39**: 309-17.

CHAPTER II

SB-224289 ANTAGONIZES THE ANTIFUNGAL MECHANISM OF THE MARINE DEPSIPEPTIDE PAPUAMIDE A

A version of this chapter was originally published by Chelsi D. Cassilly, Marcus M. Maddox, Philip T. Cherian, John J. Bowling, Mark T. Hamann, Richard E. Lee, and Todd B. Reynolds

Chelsi D. Cassilly, Marcus M. Maddox, Philip T. Cherian, John J. Bowling, Mark T. Hamann, Richard E. Lee, Todd B. Reynolds “SB-224289 antagonizes the antifungal mechanism of the marine depsipeptide Papuamide A.” *PLoS One* 11 (2016).

This article was not revised for inclusion in the present dissertation. The author contributions are as follows: Conceived and designed the experiments: CDC REL TBR MMM PTC. Performed the experiments: CDC TBR MMM PTC. Analyzed the data: CDC TBR MMM REL PTC. Contributed reagents/materials/analysis tools: TBR JJB REL MTH. Wrote the paper: TBR CDC REL JJB PTC.

Abstract

In order to expand the repertoire of antifungal compounds a novel, high-throughput phenotypic drug screen targeting fungal phosphatidylserine (PS) synthase (Cho1p) was developed based on antagonism of the toxin papuamide A (Pap-A). Pap-A is a cyclic depsipeptide that binds to PS in the membrane of wild-type *C. albicans* and permeabilizes its plasma membrane, ultimately causing

cell death. Organisms with a homozygous deletion of the *CHO1* gene (*cho1ΔΔ*) do not produce PS and are able to survive in the presence of Pap-A. Using this phenotype (i.e. resistance to Pap-A) as an indicator of Cho1p inhibition, we screened over 5,500 small molecules for Pap-A resistance and identified SB-224289 as a positive hit. SB-224289, previously reported as a selective human 5-HT1B receptor antagonist, also confers resistance to the similar toxin theopapuamide (TPap-A), but not to other cytotoxic depsipeptides tested. Structurally similar molecules and truncated variants of SB-224289 do not confer resistance to Pap-A suggesting that the toxin-blocking ability of SB-224289 is very specific. Further biochemical characterization revealed that SB-224289 does not inhibit Cho1p, indicating that Pap-A resistance is conferred by another undetermined mechanism. Although the mode of resistance is unclear, interaction between SB-224289 and Pap-A or TPap-A suggests this screening assay could be adapted for discovering other compounds which could antagonize the effects of other environmentally- or medically-relevant depsipeptide toxins.

Introduction

Patients with a compromised immune system are prone to develop nosocomial infections which can be fungal, bacterial, parasitic, or viral in nature. *Candida spp.* are pathogenic fungi responsible for the majority of fungal infections arising within hospitals (Mishra, *et al*. 2007, Morrell, *et al*. 2005). Of these, the species

found most often is *Candida albicans* (Papon, *et al*. 2013). This fungus most commonly causes mucosal infections including vaginal infections and oral thrush, but it can also cause life-threatening infections. The most serious of these include fungal endocarditis and systemic bloodstream infections which have mortality rates around or greater than 30% (Baddley, *et al*. 2008, Pfaller and Diekema 2007).

There are currently three primary classes of antifungals used to treat invasive *Candida* infections. The first line defense includes azoles (e.g. fluconazole) and echinocandins (e.g. caspofungin). However, resistance and tolerance to these drugs can lead to treatment failures (Alexander, *et al*. 2013, Dannaoui, *et al*. 2012, Pfaller 2012, Srinivasan, *et al*. 2014). The mainstay of second line defense is the polyene amphotericin B, a drug that must be carefully administered due to its nephrotoxic potential (Ghannoum and Rice 1999, Holeman and Einstein 1963). As a result of drug resistance, poor oral availability, and toxic side effects including drug-drug interactions (Mukherjee, *et al*. 2005), there is a clear need for new antifungal drugs to treat *Candida* infections.

Previously, the fungal phosphatidylserine (PS) synthase (Cho1p) was identified as a promising antifungal drug target for several reasons. First, Cho1p has been demonstrated to be required for *Candida albicans* virulence in a mouse model of systemic infection (Chen, *et al*. 2010). Mice infected with a strain of *C. albicans* where both alleles of the Cho1p gene are deleted (*cho1ΔΔ*) were able to

survive indefinitely, whereas mice infected with the wild-type strain succumbed to infection within two weeks (Chen, *et al*. 2010). Second, the Cho1p enzyme is conserved among many pathogenic fungi (Braun, *et al*. 2005, Chen, *et al*. 2010). Last, Cho1p is absent within mammals (Atkinson, *et al*. 1980b, Braun, *et al*. 2005, Chen, *et al*. 2010, Kuge, *et al*. 1986). Based on these observations, we hypothesized that high affinity inhibitors of Cho1p should render the organism unable to cause infection within a host, be active against a broad range of fungal pathogens, and be highly selective with minimal side effects in mammals.

Based on this hypothesis, we set out to identify inhibitors of this pathway using a cell based high-throughput screening approach. The assay is based on the action of a PS-dependent toxin, papuamide A (Pap-A), which is a cyclic depsipeptide isolated from marine sponges of the genus *Theonella*. Pap-A kills *C. albicans* and other yeasts by binding to PS in the membrane and forming pores that disrupt the integrity of the membrane (Andjelic, *et al*. 2008, Parsons, *et al*. 2006). We wished to exploit the PS-specific nature of Pap-A toxicity and identify compounds that block PS synthesis or alternatively interfere with PS metabolism, by selecting those small molecules that allow *C. albicans* survival in the presence of Pap-A. Thus, the Pap-A killing assay was adapted into a robust 384-well plate screening assay and tested against a reference set of bioactive compounds including many known drugs.

This screen showed a good statistical window and yielded several promising hits. However, we found that Pap-A resistance is not specific enough

to conclude that a compound targets Cho1p, as other mechanisms can be responsible for this protection phenotype. In this study we describe the characterization of a positive hit, SB-224289, which in turn showed interesting and highly specific behavior that blocks Pap-A mediated cellular poisoning.

Materials and Methods

Strains Used

The SC5314 (wild-type) strain of *C. albicans* and mutants used in this study have been previously described (Chen, *et al*. 2010) and are as follows: *cho1*ΔΔ (YLC337), and *cho1*ΔΔ*::CHO1* (YLC344). The media used to culture strains was YPD (1% Bacto yeast extract, 2% Bacto peptone, and 2% dextrose (Thermo Fisher Scientific, San Jose, CA)) (Guthrie 2002).

Compounds

The 5,760 bioactive compound library is a collated compound set of approved drugs (675 compounds) and biologically active compounds that have been documented to interact with wide range of targets (approximately 5095 compounds) including Sigma Aldrich's Library of Pharmacologically Active Compounds (LOPAC), Prestwick, and Microsource compound libraries. The library compounds were all independently verified for purity and identity by UPLC-MS analysis. Papuamide A was obtained from Flintbox in association with David Williams from the University of British Colombia, Canada. SB-224289

(Cat. # 1221), MG-624 (Cat. # 1356), and valinomycin (VA; Cat. # 3373) were ordered from Tocris Bioscience. GMC 2-29 (Cat. # 1080) and SB-216641 (Cat. # 1085) were ordered from Axon MedChem. Staurosporine (CGP 41251) was ordered from Selleckchem. Kahalalide F (KF) was a kind gift from Dr. Fernando Albericio at the Institute for Research in Biomedicine, Barcelona, Spain. Theopapuamide (TPap-A) was provided by Dr. Mark Hamann at University of Mississippi, University, Mississippi, USA. Compounds 2945, 2946, 3047, and 3048 were synthesized as described previously (Gaster, *et al*. 1998). Details of the synthesis and compound characterization data are provided the manuscript (Cassilly *et al*., 2016).

Papuamide A resistance assay

Strains were grown overnight in liquid YPD shaking at 30°C to saturation, and cultures were diluted to 2 x 10^4 cells/ml in YPD. Compounds of interest were diluted to twice the working concentration by serial dilution in a 96 well plate or by preparing separately and adding to the wells directly, in a volume of 37.5 µl of YPD. Then 37.5 µl of cells at 2 x 10^4 cells/ml in YPD were added. Plates were incubated at 37°C for 6 hours or 3 hours depending on the experiment, and then 75 µl of YPD containing depsipeptide (Pap-A at 8 µg/ml, VA at 6 µg/ml, KF at 30 µg/ml, or TPap-A at 12 µg/ml) was added to each well, diluting those concentrations by half. This addition was followed by a 37°C overnight incubation.

Cell survival was measured the next day by fluorescence intensity or optical density. For fluorescence intensity, Alamar Blue (Invitrogen, Waltham, MA) was added to the wells at a 1:10 dilution. Plates were allowed to incubate again at 37°C for 30 minutes to 2 hours until color change was apparent. Fluorescence was then read at excitation 550 nm and emission 590 nm. For optical density, plates were removed from overnight incubation and absorbance was read in a plate reader at a wavelength of 600 nm. All measurements were performed on a Cytation3 BioTek plate reader using Gen 5 software.

High throughput screen for Pap-A resistance

The 5,760 compound library was screened in a total of eighteen 384 well plates (Nunc) at a final concentration of 50-75 μM. Approximately 0.155 μl of compound dissolved in DMSO were inoculated into 10 μl of YPD in each well from ~10 mM stock plates using a BioMek robot with pin tools. Wild-type and *cho1*ΔΔ (positive control strain) were grown in liquid YPD in a 30°C shaker overnight and cultures were diluted to 10^4 cells/ml in YPD, and 10 μl were added to each well of the 384 well plate containing the test compound using a Wellmate. Plates were incubated for 6 hours at 37°C, and then 10 μl of YPD containing 12 μg/ml Pap-A was added to give a final concentration of 4 μg/ml in 30 μl of YPD. Plates were then incubated for another 16 hours at 37°C to allow selection for Pap-A resistance. The following day, cell survival was measured by adding Alamar Blue (Invitrogen, Waltham, MA) at a 1:10 dilution using a Wellmate. Plates were allowed to

incubate again at 37°C for 2 hours. Fluorescence was then read at excitation 550 nm and emission 590 nm on an Envision plate reader (Perkin Elmer, Waltham, MA). In each plate, three of the columns of wells were used as controls. One column contained no compounds and no cells and served as background control. The positive control column contained *cho1ΔΔ* plus Pap-A, as it showed resistance. An additional control was wild-type with no drugs and no Pap-A for maximal wild-type growth. The averaged background readings from the wild-type cells plus compounds in the presence of Pap-A served as the negative control in each plate.

Phosphatidylserine Synthase Assay

This procedure was done as described in (Bae-Lee and Carman 1984, Matsuo, *et al*. 2007) with minor alterations. Cultures were grown overnight and then diluted to approximately 0.1 OD_{600}/ml in 1 L YPD, and were shaken at 30°C for 6 to 10 hours. Cells were harvested by centrifugation at 6,000 x g for 20 minutes. Pellets were then transferred to 50 ml conical tubes and washed with water and re-pelleted. Supernatant was removed and the wet weight of the samples was taken. Cell pellets were stored overnight in -80°C. The following day, a cold mixture of 0.1 M Tris-Cl pH 7.5, 5 mM β-mercaptoethanol (BME), 10% glycerol , and protease inhibitors 1.7 μg/ml PMSF, 1 μg/ml leupeptin, and 1 μg/ml pepstatin (RPI, Corp., Mount Prospect, IL, USA) was added to the frozen pellets (1 ml/g [wet weight]) and allowed to thaw on ice. Cells were lysed using a French press

(three passes at approximately 13,000 lb/in^2). The homogenate was centrifuged at 4°C for 5 minutes at 3,000 rpm to clear unbroken cells and heavy material. Supernatant was then spun again at 27,000 x g for 10 minutes at 4°C. For some experiments, the resulting supernatant was then spun at 100,000 xg to collect the lower density membranes. Pellets were resuspended in 500 µl to 1 ml of 0.1 M Tris-Cl pH 7.5, 5 mM BME, 10% glycerol, and protease inhibitors. This mixture was aliquoted into microcentrifuge tubes and homogenized to break apart clumps, keeping on ice as much as possible. Total crude protein concentration was determined using a Bradford Assay. The optimal assay mixture contained 50 mM Tris-HCl pH 7.5, 0.1% Triton X-100, 0.5 mM $MnCl_2$, 0.1 mM CDP-DAG (Avanti Polar Lipids, Alabaster, AL) added as a suspension in 1% - 20% Triton X-100, and 0.4 - 0.5 mg protein in a total volume of 0.1 ml. SB-224289 and MG-624 were added to the reaction mixture at varying concentrations to monitor their ability to inhibit [^{3}H]-PS production. The PS synthase assay was performed by monitoring the incorporation of 0.5 mM L-serine spiked with 5% [^{3}H]-L-serine (or 0.02 µM) (Cat# ART 0246, ARC, Inc., St. Louis, MO, USA) into the chloroform-soluble product at 37°C for a predetermined amount of time. The reaction was terminated by the addition of 1 ml chloroform: methanol (2:1). Following a low-speed spin, 800 - 1000 µl of the supernatant was removed to a fresh tube and washed with 200 µl 0.9% NaCl. Following a second low-speed spin, 400 - 500 µl of the organic phase was removed to a new tube and washed with 500 µl of chloroform: methanol: 0.9% NaCl (3:48:47). Following a third low-speed spin,

200 - 300 µl was transferred into scintillation vials (Thermo Fisher Scientific, San Jose, CA). Tubes were dried under the chemical hood and 2.5 ml Cytoscint-ES liquid scintillation cocktail (MP Bio, Santa Ana, CA, USA) was added to each tube and counted in a Packard TriCarb 2900TR Liquid Scintillation Analyzer.

Statistical analysis

Graphs were made using GraphPad Prism version 6.04. Unpaired t-tests were used to determine significance between results. RISE (Robust Investigation of Screening Experiments) software was used to analyze data from the high throughput screen and was used to calculate Z-factors, identify 95th and 99th quantile data, and identify compounds that yielded hits of greater than 90% of positive control (*cho1*ΔΔ).

Results

Screen for compounds that confer Pap-A resistance

A novel screen was developed with an original goal of identifying compounds that inhibit the Cho1p PS synthase enzyme. This screen utilizes the unique activity of Pap-A, a toxin isolated from *Theonella spp*. of sponges (Ford 1999). Pap-A has been shown to selectively compromise the integrity of membranes containing PS (Andjelic, *et al*. 2008, Parsons, *et al*. 2006). As a result, Pap-A is toxic to wild-type *C. albicans*. However, the *cho1ΔΔ* mutant, which lacks Cho1p, and thus has no PS in its membranes, is able to survive in the presence of Pap-A

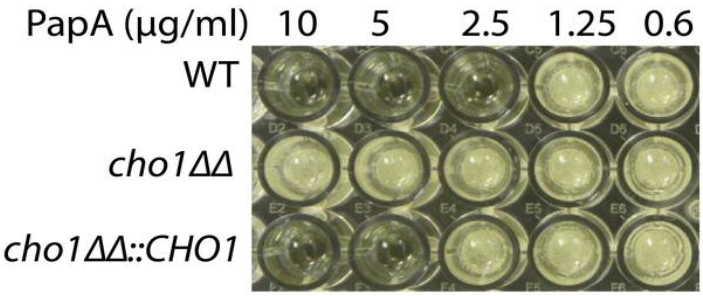

Figure 2. 1. Resistance to Pap-A Correlates with Decreases in PS.
The *cho1ΔΔ* mutant is resistant to all concentrations of papuamide A (Pap-A) indicating a total lack of PS. The *cho1ΔΔ*::*CHO1* reintegrant strain is more resistant to Pap-A than the wild-type (WT), but less resistant than the *cho1ΔΔ* mutant.

(Fig. 2.1) (Chen, *et al*. 2010). A reintegrated strain, *cho1ΔΔ::CHO1* which has one allele of *CHO1* and intermediate levels of PS (Chen, *et al*. 2010) shows intermediate resistance (Fig. 2.1). This feature of Pap-A was employed as a selection tool in our screen to identify those compounds that inhibit Cho1p. We hypothesized that some compounds that allow wild-type growth in the presence of Pap-A would do so by decreasing levels of PS in membranes.

The screen was performed on approximately 5,600 diverse pharmacologically active compounds as representative set of chemical space. Each plate contained a column for each control: 1) *cho1ΔΔ* + Pap-A as a positive control 2) no cells/no Pap-A as a background control 3) wild-type cells with no drugs or Pap-A for a wild-type growth control. The remainder of the plate was reserved for compound testing by pin transfer, and served as a control for background of wild-type cells killed by Pap-A.

The majority of test wells (black open circles in Fig. 2.2), which contained cells that were killed by Pap-A, read near the no drug/no cell background control (red circles, Fig. 2.2). Compounds were tested at a final concentration of 50-75 μM for their ability to provide resistance to wild-type *C. albicans* against a lethal dose of Pap-A (4 μg/ml). After incubation overnight, the viability indicator Alamar Blue was added and fluorescence measured at 590 nm as a proxy for survival. Of the tested compounds, 21 (filled in blue circles) showed viability greater than or equal to 90% of the *cho1ΔΔ* positive control (green circles) (Fig. 2.2). These

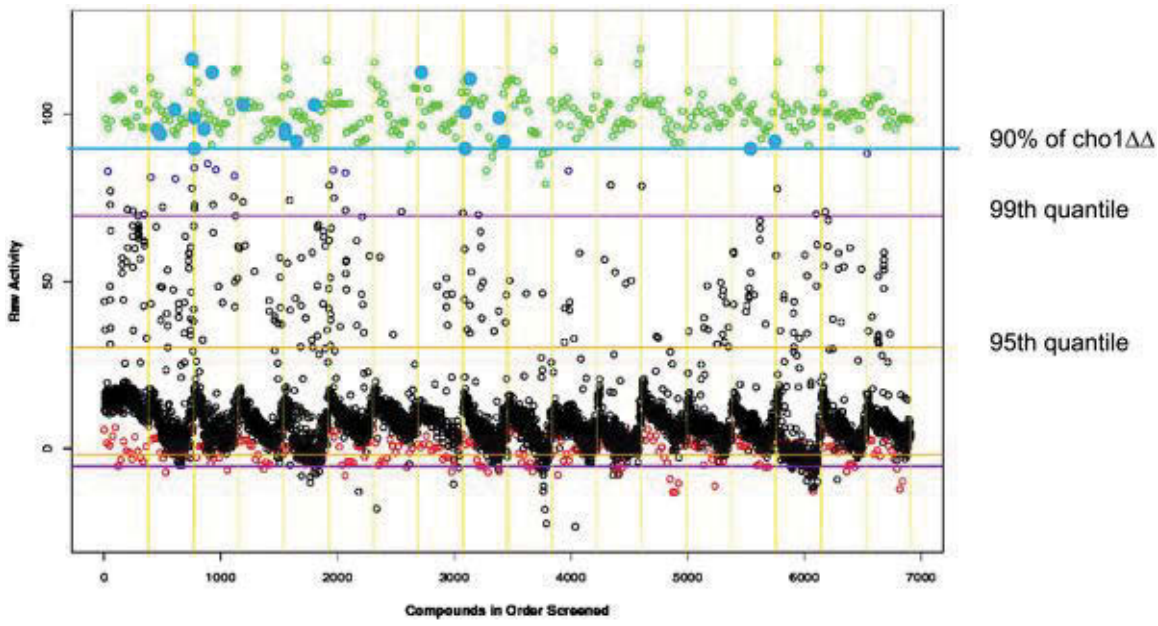

Figure 2. 2. Screen of FDA-approved Bioactive Compounds for Those that Confer Pap-A Resistance

5,760 compounds were screened for their effects on the growth of wild-type *C. albicans* (open black circles) in the presence of 4 µg/ml Pap-A. Cell growth was measured by transformation of the dye Alamar Blue over approximately 3 hours at 37°C. The *cho1ΔΔ*positive control cells growth in the presence of Pap-A with no compounds from the library are represented by green circles. Compounds that allowed wild-type cells to display >90% (above the blue line) of the growth of *cho1ΔΔ* control were designated with filled-in blue circles. Around 95% of the tested compounds showed growth levels closer to the negative control, wells which contained no cells or drugs (open red circles). The horizontal lines show the 99th quantile (purple) where 99% of the compounds exhibited growth and the 95th quantile (yellow) 95% of the compounds lie. The vertical lines divide the compounds by the 384-well plate in which they were screened which correlate to plate numbers along the bottom. A full description of the screening method is found in Materials and Methods.

21 compounds, were considered first round positive hits and were selected and tested for reproducibility in providing Pap-A resistance (data not shown). Of these 21 first round hits, two compounds reproducibly conferred Pap-A resistance to the wild-type cells: SB-224289, a serotonin receptor antagonist (Selkirk, *et al*. 1998b), and MG-624, a nicotinic acetylcholine receptor antagonist (Fig. 2.3A).

Dose response curves were performed to determine the lowest concentrations of SB-224289 and MG-624 that could confer Pap-A resistance. Serial dilutions starting at 200 μM revealed that SB-224289 could confer resistance down to 25 μM, while MG-624 was not consistently effective at producing Pap-A resistance. We found that effects of SB-224289 at concentrations above 400 μM could not be determined as this was greater than its solubility limit in the test media (data not shown). Efforts were focused on SB-224289, which showed consistent efficacy at a concentration range from 100 μM to 25 μM (Fig. 2.3B).

Identification of structural features that enable SB-224289 to confer Pap-A resistance

In order to determine if Pap-A resistance is a property common to compounds with a similar structure to SB-224289, we searched the other compounds screened in our library and found one structural analog, GR127935, which did not provide Pap-A resistance (Fig. 2.4A, data not shown). Two other structural

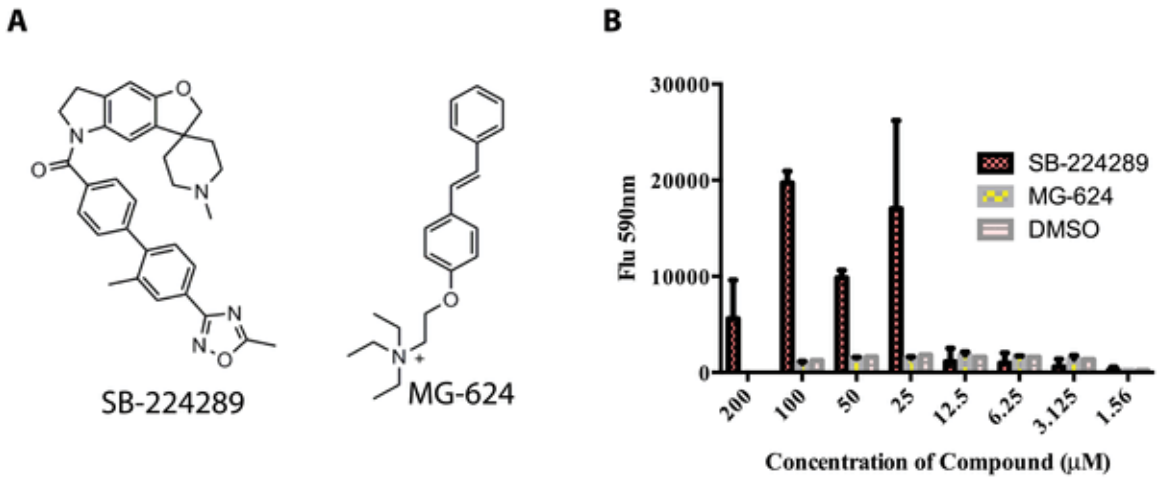

Figure 2. 3. Compounds that Conferred Pap-A Resistance to *C. albicans* Wild-type Yeast

(A) Structures of hits identified from the screen. (B) Comparison of the ability of the hits to confer Pap-A resistance to wild type *C. albicans;* SB-224289, MG-624, and DMSO as a control.

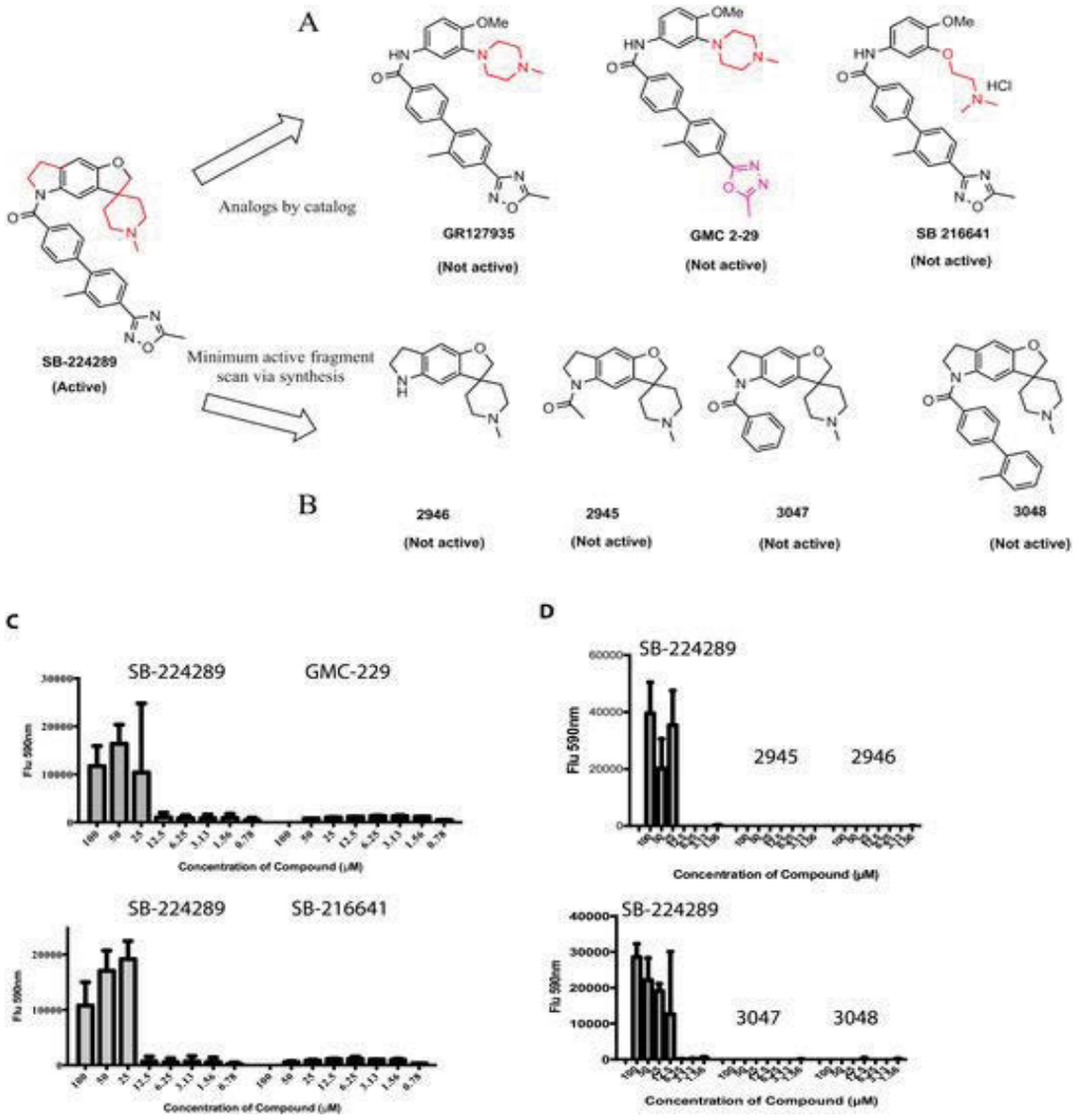

Figure 2. 4. The Full Structure of SB-224289 is Required to Provide Pap-A Resistance

(A) and (B) show the structures of purchased or synthesized analogs of SB-224289, respectively. In (C) and (D) $1x10^4$ cells/ml were treated with a serial dilution of SB-224289, test compounds or DMSO control, and then allowed to incubate for 6 hours at 37°C. Pap-A was added at either 4 μg/ml or 5 μg/ml after 6 hours the plate was incubated at 37°C overnight. Alamar Blue was added and fluorescence signal measured at 590 nm indicating survival of cells.

analogs of SB-224289, GMC 2-29 and SB-216641, were tested to assess their ability to confer Pap-A resistance to wild-type *C. albicans* (Fig. 2.4A&C). We found that neither analog rescued cells when compared with the SB-224289 control. This finding prompted us to hypothesize that the areas of structural dissimilarity between SB-224289 and GR127935, GMC 2-29, and SB-216641—specifically the spirofuro-indole ring structure unique to SB-224289—may be the key to conferring Pap-A resistance. We synthesized four SB-224289 ring structure homologues, 2945, 2946, 3047, and 3048 (Fig. 2.4B), and tested their ability to provide Pap-A resistance to wild-type *C. albicans*. Although we expected protection against Pap-A at similar or even lower concentrations, none of the synthesized SB-224289 ring structures provided resistance to Pap-A (Figs 2.4B & D). These data indicate that the full molecular structure of SB-224289 is required for producing Pap-A resistance to wild-type *C. albicans*.

Exploration of the Mechanism of Action of SB-224289

We hypothesized that SB-224289 inhibited the PS synthase enzyme, Cho1p, thus reducing levels of PS and allowing wild-type cells to survive despite the activity of Pap-A. In order to test this hypothesis, we performed a PS synthase assay to assess the activity of Cho1p with the addition of varying concentrations of SB-224289. Upon addition of SB-224289, no changes were seen in the activity of the Cho1p enzyme as compared to the wild-type control, indicating that SB-224289 does not directly inhibit the PS synthase enzyme in this *in vitro* assay

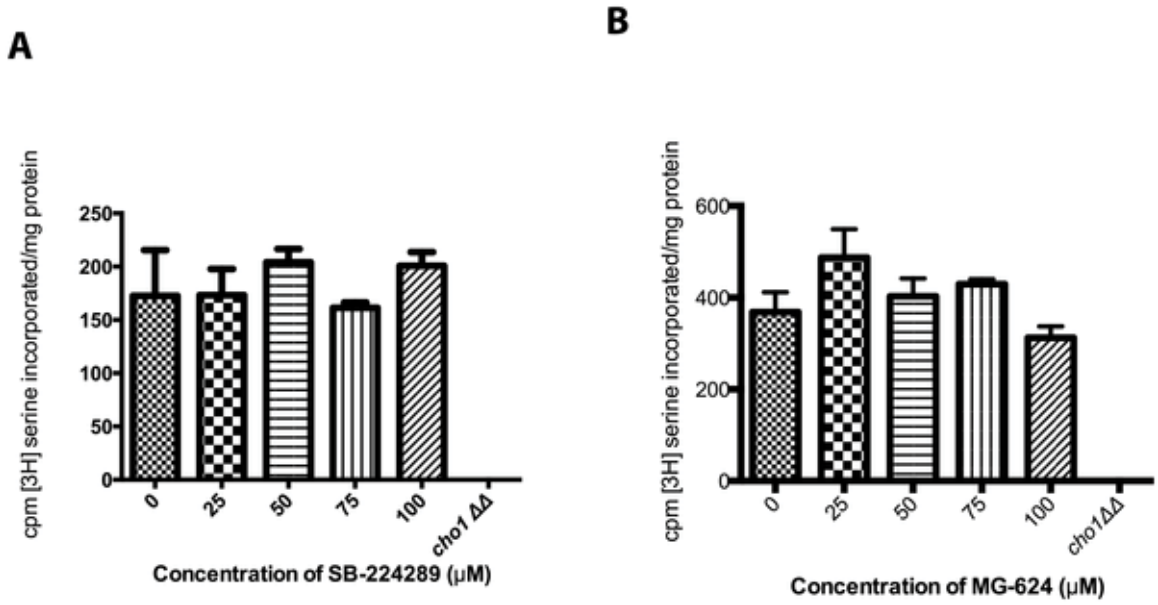

Figure 2. 5. SB-224289 and MG-624 Do Not Inhibit the Activity of Cho1p.
PS synthase activity shown as counts per minute per milligram of protein, quantifying ^{3}H-L-serine incorporated into PS. Addition of varying concentrations of SB-224289 (A) and MG-624 (B) did not have an inhibitory effect on PS production.

(Fig. 2.5A). Furthermore, a PS synthase assay was performed with MG-624 at varying concentrations. Again, no PS synthase inhibition was observed in any concentration tested (Fig. 2.5B).

To further investigate the mode of action of SB-224289, we assessed the compound's ability to inhibit PS synthesis *in vivo*. If the compound must be metabolized or modified internally in order to inhibit Cho1p, we should see a decrease in PS levels only when treating live cells with SB-224289. Previous studies showed that *cho1ΔΔ*, which has no PS, shows a distinct phenotype of β (1-3)-glucan unmasking (Davis, *et al*. 2014b). Based on this, we performed an assay to determine if treatment with SB-224289 would cause the β (1-3)-glucan in the cell wall to become exposed. Cells were treated with SB-224289 for 3 hours and then stained with β (1-3)-glucan antibody. However, epifluorescence microscopy showed no indication that β (1-3)-glucan was exposed in SB-224289-treated cells (data not shown). PS is also a precursor for the synthesis of phosphatidylethanolamine (PE), in a pathway where PS is decarboxylated to form PE. As a result, the *cho1*ΔΔ mutant, since it lacks PS, requires ethanolamine in the medium so it can make PE from imported ethanolamine via the Kennedy pathway. If SB-224289 is a PS synthase inhibitor, then it should have caused ethanolamine auxotrophy in wild-type *C. albicans*, however, this was not the case (data not shown).

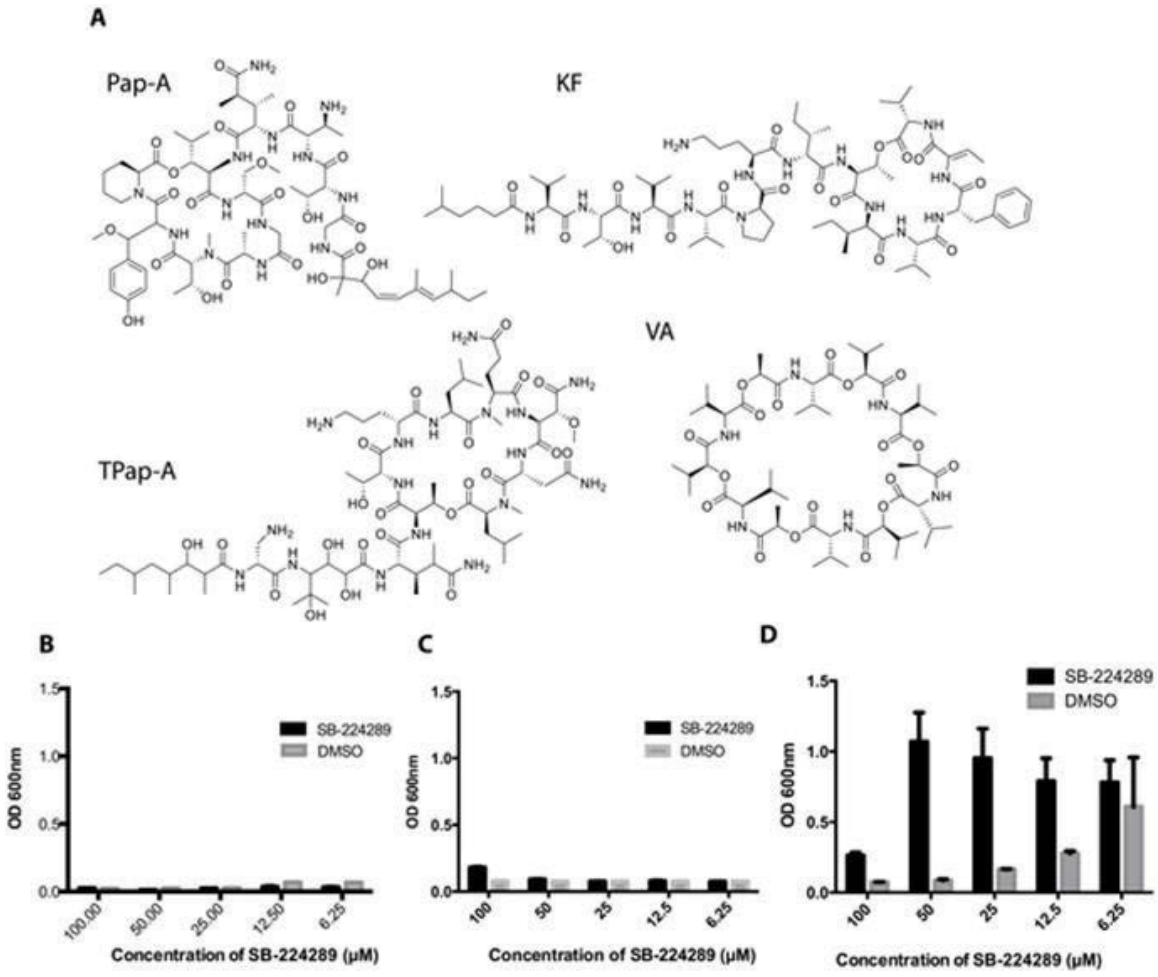

Figure 2. 6. SB-224289 Protects Against Theopapuamide, but Not Other Depsipeptides.

(A) The structure of several depsipeptides are shown. For each of these compounds, $1x10^4$ cells/ml were treated with serially diluted concentrations of SB-224289 (SB) and were incubated for 3 hours at 37°C. Following this incubation, (B) 3 μg/ml valinomycin (VA), (C) 15 μg/ml kahalalide F (KF), or (D) 6 μg/ml theopapuamide (TA) was added and further allowed to incubate overnight. Optical density (OD) was read at 600 nm the next day as a measure of cell survival.

SB-224289 specifically blocks the activity of Pap-A and not other membrane disruptors

Naturally-produced depsipeptides share similar structures (Fig. 2.6) and can be medically relevant like the antibiotic valinomycin (VA) produced from *Streptomyces spp*. (Kroten, *et al*. 2010, Tempelaars, *et al*. 2011), the emetic toxin cereulide produced by the foodborne pathogen *Bacillus cereus* (Agata, *et al*. 1995, Andersson, *et al*. 1998, Kroten, *et al*. 2010, Zuberovic Muratovic, *et al*. 2014), and anti-tumor drug prospect kahalalide F (KF) found in sea slugs (Suarez, *et al*. 2003). A previous study found that a serotonin receptor antagonist, ondansetron hydrochloride, abolished the emetic effect of cereulide in Asian house shrews (Agata, *et al*. 1995). Theopapuamide A (TPap-A) is a close structural relative of Pap-A and was previously shown to have potent antifungal activity (Plaza, *et al*. 2009, Ratnayake, *et al*. 2006). Based on these studies, we were interested in determining if SB-224289 would block the activities of similar depsipeptide toxins.

First, we tested if SB-224289 could rescue cells from toxic levels of VA. We treated *C. albicans* with serially diluted concentrations of SB-224289, followed by treatment with 6 µg/ml of VA. We found that no concentration of SB-224289 was sufficient to provide protection to cells (Fig. 2.6A). We further measured the ability of SB-224289 to mitigate the toxicity of KF and TPap-A (Fig. 2.6B & C). SB-224289 was unable to protect wild-type cells against KF, but we found that SB-224289 was able to provide protection against TPap-A.

Discussion

The screen described in this communication was originally intended to identify inhibitors of the fungal PS synthase. However, the identified hit compound, SB-224289, does not inhibit PS synthesis even though it interferes with the lethal effects of Pap-A on *C. albicans* cells that contain PS. The evidence that SB-224289 does not block PS synthesis comes from several secondary screens based on the *cho1ΔΔ* mutant's characteristic phenotype (Chen, *et al*. 2010). For example, the *cho1*ΔΔ mutant is an ethanolamine auxotroph because *C. albicans* uses PS as a precursor for production of PE, a vital phospholipid, in one of its two PE synthesis pathways. Thus, ethanolamine must be supplemented in the medium so that the organism can produce PE through the alternative Kennedy Pathway. We saw no indication that treatment with SB-224289 caused wild-type *C. albicans* to become an ethanolamine auxotroph (data not shown), indicating that it does not interfere with PS synthesis. A second useful phenotype is increased exposure of β (1-3)-glucan in the cell wall upon loss of PS. The cause of this exposure in *cho1ΔΔ* is currently unknown, but it is very specific to the loss of PS rather than PE (Davis, *et al*. 2014b). As with the previous assay, treatment with SB-224289 does not lead to exposure of ß (1-3)-glucan, thus indicating that it does not interfere with PS synthesis (data not shown). Finally, SB-224289 did not interfere with PS synthesis in an *in vitro* assay (Fig. 2.5A).

The most interesting aspect of the blockade of the lethal effects of Pap-A on *C. albicans* by SB-224289 is its specificity. Seven different analogs

representing fragments of SB-224289 or the entire molecule fail to rescue *C. albicans* from Pap-A-induced cytotoxicity. These results indicate that the activity of SB-224289 is specific and relies on the entire structure of the molecule (Fig. 2.4), possibly, due to a specific three-dimensional conformation which could only be adopted by the full SB-224289. In addition, SB-224289 could only inhibit the toxicity of depsipeptides that were structurally highly similar. For example, we saw no indication that SB-224289 provided protection to wild-type *C. albicans* treated with VA or KF (Fig. 6). However, as expected, SB-224289 was able to abrogate the cytotoxicity of TPap-A, a close structural relative of Pap-A (Fig. 6) likely to bind PS as well. Altogether, these data suggest that there might be a physical interaction between the two compounds that inhibits the toxic effects of Pap-A. More specifically, structural differences in the tail regions of these related depsipeptides may confer their selectivity. It is also possible that SB-224289 impacts cellular physiology in a way that creates a protective response, but it is unclear what such a mechanism might entail.

Further studies are needed to understand the nature of the interaction between SB-224289 and Pap-A and the mechanism that leads to protection of *C. albicans* cells against Pap-A toxicity. Although SB-224289 is clearly not acting by inhibiting Cho1p, the selective inactivation of the Pap-A toxin by SB-224289 indicates a path to the discovery of other compounds that can inactivate similar membrane active toxins. In fact, the assay described herein could be easily adapted from use with Pap-A to any number of membrane potent toxins to find

antagonists. The compounds discovered by this approach would be useful for treatments against environmental toxins that occur during algal blooms that affect drinking water, food contamination, etc. It could also be useful as a method for identifying potential drug interactions that would counter-indicate compounds or combination therapies being considered as potential anti-cancer or anti-microbial drugs.

References

Agata N, Ohta M, Mori M *et al.,* A novel dodecadepsipeptide, cereulide, is an emetic toxin of Bacillus cereus. *FEMS Microbiol Lett* 1995;**129**: 17-20.

Alexander BD, Johnson MD, Pfeiffer CD *et al.,* Increasing echinocandin resistance in *Candida* glabrata: clinical failure correlates with presence of FKS mutations and elevated minimum inhibitory concentrations. *Clin Infect Dis* 2013;**56**: 1724-32.

Andersson MA, Mikkola R, Helin J *et al.,* A novel sensitive bioassay for detection of Bacillus cereus emetic toxin and related depsipeptide ionophores. *Appl Environ Microbiol* 1998;**64**: 1338-43.

Andjelic CD, Planelles V, Barrows LR. Characterizing the anti-HIV activity of papuamide A. *Mar Drugs* 2008;**6**: 528-49.

Atkinson K, Fogel S, Henry SA. Yeast mutant defective in phosphatidylserine synthesis. *J Biol Chem* 1980;**255**: 6653-61.

Baddley JW, Benjamin DK, Jr., Patel M *et al., Candida* infective endocarditis. *Eur J Clin Microbiol Infect Dis* 2008;**27**: 519-29.

Bae-Lee MS, Carman GM. Phosphatidylserine synthesis in *Saccharomyces cerevisiae*. Purification and characterization of membrane-associated phosphatidylserine synthase. *J Biol Chem* 1984;**259**: 10857-62.

Braun BR, van Het Hoog M, d'Enfert C *et al.,* A human-curated annotation of the *Candida albicans* genome. *PLoS Genet* 2005;**1**: 36-57.

Chen YL, Montedonico AE, Kauffman S *et al.,* Phosphatidylserine synthase and phosphatidylserine decarboxylase are essential for cell wall integrity and virulence in *Candida albicans*. *Mol Microbiol* 2010;**75**: 1112-32.

Dannaoui E, Desnos-Ollivier M, Garcia-Hermoso D *et al., Candida* spp. with acquired echinocandin resistance, France, 2004-2010. *Emerg Infect Dis* 2012;**18**: 86-90.

Davis SE, Hopke A, Minkin SC, Jr. *et al.,* Masking of beta(1-3)-glucan in the cell wall of *Candida albicans* from detection by innate immune cells depends on phosphatidylserine. *Infect Immun* 2014;**82**: 4405-13.

Ford PW, Gustafson K. R., McKee T. C., Shigematsu N., Maurizi L. K., Pannell L. K., Williams D. E., de Silva E. D., Lassota P., Allen T. M., Van Soest R., Andersen R. J., Boyd M. R. Papuamides A-D, HIV-Inhibitory and Cytotoxic Depsipeptides from the Sponges Theonella mirabilis and Theonella swinhoei Collected in Papua New Guinea. *J Am Chem Soc* 1999;**121**: 5899–909.

Gaster LM, Blaney FE, Davies S *et al.,* The Selective 5-HT1B Receptor Inverse Agonist 1‘-Methyl-5-[[2‘-methyl-4‘- (5-methyl-1,2,4-oxadiazol-3-yl)biphenyl-4-yl]carbonyl]-2,3,6,7-tetrahydro- spiro[furo[2,3-f]indole-3,4‘-piperidine] (SB-224289) Potently Blocks Terminal 5-HT Autoreceptor Function Both *in vitro* and *in vivo*. *Journal of Medicinal Chemistry* 1998;**41**: 1218-35.

Ghannoum MA, Rice LB. Antifungal agents: mode of action, mechanisms of resistance, and correlation of these mechanisms with bacterial resistance. *Clin Microbiol Rev* 1999;**12**: 501-17.

Guthrie C, Fink, G. R. (ed.) *Methods in Enzymology* volume 350: Academic Press, 2002.

Holeman CW, Jr., Einstein H. The toxic effects of amphotericin B in man. *Calif Med* 1963;**99**: 90-3.

Kroten MA, Bartoszewicz M, Swiecicka I. Cereulide and valinomycin, two important natural dodecadepsipeptides with ionophoretic activities. *Pol J Microbiol* 2010;**59**: 3-10.

Kuge O, Nishijima M, Akamatsu Y. Phosphatidylserine biosynthesis in cultured Chinese hamster ovary cells. III. Genetic evidence for utilization of phosphatidylcholine and phosphatidylethanolamine as precursors. *J Biol Chem* 1986;**261**: 5795-8.

Matsuo Y, Fisher E, Patton-Vogt J *et al.,* Functional characterization of the fission yeast phosphatidylserine synthase gene, pps1, reveals novel cellular functions for phosphatidylserine. *Eukaryot Cell* 2007;**6**: 2092-101.

Mishra NN, Prasad T, Sharma N *et al.,* Pathogenicity and drug resistance in *Candida albicans* and other yeast species. A review. *Acta Microbiol Immunol Hung* 2007;**54**: 201-35.

Morrell M, Fraser VJ, Kollef MH. Delaying the empiric treatment of *Candida* bloodstream infection until positive blood culture results are obtained: a

potential risk factor for hospital mortality. *Antimicrob Agents Chemother* 2005;**49**: 3640-5.

Mukherjee PK, Sheehan DJ, Hitchcock CA *et al.,* Combination treatment of invasive fungal infections. *Clin Microbiol Rev* 2005;**18**: 163-94.

Papon N, Courdavault V, Clastre M *et al.,* Emerging and emerged pathogenic *Candida* species: beyond the *Candida albicans* paradigm. *PLoS Pathog* 2013;**9**: e1003550.

Parsons AB, Lopez A, Givoni IE *et al.,* Exploring the mode-of-action of bioactive compounds by chemical-genetic profiling in yeast. *Cell* 2006;**126**: 611-25.

Pfaller MA. Antifungal drug resistance: mechanisms, epidemiology, and consequences for treatment. *Am J Med* 2012;**125**: S3-13.

Pfaller MA, Diekema DJ. Epidemiology of invasive candidiasis: a persistent public health problem. *Clin Microbiol Rev* 2007;**20**: 133-63.

Plaza A, Bifulco G, Keffer JL *et al.,* Celebesides A-C and theopapuamides B-D, depsipeptides from an Indonesian sponge that inhibit HIV-1 entry. *J Org Chem* 2009;**74**: 504-12.

Ratnayake AS, Bugni TS, Feng X *et al.,* Theopapuamide, a cyclic depsipeptide from a Papua New Guinea lithistid sponge Theonella swinhoei. *J Nat Prod* 2006;**69**: 1582-6.

Selkirk JV, Scott C, Ho M *et al.,* SB-224289--a novel selective (human) 5-HT1B receptor antagonist with negative intrinsic activity. *Br J Pharmacol* 1998;**125**: 202-8.

Srinivasan A, Lopez-Ribot JL, Ramasubramanian AK. Overcoming antifungal resistance. *Drug Discov Today Technol* 2014;**11**: 65-71.

Suarez Y, Gonzalez L, Cuadrado A *et al.,* Kahalalide F, a new marine-derived compound, induces oncosis in human prostate and breast cancer cells. *Mol Cancer Ther* 2003;**2**: 863-72.

Tempelaars MH, Rodrigues S, Abee T. Comparative analysis of antimicrobial activities of valinomycin and cereulide, the Bacillus cereus emetic toxin. *Appl Environ Microbiol* 2011;**77**: 2755-62.

Zuberovic Muratovic A, Troger R, Granelli K *et al.,* Quantitative analysis of cereulide toxin from bacillus cereus in rice and pasta using synthetic cereulide standard and 13C6-cereulide standard-a short validation study. *Toxins (Basel)* 2014;**6**: 3326-35.

CHAPTER III

SB-224289 DISRUPTS THE PROPER LOCALIZATION OF PHOSPHATIDYLSERINE, PHOSPHATIDYLINOSITOL (4,5)-BISPHOSPHATE, AND THE PLASMA MEMBRANE ATPASE 1 IN *SACCHAROMYCES CEREVISIAE*

Contributing authors to this work include: Chelsi D. Cassilly, Rebecca E. Fong, Elizabeth R. Emanuel, Sabrina V. Williamson, Robert E. Burks, Todd B. Reynolds

This article has not been published elsewhere at this time, nor will it be before completion of this ETD. The author contributions are as follows: Conceived and designed the experiments: CDC TBR. Performed the experiments: CDC REF ERE SVW REB. Analyzed the data: CDC TBR. Contributed reagents/materials/analysis tools: TBR. Wrote the paper: CDC.

Abstract

In previous work, a series of drug screens were performed in order to identify chemical inhibitors of the fungal phosphatidylserine (PS) synthase, as it represents an excellent drug target in pathogenic fungi. Preliminary studies on a promising hit, SB-224289, showed that this compound did not inhibit the PS synthase as was hypothesized, but acted by an unknown mechanism to provide resistance to the PS-specific toxin papuamide A. Further studies were conducted in order to understand the mechanism of action of SB-224289 using fluorescent microscopy of plasma-membrane-localized probes. Our studies suggest that SB-224289 causes a physiological response in the model yeast *Saccharomyces cerevisiae* which we hypothesize is a disruption of cellular trafficking (i.e.

endocytosis). Further, preliminary screening of a lethal concentration of SB-224289 against a mutant library of *S. cerevisiae* identified Rho5 as a possible target of SB-224289. Although this is speculation and remains to be experimentally tested, it is possible that SB-224289 interferes with this protein in some way. A compound that modulates endocytosis, like SB-224289 may, could prove useful in research on membrane trafficking.

Introduction

Our lab previously performed a drug screen to identify small molecule inhibitors of the fungal phosphatidylserine (PS) synthase. This enzyme represents an excellent drug target as it is absent in mammals, and has been shown to be important for virulence (Cassilly, *et al*. 2016, Chen, *et al*. 2010). This drug screen worked by identifying compounds that allowed *Candida albicans* to survive in the presence of the PS-specific toxin papuamide A. Pap-A works by binding PS and causing lysis and eventual death of cells (Andjelic, *et al*. 2008, Chen, *et al*. 2010). We hypothesized that compounds that allowed survival of *C. albicans* in the presence of Pap-A could be PS synthesis or trafficking inhibitors.

From this screen, we identified SB-224289 as possible inhibitor of PS synthesis in *Candida albicans*. We found that certain concentrations of SB-224289 resulted in cell survival in the presence of this toxin. Initial hypotheses were formed that SB-224289 inhibited PS synthesis, but these were rejected because cells treated with the drug did not share the same phenotypic

characteristics as the *cho1ΔΔ* mutant control. In addition, no direct evidence was observed that SB-224289 inhibited the function of the *C. albicans* PS synthase in an *in vitro* enzyme assay. Based on these findings, it was concluded that SB-224289 likely interacted with Pap-A to produce resistance to the toxin, but no data could confirm this suspicion (Cassilly, *et al*. 2016).

Continued studies of the SB-224289 mechanism of action indicated that the compound may have a physiological effect on the fungus that was hidden from our previous methods of experimentation. We made various strains of *Saccharomyces cerevisiae* expressing fluorescent probes specific for PS, phosphatidylinositol 4,5-bisphosphate (PI4,5P2), and plasma membrane ATPase 1 (Pma1), and determined the effect of SB-224289 on these probes. Our findings show that SB-224289 causes a disruption in the normal plasma membrane localization of all three fluorescent markers. These results indicate that SB-224289 may disrupt normal plasma membrane trafficking in yeast.

In order to test these hypotheses, we performed a screen on the Boone Mutant Library of *S. cerevisiae* looking for mutants that were resistant to a lethal concentration of SB-224289 (Owen Ryan Ph.D. Thesis). From this screen, we were able to identify possible targets of SB-224289.

Based on our findings, it appears that SB-224289 does not interfere solely with phospholipid trafficking and localization, as was previous suspected. Rather, the results indicate that SB-224289 may disrupt the trafficking of some cellular components within cells. This conclusion is supported by the punctate

localization of GFP-Pma1p inside the cells treated with SB-224289. These punctate spots are likely vaculolar, where the protein is transported for degradation; however, further studies will need to be performed to confirm and support this hypothesis. Although SB-224289 does not act as an inhibitor of PS synthesis or trafficking, a compound that disrupts cellular trafficking could still be useful as a tool in general biological research.

Materials and Methods

Strain Production

Wild-type Σ *S. cerevisiae* (TRY181) and a *cho1Δ* deletion mutant (BMY2), which is unable to produce PS, were used. Using a standard lithium acetate transformation method we created the strains used in this study (Gietz and Woods 2002). Transformation of GFP-Lact-C2 into WT and *cho1Δ S. cerevisiae*: GFP-Lact-C2 (pGFP-Lact-C2) was transformed into wild-type and *cho1Δ* using the *URA3* marker to produce *ura3Δ his3Δ* pGFP-Lact-C2 and *ura3Δ his3Δ cho1Δ* pGFP-Lact-C2, respectively. Transformation of mCherry-Lact-C2 into WT and *cho1Δ S. cerevisiae*: mCherry-Lact-C2 (pGPD416-mCherry-Lact-C2) was transformed into wild-type and *cho1Δ* using the *URA3* marker to produce *ura3Δ his3Δ* pGPD416-mCherry-Lact-C2 and *ura3Δ his3Δ cho1Δ* pGPD416-mCherry-Lact-C2, respectively. Transformation of GFP-2x Ph(PLCδ) into *ura3Δ his3Δ* pGPD416-mCherry-Lact-C2 and *ura3Δ his3Δ cho1Δ* pGPD416-mCherry-Lact-C2 *S. cerevisiae*: The GFP-2x Ph(PLCδ) was cut from pRS426GFP-2×PH(PLCδ)

using BamHI and SalI and ligated into pRS423 to produce pRF1. pRS423GFP-2×PH(PLCδ) (pRF1) was transformed into *ura3Δ his3Δ* pGPD416-mCherry-Lact-C2 and *ura3Δ his3Δ cho1*Δ pGPD416-mCherry-Lact-C2 using the *HIS3* marker to produce *ura3Δ his3Δ* pGPD416-mCherry-Lact-C2 pRS426GFP-2×PH(PLCδ) and *ura3Δ his3Δ cho1Δ* pGPD416-mCherry-Lact-C2 pRS426GFP-2×PH(PLCδ),respectively. Transformation of the *CEN* plasmid PMA1-GFP into WT and *cho1Δ S. cerevisiae*: pCEN PMA1-GFP wild-type and *cho1Δ* using the *URA3* marker to produce *ura3Δ his3Δ* pCEN PMA1-GFP and *ura3Δ his3Δ cho1Δ* pCEN PMA1-GFP, respectively.

All strains and plasmids used in this study can be found in Tables 3.1 and 3.2, respectively.

Fluorescent Microscopy

To confirm the presence and assess the localization of all fluorescent probes used, overnight cultures were diluted back to 0.1 or 0.2 OD_{600}/ml and allowed to grow for 2-4 hours shaking at 30° C before fluorescent microscopy was performed on a Leica DMRXA microscope. All images were analyzed using Leica Application Suite 3.4.

SB-224289 Treatment

Overnight cultures of selected strains were diluted to 0.2 OD_{600} and allowed to grow for 3-4 hours. Cultures were then diluted to 0.1 OD_{600}/ml and 100 - 200 µL

Table 3. 1. Strains Produced in this Study

Strain	Organism	Genotype	Source
Σ (TRY 181)	*S. cerevisiae*	*ura3Δ his3Δ*	Lab Strain
BMY2	*S. cerevisiae*	*ura3Δ his3Δ cho1 Δ*	Lab Strain
RF01	*S. cerevisiae*	*ura3Δ his3Δ* pGFP-Lact-C2	This study
RF04	*S. cerevisiae*	*ura3Δ his3Δ cho1Δ* pGFP-Lact-C2	This study
RF09	*S. cerevisiae*	*ura3Δ his3Δ* pGPD416-mCherry-Lact-C2	This study
RF10	*S. cerevisiae*	*ura3Δ his3Δ cho1Δ* pGPD416-mCherry-Lact-C2	This study
RF21	*S. cerevisiae*	*ura3Δ his3Δ* pGPD416-mCherry-Lact-C2 pRS426GFP-2×PH(PLCδ)	This study
RF18	*S. cerevisiae*	*ura3Δ his3Δ cho1Δ* pGPD416-mCherry-Lact-C2 pRS426GFP-2×PH(PLCδ)	This study
CDCS41	*S. cerevisiae*	*ura3Δ his3Δ* pCEN PMA1-GFP	This study
CDCS42	*S. cerevisiae*	*ura3Δ his3Δ cho1Δ* pCEN PMA1-GFP	This study

Table 3. 2. Plasmids Used in this Study

Plasmid	Inserts	Source
p200 (pGFP-Lact-C2)	GFP-Lact-C2, *URA3*, Cen/Ars, Amp^R	Yeung *et al.,* 2008
pGPD416-mCherry-Lact-C2	mCherry-Lact-C2, *URA3*, Amp^R	Fairn *et al.,* 2011
pRS423	*HIS3*, Amp^R	Lab Strain
pRS426GFP-2×PH(PLCδ)	GFP-2x Ph(PLCδ), *URA3*, Amp^R	Addgene plasmid # 36092
pRF1	GFP-2x Ph(PLCδ), *HIS3*, Amp^R	This study
pCENPMA1-GFP	*PMA1-GFP*, *URA3*, Cen, Amp^R	Balguerie *et al.,* 2002

of the cells were either treated with 100 μM SB-224289 or an equivalent volume of DMSO as a negative control. This concentration of SB-224289 was shown to be non-fungicidal to the tested cell concentration in viable plate counts. All samples were then incubated at 30˚C shaking for 1 hour followed by fluorescent microscopy.

SB-224289 Mutant Library Screen

For every *Saccharomyces cerevisiae* mutant library 96-well plate being tested, 10 ml of YPD was made containing either 50 μM SB-224289 or an equal volume of DMSO as a negative control. For every library 96-well plate being tested, 100 μl of the corresponding media was added to each well, having one set of plates for SB-224289 and another set for DMSO. The 96-pin tool inoculator was placed in 100% ethanol and flamed to sterilize. The pins were then dipped into the stock *S. cerevisiae* mutant library plate after cooling. The pins were then dipped into the test plates to inoculate each well. Inoculated plates were placed in a stationary 30ºC incubator for 48 hours.

To measure the optical density, each well's contents were resuspended by pipeting several times up and down to mix, then measuring the OD_{600} in a Biotek Cytation 5 Imaging Reader plate reader. Plates were incubated again at room temperature and checked again for growth after 72 or 96 hours. If growth was observed, OD_{600} was measured again. To ensure that no bacterial contamination had occurred during the experimental proceedings, all "positive hit mutant

strains" found in the SB-224289 plates were viewed under a Leica DMRXA microscope.

Once positive hits were found, the strains were streaked onto YPD and incubated at 30ºC for 1-2 days. After strains were grown up on YPD plates, liquid cultures of 5ml YPD with were inoculated and incubated in a shaking incubator at 30ºC overnight. These cultures were diluted back to a 0.01 OD_{600}/ml in 1ml YPD. A serial dilution of SB-224289 was then performed in a 96-well plate, with the highest final concentration of SB-224289 being 100 µM. Wild-type (TRY181) *S. cerevisiae* was used as a negative control. Plates were incubated at 30ºC for 1-2 days and then optical density was measured, after mixing the wells, at 24, 48, and 72 hours. All strains that exhibited greater growth than TRY 181 at 50-100 µM SB-224289 concentrations were considered hits and streaked again on YPD plates.

Results

After previous research with SB-224289 (Selkirk, *et al*. 1998b), we concluded that the compound did not inhibit PS synthesis within *Candida albicans*, as was hypothesized, but likely had a compound-compound interaction with Papuamide-A (Cassilly, *et al*. 2016). The hypothesis of a compound-compound interaction, though explanatory for the Pap-A resistance provided by SB-224289, was never confirmed via experimentation (HPLC runs performed with both compounds were inconclusive (data not shown)). PS localization can be analyzed in the model yeast, *Saccharomyces cerevisiae* using a GFP labeled version of the C2 domain

of the bovine protein Lactadherin (Lact-C2) that specifically binds PS (Andersen, *et al*. 2000, Shi, *et al*. 2004). We acquired a version of GFP-tagged Lact-C2 (pGFP-Lact-C2) (Yeung, *et al*. 2008) which we transformed into our TRY181 and *cho1Δ* lab strains of *Saccharomyces cerevisiae*. The strains produced were: wildtype carrying pGFP-Lact-C2 and *cho1Δ* carrying pGFP-Lact-C2. Attempts were made to transform a codon-optimized GFP-Lact-C2 into *C. albicans*; however, the probe seemed to be expressed too highly in the chosen strains and did not show proper or expected localization (data not shown). Because of this problem, and the fact that many fluorescent probes can be easily used in *S. cerevisiae*, all studies done using GFP-Lact-C2 were performed in *S. cerevisiae*.

GFP-Lact-C2 localizes to the membrane in the wild-type where PS is enriched. In *cho1Δ* which is devoid of PS, GFP-Lact-C2 is diffuse throughout the cell. In an effort to understand the effect of various compounds on PS-localization, we performed a series of compound treatments followed by fluorescent microscopy to determine where GFP-Lact-C2 localized as an indication of what might be happening to PS localization. In these experiments, we expected that SB-224289 would have no effect on GFP-Lact-C2 localization if the compound truly acted via an indirect method to inhibit Pap-A toxicity. However, our findings showed that treatment with 100 μM SB-224289 (shown to be non-lethal at the cell concentration in this plate assay as assessed by viable plate counts) caused a dramatic alteration in localization of the GFP-Lact-C2 in the cell (Fig. 3.1). These results indicated that SB-224289 could have a major

effect on PS trafficking or turn-over within the cell. In addition, the specificity of this physiological response is demonstrated by the fact that two structural analogs of SB-224289—GMC 2-29 and SB-21664—did not produce any disruption in GFP-Lact-C2 localization (Fig 3.1C). These data were replicated in wildtype and *cho1Δ* strains of *S. cerevisiae* carrying the red-fluorescently-marked Lact-C2 plasmid (pGPD416-mCherry-Lact-C2) (data not shown).

In order to further understand the extent of SB-224289 activity, we wished to determine if the compound had an effect on other phospholipid localization. The Plekstrin homology domain (PH domain) is a domain of approximately 120 amino acids that has been shown to bind PI(4,5)P2 in the membrane of *S. cerevisiae* (Lemmon 2007). We hypothesized that localization of the PH domain fused with GFP (GFP-2x Ph(PLCδ)) would be unaffected by SB-224289 if the activity of the compound is specific to PS trafficking.

The plasmid pRS426GFP-2×PH(PLCδ) was transformed into wild-type and *cho1Δ* strains carrying pGPD416-mCherry-Lact-C2 to produce strains with a red fluorescent signal showing PS localization and green fluorescent signal showing PI4,5P2 localization. As expected, in the wild-type we saw localization of the GFP-2x Ph(PLCδ) at the membrane. Surprisingly, in *cho1Δ* we saw variable localization at the membrane, with part of the GFP-2x Ph(PLCδ) present as diffuse signal in the cytoplasm (Fig. 3.2). This is likely due to problems with phospholipid trafficking that are produced by the loss of PS. A recent paper

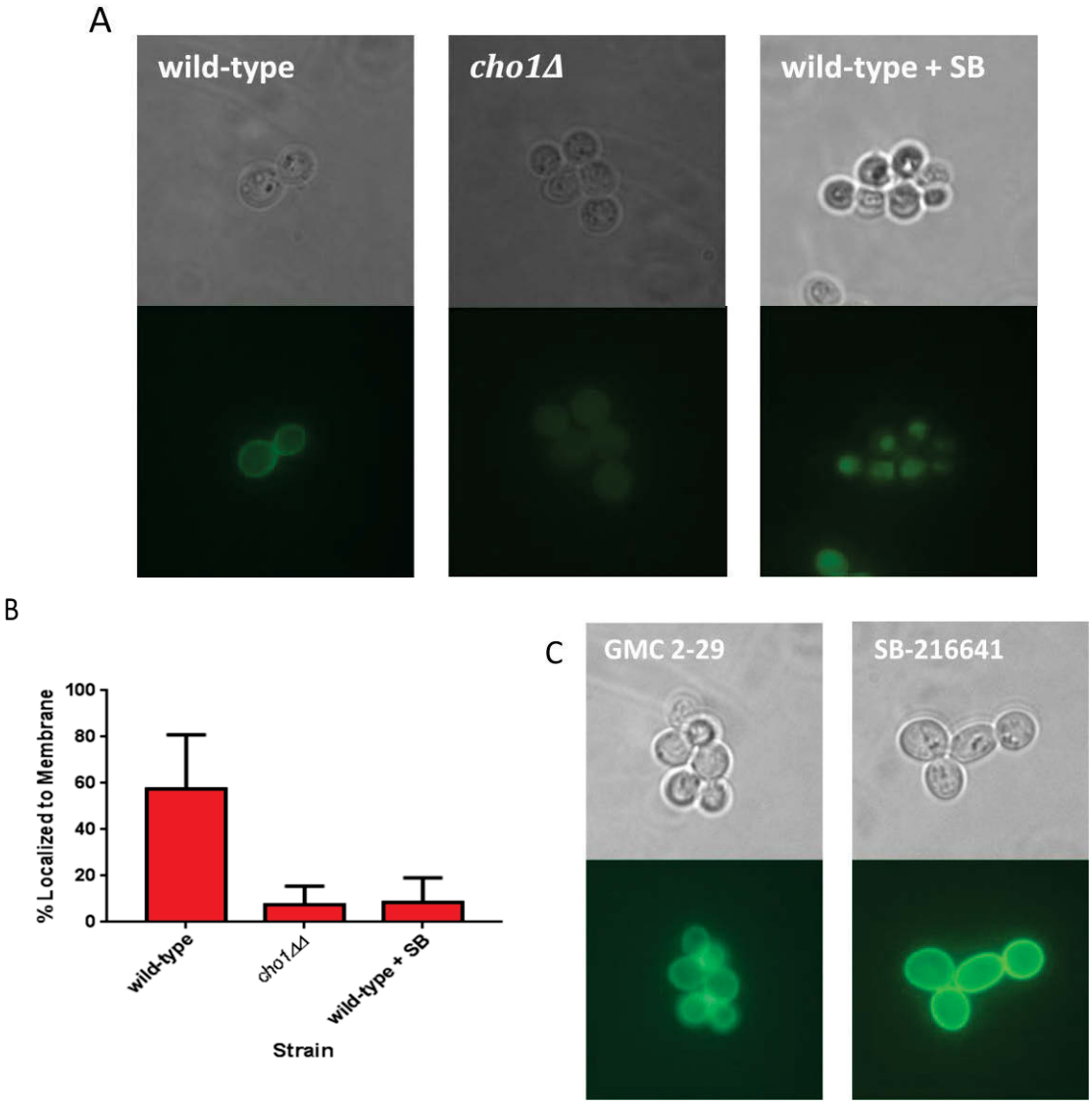

Figure 3. 1. SB-224289 Disrupts GFP-Lact-C2 Localization to PS
(A) Fluorescent micrographs of GFP-Lact-C2 localization in *cho1Δ*, wild-type, or wild-type treated with SB-224289. (B) Quantification of GFP-Lact-C2 localization to the plasma membrane in *cho1Δ*, wild-type, or wild-type treated with SB-224289. (C) Structural analogs of SB-224289, GMC 2-29 and SB-216641 do not cause a disruption in GFP-Lact-C2 localization.

described a model where PS is delivered to the plasma membrane in a protein-mediated exchange with PI4P (Moser von Filseck, *et al*. 2015). It is possible that the loss of PS causes a disruption in proper localization of PI species, and thus an alteration in the localization of the GFP-2x Ph(PLCδ), although this has yet to be confirmed.

We performed treatment of wildtype *S. cerevisiae* carrying pRS426GFP-2×PH(PLCδ) and pGPD416-mCherry-Lact-C2 with 100 μM concentration of SB-224289. Our expectation was that if SB-224289 activity was specifically altering PS localization or trafficking, that we may see no difference or change in GFP-2x Ph(PLCδ) localization, indicating no change in PI4,5P2 localization or trafficking. However, we saw diffusion of the GFP-2x Ph(PLCδ) away from the plasma membrane in cells treated with SB-224289 (Fig. 3.2). These results are similar to the GFP-Lact-C2 localization studies which may indicate that SB-224289 inhibits trafficking or turnover of PS at the plasma membrane, and further, has an impact on some PI species' localization as well.

In order to determine if SB-224289 activity was specific to phospholipid trafficking, we wished to determine the effect of SB-224289 on membrane protein localization. To do this, we selected the highly abundant, membrane-bound ATPase, Pma1 (Schmitt, *et al*. 2006). We acquired the plasmid CEN PMA1-GFP from Dr. Amy Chang and Dr. Annick Breton (Balguerie, *et al*. 2002, Huang and Chang 2011) and transformed it into our TRY181 and *cho1Δ* lab strains. In both strains, Pma1-GFP is localized to the plasma membrane (Fig. 3.3). Our

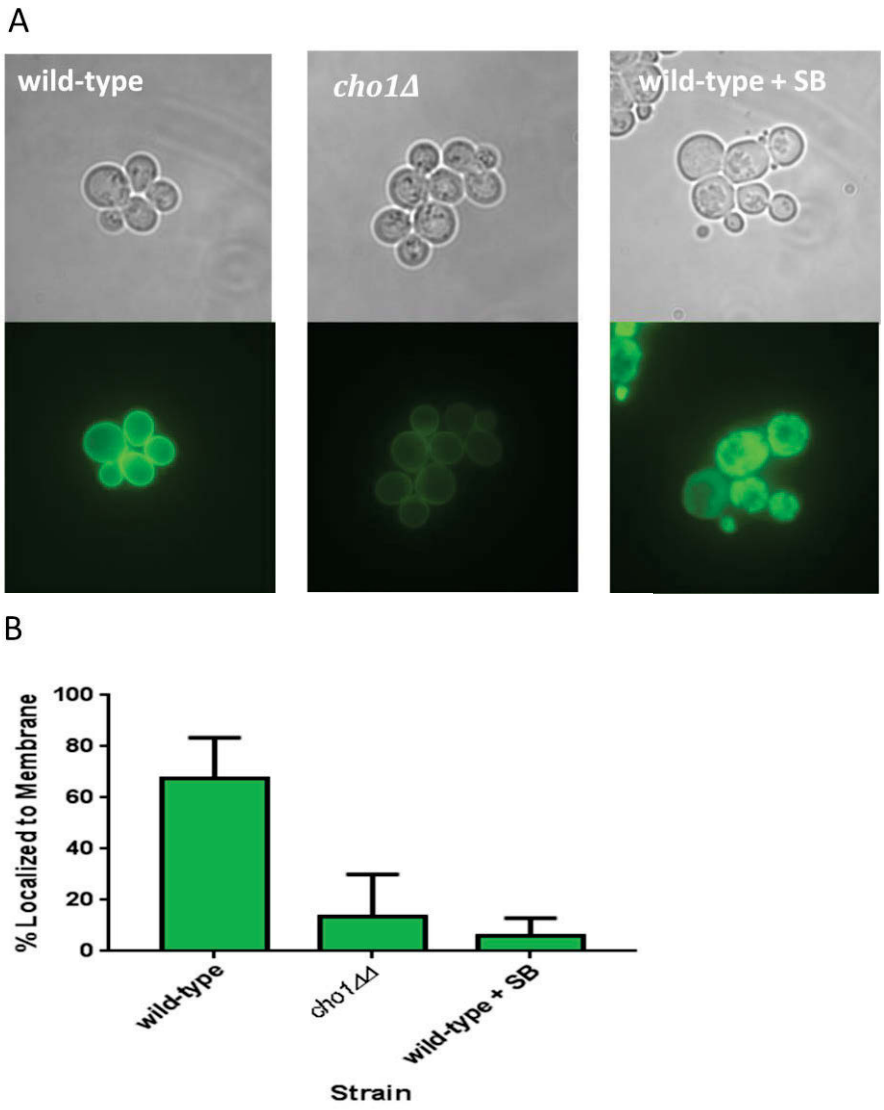

Figure 3. 2. SB-224289 Disrupts GFP-2x Ph(PLCδ) Localization to PI(4,5)P2

(A) Fluorescent micrographs of GFP-2x Ph(PLCδ) localization in *cho1Δ*, wild-type, or wild-type treated with SB-224289. (B) Quantification of GFP-2x Ph(PLCδ) localization to the plasma membrane in *cho1Δ*, wild-type, or wild-type treated with SB-224289.

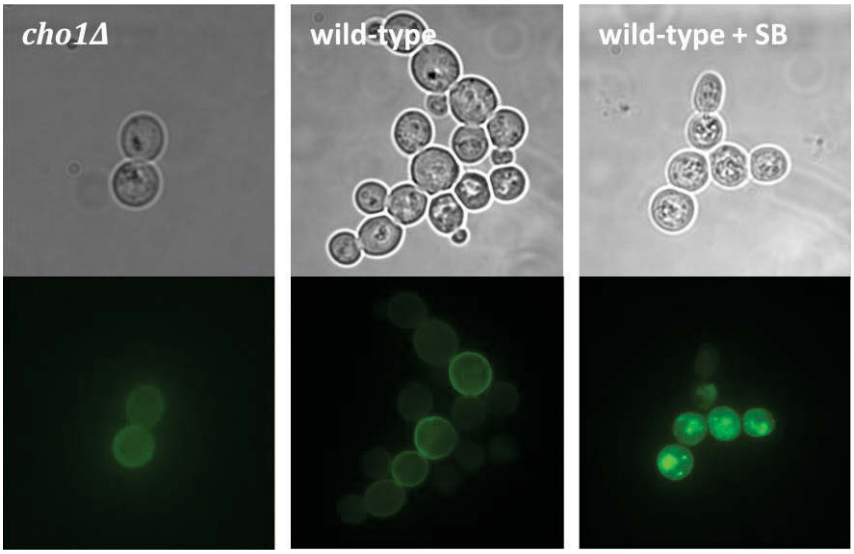

Figure 3. 3. SB-224289 Disrupts *CEN* PMA1-GFP Localization
Fluorescent micrographs of CEN PMA1-GFP localization in *cho1Δ*, wild-type, or wild-type treated with SB-224289.

hypothesis was that if the SB-224289 activity is specific to phospholipid trafficking, it would not affect the localization of Pma1-GFP. Interestingly, when the wildtype and *cho1Δ* were treated with 100 μM concentration of SB-224289, we saw a mislocalization of Pma1-GFP into intracellular punctate spots (Fig. 3.3). These findings led us to hypothesize that SB-224289 causes a disruption in normal trafficking of cellular material (i.e. endocytosis), instead of having a specific effect on phospholipid trafficking alone.

In order to test this hypothesis, we attempted to treat Pma1-GFP cells with 100 μM concentration of SB-224289 and then perform a western blot to compare expression of Pma1 protein to an untreated control. Our expectation was that if SB-224289 was causing an internalization of Pma1 that it would be degraded in the vacuole, causing a decrease in signal on the western blot. However, because of non-specificity of several GFP antibodies tested and the concentration of SB-224289 required for treatment, we were unable to detect differences in Pma1-GFP expression via western blot (data not shown).

Thus, we took a new approach to identify the pathway(s) targeted by SB-224289 activity. To do this, we screened a Whole Genome Mutant Library of *S. cerevisiae* against a lethal concentration of SB-224289 (50 μM at this cell concentration) in a 96 well plate format (Ryan, *et al*. 2012). Cells that survived the high dosage of SB-224289 were considered hits and re-screened against a serial dilution of SB-224289.

Of 3648 total strains tested, we found 96 resistant strains in the initial screen, resulting in a positive hit rate of 2.63% (Fig. 3.4). Of these initial hits, 27 mutant strains came out as true positive hits from the serial dilutions, resulting in a positive hit rate of 28.12% from the initial screen hits, or 0.74% from the total library. Although this project has not been fully completed and our results are speculation at this point, one possible target in particular (Rho5p) seemed to be connected to many of the other possible targets identified (Fig. 3.5) indicating that it may be inhibited or affected in some way by SB-224289.

Discussion

In this project, we utilized fluorescent markers to examine the effects of SB-224289 on localization of PS; PI4, 5P2; and Pma1p. In all cases, SB-224289 caused a re-distribution of the fluorescent probes away from the membrane into cytosolic or punctate spots (Figs 3.1 – 3.3). These findings demonstrate that SB-224289 has a physiological effect on yeast cells as opposed to prior conclusions that SB-224289 simply produced Pap-A resistance via physical compound-compound interactions. Based on the membrane probe disruption observed in our experiments, we hypothesized that SB-224289 might disrupt trafficking, (i.e. endocytosis) of cellular material.

In order to test this, we performed a large scale *S. cerevisiae* mutant library screen against a lethal concentration of SB-224289. We were able to identify a few possible targets of SB-224289. One target in particular seemed to have a connection to several of the other identified targets: a GTP-binding

Figure 3. 4. Screen of Mutant *S. cerevisiae* Library
Of 3648 total strains tested, 96 were resistant to 50 μM SB-224289, resulting in a positive hit rate of 2.63%. All mutants treated with SB-224289 are shown in navy and hits are shown above the arbitrary hit line of 0.5 OD_{600}. Negative control strains, treated only with DMSO, are shown in purple.

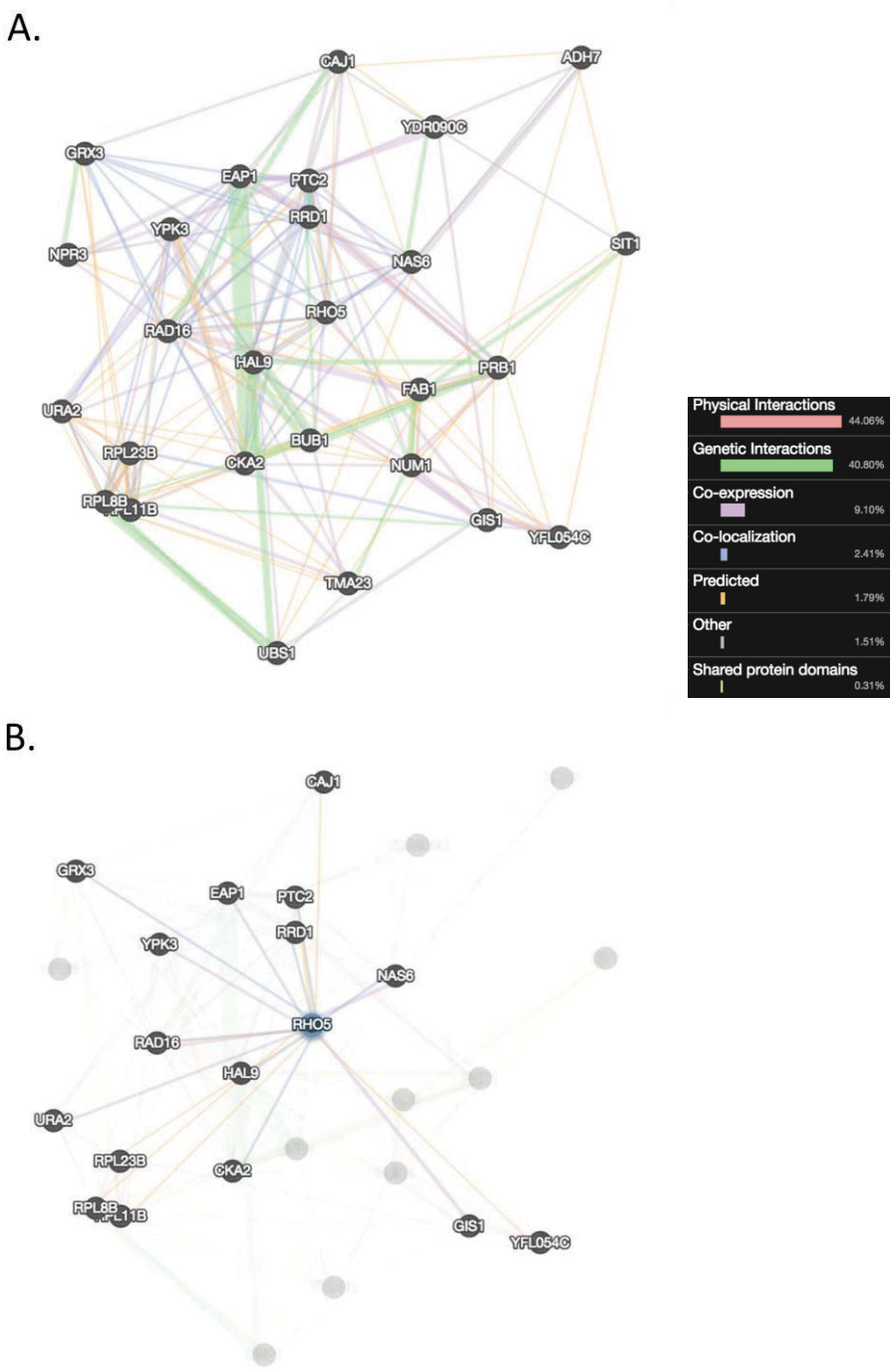

Figure 3. 5. Gene Maps Connecting True Hits from the Mutant Screen
(A) All hits from the screen (shown in Table 3.3) are shown mapped with connections to one another. (B) RHO5 demonstrates a great number of connections with several other identified targets, supporting the case that this could be a main target of SB-224289.

protein, Rho5p. Rho5p regulates a MAP kinase branch of the PKC1-mediated signal transduction pathway, which is globally important for yeast physiology (Schmitz, *et al*. 2002). Thus, it is possible that by targeting Rho5p, SB-224289 could interfere with this pathway and thus cause a disruption in normal celluar processes. However, because this is unconfirmed, these are only hypotheses that remain to be tested.

Currently we are in the process of transforming the true positive hit mutant strains of *S. cerevisiae* with the GFP-PMA1 and GFP-Lact-C2 probes to investigate how their localization differs with or without SB-224289 treatment. We are interested in both of these probes to assess whether SB-224289 continues to disrupt the localization of all components of the cell membrane by affecting certain proteins hypothesized as targets of SB-224289 function.

Further, we would like to analyze how SB-224289 might be impacting the localization of other proteins at the plasma membrane, like Ste2p. A GFP-tagged version of this lab has been produced in *S. cerevisiae* (Becker Lab) and we plan to treat this strain with SB-224289 to determine its effect on Ste2p.

Last, this project would also benefit by futher treating our fluorescent-probe-expressing strains of *S. cerevisiae* with compounds known to block endocytosis, like Latrunculin, to determine which facet of cellular trafficking specifically is affected by SB-224289 treatment.

Although this project does not have a firm conclusion, it furthers research into the mechanism of action of SB-224289. We also were able to optimize

conditions for the mutant library screen, to which SB-224289 appeared to be very sensitive. This screening approach could easily be translated for use against other compounds with unknown mechanisms of action.

References

Andersen MH, Graversen H, Fedosov SN *et al.,* Functional analyses of two cellular binding domains of bovine lactadherin. *Biochemistry* 2000;**39**: 6200-6.

Andjelic CD, Planelles V, Barrows LR. Characterizing the anti-HIV activity of papuamide A. *Mar Drugs* 2008;**6**: 528-49.

Balguerie A, Bagnat M, Bonneu M *et al.,* Rvs161p and sphingolipids are required for actin repolarization following salt stress. *Eukaryot Cell* 2002;**1**: 1021-31.

Cassilly CD, Maddox MM, Cherian PT *et al.,* SB-224289 Antagonizes the Antifungal Mechanism of the Marine Depsipeptide Papuamide A. *PLoS One* 2016;**11**: e0154932.

Chen YL, Montedonico AE, Kauffman S *et al.,* Phosphatidylserine synthase and phosphatidylserine decarboxylase are essential for cell wall integrity and virulence in *Candida albicans*. *Mol Microbiol* 2010;**75**: 1112-32.

Gietz RD, Woods RA. Transformation of yeast by lithium acetate/single-stranded carrier DNA/polyethylene glycol method. *Methods Enzymol* 2002;**350**: 87-96.

Huang C, Chang A. pH-dependent cargo sorting from the Golgi. *J Biol Chem* 2011;**286**: 10058-65.

Lemmon MA. Pleckstrin homology (PH) domains and phosphoinositides. *Biochem Soc Symp* 2007: 81-93.

Moser von Filseck J, Copic A, Delfosse V *et al.,* INTRACELLULAR TRANSPORT. Phosphatidylserine transport by ORP/Osh proteins is driven by phosphatidylinositol 4-phosphate. *Science* 2015;**349**: 432-6.

Ryan O, Shapiro RS, Kurat CF *et al.* Global gene deletion analysis exploring yeast filamentous growth. *Science* 2012;**337**: 1353-6.

Schmitt M, Schwanewilm P, Ludwig J *et al.,* Use of PMA1 as a housekeeping biomarker for assessment of toxicant-induced stress in *Saccharomyces cerevisiae*. *Appl Environ Microbiol* 2006;**72**: 1515-22.

Schmitz HP, Huppert S, Lorberg A *et al.,* Rho5p downregulates the yeast cell integrity pathway. *J Cell Sci* 2002;**115**: 3139-48.

Selkirk JV, Scott C, Ho M *et al.,* SB-224289--a novel selective (human) 5-HT1B receptor antagonist with negative intrinsic activity. *Br J Pharmacol* 1998;**125**: 202-8.

Shi J, Heegaard CW, Rasmussen JT *et al.,* Lactadherin binds selectively to membranes containing phosphatidyl-L-serine and increased curvature. *Biochim Biophys Acta* 2004;**1667**: 82-90.

Yeung T, Gilbert GE, Shi J *et al.,* Membrane phosphatidylserine regulates surface charge and protein localization. *Science* 2008;**319**: 210-3.

CHAPTER IV

MAPPING THE SUBSTRATE BINDING SITES IN THE PHOSPHATIDYLSERINE SYNTHASE IN *CANDIDA ALBICANS*

Contributing authors to this work include: Chelsi D. Cassilly,[1] Tanei J. Ricks,[2] Jerome Baudry,[3] Billy J. Carver,[1] Madison N. Steiner,[1] Michael D. Best,[2] Todd B. Reynolds[1]

[1] Department of Microbiology, University of Tennessee, Knoxville

[2] Department of Chemistry, University of Tennessee, Knoxville

[3] The University of Alabama, Huntsville

This article has not been published elsewhere at this time, nor will it be before completion of this ETD. The author contributions are as follows: Conceived and designed the experiments: CDC TJR JB BJC MDB TBR. Performed the experiments: CDC TJR JB BJC MNS TBR. Analyzed the data: CDC TJR BJC MDB TBR. Contributed reagents/materials/analysis tools: TBR MDB. Wrote the paper: CDC.

Abstract

The fungal phosphatidylserine (PS) synthase is required for virulence, conserved in fungi, but does not have a homolog in mammals, and thus represents a potential drug target in pathogenic fungi, such as *Candida albicans*. The substrate-binding sites of Cho1 have not been previously characterized, therefore we have performed biochemical characterization of this enzyme. Cho1 has two substrates: cytidyldiphosphate-diacylglycerol (CDP-DAG) and serine.

Previous studies in phospholipid biosynthetic enzymes from a variety of microorganisms have identified a conserved CDP-alcohol binding motif, known as the CAPT motif, which is also present within the sequence of *C. albicans* Cho1. Sequence alignments between PS synthase and phosphatidylinositol (PI) synthases from several microbes were used to identify a putative serine binding site as well. Alanine site directed mutagenesis of both motifs has defined the crucial residues within both motifs that are required for PS synthesis, but are not required for protein expression or stability. The results of this project will lead to more direct and rational approaches for finding Cho1 inhibitors, helping ultimately to identify more effective antifungals. In addition, these findings provide a greater understanding of enzymes involved in fungal phospholipid biosynthesis.

Introduction

The phosphatidylserine (PS) synthase enzyme in *Candida albicans* represents an excellent drug target for three reasons: 1) It is required for virulence (Chen, *et al*. 2010), indicating that inhibitors of this enzyme would render the organism incapable of causing infection; 2) it is absent in mammals (Braun, *et al*. 2005), so inhibitors potentially would have no toxic side effects for the host; and 3) it is conserved among many fungi, so a drug could potentially be effective against multiple fungal pathogens.

An important goal then is to discover an inhibitor of Cho1 that can be used as a lead compound for drug development. In order to better facilitate this, the

binding sites for the two substrates of Cho1, cytidyldiphosphate-diacylglycerol (CDP-DAG) and serine need to be described. Small molecule screening is very effective approach to identify inhibitors of enzymes (Cassilly, *et al*. 2016), but we are also interested in taking a more rational approach for identifying inhibitors. This included biochemically identifying substrate binding motifs. Identification of these sites in the protein can allow a more directed approach for identifying and modifying inhibitors via small molecule screening, which could ultimately increase chances of finding PS synthase inhibitors.

The PS synthase enzyme (originally denoted as: cytidine 5'-diphospho-1,2-diacyl-sn-glycerol: L-serine O-phosphatidyltransferase) was first identified in *Saccharomyces cerevisiae* in 1980 (Atkinson, *et al*. 1980a, Atkinson, *et al*. 1980c, Kovac, *et al*. 1980). Initial characterization of the yeast PS synthase included protein purification (Bae-Lee and Carman 1984, Letts, *et al*. 1983), determination of Michaelis-Menton kinetics (Bae-Lee and Carman 1984, Carman and Matas 1981, Carson, *et al*. 1982, Kovac, *et al*. 1980), understanding the regulation of Cho1 (Bae-Lee and Carman 1990, Bailis, *et al*. 1987, Carson, *et al*. 1982, Hromy and Carman 1986, Kelley, *et al*. 1988, Kinney and Carman 1988, Letts and Henry 1985, Poole, *et al*. 1986), and identifying the localization of the enzyme (Kohlwein, *et al*. 1988, Kuchler, *et al*. 1986b). Beyond the fungal PS synthase, characterization of bacterial PS synthases was also performed (DeChavigny, *et al*. 1991, Dowhan 2013, Dutt and Dowhan 1977, Dutt and Dowhan 1981, Dutt and Dowhan 1985, Ge and Taylor 1997, Kanfer and

Kennedy 1964, Okada, *et al*. 1994, Raetz and Kennedy 1972, Rilfors, *et al*. 1999). Within these studies, a distinction between the two subclasses of PS synthases was formed. Subclass I is present primarily in some Gram negative bacteria and subclass II is primarily found in Gram positive bacteria and yeast (Koonin 1996, Matsumoto 1997, Sohlenkamp, *et al*. 2004, Sung, *et al*. 1997). Last, characterization of mammalian PS synthases have also been performed, although these enzymes share little similarity to any microbial PS synthases, and indeed function by a completely different mechanism (Kuge and Nishijima 1997, Ohsawa, *et al*. 2004, Sturbois-Balcerzak, *et al*. 2001, Vance and Steenbergen 2005b).

A highly conserved motif, D-$(X)_2$-D-G-$(X)_2$-A-R-$(X)_2$-N-$(X)_5$-G-$(X)_2$-L-D-$(X)_3$-D, was identified in yeast phosphatidylinositiol synthase (PIS1), phosphatidylserine synthase (CHO1), and the *E. coli* phosphatidylglycerophosphate synthase (PGPS) (Gopalakrishnan, *et al*. 1986, Nikawa, *et al*. 1987a, Nikawa, *et al*. 1987b). This motif was further identified in yeast cholinephosphotransferase (CPT1) and ethanolaminephosphotransferase (EPT1) (Hjelmstad and Bell 1990, Hjelmstad and Bell 1991, McMaster and Bell 1994). All of these enzymes bind alcohols and CDP-alcohols, and catalyze the formation of a phosphodiester bond between the CDP-alcohols and the secondary alcohol (Hjelmstad and Bell 1990, Hjelmstad and Bell 1991). Subsequently, threonine and serine residues located within this motif in *E. coli* phosphatidylglycerolphosphate synthase (PGPS) and *Bacillus subtilis*

phosphatidylserine synthase (PSS), respectively, were mutated to proline to determine the importance of this motif. While not a part of the conserved motif itself, this amino acid change in both circumstances was non-conservative and decreased enzyme activity, supporting the hypothesis that this motif is crucial for enzyme function (Saha, *et al*. 1996, Usui, *et al*. 1994), although with the caveat that proline could be disrupting the secondary structure of the protein. Since these initial studies, this CDP-alcohol phosphatidyltransferase (CAPT) motif, was narrowed to D-G-$(X)_2$-A-R-$(X)_8$-G-$(X)_3$-D-$(X)_3$-D, and was identified to be almost invariably conserved in numerous other lipid biosynthetic enzymes, including those of Gram positive and Gram negative bacteria, archea, fungi, plants, and mammals (Dewey, *et al*. 1994, Dryden and Dowhan 1996, Matsumoto 1997, Matsuo, *et al*. 2007, Sohlenkamp, *et al*. 2004, Tanaka, *et al*. 1996). In 1998, Williams *et al.,* characterized the CAPT motif in yeast *CPT1* by alanine scanning mutagenesis which provided detailed importance of each residue within the conserved motif (Williams and McMaster 1998).

More recently, two enzymes from the CDP-alcohol phosphatidyltransferase family from *Archaeoglobus fulgidus* were shown to contain this motif on helices TM2 and TM3 of the solved crystal structures. In these studies, the CAPT motif was also widened to include an N-terminal aspartic acid, making the current, more general motif: D-$(X)_2$-D-G-$(X)_2$-A-R-$(X)_{7-12}$- G-$(X)_3$-D-$(X)_3$-D (Nogly, *et al*. 2014, Sciara, *et al*. 2014). This was further confirmed in the phosphatidylinositol-phosphate synthase from *Renibacterium*

salmoninarum where the CAPT motif was again found within TM2 and TM3 of the solved crystal structure (Clarke, *et al*. 2015). To our knowledge, these are the only three CDP-alchohol phosphatidyltransferase enzymes with solved crystal structures.

Based on the above studies there is sequence homology to guide a search for the CAPT motif in Cho1, but the motif specific for the other substrate, serine, is unknown. In fact, for many of the CDP-DAG binding enzymes such as PI synthase and PGP synthase, the binding sites for the non-CDP substrate are unclear. Thus, identification of the serine binding site—or some residues involved in serine binding, even if it is not the full motif—in Cho1 will facilitate a better understanding of this class of enzymes which are crucial for phospholipid biosynthesis in all kingdoms of life.

Previously we described the apparent K_m and V_{max} for PS synthase, as well as its role in the phospholipidome of *C. albicans*. Further, we probed the specificity of the active site of this protein for L-serine by competition assays with the closely related amino acids L-threonine and D-serine to an *in vitro* assay. We found that only very high concentrations of these substrates could compete with serine, indicating that the enzyme seems to be fairly specific for L-serine, which agrees with previous studies in *S. cerevisiae* and even *E. coli* (Bae-Lee and Carman 1984, Cassilly, *et al*. 2017, Kanfer and Kennedy 1964, Mitoma, *et al*. 1998). Although these studies provided important preliminary information, they

did not reveal insights into the active sites themselves. In the present communication, we map the substrate binding sites for Cho1p.

Materials and Methods

Strains and Media

In this study we used the *cho1*ΔΔ (YLC337) and *cho1*ΔΔ*::CHO1* (YLC344) mutants created within the SC5314 (wild-type) strain of *C. albicans,* which have been described previously (Chen, *et al*. 2010). The media used to culture strains was YPD (1% Bacto yeast extract, 2% Bacto peptone, and 2% dextrose (Thermo Fisher Scientific)) or minimal medium (0.67% yeast nitrogen base, 2% dextrose) supplemented with 1 mM ethanolamine where indicated (Guthrie 2002).

Genetic Cloning and Site-Directed Mutagenesis

The plasmid pYLC314 containing the *MET3* promoter (P_{MET3}) was generated by digesting pBluescript SK+ with *EcoRI* and ligating this to a PCR product carrying the *SAT1* marker and P_{MET3} generated from pYLC229 that is flanked by *EcoRI* sites that were created by primers JCO165 and JCO166 (Chen, *et al*. 2008). We also derived a vector from this one that lacks P_{MET3}, but retains the *SAT1* marker by digesting the plasmid with *PstI*, which cut on either side $P_{MET3,}$ to remove it, and then religated the vector to itself to create pBluescript-SAT1. The *CHO1* gene was amplified from SC5314 genomic DNA using primer CCO54, which sits 1000 bp upstream of *CHO1* start site and includes a 5' *XhoI* cut site, and CCO55

which sits at the 5' end of *CHO1* and includes a 3' 2x HA tag followed by an *AatII* cut site. The downstream region of *CHO1* was amplified using CCO56, which sits immediately downstream of the *CHO1* stop codon and contains a 5' *AatII* cut site followed by a 1x HA tag before the downstream sequence, and CCO57, which sits 500 bp downstream of the *CHO1* stop site and includes a 3' *HindIII* cut site. Once amplified, both fragments were double digested with their respective enzyme combinations. The plasmid pBluescript-SAT1 was digested with *XhoI* and *HindIII* and all three fragments were ligated together to create pCDC4.

Site-directed mutagenesis was performed using a primer based method. Forward and reverse primers approximately 35-40 bp in length were made for each mutation where the codon of interest was modified as conservatively as possible to produce alanine (Table 4.1). The plasmids were linearized with *MluI* prior to transformation into *cho1*$\Delta\Delta$ by electroporation. PCR products generated from isolated genomic DNA from all SDM *CHO1* transformant strains using primers CCO136 and CCO137 were sequenced using CCO105 or CCO20 to ensure that the genes were reintegrated correctly and that no spurious mutations had arisen.

To generate P_{MET3}-*PIS1*, a 3X FLAG tagged version of *PIS1* gene was amplified from pCDC21 using primers TRO1039 and TRO1043 which introduced *BamHI* and *NotI* sites, which were used to clone it into pYLC314 in front of the P_{MET3} promoter to produce pCDC27. For insertion of the putative PS synthase serine-binding motif into the *PIS1* sequence, primers CCO141 and CCO142 were

Table 4. 1. Primers Used in this Study.

Oligonucleotide	Sequence	Mutation
CCO20	GGAATCAAAAGATACTGTG	
CCO54	**aaaactcgag**CTGTAGAGCAGTTGGTTG	
CCO55	**aaaaGACGTC**ATAGGGATAGCCGGCATAGTCAGGAACAT CGTATGGGTAAACGGCCGC***TGGTTTAGGAATTTTTAAA GAT***	
CCO56	**aaaaGACGTC**CCGGACTATGCAGGATCCTATCCATATGA CGTTCCAGATTACGCTCCGGCCGCC***TAGAGATGATTCT AAAATAGAAT***	
CCO57	**aaaaaagctt**CAGAACCAGAATTATTGTTTC	
CCO58	GGGGTTATTTTTCGATTTTTTTGctGGTAGAGTTGCAAG	D128A
CCO59	CTTGCAACTCTACCagCAAAAAAATCGAAAAATAACCCC	D128A
CCO60	ATTTTTCGATTTTTTTGATGctAGAGTTGCAAGATTAAG	G129A
CCO61	CTTAATCTTGCAACTCTagCATCAAAAAAATCGAAAAAT	G129A
CCO62	TTTTTGATGGTAGAGTTGCAgctTTAAGAAATAAATCATC	R133A
CCO63	GATGATTTATTTCTTAAagcTGCAACTCTACCATCAAAAA	R133A
CCO64	ATAAATCATCATTAATGGctCAAGAGTTAGATTCATTAG	G142A
CCO65	CTAATGAATCTAACTCTTGagCCATTAATGATGATTTAT	G142A
CCO66	TAATGGGACAAGAGTTAGctTCATTAGCTGATTTGGTATC	D146A
CCO67	GATACCAAATCAGCTAATGAagCTAACTCTTGTCCCATTA	D146A
CCO68	GTTAGATTCATTAGCTGctTTGGTATCATTTGGGGTATC	D150A
CCO69	GATACCCCAAATGATACCAAagCAGCTAATGAATCTAAC	D150A
CCO82	GTTGGGGTTATTTTTCGcTTTTTTTGATGGTAGAGTTG	D125A
CCO83	CAACTCTACCATCAAAAAAAgCGAAAAATAACCCCAAC	D125A
CCO88	GGTTTTATGTGGATTAACA***gct***TTGGCTAGATTTAATATC	R186A
CCO89	GATATTAAATCTAGCCAA***agc***TGTTAATCCACATAAAACC	R186A
CCO90	GATTAACAAGATTGGCT***gct***TTTAATATCTCCGTC	R189A
CCO91	GACGGAGATATTAAA***agc***AGCCAATCTTGTTAATC	R189A
CCO94	GGTTTTATGTGGATTAACAAGA***gct***GCTAGATTTAATATC	L187A
CCO95	GATATTAAATCTAGC***agc***TCTTGTTAATCCACATAAAACC	L187A
CCO96	CAAGATTGGCTAGA***gc***TAATATCTCCGTCAATAAC	F190A
CCO97	GTTATTGACGGAGATATTA***gc***TCTAGCCAATCTTG	F190A
CCO105	CTCTCAGTATTGTTCAAAC	
CCO141	CTGATAACATAGCATACATATGCATATAAAATCTAGCCAA TCTTGTTAATCCACATAAAACCCAATGAGATGATAAATCT AAACTGACTAGT	
CCO142	ACTAGTCAGTTTAGATTTATCATCTCATTGGGTTTTATGT GGATTAACAAGATTGGCTAGATTTTATATGCATATGTATG CTATGTTATCAG	

used for site-directed mutagenesis to produce pCDC28. These plasmids were linearized with *XbaI* prior to transformation into *C. albicans cho1*ΔΔ by electroporation (Chen, *et al*. 2010). All plasmids and strains can be found in Tables 4.2 and 4.3, respectively.

Western Blots

Protein isolation and western blotting were performed with some modifications to previously published methods (Piispanen, *et al*. 2013) and according to the manufacturers' protocols (LI-COR). Cultures were grown overnight in 5 ml YPD, diluted to 0.1 OD_{600}/ml in 25 ml of YPD and allowed to grow until reaching early log phase (0.7 – 1 OD_{600}/ml). In the case of *PIS1*, the strains were grown overnight in minimal medium containing 1 mM ethanolamine until cultures reached log phase. Cultures were pelleted, washed with water and frozen overnight at -80°C. Pellets were then thawed on ice, resuspended in 1X PBS containing a protease inhibitor cocktail (Roche 4693124001) along with additional protease inhibitors (phenylmethylsuphonylfluoride (PMSF), leupeptin, and pepstatin (RPI P20270-5.0, L22035-0.005, P30100-0.005) and broken with 200 µl volume of glass beads (Sigma G1145-500G) in a bead-beater at 4°C for one minute six times, with one minute pauses in between. Samples were spun at 5,000 rpm for 1 minute to clear debris and transferred to a new tube on ice. Again, samples were cleared by spinning at 5,000 rpm for 8 minutes. This twice-

Table 4. 2. Plasmids Used in this Study

Plasmid	Inserts	Source
pYLC314-TBR	NAT^R, Amp^R	Lab Strain
pCDC4	NAT^R, Amp^R , *CHO1*	Shaner *et al.,* 2004
pCDC15	NAT^R, Amp^R , $CHO1^{D125A}$	Fairn *et al.,* 2011
pCDC8	NAT^R, Amp^R , $CHO1^{D128A}$	Lab Strain
pCDC14	NAT^R, Amp^R , $CHO1^{G129A}$	Addgene plasmid # 36092
pCDC10	NAT^R, Amp^R , $CHO1^{R133A}$	This study
pCDC12	NAT^R, Amp^R , $CHO1^{G142A}$	Lab Strain
pCDC11	NAT^R, Amp^R , $CHO1^{D146A}$	Lab Strain
pCDC9	NAT^R, Amp^R , $CHO1^{D150A}$	This study
pCDC23	NAT^R, Amp^R , $CHO1^{R186A}$	This study
pCDC24	NAT^R, Amp^R , $CHO1^{L187A}$	This study
pCDC22	NAT^R, Amp^R , $CHO1^{R189A}$	This study
pCDC25	NAT^R, Amp^R , $CHO1^{F190A}$	This study
pYLC314	*pMET3*, NAT^R, Amp^R	Joseph Chen, Reynolds Lab

Table 4. 3. Strains Produced in this Study.

Organism	Marker	Plasmid	Gene/Mutation	Name
C. albicans	Nourseothricin	pCDC4	CHO1-HAx3	CDCS59
C. albicans	Nourseothricin	pCDC15	CHO1-HAx3^{D125A}	CDCS60
C. albicans	Nourseothricin	pCDC8	CHO1-HAx3^{D128A}	CDCS61
C. albicans	Nourseothricin	pCDC14	CHO1-HAx3^{G129A}	CDCS62
C. albicans	Nourseothricin	pCDC10	CHO1-HAx3^{R133A}	CDCS63
C. albicans	Nourseothricin	pCDC12	CHO1-HAx3^{G142A}	CDCS64
C. albicans	Nourseothricin	pCDC11	CHO1-HAx3^{D146A}	CDCS65
C.albicans	Nourseothricin	pCDC9	CHO1-HAx3^{D150A}	CDCS66
C. albicans	Nourseothricin	pCDC23	CHO1-HAx3^{R186A}	CDCS67
C. albicans	Nourseothricin	pCDC24	CHO1-HAx3^{L187A}	CDCS68
C. albicans	Nourseothricin	pCDC22	CHO1-HAx3^{R189A}	CDCS69
C.albicans	Nourseothricin	pCDC25	CHO1-HAx3^{F190A}	CDCS70

cleared supernatant was moved to fresh tubes on ice and a Bradford assay was performed to determine protein concentration.

Proteins were separated by SDS-PAGE. 40 µg of protein per sample were loaded into the wells of a 6% stacking/10% separating gel and run at 35 mAmps, followed by transfer to PVDF membranes (926-31099 LI-COR) using a blot module (GE Healthcare Life Sciences 80-6418-96) for one hour at 400 mAmps. Membranes were dried for one hour at room temperature, blocked using TBS:Odyssey Blocking Buffer (1:1) (927-50100 LI-COR), and incubated overnight at 4˚C in TBST:Odyssey Blocking Buffer (1:1) with primary antibodies according to the tag (HA.11; Covance (Reynolds, *et al*. 2008) or FLAG 637301; BioLegend 637301). The following day, after 4 washes in TBST at room temperature, membranes were incubated with IRDye® 680RD Goat-anti-Rat (926-68076) or IRDye® 800CW Goat-anti-Mouse (926-32210) secondary antibodies (LI-COR) at room temperature for at least one hour. Membranes were then washed 4x with TBST and then imaged using a LI-COR Odyssey scanner.

In vitro PS Synthase Assay

The PS Synthase assay was performed as described previously in (Cassilly, *et al*. 2017) with the exception that the 37°C incubation times were increased to 45 minutes.

Protein Pull Down

Protein was isolated as partially described in (Graham, *et al*. 1994) by growing 200 ml YPD cultures to approximately 1.5 to 2.5 OD_{600}/mL. Samples were centrifuged at 3,300 rpm for 5 minutes, then resuspended in 20 ml YPD (approximately 18 - 20 OD_{600}/mL). Protease inhibitors (phenylmethylsuphonyl fluoride, leupeptin and pepstatin), 50 mM HEPES buffer, and 40 mM β-mercaptoethanol (BME) was added. Zymolyase (~100 ug/ml) (120493-1 AmsBio) was added and cultures were shaken at 37°C for 1 hour. Resulting spheroplast cultures were centrifuged at 3,300 rpm for 5 min. Pellets were washed with spheroplasting buffer (1 M sorbitol, 20 mM Tris-HCl pH 7.5), then resuspended in approximately 5 ml resuspension buffer (1 M sorbitol, 10 mM triethanolamine pH 7.5, 1 mM EDTA) and stored at –80°C.

The next day, cells were lysed using osmotic lysis (Graham, *et al*. 1994). Pellets were thawed on ice and then 20 ml of lysis buffer (0.1 M sorbitol, 10 mM triethanolamine pH 7.5, 1 mM EDTA) was added, sitting for 5 min. Dounce homogenization (>30 strokes) was then used on ice to break cells further. Homogenate was centrifuged at 4°C for 6 min at 1000 xg to clear unbroken cells. Supernatant was spun at 27,000× g for 10 min at 4°C and pellets were resuspended in residual liquid after eluting the supernatant. The thick mixture was mini-homogenized to break clumps. Last a Bradford assay was performed to quantify protein.

The protein pull-down was described in part as in (Hauser, *et al*. 2007). 2.5 mg of *cho1ΔΔ::CHO1-HAx3* and *cho1ΔΔ::CHO1* protein was incubated at 37°C with 0.1 mM L-serine and 25 mM cysteine analog for 30 minutes. There was also an untreated control for both *cho1ΔΔ::CHO1-HAx3* and *cho1ΔΔ::CHO1.* Following this incubation, the protein was solubilized in RIPA buffer (1X TBS, 0.1% SDS, 1% Triton X-100) overnight, rotating at 4°C. The next day, according to the manufacturer's protocol, Anti-HA magnetic beads (Pierce PI88836) were washed 2x in TBS-T (500 mM Tris Base, 1.5 M NaCl, pH 7.5, 0.05% Tween-20) using a magnetic stand. The beads were then added to the protein samples and again incubated overnight, rotating at 4°C. The following day, the samples were washed with RIPA buffer 4-5x. The samples were then washed 4x with TBS to remove all detergent. Samples were stored at 4°C or given directly for MS/MS analysis.

Homology Modeling

The homology model was produced using Molecular Operating Environment (MOE) software. A Protein Data Bank (PDB) search was performed using the Cho1 protein sequence, and was found to have at least 25% sequence similarity to the three published crystal structures in (Clarke, *et al*. 2015, Nogly, *et al*. 2014, Sciara, *et al*. 2014). Several homology models were produced using each of the three crystal structures as templates. The final homology model of Cho1p presented in this manuscript was produced by threading the sequence of Cho1p

onto AF2299, a CDP-alcohol phosphotransferase, which had approximately 32.4% sequence similarity and 18.7% sequence identity with Cho1p (using the EMBOSS Stretcher alignment tool).

Statistical Analysis

All statistical analysis was performed on GraphPad Prism 7 using a student's t-test.

Results

The CDP-alcohol phosphatidyltransferase (CAPT) binding motif (D-G-$(X)_2$-A-R-$(X)_8$-G-$(X)_3$-D-$(X)_3$-D) is almost invariably conserved in enzymes binding CDP-alcohols even across kingdoms (Table 4.4), indicating the importance of this motif in the function of these types of enzymes (Okada, *et al*. 1994). One exception lies in some Gram negative bacteria, such as *E. coli*, where this motif is not present within certain enzymes (e.g. Pss) binding CDP-DAG, indicating divergence (Matsumoto 1997).

Previously Williams *et al.,* performed detailed site directed mutagenesis on the CAPT motif in *CPT1* cholinephosphotransferase in *S. cerevisiae* (Table 4.4). They found that mutation of Gly114, Gly127, Asp131, and Asp135 caused loss of activity while mutants of Ala117 and Arg118 showed a decrease in activity, and Asp113 showed wild-type activity (Williams and McMaster 1998). Using *S. cerevisiae* Cpt1 as a guide, we tested whether amino acids conserved in the

Table 4. 4. CAPT Motif Largely Conserved in Enzymes Binding CDP-Alcohols Across Kingdoms

Organism	Enzyme	CDP-Binding Motif	Reference
C. albicans	PS Synthase	DFFDGRVARLRNKSSLMGQELDSLAD	This research
C. albicans	PI Synthase	DAFDGYAARKFNQGTRFGAVLDMVTD	This research
C. parapsilosis	PS Synthase	DFFDGRVARLRNKSSLMGQELDSLAD	This research
C. glabrata	PS Synthase	DFFDGRVARLRNRSSLMGQELDSLAD	This research
S. cerevisiae	PS Synthase	DFLDGRVARLRNRSSLMGQELDSLAD	Takeda *et al.,* 2014; Matsuo *et al.,* 2007
S. cerevisiae	CPT	DMHDGMHARRTGQQGPLGELFDHCID	Williams *et al.,* 1998
S. pombe	PS Synthase	DFLDGKVARWRGKSSLMGQELDSLAD	Matsuo *et al.,* 2007
B. subtilis	PS Synthase	DFFDGMAARKLNAVSDMGRELDSFAD	Okada *et al.*, 1994
R. salmoninarum	PIP synthase	DIIDGLMARLLFREGPWGAFLDSYLD	Clarke *et al.*, 2015
S. meliloti	PS Synthase	DGIDGRIARLLKATSSFGVQMDSLAD	Sohlenkamp *et al.*, 2003; KEGG *Sinorhizobium meliloti* 1021
A. fulgidus	CDP-alcohol phosphotransferase AF2299	DGCDGEIARLKFMESKYGAWLDGVLD	Sciara *et al.,* 2014
A. fulgidus	IPCT-DIPPS	AYYDGWIAREINRKVSLRISRL—LAD	Nogly *et al.*, 2014

* gray highlighted residues represent the conserved amino acids

CAPT motif of multiple enzymes shown in Table 4.4 were important for catalysis in the *Candida albicans* PS synthase using alanine site directed mutagenesis.

We generated an HAx3-tagged version of the *CaCHO1* on a SAT1 marked plasmid and integrated it into the *cho1*ΔΔ mutant genome. Transformants were screened for expression of Cho1-HAx3 by Western blot (Fig 4.1A) and the ability of a representative transformant expressing Cho1-HAx3 expression to complement *cho1*ΔΔ for PS synthase enzyme activity was tested. Cho1-HAx3 restored PS synthase activity to the *cho1*ΔΔ strain (Fig. 4.1B). In addition, the *CHO1-HAx3* gene was able to at least partially restore growth to *cho1*ΔΔ on minimal medium lacking ethanolamine (data not shown).

It should be noted that several bands were observed that bound to an anti-HA antibody, but none of these were present in the *cho1*ΔΔ control (Fig. 4.1B). We suspect that the band at 34 KDa is the full-length protein, which correlates with the predicted molecular weight of 34.8 KDa. Proteolytic maturation of enzymes is a well-documented phenomenon (Hartmann, *et al*. 2014) and previous studies found similar findings with the PS synthase in *S. cerevisiae* (Choi, *et al*. 2010, Dey, *et al*. 2017, Kinney and Carman 1988), showing a 30 KDa band and a 23 KDa band in western blot analysis. Although our band sizes differ (36, 34, and 29 KDa), we do see a difference of 7 KDa between our largest band and our smallest, which matches with what has been seen in *S. cerevisiae*. These previous studies found that the 30 KDa band was likely proteolytically degraded to produce the 23 KDa band, but that both forms of the protein were

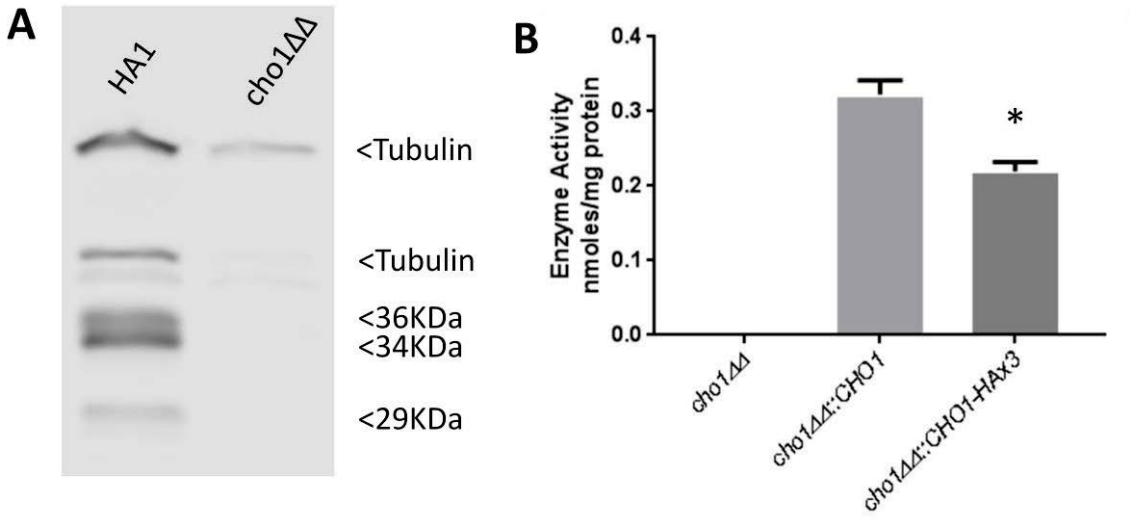

Figure 4. 1. Enzyme Activity and Expression of Cho1p-HAx3
(A) Western blot showing expression of Cho1p-HAx3 (HA1) as compared to a negative control. Several bands are present, possibly indicating degradation (29 KDa) or phosphorylation of Cho1p (36 KDa). (B) Protein was collected from *cho1ΔΔ*, *cho1ΔΔ::CHO1-HA*, *cho1ΔΔ::CHO1-HAx3* and used in an *in vitro* PS synthase assay. A small, but statistically significant decrease is seen in the HAx3 tagged version of Cho1p. * p = 0.0013

active (Kinney and Carman 1988, Kohlwein, *et al*. 1988).

Confirmation of the CAPT-Motif's Importance in Enzyme Activity

We performed site-directed mutagenesis of the non-alanine residues in the CAPT motif. Each residue was mutated to alanine within the *CHO1-HAx3* in the pCDC4 plasmid as described in materials and methods. The mutant plasmids were transformed into *cho1ΔΔ*, checked for correct reintegration by PCR and then colonies representing each mutation were screened for those that showed expression of Cho1-HAx3 similar to wild-type by western blot (Fig. 4.2, Table 4.5). Membranes were isolated from each of the amino acid substitution mutants, along with *cho1ΔΔ::CHO1-HAx3* and *cho1ΔΔ* controls, to assess activity of each mutant protein by the *in vitro* PS synthase assay. In contrast to the findings in the CAPT domain from *S. cerevisiae* Cpt1p (Williams and McMaster 1998), the D125A, D128A, G142A, and D146A from the Cho1 PS synthase CAPT motif showed 0% of Cho1p-HAx3 activity. G129A and D150A showed 4% and 67.5% of the Cho1p-HAx3 activity, respectively (Fig. 4.3). The R133A mutant originally showed decreased activity, however this reintegrated plasmid also showed lower expression levels by western blot, so, we performed another enzyme assay on a highly expressed R133A mutant and found that activity correlated with expression, leading us to believe that R133A does not significantly impact the activity of Cho1p-HAx3 (Fig. 4.3, data not shown).

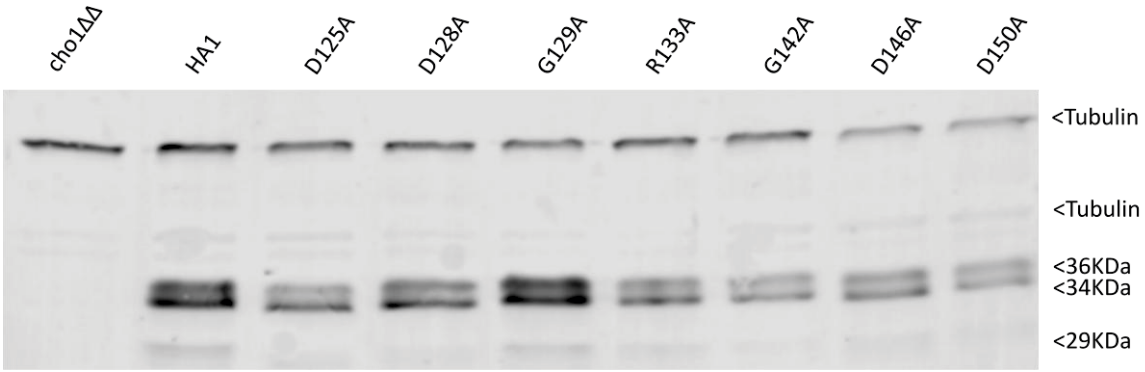

Figure 4. 2. Expression of Cho1p-HAx3 CAPT Motif Mutants
Protein was collected from *cho1ΔΔ*, *cho1ΔΔ::CHO1-HAx3* (HA1) and each CAPT motif point mutant used in a western blot to assess expression. Expression from two western blots per mutant were quantified against tubulin standards using Image J and the average was taken to determine approximate expression values (shown in Table 4.5).

Table 4. 5. Average (AVG) expression via western blotting (WB) CAPT motif (top) and predicted serine binding motif (bottom) mutants

Strain	WB#1	WB#2	AVG	% WT
cho1ΔΔ	1.724	0.887	**1.3055**	**4.3**
HA1	31.685	28.325	**30.005**	**100**
D125A	36.884	18.863	**27.874**	**93**
D128A	67.666	27.896	**47.781**	**159**
G129A	131.73	53.005	**92.368**	**308**
R133A	16.29	20.702	**18.496**	**62**
G142A	20.758	13.762	**17.26**	**58**
D146A	14.069	35.931	**25**	**83**
D150A	26.714	24.955	**25.835**	**86**
cho1ΔΔ	0.061	0.1421	**0.1015**	**0.9**
HA1	3.1951	20.359	**11.777**	**100**
R186A	3.4295	14.435	**8.9324**	**81**
L187A	2.1733	12.09	**7.1315**	**65**
R189A	1.7103	19.024	**10.367**	**95**
F190A4	1.3978	17.989	**9.6934**	**88**

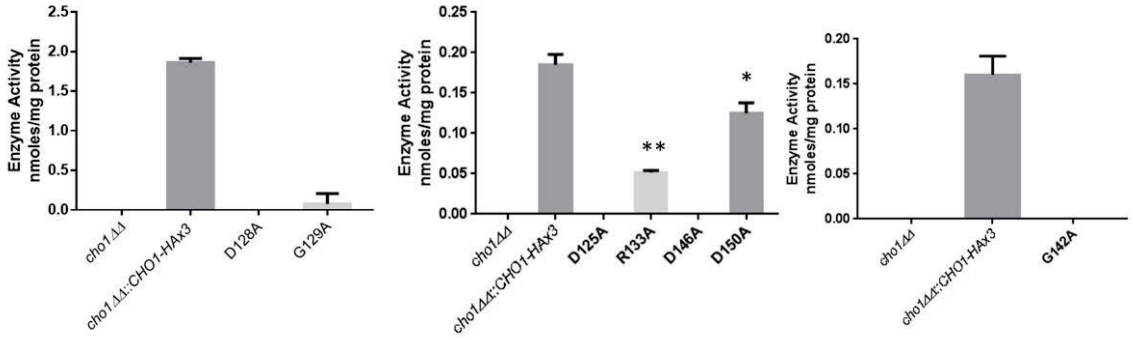

Figure 4. 3. Enzyme Activity of Cho1p-HAx3 CAPT-Motif Mutants
Protein was collected from *cho1ΔΔ*, *cho1ΔΔ::CHO1-HA*, *cho1ΔΔ::CHO1-HAx3* and each of the CAPT motif point mutants and used in an *in vitro* PS synthase assay. All mutants show statistically significant decrease or abolishment of activity. * $p = 0.0046$, ** $p = 0.0016$, all other = $p < 0.0003$

Assessment of Predicted Serine Binding Motif's Role in Enzyme Activity

In addition to CDP-DAG, Cho1 also binds serine as a substrate, and we were interested in determining the serine binding site of Cho1. The serine binding site is of particular interest in this study as CDP-DAG binding is common to several enzymes that bind CDP-alcohols, whereas the serine binding site is more specific to this enzyme.

However, unlike the CAPT motif, there is little known, to our knowledge, about where serine binds in Cho1. Previous work on the mammalian PS synthase, PSS1, identified an asparagine (Asn-209) residue as likely playing a role in serine binding or recognition (Ohsawa, *et al*. 2004). However, as the Cho1 protein from *C. albicans* shares little amino acid similarity with mammalian PSS1, and in sequence alignment, a corresponding Asn-209 residue is entirely absent within *CHO1*, this informed our search relatively little.

We took a two-pronged approach to identify where serine might bind in Cho1. PI synthase and PS synthase from yeast are similar enzymes in that both bind CDP-DAG and a small molecule as substrates to generate their respective phospholipids. *Candida albicans* Pis1 shares 28.5% amino acid similarity with Cho1 and only differs enzymatically in binding inositol instead of serine. We hypothesized that alignment and comparison of sequences between the two genes might reveal a conserved serine binding site in Cho1. We aligned the Pis1 amino acid sequences from *C. albicans*, *Saccharomyces cerevisiae*, and *Schizosaccharomyces pombe* with the Cho1 amino acid sequence from the

same organisms (Fig. 4.4). From this alignment, we found a highly conserved sequence in all of the PS synthase linear sequences that was entirely absent from the Pis1 linear sequences (X-V-L-C-G-L-X-R-L-A-R-F). We predicted that this might be part of the serine binding motif. Site directed mutagenesis of the latter portion of the motif was performed as described previously for the CAPT motif. We screened for colonies with roughly equal average expression of mutant forms of *CHO1-HAx3* compared to the *cho1ΔΔ::CHO1-HAx3* background strain (Fig. 4.5A, Table 4). We isolated membranes from each mutant and the control (wild-type and *cho1*ΔΔ) strains and performed an *in vitro* PS synthase assay to compare them. Each mutated residue in the latter portion of this motif demonstrated a complete abolishment of activity as assayed in our *in vitro* enzyme experiment with the exception of F190A which showed 59% of the background activity (Fig. 4.5B).

Homology Model Predicting Cho1p Structure

Cho1 is a membrane protein that has not yet been crystalized. However, there are several CDP-alcohol binding phospholipid biosynthetic proteins that have been crystalized recently. Using Molecular Operating Environment software, we threaded the sequence of *CHO1* onto the solved crystal structures of these proteins: two archeal and one bacterial membrane-bound proteins with CAPT motifs (Clarke, *et al*. 2015, Nogly, *et al*. 2014, Sciara, *et al*. 2014). This experiment produced a homology model that demonstrates the close proximity of

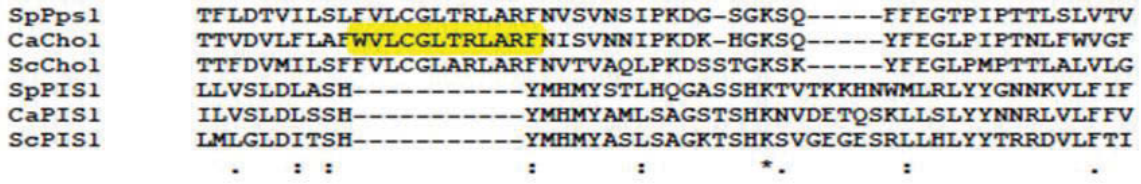

Figure 4. 4. Sequence Alignment Reveals Possible Serine Binding Motif
Alignment of a portion of the PS synthases and PI synthases from *C. albicans*, *S. cerevisiae*, and *S. pombe*. Highly conserved sequence, hypothesized to be serine binding site in PS synthases, is highlighted in yellow.

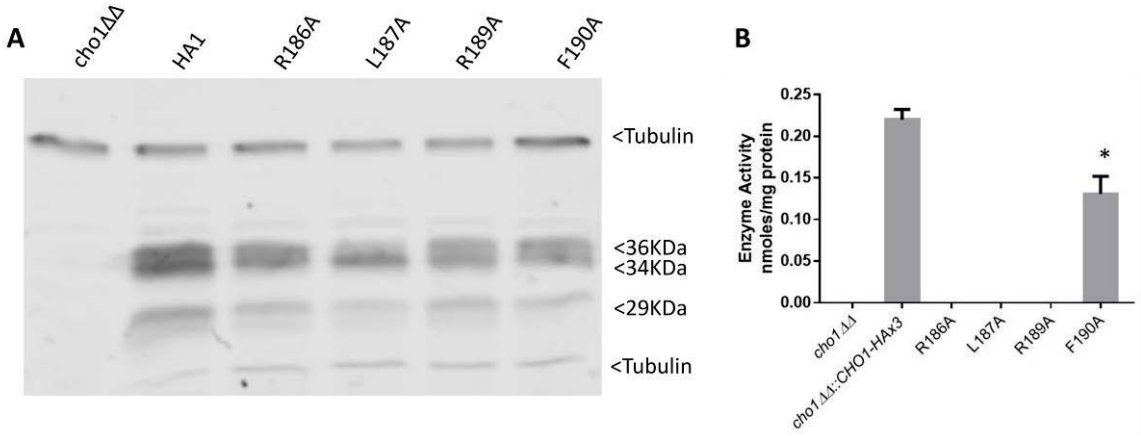

Figure 4. 5. Expression and Enzyme Activity of Cho1p-HAx3 Predicted Serine Binding Motif Mutants

(A) Protein was collected from *cho1ΔΔ*, *cho1ΔΔ::CHO1-HAx3* (HA1) and each predicted serine binding motif point mutant used in a western blot to assess expression. Expression from two western blots per mutant were quantified against tubulin standards using Image J and the average was taken to determine approximate expression values (shown in Table 4.5). (B) Protein was collected from *cho1ΔΔ*, *cho1ΔΔ::CHO1-HA*, *cho1ΔΔ::CHO1-HAx3* and each of the predicted serine motif point mutants and used in an *in vitro* PS synthase assay. All mutants show statistically significant decrease or abolishment of activity. * $p = 0.0032$, all other = $p < 0.0001$

the serine binding site (yellow) with the CAPT motif (cyan) (Fig 4.6). These data further support the findings in our experimental work.

Discussion

In this study we found that most of the amino acids in the predicted CAPT motif in *C. albicans* Cho1-HAx3 are necessary for PS synthesis. However, there were some differences from what has been observed in the CAPT motifs from some other enzymes. For example, as opposed to the findings in *S. cerevisiae* Cpt1 (Williams and McMaster 1998), only mutations of Asp125, Asp128, Gly142, and Asp146 caused loss of activity, while mutations of Gly129 and Asp150 showed a severe to modest decrease in activity, and Arg133 showed nearly wild-type level activity (Fig. 4.3). In the Cpt1 enzyme from *S. cerevisiae,* Williams *et al.,* published that replacing Gly114, Gly127, Asp131, and Asp135 with alanine abolished enzyme activity, while Ala117 and Arg118 mutants displayed decreased activity and mutation of Asp113 had no detectable effect on enzyme function (Williams and McMaster 1998). Williams and McMaster noted that, because the amino acid glycine does not have a functional group, it is possible that the importance of the glycine residues could be steric and control binding or positioning of the substrates. Further, the alanine and arginine residues within the Cpt1 CAPT motif were predicted to be important in binding and positioning of the CDP-alcohol substrate (Williams and McMaster 1998).

Figure 4. 6. Predicted Structure of Cho1p Based on Homology Modeling
(A) Cho1p amino acid sequence was threaded onto the crystal structure of the AF2299 CDP-alcohol phosphotransferase (PDB accession number 4O6N via Clarke *et al*., 2014) using Molecular Operating Environment 2015.1 software. The CAPT motif is shown in cyan and the predicted serine binding motif is shown in yellow. (B) Shows a closer view of the proximity of the CAPT motif to four amino acids of the predicted serine binding site.

A

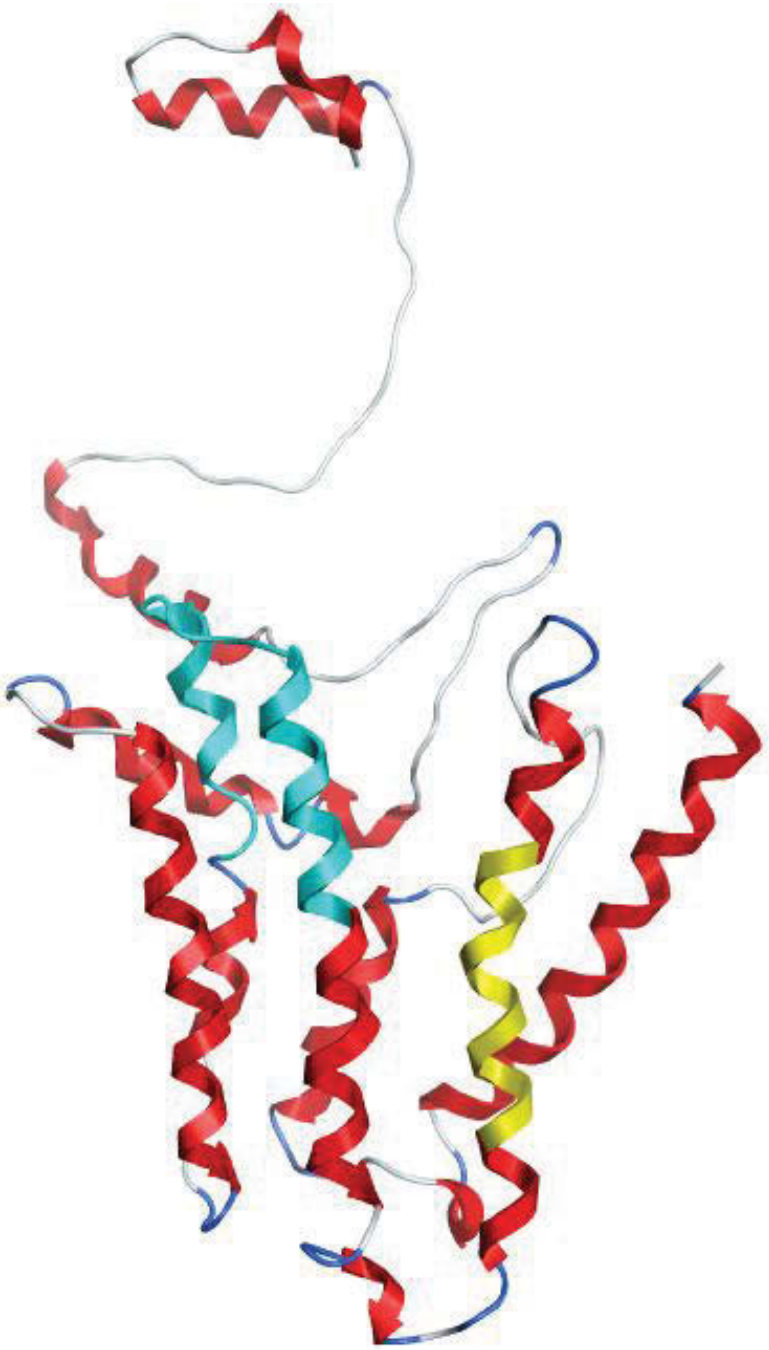

Figure 4.6 continued

B

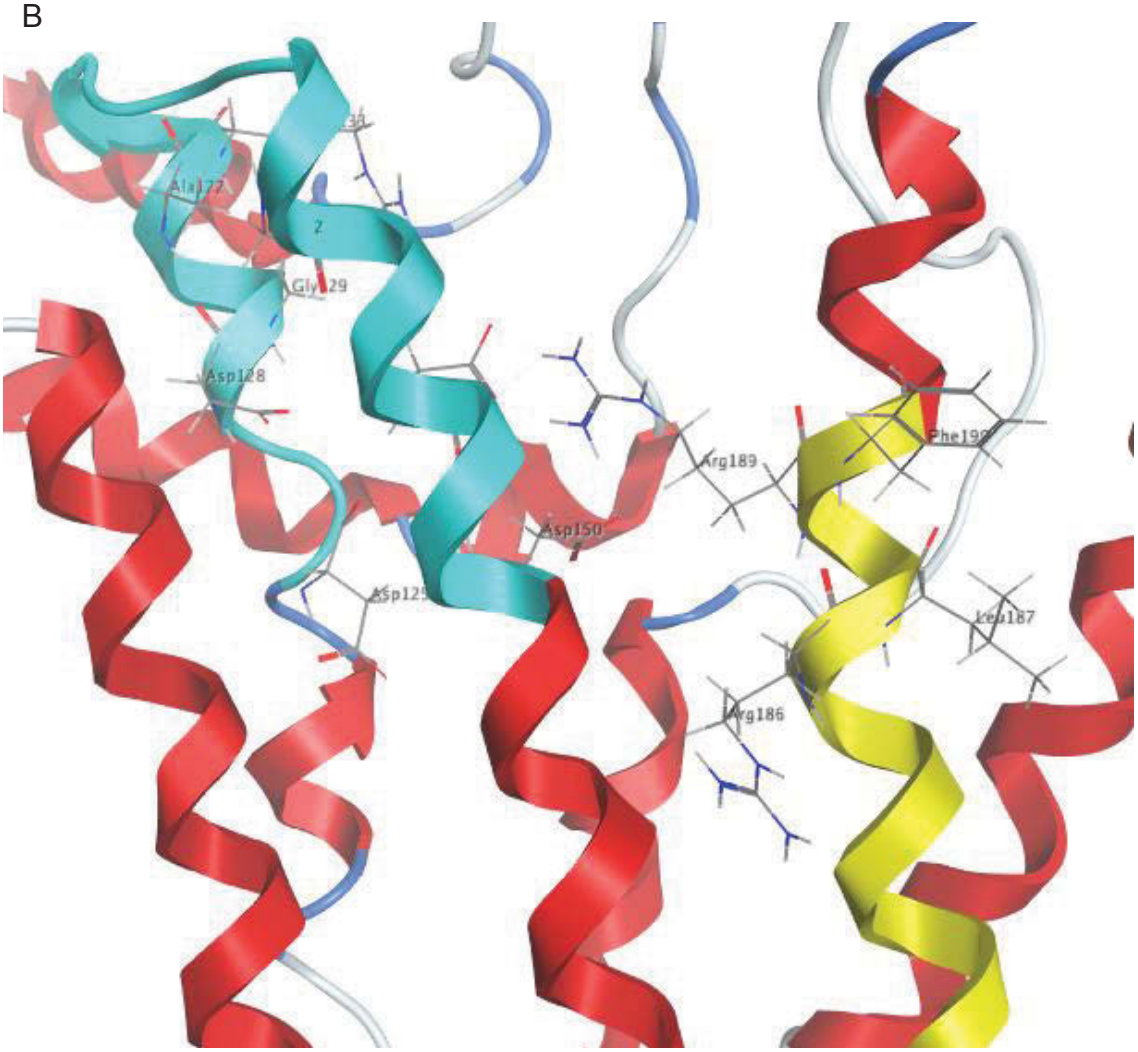

Figure 4.6 continued

Last, the final two aspartic acid residues within the yeast Cpt1 were identified as probable catalytic residues (Williams and McMaster 1998). Within *C. albicans* Cho1p-HAx3, we did not see a severe loss of activity for the D150A mutation, which was the case for the second aspartic acid in the motif in yeast *CPT1*. As a result, we suspect the catalytic residue in *C. albicans* Cho1p is one of the three remaining aspartic acids: D125, D128, or D146. Despite the slight differences between our findings and those of the yeast *CPT1*, which is not totally unexpected given the difference in substrate and organism, our data supports and confirms the importance of the CAPT motif in proper enzyme function of Cho1p in *C. albicans* (Williams and McMaster 1998).

In addition to confirming the importance of the predicted CAPT motif in Cho1, we predicted a possible serine-binding motif based on sequence alignment from three different yeasts. This motif, X-V-L-C-G-L-X-R-L-A-R-F, is highly conserved across PS synthase orthologs in these organisms, while it is entirely absent from the Pis1p enzymes of the same three organisms (Fig. 4.4). Site directed mutagenesis of the latter four residues in the motif produced an almost complete abolition of activity. The only exception was the F190A mutation which statistically significantly decreased activity, but only to 59% that of the background strain (Fig. 4.5B). Although from these results we cannot say for certain whether our mutations are affecting substrate binding, catalysis, or protein stability/folding, it is clear that this sequence is critical for enzyme function.

In order to gain some insight into how these motifs might be arranged relative to one another, we produced a homology model of Cho1. This homology model, created by threading Cho1 sequence on the solved structures of other membrane-bound CAPT-motif-containing proteins (Clarke, *et al*. 2015, Nogly, *et al*. 2014, Sciara, *et al*. 2014), has provided at least a preliminary view of what Cho1 might look like. The model predicts a six-transmembrane domain protein structure with relatively close proximity of the predicted substrate binding sites. Many of the residues within the CAPT motif are charged and have been found to be part of a hydrophilic face of the 2nd and 3rd transmembrane domains of this protein (Saha, *et al*. 1996). This correlates well with the homology model which shows the CAPT motif spanning TM (2/3). The predicted serine-binding motif (yellow) is located deep within the hypothesized membrane-bound portion, but it is possible that there is a hydrophilic core that might allow substrate entry into this site. This correlates well with the hypothesis that *C. albicans* Cho1 has a cytosolic-facing hydrophilic core where substrates bind, which has been demonstrated in PIS1 in yeast (Bochud and Conzelmann 2015). There is a long, unstructured N-terminus that is predicted to be soluble and is likely important for proper membrane insertion, although this has yet to be confirmed in *C. albicans* (Sperka-Gottlieb, *et al*. 1990).

We have demonstrated here, for the first time, the importance of the CAPT motif within the PS synthase from a medically-relevant, pathogenic fungus. Further, we have begun efforts to identify binding location of the second

substrate in this reaction, an area that is still relatively unstudied. We have produced a homology model of Cho1p that places both of the substrate binding sites in close proximity. These findings contribute not only to the general understanding of phospholipid synthesizing enzymes, but also provide crucial information on candidate locations of this protein where binding of small molecules may inhibit activity. Because Cho1p represents such a promising drug target, this data may lead to a more refined approach for discovering inhibitors.

References

Atkinson K, Fogel S, Henry SA. Yeast mutant defective in phosphatidylserine synthesis. *J Biol Chem* 1980a;**255**: 6653-61.

Atkinson KD, Jensen B, Kolat AI *et al.,* Yeast mutants auxotrophic for choline or ethanolamine. *J Bacteriol* 1980b;**141**: 558-64.

Bae-Lee M, Carman GM. Regulation of yeast phosphatidylserine synthase and phosphatidylinositol synthase activities by phospholipids in Triton X-100/phospholipid mixed micelles. *J Biol Chem* 1990;**265**: 7221-6.

Bae-Lee MS, Carman GM. Phosphatidylserine synthesis in *Saccharomyces cerevisiae*. Purification and characterization of membrane-associated phosphatidylserine synthase. *J Biol Chem* 1984;**259**: 10857-62.

Bailis AM, Poole MA, Carman GM *et al.,* The membrane-associated enzyme phosphatidylserine synthase is regulated at the level of mRNA abundance. *Mol Cell Biol* 1987;**7**: 167-76.

Bochud A, Conzelmann A. The active site of yeast phosphatidylinositol synthase Pis1 is facing the cytosol. *Biochim Biophys Acta* 2015;**1851**: 629-40.

Braun BR, van Het Hoog M, d'Enfert C *et al.,* A human-curated annotation of the *Candida albicans* genome. *PLoS Genet* 2005;**1**: 36-57.

Carman GM, Matas J. Solubilization of microsomal-associated phosphatidylserine synthase and phosphatidylinositol synthase from *Saccharomyces cerevisiae*. *Can J Microbiol* 1981;**27**: 1140-9.

Carson MA, Atkinson KD, Waechter CJ. Properties of particulate and solubilized phosphatidylserine synthase activity from *Saccharomyces cerevisiae*. Inhibitory effect of choline in the growth medium. *J Biol Chem* 1982;**257**: 8115-21.

Cassilly CD, Farmer AT, Montedonico AE *et al.,* Role of phosphatidylserine synthase in shaping the phospholipidome of *Candida albicans*. *FEMS Yeast Res* 2017;**17**.

Cassilly CD, Maddox MM, Cherian PT *et al.,* SB-224289 Antagonizes the Antifungal Mechanism of the Marine Depsipeptide Papuamide A. *PLoS One* 2016;**11**: e0154932.

Chen YL, Kauffman S, Reynolds TB. *Candida albicans* uses multiple mechanisms to acquire the essential metabolite inositol during infection. *Infect Immun* 2008;**76**: 2793-801.

Chen YL, Montedonico AE, Kauffman S *et al.,* Phosphatidylserine synthase and phosphatidylserine decarboxylase are essential for cell wall integrity and virulence in *Candida albicans*. *Mol Microbiol* 2010;**75**: 1112-32.

Choi HS, Han GS, Carman GM. Phosphorylation of yeast phosphatidylserine synthase by protein kinase A: identification of Ser46 and Ser47 as major sites of phosphorylation. *J Biol Chem* 2010;**285**: 11526-36.

Clarke OB, Tomasek D, Jorge CD *et al.,* Structural basis for phosphatidylinositol-phosphate biosynthesis. *Nat Commun* 2015;**6**: 8505.

DeChavigny A, Heacock PN, Dowhan W. Sequence and inactivation of the pss gene of *Escherichia coli*. Phosphatidylethanolamine may not be essential for cell viability. *J Biol Chem* 1991;**266**: 10710.

Dewey RE, Wilson RF, Novitzky WP *et al.,* The AAPT1 gene of soybean complements a cholinephosphotransferase-deficient mutant of yeast. *Plant Cell* 1994;**6**: 1495-507.

Dey P, Su WM, Han GS *et al.,* Phosphorylation of lipid metabolic enzymes by yeast protein kinase C requires phosphatidylserine and diacylglycerol. *J Lipid Res* 2017;**58**: 742-51.

Dowhan W. A retrospective: use of *Escherichia coli* as a vehicle to study phospholipid synthesis and function. *Biochim Biophys Acta* 2013;**1831**: 471-94.

Dryden SC, Dowhan W. Isolation and expression of the Rhodobacter sphaeroides gene (pgsA) encoding phosphatidylglycerophosphate synthase. *J Bacteriol* 1996;**178**: 1030-8.

Dutt A, Dowhan W. Intracellular distribution of enzymes of phospholipid metabolism in several gram-negative bacteria. *J Bacteriol* 1977;**132**: 159-65.

Dutt A, Dowhan W. Characterization of a membrane-associated cytidine diphosphate-diacylglycerol-dependent phosphatidylserine synthase in bacilli. *J Bacteriol* 1981;**147**: 535-42.

Dutt A, Dowhan W. Purification and characterization of a membrane-associated phosphatidylserine synthase from Bacillus licheniformis. *Biochemistry* 1985;**24**: 1073-9.

Ge Z, Taylor DE. The *Helicobacter pylori* gene encoding phosphatidylserine synthase: sequence, expression, and insertional mutagenesis. *J Bacteriol* 1997;**179**: 4970-6.

Gopalakrishnan AS, Chen YC, Temkin M *et al.,* Structure and expression of the gene locus encoding the phosphatidylglycerophosphate synthase of *Escherichia coli*. *J Biol Chem* 1986;**261**: 1329-38.

Graham TR, Seeger M, Payne GS *et al.,* Clathrin-dependent localization of alpha 1,3 mannosyltransferase to the Golgi complex of *Saccharomyces cerevisiae*. *J Cell Biol* 1994;**127**: 667-78.

Guthrie C, Fink, G. R. (ed.) *Methods in Enzymology* volume 350: Academic Press, 2002.

Hartmann A, Hellmund M, Lucius R *et al.,* Phosphatidylethanolamine synthesis in the parasite mitochondrion is required for efficient growth but dispensable for survival of *Toxoplasma gondii*. *J Biol Chem* 2014;**289**: 6809-24.

Hauser M, Kauffman S, Lee BK *et al.,* The first extracellular loop of the *Saccharomyces cerevisiae* G protein-coupled receptor Ste2p undergoes a conformational change upon ligand binding. *J Biol Chem* 2007;**282**: 10387-97.

Hjelmstad RH, Bell RM. The sn-1,2-diacylglycerol cholinephosphotransferase of *Saccharomyces cerevisiae*. Nucleotide sequence, transcriptional mapping, and gene product analysis of the CPT1 gene. *J Biol Chem* 1990;**265**: 1755-64.

Hjelmstad RH, Bell RM. sn-1,2-diacylglycerol choline- and ethanolaminephosphotransferases in *Saccharomyces cerevisiae*. Nucleotide sequence of the EPT1 gene and comparison of the CPT1 and EPT1 gene products. *J Biol Chem* 1991;**266**: 5094-103.

Hromy JM, Carman GM. Reconstitution of *Saccharomyces cerevisiae* phosphatidylserine synthase into phospholipid vesicles. Modulation of activity by phospholipids. *J Biol Chem* 1986;**261**: 15572-6.

Kanfer J, Kennedy EP. Metabolism and Function of Bacterial Lipids. Ii. Biosynthesis of Phospholipids in *Escherichia coli*. *J Biol Chem* 1964;**239**: 1720-6.

Kelley MJ, Bailis AM, Henry SA *et al.,* Regulation of phospholipid biosynthesis in *Saccharomyces cerevisiae* by inositol. Inositol is an inhibitor of phosphatidylserine synthase activity. *J Biol Chem* 1988;**263**: 18078-85.

Kinney AJ, Carman GM. Phosphorylation of yeast phosphatidylserine synthase *in vivo* and *in vitro* by cyclic AMP-dependent protein kinase. *Proc Natl Acad Sci U S A* 1988;**85**: 7962-6.

Kohlwein SD, Kuchler K, Sperka-Gottlieb C *et al.,* Identification of mitochondrial and microsomal phosphatidylserine synthase in *Saccharomyces*

cerevisiae as the gene product of the CHO1 structural gene. *J Bacteriol* 1988;**170**: 3778-81.

Koonin EV. A duplicated catalytic motif in a new superfamily of phosphohydrolases and phospholipid synthases that includes poxvirus envelope proteins. *Trends Biochem Sci* 1996;**21**: 242-3.

Kovac L, Gbelska I, Poliachova V *et al.,* Membrane mutants: a yeast mutant with a lesion in phosphatidylserine biosynthesis. *Eur J Biochem* 1980;**111**: 491-501.

Kuchler K, Daum G, Paltauf F. Subcellular and submitochondrial localization of phospholipid-synthesizing enzymes in *Saccharomyces cerevisiae*. *J Bacteriol* 1986;**165**: 901-10.

Kuge O, Nishijima M. Phosphatidylserine synthase I and II of mammalian cells. *Biochim Biophys Acta* 1997;**1348**: 151-6.

Letts VA, Henry SA. Regulation of phospholipid synthesis in phosphatidylserine synthase-deficient (chol) mutants of *Saccharomyces cerevisiae*. *J Bacteriol* 1985;**163**: 560-7.

Letts VA, Klig LS, Bae-Lee M *et al.,* Isolation of the yeast structural gene for the membrane-associated enzyme phosphatidylserine synthase. *Proc Natl Acad Sci U S A* 1983;**80**: 7279-83.

Matsumoto K. Phosphatidylserine synthase from bacteria. *Biochim Biophys Acta* 1997;**1348**: 214-27.

Matsuo Y, Fisher E, Patton-Vogt J *et al.,* Functional characterization of the fission yeast phosphatidylserine synthase gene, pps1, reveals novel cellular functions for phosphatidylserine. *Eukaryot Cell* 2007;**6**: 2092-101.

McMaster CR, Bell RM. Phosphatidylcholine biosynthesis in *Saccharomyces cerevisiae*. Regulatory insights from studies employing null and chimeric sn-1,2-diacylglycerol choline- and ethanolaminephosphotransferases. *J Biol Chem* 1994;**269**: 28010-6.

Mitoma J, Kasama T, Furuya S *et al.,* Occurrence of an unusual phospholipid, phosphatidyl-L-threonine, in cultured hippocampal neurons. Exogenous L-serine is required for the synthesis of neuronal phosphatidyl-L-serine and sphingolipids. *J Biol Chem* 1998;**273**: 19363-6.

Nikawa J, Kodaki T, Yamashita S. Primary structure and disruption of the phosphatidylinositol synthase gene of *Saccharomyces cerevisiae*. *J Biol Chem* 1987a;**262**: 4876-81.

Nikawa J, Tsukagoshi Y, Kodaki T *et al.,* Nucleotide sequence and characterization of the yeast PSS gene encoding phosphatidylserine synthase. *Eur J Biochem* 1987b;**167**: 7-12.

Nogly P, Gushchin I, Remeeva A *et al.,* X-ray structure of a CDP-alcohol phosphatidyltransferase membrane enzyme and insights into its catalytic mechanism. *Nat Commun* 2014;**5**: 4169.

Ohsawa T, Nishijima M, Kuge O. Functional analysis of Chinese hamster phosphatidylserine synthase 1 through systematic alanine mutagenesis. *Biochem J* 2004;**381**: 853-9.

Okada M, Matsuzaki H, Shibuya I *et al.,* Cloning, sequencing, and expression in *Escherichia coli* of the *Bacillus subtilis* gene for phosphatidylserine synthase. *J Bacteriol* 1994;**176**: 7456-61.

Piispanen AE, Grahl N, Hollomon JM *et al.,* Regulated proteolysis of *Candida albicans* Ras1 is involved in morphogenesis and quorum sensing regulation. *Mol Microbiol* 2013;**89**: 166-78.

Poole MA, Homann MJ, Bae-Lee MS *et al.,* Regulation of phosphatidylserine synthase from *Saccharomyces cerevisiae* by phospholipid precursors. *J Bacteriol* 1986;**168**: 668-72.

Raetz CR, Kennedy EP. The association of phosphatidylserine synthetase with ribosomes in extracts of *Escherichia coli*. *J Biol Chem* 1972;**247**: 2008-14.

Reynolds TB, Jansen A, Peng X *et al.,* Mat formation in *Saccharomyces cerevisiae* requires nutrient and pH gradients. *Eukaryot Cell* 2008;**7**: 122-30.

Rilfors L, Niemi A, Haraldsson S *et al.,* Reconstituted phosphatidylserine synthase from *Escherichia coli* is activated by anionic phospholipids and micelle-forming amphiphiles. *Biochim Biophys Acta* 1999;**1438**: 281-94.

Saha SK, Furukawa Y, Matsuzaki H *et al.,* Directed mutagenesis, Ser-56 to Pro, of *Bacillus subtilis* phosphatidylserine synthase drastically lowers

enzymatic activity and relieves amplification toxicity in *Escherichia coli*. *Biosci Biotechnol Biochem* 1996;**60**: 630-3.

Sciara G, Clarke OB, Tomasek D *et al.,* Structural basis for catalysis in a CDP-alcohol phosphotransferase. *Nat Commun* 2014;**5**: 4068.

Sohlenkamp C, de Rudder KE, Geiger O. Phosphatidylethanolamine is not essential for growth of *Sinorhizobium meliloti* on complex culture media. *J Bacteriol* 2004;**186**: 1667-77.

Sperka-Gottlieb C, Fasch EV, Kuchler K *et al.,* The hydrophilic and acidic N-terminus of the integral membrane enzyme phosphatidylserine synthase is required for efficient membrane insertion. *Yeast* 1990;**6**: 331-43.

Sturbois-Balcerzak B, Stone SJ, Sreenivas A *et al.,* Structure and expression of the murine phosphatidylserine synthase-1 gene. *J Biol Chem* 2001;**276**: 8205-12.

Sung TC, Roper RL, Zhang Y *et al.,* Mutagenesis of phospholipase D defines a superfamily including a trans-Golgi viral protein required for poxvirus pathogenicity. *Embo J* 1997;**16**: 4519-30.

Tanaka S, Nikawa J, Imai H *et al.,* Molecular cloning of rat phosphatidylinositol synthase cDNA by functional complementation of the yeast *Saccharomyces cerevisiae* pis mutation. *FEBS Lett* 1996;**393**: 89-92.

Usui M, Sembongi H, Matsuzaki H *et al.,* Primary structures of the wild-type and mutant alleles encoding the phosphatidylglycerophosphate synthase of *Escherichia coli*. *J Bacteriol* 1994;**176**: 3389-92.

Vance JE, Steenbergen R. Metabolism and functions of phosphatidylserine. *Prog Lipid Res* 2005;**44**: 207-34.

Williams JG, McMaster CR. Scanning alanine mutagenesis of the CDP-alcohol phosphotransferase motif of *Saccharomyces cerevisiae* cholinephosphotransferase. *J Biol Chem* 1998;**273**: 13482-7.

CONCLUSION

The findings from the projects in this dissertation have not always returned expected results; however, they have provided some interesting and beneficial data nonetheless. The primary goal of this work began as a search for small molecules that inhibit the phosphatidylserine (PS) synthase enzyme in *Candida albicans*. The secondary goal, which became equally as important as the primary, was the characterization of the PS synthase protein itself.

One of the first projects undertaken in this work was to describe the PS synthase's contribution in the phospholipidome of *C. albicans*. Previous studies described the phospholipid content of *C. albicans*, or showed PL mutant's phospholipid profile via TLC, but the work described in chapter two is the first time mass spectrometry was used to define the lipid profiles of certain PL mutants. In this study, we were able to identify that specific species of PS were preferentially used to produce PE. In addition, we found that, in the event that ethanolamine and choline are readily available within the medium, the Kennedy pathway is able to compensate for the *de novo* loss of PE and PC production. We were also able to describe the enzyme kinetics for the PS synthase, the values of which correspond well with previously published data for *Saccharomyces cerevisiae*. These data helped to inform our screening approaches described next.

In chapter three, the use of *cho1ΔΔ* mutant phenotypic traits as indicators that compounds inhibit the PS synthase is discussed. This project looked for compounds that could counteract Papuamide A, which is toxic to cells containing

PS in their membranes. Thus, by counteracting Pap-A toxicity, hit compounds were hypothesized to inhibit PS production by inhibiting PS synthase activity.

We identified a compound, SB-224289, which showed reproducible Pap-A resistance. After further characterization, we concluded that SB-224289 did not behave as we hypothesized, indicating that this trait of providing Pap-A resistance was not specific enough for use in large scale screens. Indeed, at the end of this chapter, we concluded that SB-224289 likely physically interacted with Pap-A to abrogate the negative effects of the toxin.

Interestingly, as described in chapter four we found that when we continued experimentation on SB-224289 in *S. cerevisiae*, it seemed to disrupt proper localization of PS and another phospholipid PI54P. Thus, SB-224289 did not behave by inhibiting the PS synthase enzyme, but instead controlled some facet of phospholipid trafficking. Further investigation showed that SB-224289 treatment also caused a disruption in proper localization of Pma1p, a membrane bound ATPase. Based on this, it seemed that SB-224289 activity acted more generally by disrupting some component of cellular trafficking, possibly endocytosis. We performed a screen on yeast homozygous mutants to determine the intracellular target of SB-224289. In this assay, although it is as yet incomplete, we identified Rho5p as a possible target for SB-224289. The direct mechanism is unclear at the current time, but as Rho5p is active in many pathways, it is conceivable that SB-224289 could interfere with one branch pathway that controls endocytosis within yeast. However, this is speculation at

the current time and further research will be conducted to either confirm or refute these hypotheses. While unexpected given our initial goals of the Pap-A toxicity screen, it still produced interesting results as a compound that induces large-scale endocytosis could be useful in laboratory work.

In addition, as described in appendix three we performed a second Pap-A toxicity screen, this time on plant extract fractions. It is well known that many plants have innate defenses against fungal pathogens. Thus, we hypothesized that there might be PS synthase inhibitors in the secondary metabolite milieu produced by plants. We performed another screen and identified a fraction from the leaf extract of the rain tree that allowed *C. albicans* to survive in the presence of Pap-A. As described for SB-224289, we found that the rain tree extract did not inhibit PS synthase as we hypothesized. We continued characterization of this plant extract in an attempt to identify the bioactive component, but found that the complexity of molecules within the plant extract precluded our ability to isolate the single molecule producing our phenotypic trait.

Because of the difficulties encountered with our Pap-A toxicity screening, we tried to take a more direct approach to identify compounds that inhibit the fungal PS synthase. To do this, we used a phenotypic trait of *cho1ΔΔ* as an indicator that the PS synthase had been inhibited. As described in appendix one, this phenotypic trait was ethanolamine auxotrophy. Ethanolamine auxotrophy describes cells that must have ethanolamine provided in the medium to survive. This is a trait of *cho1ΔΔ* because PS is a precursor to the *de novo* production of

PE, which is an essential phospholipid. Without PE, the cells cannot grow. However, there is a secondary, scavenging pathway called the Kennedy pathway that produces PE without the requirement for PS first. We hypothesized that PS synthase inhibitors would cause the cells to become ethanolamine auxotrophs, and thus unable to grow in minimal medium deplete of ethanolamine. We performed a screen on small molecules, looking to identify ones that might cause ethanolamine auxotrophy in minimal medium. Any positive hits that were identified in this initial screen were then further confirmed by adding ethanolamine back to the medium and looking for a recovery of growth (via the Kennedy pathway of producing PE from exogenous ethanolamine).

Although we found positive hits in our initial screen, we never identified a compound that showed a reproducible return of growth when ethanolamine was returned to the medium. However, although we did not find compounds that induced ethanolamine auxotrophy, and thus inhibit the PS synthase, we did identify a compound that showed effective inhibition of growth of *C. albicans*. This compound, called Lee-3664, showed effective killing of *C. albicans* at low concentrations, while also showing relatively low cytotoxicity against mammalian cells. Based on this, further characterization of this compound, as well as chemical modification of its structure, is underway with collaborators at St. Jude.

Because of the difficulties we faced with the high-throughput screening approaches with small molecules, we became interested in taking a different approach for identifying PS synthase inhibitors. We hypothesized that, by

identifying the important functional locations on PS synthase, we might be better able to target those in a rational manner. Thus, in order to do this, we performed various site-directed mutagenesis experiments to identify substrate binding sites on the protein.

As described in chapter five, the fungal PS synthase is known to bind to CDP-DAG and serine. Previously published data has shown a well-conserved motif for many enzymes that bind CDP- molecules. We performed site-directed mutagenesis on this sequence within the PS synthase and found that indeed there was a significant decrease in enzymatic activity upon loss of many of these amino acids. In addition to the CDP-DAG binding site, we were interested, perhaps more so, in determining where serine binds the protein. Unlike CDP-DAG, there is little in the literature known about where serine binds in any protein. Thus, we performed sequence alignments of fungal PS synthase and PI synthases to guide our hypothesis of where serine binds. We identified an amino acid sequence that was well conserved across several fungal PS synthases but absent in PI synthases. When the amino acids in this sequence were mutated individually to alanines, the enzyme showed a complete abolishment of activity. Although at this point we cannot say for certain whether this is the true binding site of serine or these amino acids are important in another way for the enzyme function, this characterization has revealed another location on the protein where inhibition may be beneficial in stopping the function of the enzyme.

Last, there is little known about PS trafficking and dynamics within any organism. Because of this, we were interested in determining how long PS remains at the plasma membrane of *S. cerevisiae*. As described in appendix two, we produced several yeast strains carrying fluorescent molecules to demonstrate localization of PS. We also wished to put the PS synthase under a repressible promoter whereby we could control the production of PS and follow its movement, appearance, or disappearance within the cell. Unfortunately, all attempts at producing repressible PS synthase in this yeast were not entirely successful at producing a clean shut off of PS expression. As a result, we used lyso-PS treatment in a *cho1Δ* to measure PS duration at the membrane. This lyso-PS was added exogenously into the medium of *cho1Δ* cells which took up the lyso-PS, modified it in the ER, and then returned it to the plasma membrane. We observed an appearance of PS at the membrane within fifteen to thirty minutes that remained up to 300 minutes after removal of exogenous lyso-PS, although diffusion began to occur at later time points. These findings, although not exactly as occurs naturally, demonstrate the potential for PS to remain in the membrane for extended periods of time.

The last project we worked on was crystallization of Cho1p as described in appendix four. Although this project was begun too late for a structure to be solved, we did take the first important steps for protein crystallization. Strains of *S. cerevisiae* were produced where both the *S. cerevisiae* and *C. albicans* PS synthase were highly expressed and tagged with Hisx6. These strains will allow

isolation and purification of the protein in future experiments using affinity chromatography. Although it may be a daunting task, once a crystal structure is solved, it will greatly advance our understanding of the protein in general, and as a drug target. In fact, modern technology allows for computational screening with solved protein structures whereby small molecules can be docked within the proposed active site of the protein. These identified molecules that "fit" well into the active site would then further be tested in *in vitro* and *in vivo* assays to determine efficacy. As described in chapter five, a homology model was produced that predicted the structure of the PS synthase, but it is well documented that homology models are not always accurate. We attempted to use the homology model of Cho1p in the computational screen, but the parameters determining "hit" compounds were too loose, allowing too many hits to be identified. Thus, it is our intention to perform another computational screen with increased confidence once a crystal structure is solved.

In addition to the future computational screen, another screening approach is underway. This approach utilizes three different expression profiles of the drug target in genetically altered *C. albicans*. First is an overexpressed version of the protein, second is a wild-type version, and third is an under- or non-expressed protein. Each of these strains also expresses a unique fluorescent marker that differentiates it from the other strains. These strains are pooled in 96-well plates and treated with the compound of interest. After incubation, fluorescence is monitored to determine if there has been an effect on

the strains. If the target itself is being specifically inhibited, there should be a dose-response of efficacy. For instance, the overexpressed strain should be completely inhibited as there is more target for the compound to inhibit. The wild-type should also be susceptible, but perhaps to a lesser degree. And last, the deletion or under-expressed protein strain should grow relatively well since the drug target is present in decreased levels. Thus, this method allows differentiation of compounds that are outright toxic (i.e. kill all of the strains) and those that are selectively toxic based on the drug target.

This approach is in the beginning stages with Glen Palmer and collaborators from the UT Health Science Center. Strains have been constructed and large scale screens are slated to go forward. This methodology seems promising and will hopefully reduce much of the nonspecific activity of drugs that we have seen in our previous screening approaches.

In conclusion, the work in this dissertation has described an entirely new physiological behavior for the compound SB-224289. Although a clear answer for its exact mechanism is not known, a molecule that disrupts proper trafficking of cellular material (i.e. endocytosis) could be useful in labs that study of these processes in yeast.

Further, the findings of this dissertation have provided a greater general understanding of Cho1p and its importance and activity within the pathogenic *C. albicans.* Research is still underway to more-confidently describe the substrate-binding sites of Cho1p, but our findings demonstrate two motifs that may play

important roles in enzyme function. Because of the highly conserved nature of the CAPT motif residues, it seems likely that decreases in activity in the CAPT-motif mutant versions of Cho1p are likely a result of disruption of CDP-DAG binding or catalytic activity of the enzyme. To further confirm this, K_m and V_{max} analysis would need to be performed on some of the still-functional mutant versions of Cho1p to determine where the true disruption lies.

Second, although there is little evidence to confidently demonstrate that our predicted serine-binding motif is truly important in serine binding, three of the four residues within this motif were shown to abolish activity of the protein, indicating at least that they are important in some way to enzyme function. Because of the questions that still remain regarding this motif, and the possibility that it is not involved in serine-binding as hypothesized, it will be even more important that future experiments include active site labeling which can more definitively identify residues important in serine binding.

Last, this research has made possible many Cho1p inhibitor screening approaches that were not possible before its completion. Although there are clearly difficulties in screening for inhibitors of Cho1p, this research has provided an excellent path forward in further screening approaches to identifyi inhibitors. Plus, it has lended credence to the hypothesis that Cho1p represents an excellent drug target. Because Cho1p is crucial to the *de novo* production of several major phospholipids (PS, PE, and PC), its disruption renders this organism unable to grow and cause infection in the host. In addition, although it

is not required that a drug target be absent within the host organism for specificity, the fact that Cho1p is absent within mammals may remove the added possibility of toxicity to the host, as it is an issue in some antifungal drugs on the market today.These reasons alone support the usefulness of pursuing Cho1p as a drug target; however, there are also many tools that allow for the study of Cho1p as well as PS levels, localization, and biosynthesis. These tools include the *in vitro* PS synthase assay, microscopy of GFP-Lact-C2-expressing strains of *S. cerevisiae*, lipidomics, and more. Further, there are excellent phenotypic traits that can be used in secondary screens to confirm the activity of possible Cho1p inhibitors (i.e. Papuamide-A assay, ethanolamine auxotrophy, β-glucan unmasking in the cell wall). These tools and secondary screening traits have been developed, utilized, or optimized within this dissertation work. This array of tools and secondary screens available for use in studying Cho1p support its excellent potential as a drug target.

APPENDICES

APPENDIX I

SCREEN FOR COMPOUNDS INDUCING ETHANOLAMINE AUXOTROPHY IN *CANDIDA ALBICANS*

Contributing authors to this work include: Chelsi D. Cassilly, [1] Martin Cheramie, [2] Robin B. Lee, [2] Dinesh M. Fernando., [2] Miranda J. Crouch, [1] Richard E. Lee, [2] Todd B. Reynolds [1]

University of Tennessee, Knoxville [1]

St. Jude Children's Research Hospital [2]

This article has not been published elsewhere at this time, nor will it be before completion of this ETD. The Abstract is a modified version of one submitted for presentation at the Comparative and Experimental Medicine and Public Health Research Symposium at the University of Tennessee, Knoxville, in 2015. The author contributions are as follows: Conceived and designed the experiments: CDC MC RBL REL TBR. Performed the experiments: CDC MC RBL DMF MJC TBR. Analyzed the data: CDC MC RBL DMF REL TBR. Contributed reagents/materials/analysis tools: TBR REL. Wrote the paper: CDC DMF

Abstract

The pathogenic fungus *Candida albicans* is the leading cause of hospital-acquired fungal infections in immunocompromised individuals. Invasive bloodstream infections have a 30% mortality rate. Three antifungal classes are used to treat invasive fungal infections including azoles, echinocandins, and polyenes. Rising drug resistance and drug toxicity have made these compounds less effective and new drugs are needed. The fungal phosphatidylserine (PS)

synthase (Cho1p) has been suggested as a drug target because it is: 1) required for *C. albicans* virulence, 2) conserved among fungi, and 3) absent from mammals. Thus, Cho1p inhibitors could be broad-range antifungals with few detrimental side effects. To identify Cho1p inhibitors, we have taken a novel compound screening approach. Cells lacking Cho1p cannot survive without supplemented ethanolamine because *de novo* biosynthesis of phosphatidylethanolamine (PE), a vital phospholipid, is downstream of PS production. Thus, these cells only survive by making PE from imported ethanolamine by an alternative pathway. We screened compounds for their ability to inhibit growth of wildtype *C. albicans* in media lacking ethanolamine, but not in media containing ethanolamine, thus indicating ethanolamine auxotrophy. A set of three large-scale, high-throughput screens were performed. Although we did not succeed in identifying PS synthase inhibitors from these screens, we were able to identify a compound of interest, named Lee-3664, that seems highly toxic to fungi. Further compound modifications and testing are underway on this compound.

Introduction

In addition to the drug screen performed with Papuamide A (Cassilly, *et al.* 2016), we also screened compounds for their ability to phenocopy the *cho1*ΔΔ mutant. One particularly useful phenotypic trait is ethanolamine auxotrophy (i.e. the inability to survive without ethanolamine supplemented in the medium). In the

de novo pathway, PS is a precursor for synthesis of PE, so PE synthesis is also blocked when PS synthesis is disrupted, as in the case of the *cho1*ΔΔ mutant (Chen, *et al.* 2010). PE is an essential phospholipid, and without it *C. albicans* is unable to survive. The *cho1*ΔΔ can circumvent this blockage of the *de novo* pathway by using the alternative Kennedy Pathway to import exogenous ethanolamine for the production of PE (Cassilly, *et al.* 2017). However, this only works in culture media as there is insufficient ethanolamine in the mouse host to support PE synthesis during an infection, which likely contributes to avirulence in the *cho1*ΔΔ mutant (Davis *et al.*, in preparation). We hypothesized that compounds that cause wild-type *C. albicans* to become an ethanolamine auxotroph could be inhibiting an enzyme within the PS synthesis pathway.

In order to test this hypothesis, we developed a screen where we grew the wild-type organism in ethanolamine deplete synthetic medium. The organism was then treated with compounds from a selected library and allowed to incubate overnight. Wells that contained actively growing cells, like the wild-type DMSO negative control, were considered negative hits (because they are not ethanolamine auxotrophs) while wells that contained no growth were considered initial hits.

To eliminate false positives, specifically compounds that are inherently toxic to the cells, we developed a secondary screen that supplemented 1 mM ethanolamine to the medium. This exogenous ethanolamine would be substrate for the Kennedy Pathway to circumvent the need for PS, and thus allow growth of

the *cho1*ΔΔ mutant. As a result, in this secondary screen, compounds that inhibited growth in the ethanolamine negative screen, but not in the presence of ethanolamine, were considered true hits. True hits were then further screened more stringently to determine the lowest concentration at which the compounds were effective.

We performed three different small-scale but high-throughput screens for compounds that caused a loss of growth in minimal medium. These compounds were then tested in a minimum inhibitory concentration (MIC) curve in duplicate with media +/- ethanolamine to find the minimum concentration that caused ethanolamine auxotrophy. Unfortunately, we were unable to identify any hits that induced ethanolamine auxotrophy in the wild-type organism reproducibly. However, one beneficial aspect of our screening approach was the alternative ability to identify compounds that are fungicidal (i.e. compounds that inhibited growth in both +/-ethanolamine conditions, indicating that they might be toxic to fungi instead of simply inhibitory to a particular pathway). Although we were unable to identify PS synthase inhibitors through this screen, we did identify one compound in particular with promise as a fungicidal drug.

Materials and Materials

Strains and culture methods

The strains used in this study were wild-type (SC5314), *cho1Δ*, *cho1ΔΔ* (YLC337), and *psd1Δ/Δpsd2Δ/Δ::*P_{Met3}*-PSD1* (YLC331). Strains were previously published and described (Chen, *et al.* 2010) and can be found in Table A1.1.

Minimal medium (0.67% yeast nitrogen base without amino acids (Difco), 2% dextrose (ThermoFisher Scientific)) and YPD rich medium (1% yeast extract, 2% peptone, 2% dextrose) were used where indicated (Guthrie 2002).

Genetics and Cloning

The plasmid pYLC314 which contains an *ACT1* promoter and nourseothricin resistance gene (*SAT1*) followed by P_{MET3} was isolated from *E. coli*. To insert this sequence in front of the *CHO1* gene in *cho1Δ*, we designed one primer containing the sequence upstream of *CHO1* followed by the *ACT1* promoter beginning (CCO14) and a second, reverse primer containing the 3' portion of P_{MET3} followed by sequence just before the start codon of *CHO1* (CCO15) (Table A1.1) This portion was amplified using PCR, then purified and transformed into *cho1Δ*. Selection was performed on YPD-nourseothricin plates. This produced *cho1Δ* P_{MET3}-*CHO1*.

Secondary Screens for Ethanolamine Auxotrophy

Further screening of transformants was performed using serial dilution on minimal medium agar plates supplemented with: 1) nothing, 2) 2.5 mM cysteine/ 2.5 mM methionine, 3) 1 mM ethanolamine, or 2.5 mM cysteine/ 2.5 mM methionine 1 mM ethanolamine. A starting culture of 0.1 OD_{600}/ml was diluted 1:10 five times and then spotted on each plate. Positive and negative growth

Table A1. 1. Strains, Plasmids, and Primers Used or Produced in this Study

Name	Organism	Genotype	Source
SC5314 (Ca157)	*C. albicans*		Lab Strain
Ca159 (YLC337)	*C. albicans*	*cho1ΔΔ*	Chen *et al*., 2010
YLC331	*C. albicans*	*psd1Δ/Δpsd2Δ/Δ::pMet3-PSD1*	Joseph Chen
CDCS11	*S. cerevisiae*	*cho1Δ* P_{MET3}*-CHO1*	Becker Lab

pYLC314	*E. coli*	P_{MET3}, Amp^R, *SAT1*	Joseph Chen

CCO14		*TTCAAACAAGCATTTTGTTATATATAA CGGTTTTCTTTTTTTCATCTCGTTTTA TTTATTTACACATTTTTT*CGTCAAAAC TAGAGAATAATAAAG	This Study
CCO15		*TTCTGAATCTGATACAATTGCTGATTC TTGGTGCTTGGAGAACCCGGTAGCT GATGAGTCTGTCATGAATAG*GTTTTC TGGGGAGGGTATTT	This Study

controls included the wild-type and *cho1ΔΔ*. Plates were allowed to dry and incubated at 30°C overnight before pictures were taken.

Additionally, a form of the above assay was performed in 96-well plates with liquid medium instead. Appropriate cell cultures were grown overnight in 5 ml to stationary phase in 5 ml YPD shaking at 30°C. Cultures were pelleted and washed with sterile water 2x. Cells were resuspended in minimal medium and diluted to an OD_{600}/ml of 0.1. Cells were then counted on a hemocytometer twice and diluted to 2.5 x 10^3 cells/ml. 50 µl of the dilutions were pipetted into a 96-well plate, then additional medium was added containing either 1) nothing, 2) 5 mM cysteine/ 5 mM methionine, 3) 2 mM ethanolamine, or 5 mM cysteine/ 5 mM methionine 2 mM ethanolamine. Plates were incubated at 30°C overnight. The following day, Alamar Blue was added according to the manufacturer's protocol and (Cassilly, *et al.* 2016), then fluorescence was read in a plate reader as a proxy of growth.

Ethanolamine auxotrophy screening

Wild-type and *cho1ΔΔ* were grown overnight in 5 ml of YPD shaking at 30°C. The following day cultures were transferred to 15 ml conical tubes and centrifuged at 3,000 rpm for 3 minutes. Supernatant was decanted and cells were washed 2x with sterile water. On the last wash, cells were resuspended in minimal medium and the OD_{600}/ml was taken using a spectrophotometer. Cultures were diluted to an OD_{600}/ml of 0.1 in 5 ml of minimal medium. Using a

hemocytometer, cells were counted for each strain twice then diluted to 1.6 x 10^6 cells/ml. These dilutions were pipetted into either a 96- (100 µl/well) or 384- (40 µl/well) well plate and incubated at 30°C overnight. Compounds from each library used were added to a concentration of ~10 µM using a automated pintool as described in (Cassilly, *et al.* 2016).

The following day, CellTiter Glo was added according to the manufacturer's protocol and luminescence was measured to assess growth of the organism. To define positive hits, all data was copied from BMG Pherastar software into an Excel spreadsheet. Before proceeding raw Relative Luminescence Units (RLU) were normalized to each other ($0<n<1$, 0 = positive control, 1 = negative control). Data analysis proceeded using normalized RLU (nRLU). DMSO negative control wells were averaged and Fluconazole positive control wells were averaged. These averages provided our experimental maxima and minima of nRLU for each plate. A fungicidal index (FI) was developed by dividing the nRLU in the experimental well by the average of the plate's DMSO negative control wells' nRLU in EA- plates ($0<FI<1$, lower the FI, the more fungicidal the compound). To investigate recovery between EA+ and EA- wells, a Recovery Index (RI) was developed by dividing the nRLU of corresponding wells from the EA+ plate by the nRLU from the EA- plate. Therefore, a larger value indicated greater recovery in the EA enriched media. To determine a hit in our screen, the RI was divided by the FI (RI/FI). Therefore, the larger number, the more recovery from adding EA in the presence of a compound active against *C.*

ablicans. Data was then graphed, with each compound along the x-axis and nRLU along y-axis. We followed up on the top 20 hits (top 20 highest numbers from RI/FI). Hits were follow upon by MIC determination in 96 well format in EA-/EA+ conditions. MIC was determined using Alamar Blue.

Mammalian Cytotoxicity

Vero (Kidney epithelial cells; ATCC CCL-81) and HEPG2 (Liver Hepatocellular Carcinoma cells; ATCC HB-8065) monolayers were trypsinized (ATCC 30-2101) and quantified using disposable SD100 cell counting chambers and Cellometer Auto T4 (Nexcelom Bioscience, MA). Cells were seeded at 5000 cells/well (10-15 % confluency) into white, flat bottom 96-well plates (Nunc 136101, ThermoFisher) using enriched Dulbecco's Modified Eagle's Medium (Hyclone: DMEM/ High Glucose) for Vero cells and Eagle's Minimum Essential Medium (EMEM; ATCC 30-2003) for HEPG2 cells, each containing 10 % Fetal Bovine Serum (ATCC-30-2020). Plates were incubated overnight at 37°C in the presence of 5% CO_2. All compounds were solubilized in DMSO and serially diluted in respective media for each cell line. A serial dilution of DMSO only was made to monitor for diluent toxicity against HEPG2 and Vero. Equal volume of media containing compound dilutions was transferred to plates containing seeded cells using Biomek FXP liquid handling robot (Beckman Coulter,CA). The plates were briefly spun and incubated for 72 hours. After 72 hours of incubation, viability was indirectly measured using the CellTiter-Glo®

Luminescent Cell Viability (G7572 Promega) assay. Assay plates were read at peak emission wavelength of 590 nm on a PHERAstar FS Multilabel reader (BMG, Cary,NC). The raw data was normalized to no drug (DMSO only) wells as 100% viability standard. The concentration of test compounds that inhibited growth by 50% (IC_{50} value) was computed using nonlinear regression based fitting of inhibition curves using log [inhibitor] vs. Response-variable slope (four parameters) - symmetrical equation, in GraphPad Prism version 7 (GraphPad Software, La Jolla California USA, www.graphpad.com).

Results

Initially we wanted to set strong positive and negative controls for our screen. In previous work, we found that the *cho1*ΔΔ mutant showed relatively poor growth return in the presence of ethanolamine (Chen, *et al.* 2010). Because of this, detection of recovered growth of the *cho1ΔΔ* mutant in our screen presented a possible challenge in using *cho1ΔΔ* mutant as the positive control for identifying hits.

We were interested in producing a strain of *C. albicans* with *CHO1* under the repressible promoter P_{MET3}. In this case, P_{MET3}-*CHO1* should produce Cho1p when grown in conditions where methionine and cysteine are absent, but not produce the protein when grown in the presence of methionine and cysteine (Care, *et al.* 1999). This would give us a way of controlling Cho1p expression via the action of compounds (i.e. cysteine and methionine) which is a close analog of

what we were screening for (i.e. small molecules that inhibit Cho1p). We used PCR to amplify P_{MET3} from pYLC314 (Joseph Chen) with overhangs matching to the upstream region of *CHO1*. We made many attempts to integrate the construct into the genome of a heterozygous *cho1Δ* mutant. We isolated one positive colony where P_{MET3}-CHO1 appeared to have integrated (CDCS11). As shown in Figure A1.A, *cho1ΔΔ* cannot grow on minimal medium due to ethanolamine auxotrophy while *cho1Δ::*P_{MET3}*-CHO1* grows because it is expressing Cho1p under these conditions. In Figure A1.1B, *cho1ΔΔ* grows in 1 mM ethanolamine supplemented medium because it can produce PE via the Kennedy Pathway. The *cho1Δ::* P_{MET3}*-CHO1* strain grows equally as well in minimal medium containing ethanolamine as in medium unsupplemented with ethanolamine. In Figure A1.1C, *cho1ΔΔ* cannot grow on minimal media with 2.5 mM cysteine and 2.5 mM methionine because it has to have ethanolamine to grow. In addition, *cho1Δ::* P_{MET3}*-CHO1* strain does not grow when 2.5 mM cysteine and 2.5 mM methionine are supplemented because the presence of these components shut off the P_{MET3} which is controls expression of Cho1p and thus, the organism becomes an ethanolamine auxotroph under these conditions. Last, in Figure A1.1D, the *cho1 ΔΔ* mutant has a modest return of growth on minimal medium supplemented with 2.5 mM cysteine and 2.5 mM methionine and 1 mM ethanolamine because it is able to produce PE via the Kennedy Pathway. The *cho1Δ::*P_{MET3}*-CHO1* strain also has a modest return of growth when ethanolamine is added due to the same reason. Although these results

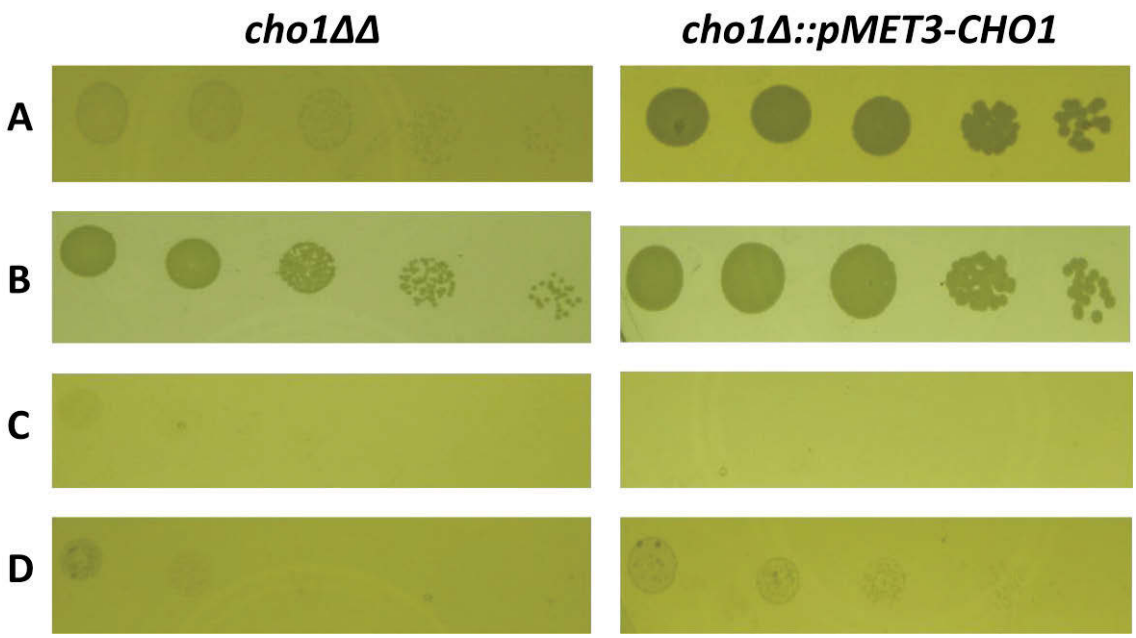

Figure A1. 1. Growth Phenotype of the *cho1Δ::P_{MET3}-CHO1* Strain
The *cho1ΔΔ* and *cho1Δ::P_{MET3}-CHO1* strains were compared for growth phenotype on minimal medium supplemented with (A) nothing, (B) 1 mM ethanolamine, (C) 2.5 mM cysteine and 2.5 mM methionine, (D) 1 mM ethanolamine and 2.5 mM cysteine and 2.5 mM methionine.

were precisely as expected, this phenotype unfortunately seemed to disappear over time and we could never replicate this data in new transformations. Thus, the project to produce *cho1Δ::P_{MET3}-CHO1* was abandoned.

Despite this problem we continued efforts to produce an adequate positive control for our screen. Previously in the Reynolds Lab, a strain had been produced where the *PSD1* gene was under P_{MET3} control: *psd1Δ/Δpsd2Δ/Δ::P_{MET3}-PSD1* (Joseph Chen). This strain is also an ethanolamine auxotroph under certain circumstances because, even though it can produce PS, it can only convert that PS to PE in medium lacking cysteine or methionine (i.e. when the Psd1p enzyme is produced). To confirm that this strain behaved as expected, we tested the ability of *psd1Δ/Δpsd2Δ/Δ::P_{MET3}-PSD1* to respond to methionine, cytsteine, and ethanolamine. We found that this strain showed no growth in the presence of cysteine and methionine alone, but that upon the addition of 1 mM ethanolamine, was recovered for growth (Fig. A1.2). This was an excellent proxy of what we expected to see with small molecule inhibitors in our screening approach. However, while *psd1Δ/Δpsd2Δ/Δ::P_{MET3}-PSD1* showed excellent ethanolamine auxotrophy recovery at UTK, reproducibility of this phenotype was never secured at St. Jude, and thus the *cho1ΔΔ* mutant was included as a positive control in our high-throughput screens instead of *psd1Δ/Δpsd2Δ/Δ::P_{MET3}-PSD1.*

At UTK we performed several assays to determine the appropriate conditions for use of *cho1ΔΔ* mutant as a positive control (Table A1.2, Fig.

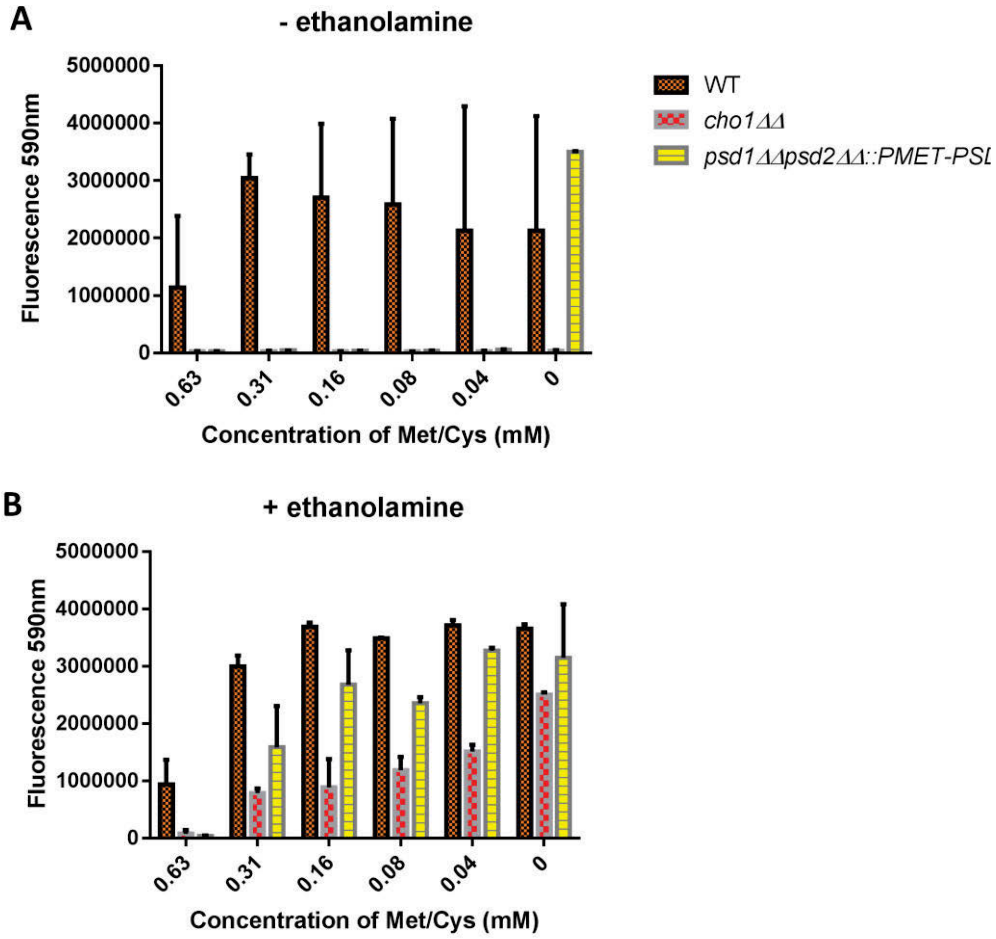

Figure A1. 2. Use of *P_{MET3}-PSD1* as a positive control
When grown without 1 mM ethanolamine (A) the *cho1ΔΔ* strain cannot grow under any circumstance and the *psd1ΔΔpsd2ΔΔ::P_{MET3}-PSD1* can grow only without the presence of met/cys. However, when 1 mM ethanolamine is added to the medium (B) there is a return of growth to both *cho1ΔΔ* and *psd1ΔΔpsd2ΔΔ::P_{MET3}-PSD1* nearly to wild-type levels in the presence of met/cys*. Medium also contained 50 mM Hepes to allow for measurement with Alamar Blue.*Too high concentrations of met/cys appear toxic (>/= 0.63 mM). Abbreviations: met/cys = methionine and cysteine.

A1.3). While the *cho1ΔΔ* mutant was sufficient as a positive control at UTK, detectable growth of this control was never observed at St. Jude for any of the screens performed.

In a pilot study at St. Jude Children's Research Hospital (St. Jude), we assessed 1,831 bioactive, FDA-approved compounds (http://www.selleckchem.com/screening/chemical-library.html) to identify those which produce ethanolamine auxotrophy in wild-type *C. albicans* growing in medium lacking ethanolamine (i.e. phenocopy the *cho1ΔΔ* mutant). This initial screen revealed 13 initial hits (0.7% hit rate). The Z-scores for most of the plates were above 0.5, indicating a reliable screen by standard HTS statistical appraisal (Zhang, *et al.* 1999). Each of the 13 hits was rescreened in triplicate under a dose-response curve in media +/-ethanolamine using controls of compounds that had no effect or were toxic. Unfortunately, this revealed that none of the bioactives induced ethanolamine auxotrophy, although several were directly inhibitory to growth.

We performed a second screen with a 510-compound library subset from the Medicines for Malaria Venture (https://www.mmv.org/). Due to the effectiveness against the eukaryotic organism *Plasmodium*, we were interested to see if these compounds were also effective against *C. albicans*. From this screen, we obtained no compounds that induced reproducible ethanolamine auxotrophy in wild-type *C. albicans*.

Table A1. 2. UTK-Determined Parameters for Ethanolamine Auxotrophy Screening

	Plate	Medium	Cell Concentration (cells/ml)	Incubation Temperature (°C)	Viability Indicator
Primary Screen	384-well	0.67% yeast nitrogen base, 2% dextrose	1×10^4	30	CellTiter Glo
Counter Screen	96-well	0.67% yeast nitrogen base, 2% dextrose, 50 mM HEPES, 1 mM Ethanolamine	1×10^4	30	Alamar Blue

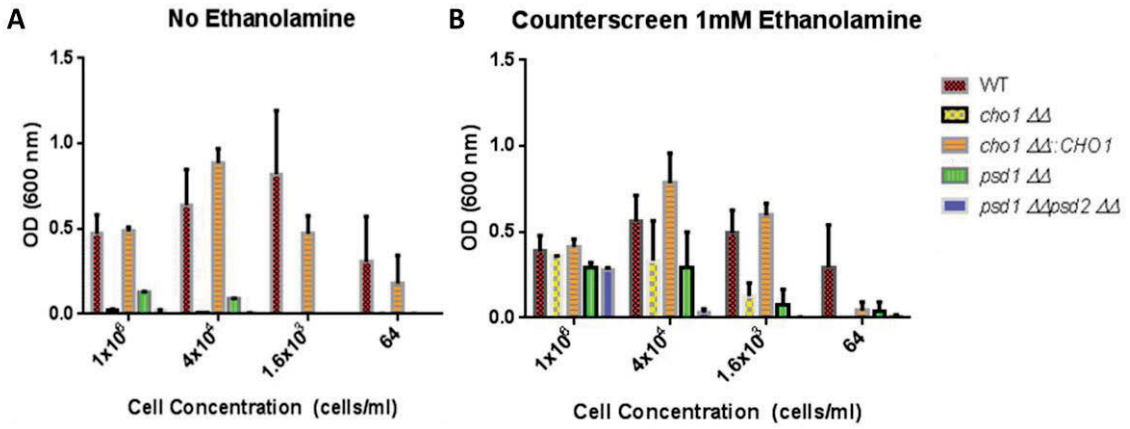

Figure A1. 3. Use of *cho1ΔΔ* as a positive control
(A) When grown without 1 mM ethanolamine the *cho1ΔΔ* and *psd1ΔΔpsd2ΔΔ* strains cannot grow due to ethanolamine auxotrophy. The *psd1ΔΔ* strain shows a severe growth defect at the highest cell concentration and is undetectable at the lower cell concentrations. The only cell growth is seen in wild-type and *cho1ΔΔ::CHO1* which can synthesize PE *de novo.* (B) When the medium is supplemented with 1 mM ethanolamine, *cho1ΔΔ*, *psd1ΔΔ,* and *psd1ΔΔpsd2ΔΔ* show a return of growth nearly equal to the wild-type and *cho1ΔΔ::CHO1* strains at the highest cell concentration.

The last library screened was the Maybridge Collection of 1,342 fragments (http://www.maybridge.com/portal/alias__Rainbow/lang__en/tabID__230/DesktopDefault.aspx). These fragments are increasingly useful due to their diversity in structure as well as their high potential to be combined or modified to improve efficacy. On average, these compounds were within the size range of 200 to 300 Da and soluble in water. From this screen we identified 20 true hits that produced ethanolamine auxotrophy; however, upon performing dose response experiments, none reproducibly retained this phenotype.

Although we saw no compounds from any screen that produced ethanolamine auxotrophy, we did find 18 total initial hits that appeared to be fungicidal. These hits thus became of primary interest and were screened further for minimum inhibitory concentration (MIC) against fungi and tested for mammalian cytotoxicity. After cytotoxicity testing against HepG and VERO cells, we identified two promising compounds. One had a fungal MIC of less than 0.57 μM and a cytotoxicity index of 27.5 μM. The second had a fungal MIC of 4.6 μM and a cytotoxicity index of greater than 109 μM. Because of the excellent cytotoxicity index of the second compound, we began to focus on this compound, now named Lee-3664.

Unfortunately, while this compound showed great promise at St. Jude, the fungal MIC experiments could not be reproduced at UTK. This seems to indicate that conditions must be completely uniform to produce desired phenotypes. However, despite the issues in reproducibility, work is currently underway at St.

Jude to further characterize Lee-3664 mechanism of action by screening a heterozygote deletion collection of *C. albicans*. Further, chemists at St. Jude are modifying the structure of Lee-3664 to produce analogs with the expectation that some of them may be more effective antifungals with lower MICs.

Discussion

It was our expectation to perform the three described small-scale, high-throughput screens and then ramp up the approach to include the 520,000 on-site compound library (Chen 2008) at St. Jude, but because of the challenges associated with this work, this goal was abandoned. Indeed, we began this screening approach in order to avoid the complexity associated with the Papuamide A screen. As these results show, using ethanolamine auxotrophy as a screening trait has its own unique set of challenges. However, although this work has been met with problems, from finding adequate controls to issues with reproducibility across work sites, there is still the potential that interesting information may come of this screen in future studies at St. Jude.

References

Care RS, Trevethick J, Binley KM *et al.* The MET3 promoter: a new tool for *Candida albicans* molecular genetics. *Mol Microbiol* 1999;**34**: 792-8.

Cassilly CD, Farmer AT, Montedonico AE *et al.* Role of phosphatidylserine synthase in shaping the phospholipidome of *Candida albicans*. *FEMS Yeast Res* 2017;**17**.

Cassilly CD, Maddox MM, Cherian PT *et al.* SB-224289 Antagonizes the Antifungal Mechanism of the Marine Depsipeptide Papuamide A. *PLoS One* 2016;**11**: e0154932.

Chen T, Guy, R. K. HIGH-THROUGHPUT SCREENING AND DRUG DISCOVERY AT ST. JUDE CHILDREN'S RESEARCH HOSPITAL. *Cell Notes* 2008: 3 - 4.

Chen YL, Montedonico AE, Kauffman S *et al.* Phosphatidylserine synthase and phosphatidylserine decarboxylase are essential for cell wall integrity and virulence in *Candida albicans*. *Mol Microbiol* 2010;**75**: 1112-32.

Guthrie C, Fink, G. R. (ed.) *Methods in Enzymology* volume 350: Academic Press, 2002.

Zhang JH, Chung TD, Oldenburg KR. A Simple Statistical Parameter for Use in Evaluation and Validation of High Throughput Screening Assays. *J Biomol Screen* 1999;**4**: 67-73.

APPENDIX II

TRAFFICKING AND STABILITY OF PHOSPHATIDYLSERINE IN THE PLASMA MEMBRANE OF YEAST

Contributing authors to this work include: Chelsi D. Cassilly, Rebecca E. Fong., Elizabeth R. Emanuel, Todd B. Reynolds

University of Tennessee, Knoxville

This article has not been published elsewhere at this time, nor will it be before completion of this ETD. Part of this appendix was submitted as REF's undergraduate honors research thesis for the University of Tennessee in 2016. While major edits have been made, permission was obtained from REF by CDC to include portions of the thesis work in this ETD. The author contributions are as follows: Conceived and designed the experiments: CDC TBR. Performed the experiments: CDC REF ERE. Analyzed the data: CDC REF TBR. Contributed reagents/materials/analysis tools: TBR. Wrote the paper: CDC REF

Abstract

Phosphatidylserine (PS) is a phospholipid that is commonly enriched in the inner leaflet of the plasma membrane of yeast and other eukaryotes. PS is produced in the endoplasmic reticulum and is trafficked to the mitochondria where it can be used to produce other phospholipids or to the plasma membrane. Although there have been some advances in understanding PS trafficking, little is known about the duration of PS at the plasma membrane. Previous studies involving extracellular addition of lyso-PS (i.e. PS where one fatty acid tail has been removed) suggested a rapid conversion of Lyso-PS into PS, followed by

incorporation into the plasma membrane. To further study this, we engineered a strain of *Saccharomyces cerevisiae* where the PS synthase gene (*CHO1*) is controlled by the repressible galactose promoter (P_{GAL1}). In the presence of galactose, Cho1p enzyme is expressed, and thus PS is synthesized. However, when glucose is present in the medium instead of galactose, P_{GAL1} represses *CHO1* and therefore PS production. In addition, we introduced a fluorescent, PS-specific probe to *S. cerevisiae* in order to visualize PS via fluorescent microscopy. We found that glucose repression of *CHO1* via P_{GAL1} caused a diffusion of the fluorescent probe away from the plasma membrane, indicating a decrease in PS levels. However, P_{GAL1} did not completely shut off Cho1p production, and thus the results were variable. In addition, we tested the effects of membrane-perturbing agents on PS localization and found that some compounds cause redistribution of PS within yeast.

Introduction

Phosphatidylserine (PS) is a glycerophospholipid and is considered a major phospholipid in eukaryotic organisms. Within most eukaryotes, PS is enriched in the inner leaflet of the plasma membrane and can have significant roles in membrane structure and cell signaling (Carman and Han 2011, Lagace and Ridgway 2013, Levin 2005, Mioka, *et al.* 2014). PS is produced in the endoplasmic reticulum (ER) by the PS synthase enzyme Cho1p (Carman and Han 2011, Cassilly, *et al.* 2017, Chen, *et al.* 2010, Osman, *et al.* 2011). After

production, PS can either be trafficked to the plasma membrane or used to make phosphatidylethanolamine (PE) in the mitochondria or endosome (Yeung, *et al.* 2008). Several studies have been conducted to study trafficking of PS to the mitochondria and plasma membrane. These studies describe the mitochondrial associated membrane (MAM) and the plasma membrane associated membrane (PAM) which are portions of the ER that are closely associated with the mitochondria or the plasma membrane, respectively. The MAM and the PAM are where the majority of phosphatidylserine synthesis and trafficking are predicted to occur (Achleitner, *et al*. 1999, Kuchler, *et al*. 1986a, Maeda, *et al*. 2013, Moser von Filseck, *et al*. 2015, Natarajan, *et al*. 2004, Osman, *et al*. 2011, Pichler, *et al*. 2001, Pomorski, *et al*. 2003, Sleight and Pagano 1983, Tamura, *et al*. 2012, Voelker 2003). Despite these studies, little is known about the dynamics of PS once it reaches the plasma membrane.

Previous work by (Maeda, *et al.* 2013, Moser von Filseck, *et al.* 2015) described a rapid (within 10 minutes) incorporation of Lyso-PS into PS in the ER, and subsequent relocation to the plasma membrane. Although this describes the movement of newly formed PS to the membrane, it is through an unnatural mechanism whereby Lyso-PS is the starting material that is converted into PS, then trafficked back to the plasma membrane (Maeda, *et al.* 2013). While this is informative, it does not describe the natural process of PS trafficking whereby PS is produced from CDP-DAG and serine. Understanding this natural trafficking and dynamics of PS was the goal of the present study.

In order to observe the movement of PS, we constructed a version of the Sc*CHO1* gene which is under the control of a repressible promoter. The galactose promoter (P_{GAL1}) allows expression of a particular gene in the presence of galactose and represses the expression of the gene in the presence of glucose. By inserting P_{GAL1} in place of the native *CHO1* promoter (P_{GAL1}-*CHO1*), we are able to control the expression of Cho1p, and thus the production of PS in the cell. Thus, when grown in medium containing galactose, *CHO1* transcribed and translated into protein, allowing the production of PS. Alternatively, when in the presence of glucose, *CHO1* is shut off, halting the production of PS.

In order to visualize changes in PS localization as a result of the above experimentation, we utilized two fluorescent, PS-specific probes GFP-Lact-C2 and mCherry-Lact-C2. Fluorescent molecules GFP and mCherry were fused to the C2 domain of Lactadherin, a bovine protein that binds specifically to PS, to create useful PS-specific probes (Fairn, *et al.* 2011a, Fairn, *et al.* 2011b). Together with the repressible production of Cho1p (P_{GAL1}-*CHO1*), these tools in theory should allow not only control of PS production, but also visualization of PS overtime. However, we found that the P_{GAL1}-*CHO1* strain was leaky, and even when grown in the presence of glucose, produced a small amount of PS. This concentration, though low, was still enough to support growth and show localization of PS, which precluded our ability to obtain total *CHO1* shut off.

As a result, we began efforts to utilize a new method using a plant system of controlled protein degradation. This system is a naturally occurring process in plants where the plant hormone auxin induces the degradation of anything bearing a particular sequence. Recently, this auxin-based degradation has been developed into a tool to control the proteolysis of specified proteins in other systems like yeast (Nishimura, *et al.* 2009). We wished to utilize this system to control degradation of Cho1p in yeast. Although final results were never obtained showing auxin-repressible degradation of Cho1p, strains were developed within this study, allowing this system to be usable in the future.

Last, because PS has been shown to be important for virulence of some fungi (Chen, *et al.* 2010, Vale-Silva, *et al.* 2016), we wished to utilize these tools in *C. albicans* and *C. glabrata*, but as a result of cloning and expression issues, were unable to adapt these techniques for the pathogenic fungi. Findings from our experiments, although incomplete, are excellent beginning steps in developing a greater understanding of PS dynamics.

Materials and Methods

Strains Used

Wild-type Σ *S. cerevisiae* (TRY181) and the *cho1Δ* deletion mutant (BMY2), which is unable to produce PS, were used. These strains contain auxotrophies for uracil and histidine (Table A2.1). All other strains were produced as described below. Details on particular strains can be found in Table A2.1.

Table A2. 1. Strains Produced or Used in this Study

Strain	Organism	Genotype	Source
Σ (TRY 181)	*S. cerevisiae*	*ura3Δ his3Δ*	Lab Strain
BMY2	*S. cerevisiae*	*ura3Δ his3Δ cho1 Δ*	Lab Strain
RF01	*S. cerevisiae*	*ura3Δ his3Δ* pGFP-Lact-C2	This study
RF04	*S. cerevisiae*	*ura3Δ his3Δ cho1Δ* pGFP-Lact-C2	This study
RF09	*S. cerevisiae*	*ura3Δ his3Δ* pGPD416-mCherry-Lact-C2	This study
RF10	*S. cerevisiae*	*ura3Δ his3Δ cho1 Δ* pGPD416-mCherry-Lact-C2	This study
RF21	*S. cerevisiae*	*ura3Δ his3Δ* pGPD416-mCherry-Lact-C2 pRS426GFP-2×PH(PLCδ)	This study
RF18	*S. cerevisiae*	*ura3Δ his3Δ cho1Δ* pGPD416-mCherry-Lact-C2 pRS426GFP-2×PH(PLCδ)	This study
RF25	*S. cerevisiae*	*ura3Δ his3Δ cho1Δ::P_{GAL1}-CHO1 G418^R*	This study
RF26	*S. cerevisiae*	*ura3Δ his3Δ cho1Δ::P_{GAL1}-CHO1 G418^R* pGFP-Lact-C2	This study
BY25594	*S. cerevisiae*	*MATaura3-1::ADH1-AtTIR1-9Myc(URA3) ade2-1 his3-11, 15 leu2-3, 112 trp1-1 can1-100*	From Minetaka Sugiyama
CDCS67	*S. cerevisiae*	*MATaura3-1::ADH1-AtTIR1-9Myc(URA3) ade2-1 his3-11, 15 leu2-3, 112 trp1-1 can1-100 cho1::CHO1-Deg-Kan^R*	This study
MG1655	*E. coli*		Gift from Fozo Lab
CDCS12	*E. coli*	*LactC2-GFP-Amp^R*	This study
CDCS16	*E. coli*	*Amp^R*	This study
Cg 27	*C. glabrata*	*ura3Δ his3Δ leu2Δ tryp1Δ*	Lab Strain
RF29	*C. glabrata*	*ura3Δ his3Δ leu2Δ tryp1Δ* pGFP-Lact-C2	This study

Table A2. 2. Continued.

Strain	Organism	Genotype	Source
SC5314 (Ca157)	*C. albicans*		Lab Strain
Ca159	*C. albicans*	*cho1ΔΔ*	Chen *et al.*, 2010
CDCS18	*C. albicans*	P_{ENO1}::P_{ENO1}-*GFP-Lact-C2-SAT1*	This study
CDCS24	*C. albicans*	*cho1ΔΔ* P_{ENO1}::P_{ENO1}-*GFP-Lact-C2-SAT1*	This study

Strain Production

We used a standard lithium acetate transformation method to construct the *S. cerevisiae* strains in this study (Gietz and Woods 2002). All strain and plasmid information can be found in Tables A2.1 and A2.2, respectively. Transformation of GFP-Lact-C2 into WT and *cho1Δ S. cerevisiae*: GFP-Lact-C2 (pGFP-Lact-C2) was transformed into wild-type and *cho1Δ* using the *URA3* marker to produce *ura3Δ his3Δ* pGFP-Lact-C2 and *ura3Δ his3Δ cho1Δ* pGFP-Lact-C2, respectively. Transformation of mCherry-Lact-C2 into WT and *cho1Δ S. cerevisiae*: mCherry-Lact-C2 (pGPD416-mCherry-Lact-C2) was transformed into wild-type and *cho1Δ* using the *URA3* marker to produce *ura3Δ his3Δ* pGPD416-mCherry-Lact-C2 and *ura3Δ his3Δ cho1Δ* pGPD416-mCherry-Lact-C2, respectively. Transformation of GFP-2x Ph(PLCδ) into *ura3Δ his3Δ* pGPD416-mCherry-Lact-C2and *ura3Δ his3Δ cho1Δ* pGPD416-mCherry-Lact-C2*S. cerevisiae*: The GFP-2xPh(PLCδ) was cut from pRS426GFP-2×PH(PLCδ) and ligated into pRS423 to produce pRF1 (Table A2.2). pRS426GFP-2×PH(PLCδ) (pRF1) was transformed into *ura3Δ his3Δ* pGPD416-mCherry-Lact-C2 and *ura3Δ his3Δ cho1Δ* pGPD416-mCherry-Lact-C2using the *HIS3* marker to produce *ura3Δ his3Δ* pGPD416-mCherry-Lact-C2 pRS426GFP-2×PH(PLCδ) and *ura3Δ his3Δ cho1Δ* pGPD416-mCherry-Lact-C2 pRS426GFP-2×PH(PLCδ), respectively. Transformation of P_{GAL1} into WT and *cho1Δ S. cerevisiae*: P_{GAL1} was amplified from p73 with primers adapted from (Longtine, *et al.* 1998) (CCO49 and CCO50) containing overhangs of the native *CHO1* promoter. The PCR product was transformed into wild-type and *cho1Δ*

Table A2. 3. Plasmids Used in this Study

Plasmid	Inserts	Source
p200 (pGFP-Lact-C2)	GFP-Lact-C2, *URA3*, Cen/Ars, Amp^R	Yeung *et al.*, 2008
pBS34	mCherry, *URA3*, Amp^R	Shaner *et al.*, 2004
pGPD416-mCherry-Lact-C2	mCherry-Lact-C2, *URA3*, Amp^R	Fairn *et al.*, 2011
pRS423	*HIS3*, Amp^R	Lab Strain
pRS426GFP-2×PH(PLCδ)	GFP-2x Ph(PLCδ), *URA3*, Amp^R	Addgene plasmid # 36092
pRF1	GFP-2x Ph(PLCδ), *HIS3*, Amp^R	This study
p73	P_{GAL1}, $G418^R$, Amp^R	Lab Strain
EBp42	NAT^R, Amp^R	Lab Strain
BYP 6740 (Pmk43)	Amp^R, KAN	Nishimura *et al.*, 2009
BYP 6742 (Pmk76)	*URA3*, Amp^R	Nishimura *et al.*, 2009
pCDC2	eGFP-Lact-C2, NAT^R, Amp^R	This study
pRI1	Ap^R	Fozo Lab, Opdyke *et al.*, 2006
pCDC5	GFP-Lact-C2, Amp^R	This study
pRS423	*HIS3*, Amp^R	Lab Strain
pUC57		Lab Strain
pCDC4	GFP-Lact-C2, NAT^R, Amp^R	This study
pCDC2	eGFP-Lact-C2, NAT^R, Amp^R	This study

using the G418/Kanamycin resistance marker to produce *ura3Δ his3Δ cho1Δ::P_{GAL1}-CHO1 G418/Kan^R*. Primer sequences can be found in Table A2.3. Transformation of GFP-Lact-C2 into *ura3Δ his3Δ cho1Δ::P_{GAL1}-CHO1 G418/Kan^R S. cerevisiae*: GFP-Lact-C2 (pGFP-Lact-C2) was transformed into *ura3Δ his3Δ cho1Δ::P_{GAL1}-CHO1 G418/Kan^R* using the *URA3* marker to produce *ura3Δ his3Δ cho1Δ::P_{GAL1}-CHO1 G418/Kan^R GFP-Lact-C2*. Cloning of Auxin-Repressible Degron System: For inserting the "degron sequence" at the C-terminus of *ScCHO1*, we adapted the primers from (Nishimura, *et al.* 2009). First we made CCO120 and CCO121 based on pYM3/6_F and pYM3/6_R with overhangs matching the ScCHO1 gene just before the stop codon and just after the stop codon, respectively. However, because we had no success with these oligonucleotides, we ordered a second reverse primer to replace CCO121, called CCO143. This primer in combination with CCO120 resulted in a band ~2.4 Kb in length when used in PCR of BYP 6740 (Pmk43) (plasmid from Minetaka Sugiyama). This PCR product was then transformed into BY25594 (from Minetaka Sugiyama). Correct orientation of the insertion was confirmed using CCO108 in combination with either CCO144 (3.3 Kb band) or CCO145 (2.1 Kb band). Sequencing to confirm the correct sequence insertion was performed using CCO140.

The strain already contained the E3 ligase with a uracil marker (BYP 6742 (Pmk76)), but to include the GFP-Lact-C2 probe, we had to move GFP-Lact-C2 into a plasmid with an alternative marker (pGFP-Lact-C2 contains a uracil marker

Table A2. 4. Primers Used in this Study

Primer	Sequence	Source
CCO49	**AAGAGAGATACACCTATTTTTTTCATTTTGTGGGTGATTGTCATTTTTAG** GAATTCGAGCTCGTTTAAAC	Adapted from Longtine *et al.*, 1998
CCO50	**TCCGTGTGTGGGAATTCTTGAGGTGCGAAATCTTCATCTGATTCAACCATTTT**CATTTTGAGATCCGGGTTTT	Adapted from Longtine *et al.*, 1998
CCO120	TTATCCATGGGTGTGGAATGATTTCGAAGAGCTTGAAAATTCCAAAGCCA AGCTTCGTACGCTGCAGGTCG	Adapted from Nishimura *et al.*, 2009
CCO121	AAAAGTTATATGTACAAATTTTTTTTGACGCCAGGCATGAACAAAAACTA GGTAAGATCTCTTGAATGATCGTTC CACTTTTTAGC	Adapted from Nishimura *et al.*, 2009
CCO143	AAAAGTTATATGTACAAATTTTTTTTGACGCCAGGCATGAACAAAAACTA CGAGTCAGTGAGCGAGGAAGC	This study
CCO108	ATGGTTGAATCAGATGAA	This study
CCO144	GAATGTCGTGTGAAGCTG	This study
CCO145	GTGAGAACTGTATCCTAGC	This study
CCO140	CAGCTGGCAAGAATTGAG	This study
CCO147	AAAAgcggccgcCCTAACAGCCCAGC AGC	This study
CCO148	AAAAgagctcATGGTGAGCAAGGGCG	This study
CCO32	*GGAATATTACAACCATGGCTGATCC ATGTCTAAAGGTG*	This study
CCO33	TACAATCATGACT*GATCCATGTCTA AAGGTG*	This study

(parent plasmid is pRS416)). Thus, we selected pRS423 which contains a *HIS3* marker. pRS423 was digested with NotI-HF and SacI, then purified. GFP-Lact-C2 was amplified from pGFP-Lact-C2 using CCO147 which contained a NotI cut site 3' of the GFP sequence and CCO148 which contained a SacI cut site 5' of the Lact-C2 sequence.

Candida glabrata

C. glabrata was transformed with pGFP-Lact-C2 using the same lithium acetate transformation method as *S. cerevisiae*. The produced strain, RF29 can be found in Table A2.1 and the plasmid in Table A2.2.

Candida albicans

Because of the special CTG codon usage in *C. albicans*, we could not utilize the same plasmids for *S. cerevisiae* or *C. glabrata*. After several attempts to perform multiple tandem site-directed mutagenesis procedures we used Genescript to synthesize the plasmid pCDC6 which contains a codon-optimized GFP-Lact-C2 in pUC57. Unfortunately, no fluorescence was seen upon transformation into *C. albicans*, and thus a new GFP gene (eGFP) was used. The present GFP gene was removed from pCDC4 using NcoI and SspI. eGFP was amplified using CCO32 which contained a 3' SspI cut site and CCO33 which contained a BspHI cut site (matched up with NcoI cut site), producing pCDC2. This plasmid was

digested in the promoter and transformed into both wild-type (CDCS18) and *cho1ΔΔ* (CDCS24).

Escherichia coli

E. coli strain MG1655 was used for this study. GFP-Lact-C2 was amplified from pGFP-Lact-C2 using primers TRO 938 and TRO939 which contain EcoRI and HinDIII cut sites respectively. pRI plasmid was then digested using EcoRI and HinDIII and gel purified. The digested GFP-Lact-C2 fragment was ligated into plasmid pRI to produce pCDC5. This plasmid and the empty vector were transformed simultaneously into chemically competent MG1655 to produce CDCS12 and CDCS16, respectively.

For the transformation, MG1655 was streaked on an LB plate and inoculated in 3 ml of LB overnight at 37°C, shaking. The following morning the cells were diluted 1:500 in LB and shaken at 37°C until the OD_{600} reached approximately 0.4 to 0.6 (~3 hours). The cells were pelleted at 3600 rpm at 4°C for 10 minutes. Pellets were resuspended in water and spun again. The pellet was then resuspended in 800 µl of ice cold water then spun down at 13,000 rpm at 4°C for 3 minutes. The supernatant was aspirated and then the pellet was resuspended in 100 µl of ice cold water. Gene Pulse cuvettes were placed on ice, then 40-50 µl of the cells were mixed with 1.5 µl of the ligation or with 0.5 – 1 µl of pRI empty vector. The cuvettes were electroporated at 25 µF with a resistance of 200 Ω and a voltage of 2.5 V. The cuvettes were then immediately

placed on ice and 500 µl of SOC medium was added to rescue for 1 hour at 37°C shaking. After the rescue, cells were plated on LB-Ampicillin plates and incubated at 37°C overnight.

Fluorescent Microscopy

To confirm the successful transformation of fluorescent probes into our yeast strains, overnight cultures were diluted back to 0.1 or 0.2 OD_{600} and allowed to grow for 2-4 hours shaking at 30°C or until early log phase was reached. Cells were then imaged via fluorescent microscopy (Leica). For quantification of localized, partially localized, and diffuse GFP-Lact-C2, 80 total frames were assessed. The percentages of each category in each frame was calculated and then averaged with the rest of the frames for both galactose- and glucose-grown strains. All images were analyzed using Leica Application Suite 4.4.

Serial Dilution Plating

To test the effectiveness of our repressible promoter, *ura3Δ his3Δ cho1Δ::*P_{GAL1}*-CHO1 G418/Kan*^{R} were grown overnight, then diluted to 0.1, 0.2, 4 x 10^{-3}, 8 x 10^{-4}, and 1.6 x 10^{-6} OD_{600}. 10 µl aliquots were spotted onto minimal medium agar plates supplemented with galactose or glucose, +/- 1 mM ethanolamine. Plates were incubated at 30°C then viewed the following day for growth.

Lipid Extraction and Thin Layer Chromatography

The *ura3Δ his3Δ cho1Δ::P_{GAL1}-CHO1 G418/Kan^R* strain was grown in 5 ml minimal medium supplemented with either glucose or galactose overnight, shaking at 30°C. Lipids were extracted using a standard hot ethanol extraction (Hanson and Lester 1980). Isolated lipids and lipid standards (Avanti) were spotted on thin layer chromatography plates (Millipore) and separated with chloroform:ethanol:water:trimethylamine (35:30:7:35) solvent system (Chen, *et al.* 2010). Lipids were imaged using primulin dye and UV-light exposure.

Lyso PS Uptake Experiment

The Lyso-PS protocols from (Maeda, *et al.* 2013, Moser von Filseck, *et al.* 2015) were adapted for this experiment. Overnight cultures of *cho1Δ* pGFP-Lact-C2 were either used directly (stationary phase study) or diluted to 0.1 and allowed to grow for 2 hours (log phase study). Cells were washed with cold water, followed by lyso-PS (Avanti) addition and a 10 minute incubation on ice. Tubes were then incubated at 30˚C and at select time points a 10 µL sample of cells was removed and mounted onto slides. For some experiments where time was constraining, Prolong Gold (Life Technologies) was used to preserve samples until microscopy could be performed. Stationary phase time points: 0, 15, 30, and 60 minutes. Log phase time points: 0, 1, 2, and 3 hours.

Compound Treatment

The *ura3Δ his3Δ* pGFP-Lact-C2 and *ura3Δ his3Δ cho1Δ* pGFP-Lact-C2 strains were used to test the effects of Papuamide-A (Pap-A) (Flintbox), SB-224289 (Tocris), and Staurosporine (CGP 41251) (SelleckChem) on PS localization. Overnight cultures were diluted to 0.2 OD_{600} and allowed to grow for 3-4 hours. Cultures were then diluted to 0.1 OD_{600} and 200 µL of the *ura3Δ his3Δ* pGFP-Lact-C2 were either treated with 50 µg/mL Pap-A, 4.5µg/mL staurosporine, 250 µM SB-224289, or the solvent (water:methanol (2:1)) for Pap-A and DMSO for SB-224289 and staurosporine) as negative controls. *ura3Δ his3Δ cho1Δ* pGFP-Lact-C2 was used as a positive control for PS mislocalization. All samples were then incubated at 30˚C for 1 hour and 20 minutes followed by fluorescent microscopy. A second trial was performed with a decreased concentration of SB-224289 (100 µM) and cell plating for viability.

Results

Phosphatidylserine is produced in the endoplasmic reticulum in yeast and can either be trafficked to the plasma membrane or the mitochondria where it is used to produce phosphatidylethanolamine (PE). Some studies have provided a greater understanding of PS trafficking to these areas; however, the duration of PS at the plasma membrane is currently unknown. In this work, we undertook experimentation to determine the length of time that PS remains at the membrane in the model yeast *Saccharomyces cerevisiae*.

In order to perform these studies, we began by creating strains harboring GFP-Lact-C2 (Yeung, *et al.* 2008). GFP-Lact-C2 binds to PS in the cell and emits a green fluorescence, allowing us to visualize PS localization within cells.

GFP-Lact-C2 (pGFP-Lact-C2) in wild-type and *cho1Δ S. cerevisiae*

Figure A2.1A shows micrographs of wildtype and *cho1Δ S. cerevisiae* lab strains carrying pGFP-Lact-C2. GFP-Lact-C2 localizes to the membrane in wild-tyep where PS is enriched. In *cho1Δ*, which has no PS, GFP-Lact-C2 is diffuse throughout the cell.

mCherry-Lact-C2 (pGPD416-mCherry-Lact-C2) in wild-type and *cho1Δ S. cerevisiae*

We further wanted to determine if the probe bound to the fluorophore mCherry might offer even clearer signal. Figure A2.1B shows micrographs of of wildtype and *cho1Δ S. cerevisiae* lab strains carrying pGPD416-mCherry-Lact-C2 grown to log phase. As was shown with GFP-Lact-C2, we see localization of mCherry-Lact-C2 at the membrane in wild-type whereas diffuse signal in *cho1Δ.* However, although overall we saw diffusion in *cho1Δ*, we did see some cells with slight localization at the membrane, which was not ideal and prompted us to focus on GFP-Lact-C2 as our fluorescent probe for PS-localization.

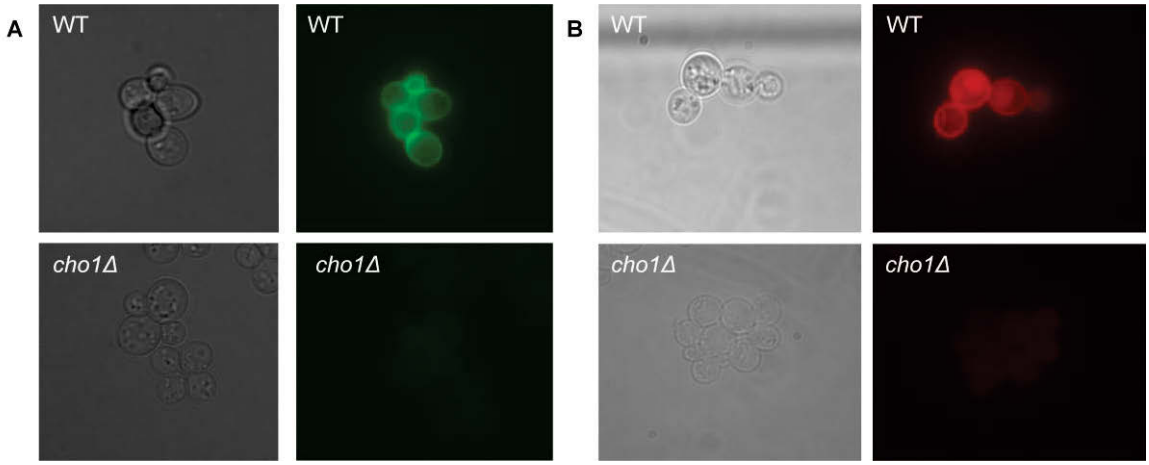

Figure A2. 1. Localization of PS in Wildtype and *cho1Δ* Yeast
Fluorescent microscopy of (A) wild-type and *cho1Δ* carrying pGFP-Lact-C2 and (B) pGPD416-mCherry-Lact-C2. Images were taken during log phase of growth.

GFP-2x Ph(PLCδ) (pRS426GFP-2×PH(PLCδ)) in wild-type and *cho1Δ S. cerevisiae*

In order to better create a distinction between membrane-bound and diffuse GFP-Lact-C2 probe (i.e. PS localization), we wished to incorporate a second, plasma membrane positive marker. The Plekstrin homology domain (PH domain) is a domain of approximately 120 amino acids that binds to PI4,5P2 in the membrane of *S. cerevisiae* (Lemmon 2007). We hypothesized that localization of the PH domain fused with GFP (GFP-2x Ph(PLCδ)) to PI4,5P2 could be used as a positive marker for the plasma membrane. This, combined with mCherry-Lact-C2 would allow us to monitor the precise location of PS in the cell.

Under this model, mCherry-Lact-C2 and GFP-2x Ph(PLCδ) would overlap (forming a yellow signal) in the wild-type organism. In the *cho1Δ*, the membrane would be green (GFP-2x Ph(PLCδ)) and the cytoplasm would appear red (diffuse mCherry-Lact-C2 signal) as a result of absence of PS. We further hypothesized that, should this tool be useful, we could add a third component to control PS production (place *CHO1* under a repressible promoter). Thus, PS should start out located at the membrane, but upon the shut off of PS production via our repressible promoter, it should visibly diffuse into the cytoplasm. Resulting overlay images of the red and green fluorescence under normal conditions should show a yellow color around the membrane. When the expression of *CHO1* is turned off, there should be a separation of colors as the red begins to diffuse into the cytoplasm, while the green stays at the membrane.

pRS426GFP-2×PH(PLCδ) was transformed into wildtype and *cho1Δ S. cerevisiae* already carrying pGPD416-mCherry-Lact-C2. As expected, in wildtype there is localization of the fluorescence under both green and red fluorescence (Fig A2.2). In addition *cho1Δ* displayed green fluorescence (GFP-2x Ph(PLCδ)) localized at the plasma membrane. When under the red fluorescence, the mCherry-Lact-C2 signal is diffuse throughout the cell. However, the results were inconsistent throughout experiments with some showing localization of mCherry-Lact-C2 in *cho1Δ*, and still others showing low mCherry-Lact-C2 signal all together (Fig A2.2). As a result, we began to focus efforts on the use of GFP-Lact-C2 alone.

Transformation of P_{GAL1}, G418^R, Amp^R (p73) into WT *S. cerevisiae*

Next, in order to study the length of time that PS remains at the membrane, we wished to create a strain where the PS synthase gene (*CHO1*) was under a repressible promoter. We engineered the strain *cho1Δ::*P_{GAL1}*-CHO1* which allows PS production when the strain is grown in galactose medium, and inhibits PS production when the strain is grown in glucose (Eckert and Muhlschlegel 2009, Longtine, *et al.* 1998).

We performed two experiments to validate *cho1Δ::*P_{GAL1}*-CHO1*. First, the strain was grown on minimal medium with: 1) histidine and uracil to account for the auxotrophies of the parent strain, 2) galactose **or** glucose to either repress or

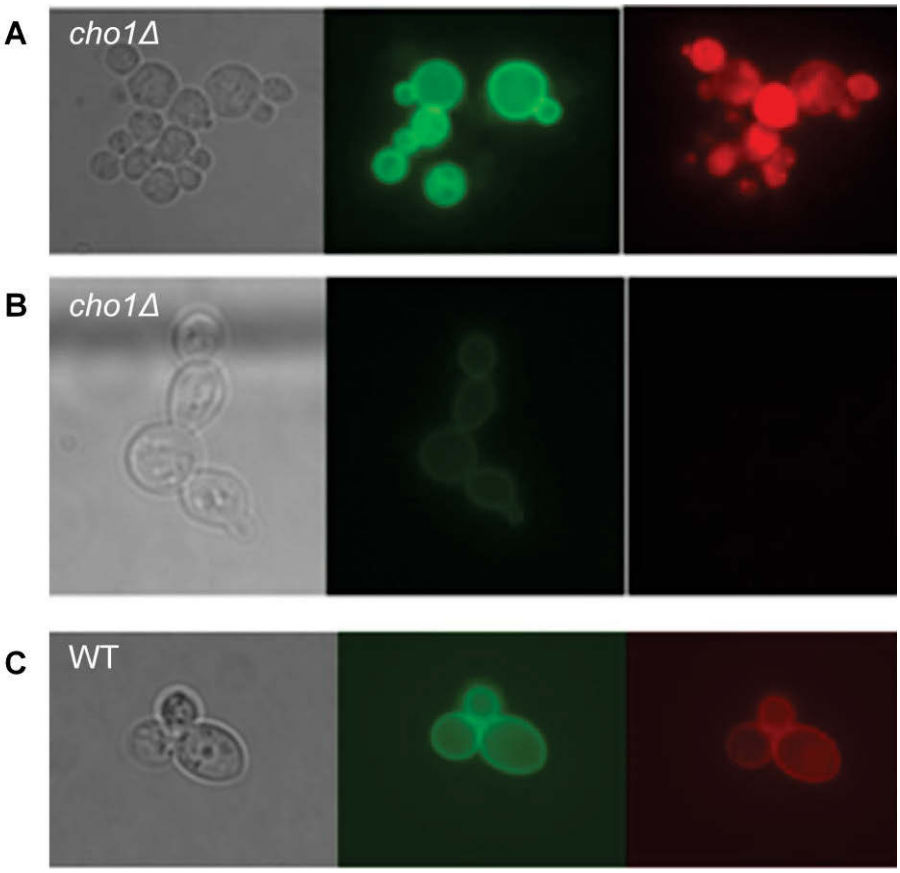

Figure A2. 2. Localization of PS and PI4,5P2 in Wild-type and *cho1Δ* Yeast
Fluorescent microscopy of (A) and (B) *cho1Δ* and (C) wild-type *S. cerevisiae* with the PH domain GFP and Lact-C2 mCherry under red and green fluorescence in stationary phase.

allow PS production, and 3) **+/-** 1 mM ethanolamine to account for any auxotrophy produced by PS decreases (Chen, *et al.* 2010).

As shown in Figure A2.3, in the presence of galactose, P_{GAL1} is turned on, allowing expression of *CHO1* and hence the production of PS (Fig. A2.3A). In the presence of glucose P_{GAL1} is shut off, turning off expression of *CHO1* and preventing PS from being made (Fig. A2.3B). Addition of ethanolamine allows for production of PE in the absence of PS via the alternative Kennedy Pathway (Cassilly, *et al.* 2017, Chen, *et al.* 2010), and allows growth (Fig. A2.3D). However, in the presence of glucose without ethanolamine, the organism should be unable to grow. Unfortunately, though there is a decrease in growth, the fact that the organism is still able to grow (Fig. A2.3C) is an indication that there is an incomplete shut off of P_{GAL1}. In this case, we hypothesize that some PS is still being produced via leaky repression of *CHO1* to the extent that PE can be made in the absence of PS.

In order to confirm our suspicions of an incomplete shut-off of *CHO1*, we isolated lipids from strains grown in all conditions mentioned above. We then performed thin layer chromatography to qualitatively measure PS levels within each condition. As shown in Figure A2.4, PS is present in *cho1Δ::*P_{GAL1}*-CHO1* grown in galactose and wild-type negative control, because the *CHO1* gene is being expressed. Inversely, there is no PS in *cho1Δ* positive control. However, as suggested by the growth of glucose-grown *cho1Δ::*P_{GAL1}*-CHO1* in Figure A2.4,

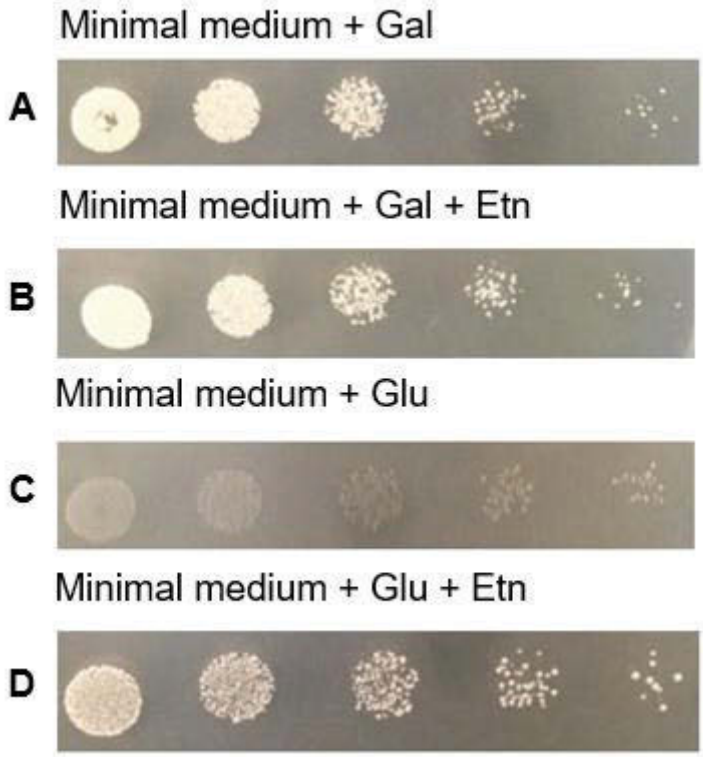

Figure A2. 3. Phenotype of the *cho1Δ::P_{GAL1}-CHO1* on Solid Medium

Serial dilutions of the *cho1Δ::P_{GAL1}-CHO1* strain in medium supplemented with (A) galactose (Gal) and (B) 1 mM ethanolamine (Etn) or (C) glucose (Glu) and (D) 1 mM ethanolamine. Results show decreased growth on medium + Glu without Etn where both *de novo* and Kennedy PE synthesis are inhibited.

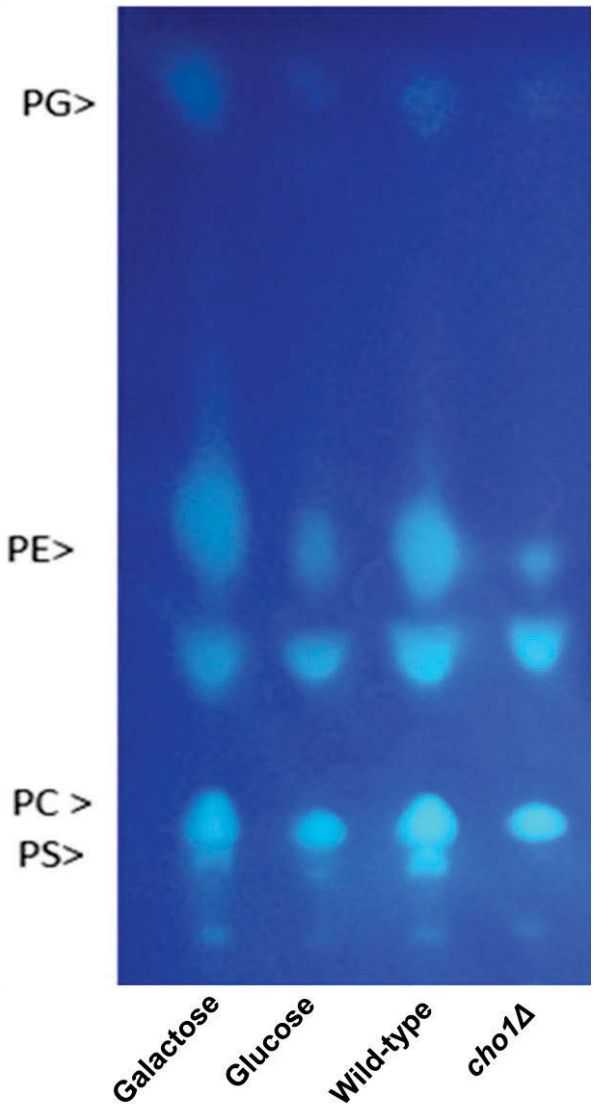

Figure A2. 4. *cho1Δ::P_{GAL1}-CHO1* TLC
cho1Δ::P_{GAL1}-CHO1 shows decreased, but not complete loss of, PS in presence of glucose as compared to strain grown in galactose, wild-type, and the *cho1Δ* negative control. These results indicate an incomplete shut off of the *CHO1* gene.

there is some PS in the strain grown in glucose, further displaying the incomplete shut off of P_{GAL1}.

Despite these data, we were interested in performing microscopy in an effort to identify any GFP-Lact-C2 localization differences in this strain. We inserted GFP-Lact-C2 within *cho1Δ::*P_{GAL1}*-CHO1*. We then performed microscopy to determine the influence of growth in glucose or galactose on PS localization. Figure A2.5A shows *cho1Δ::*P_{GAL1}*-CHO1* carrying pGFP-Lact-C2 grown in galactose. As expected, GFP-Lact-C2 localized around the cell membrane. Figure A2.5B, *cho1Δ::*P_{GAL1}*-CHO1* carrying pGFP-Lact-C2 is grown in glucose, shutting off P_{GAL1}, and hence repressing the expression of the *CHO1* gene. PS is not being produced, so the GFP-Lact-C2 is diffuse in the cytoplasm.

Unfortunately, these results were not consistent and we met with high variability when viewing the cells under the fluorescent microscope. As shown in Figure A2.5C, three localization signatures were seen: 1) distinct localization with the PS localized mainly at the membrane, 2) diffuse with no signs of fluorescence at the membrane, and 3) partial localization with some fluorescence diffuse and localized at the membrane. This further indicated that P_{GAL1} produced an incomplete shutoff of *CHO1* and that PS was still being produced to some extent in some cells.

To quantify these findings, we counted the cells falling into the three signature fluorescence types. Figure A2.5D shows the quantification of 80 frames of fluorescing cells (n=1669 fluorescing cells). Localized, partially localized, and

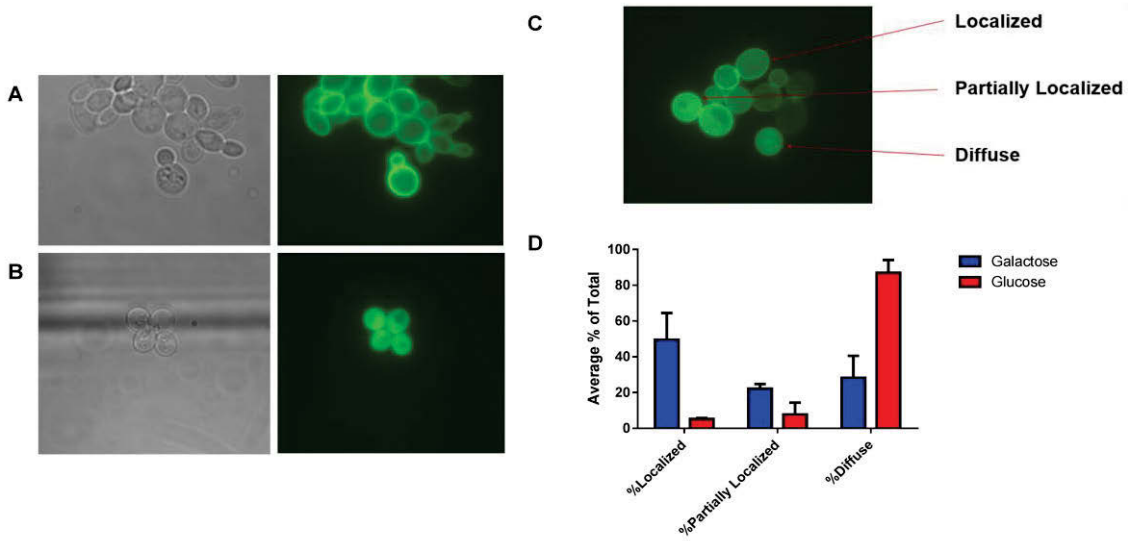

Figure A2. 5. Localization of PS in *cho1Δ::P_{GAL1}-CHO1::GFP-Lact-C2 S. cerevisiae*

(A) Shows the *cho1Δ::P_{GAL1}-CHO1::GFP-Lact-C2 S. cerevisiae* grown in galactose medium, with localized PS at the membrane. (B) shows the strain grown in glucose and the diffusion of Lact-C2-GFP into the cytoplasm. (C) Examples of cells localized, partially localized, and diffuse. (D) Quantification of GFP-Lact-C2 localization reveals that shut off of Cho1p (i.e. cells grown in glucose) causes quantitative decreases in plasma membrane localization of the probe, but that the result is not consistent. Galactose grown cells showed less growth and weaker fluorescence due to the nature of the galactose carbon source compared to glucose. Localized, partially localized, and diffuse fluorescing cells are calculated as a percent of total cells counted. n = 1669 fluorescing cells.

diffuse fluorescing cells were calculated as percentages of each frame, then averaged to produce an overall percentage. Although there is a significant increase in the mislocalization when the strain is grown in glucose, the frames are not completely uniform, and the variability was judged as too high to continue these experiments. Additionally, since galactose is not as preferable of a carbon source as glucose, the cells showed less growth, and also a weaker fluorescence signal.

Exogenous Addition of Lyso PS

Previous studies found that addition of lyso-PS (PS with one fatty acid chain) to *cho1Δ* strain which produces no PS caused the cells to uptake the lyso-PS and recycle it in the cell as PS. The lyso PS is converted to PS and transferred to the membrane from the ER (Maeda, *et al.* 2013, Moser von Filseck, *et al.* 2015). We wished to reproduce this result by adding lyso-PS to *cho1Δ* carrying pGFP-Lact-C2. Then we monitored the movement of PS through the cell over a time course via fluorescent microscopy. We added lyso PS to cultures for 10 minutes at room temperature to allow for uptake. Tubes were then placed in the 30˚C water bath to allow for trafficking within the cells.

Under the green fluorescence, the cells showed diffuse GFP-Lact-C2 signal for the 0 and 15 minute time points (Fig A2.6). We hypothesize that lyso-PS is taken up here, and in the process of being repackaged in the ER. The cells began to show localization around the 30 minute time point where they have

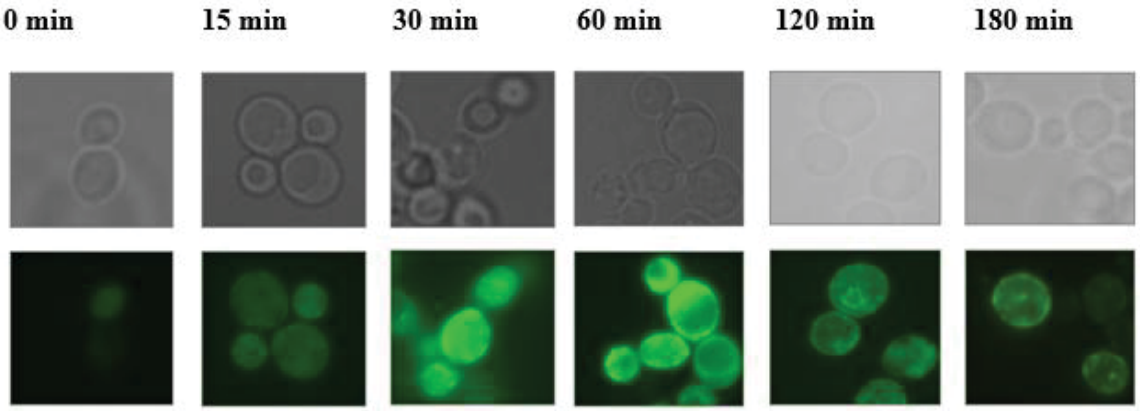

Figure A2. 6. Time Course of PS Localization in *cho1Δ* Upon Addition of Lyso PS

cho1Δ S. cerevisiae carrying pGFP-Lact-C2 shows a plasma membrane localization of PS within 30 minutes of incubation at 37°C.

likely sent re-modeled PS to the plasma membrane. At 60 minutes, the PS is more localized at the membrane. It remains localized at 120 and 180 minute time points, though some of the signal begins to diffuse back in to the cytoplasm.

Compound Experiment

After having engineered the wildtype and *cho1Δ* carrying pGFP-Lact-C2 strains, we were interested in using this tool (GFP-Lact-C2) to determine effects of membrane-perturbing agents on PS localization. Papuamide-A, SB-224289, and staurosporine were chosen because previous experiments have been performed that indicate that these compounds either disrupt PS trafficking or plasma membrane structure in *Candida albicans* (Andjelic, *et al*. 2008, Cassilly, *et al*. 2016, Cho, *et al*. 2013b, Cho, *et al*. 2012, Selkirk, *et al*. 1998a). Papuamide-A is a compound that binds to PS in the plasma membrane and causes cell lysis and death (Andjelic, *et al.* 2008, Cassilly, *et al.* 2016, Chen, *et al.* 2010). Staurosporine blocks endosomal sorting and recycling of PS, and hence inhibits the trafficking of PS to the membrane (Cho, *et al*. 2013b, Cho, *et al*. 2012). SB-224289 is 5-H_{T1}B receptor antagonist that has been shown to cause trafficking problems in *S. cerevisiae*, and likely promotes massive endocytosis (Chapter 2 and 3) (Cassilly, *et al*. 2016, Selkirk, *et al*. 1998a).

To test the effects of these compounds on PS localization, we treated log phase wild-type carrying pGFP-Lact-C2 with varying concentrations of each compound and examined the GFP-Lact-C2 probe signal via fluorescent

microscopy. All data was compared to an untreated control and *cho1Δ* (Fig A2.7A). As shown in Figure A2.7C, when wild-type was treated with Pap-A, accumulation of fluorescence inside the cells was observed, as well as a decrease in cell size, indicating the process of cell death (compare to Fig A2.7B). This was further demonstrated by plating the treated cell sample on solid medium. Samples treated with Pap-A were not viable, whereas untreated cells grew. When treated with staurosporine, which is supposed inhibit the trafficking of PS to the membrane, PS was seen trapped in punctuate spots within the cytoplasm (Fig A2.7E, compare with Fig A2.7D). Last, cells treated with SB-224289 showed accumulation of GFP-Lact-C2 in the cytoplasm, and a decrease in signal at the membrane (Fig A2.7G, H, compare with Fig A2.7F). Viability plating of staurosporine and SB-224289-treated cells indicated no signs of cell toxicity via a fungicidal mechanism.

Efforts to Adapt PS Trafficking Tools in Other Microbes

Because of the usefulness of these tools developed in *S. cerevisiae*, we wished to move them into other systems, including pathogenic fungi (*C. albicans* and *C. glabrata*) and bacteria (*E. coli*).

In *C. albicans*, we inserted the GFP-Lact-C2 gene into an *ENO1* locus of wild-type and *cho1ΔΔ* as described in materials and methods. Although fluorescent signal was observed in both strains (Fig A2.8C and D), there seemed to be a great deal of unexpected localization of GFP-Lact-C2 at the membrane in

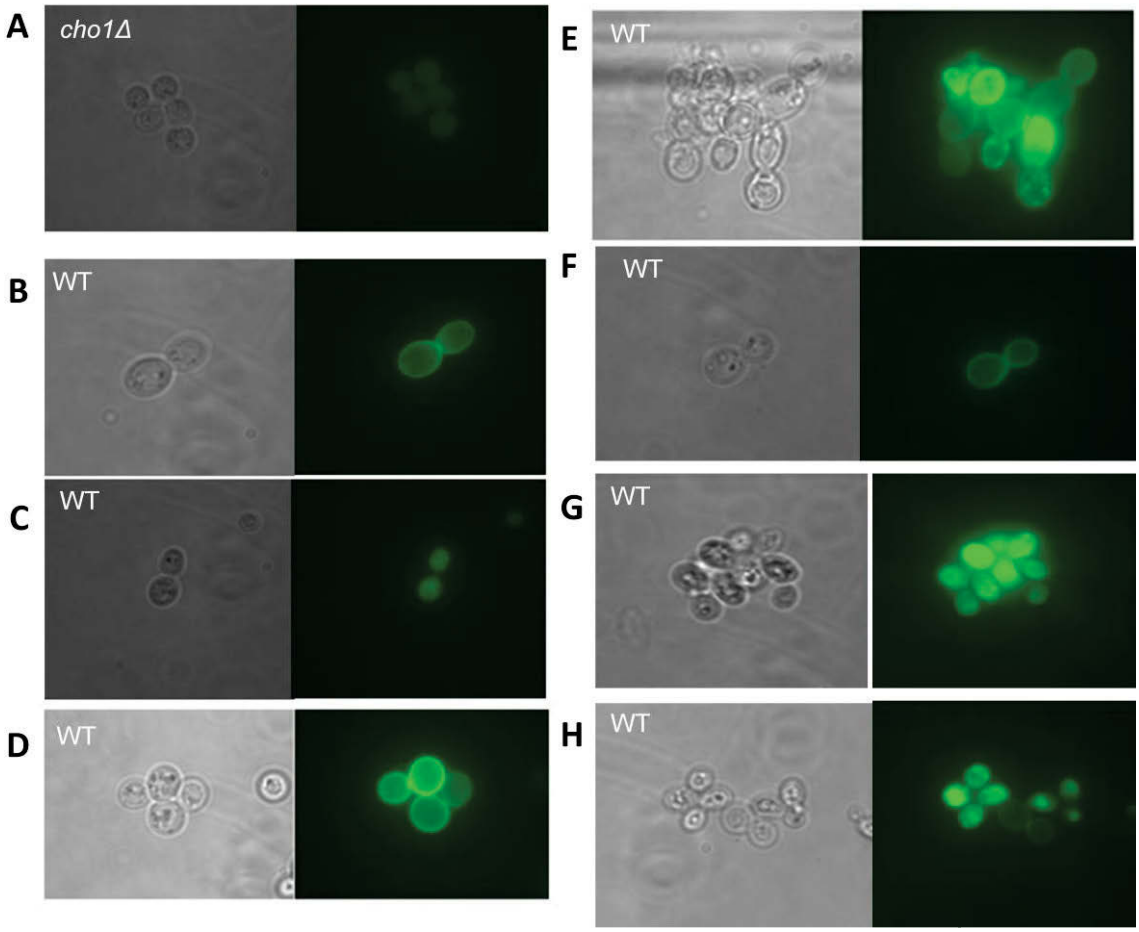

Figure A2. 7. Effect of Membrane-Perturbing Agents on Cells
(A) *cho1Δ* carrying pGFP-Lact-C2 control while (B) wild-type carrying pGFP-Lact-C2 untreated with a methanol:water solution, and (C) treated with 50 µg/mL Pap-A. (D) wild-type carrying pGFP-Lact-C2 treated with DMSO, while (E) shows the strain treated with 4.5 µg/mL Staurosporine. (F) wild-type untreated with DMSO, while (G) the strain treated with SB-224289 at 250 µM or (H) 100 µM.

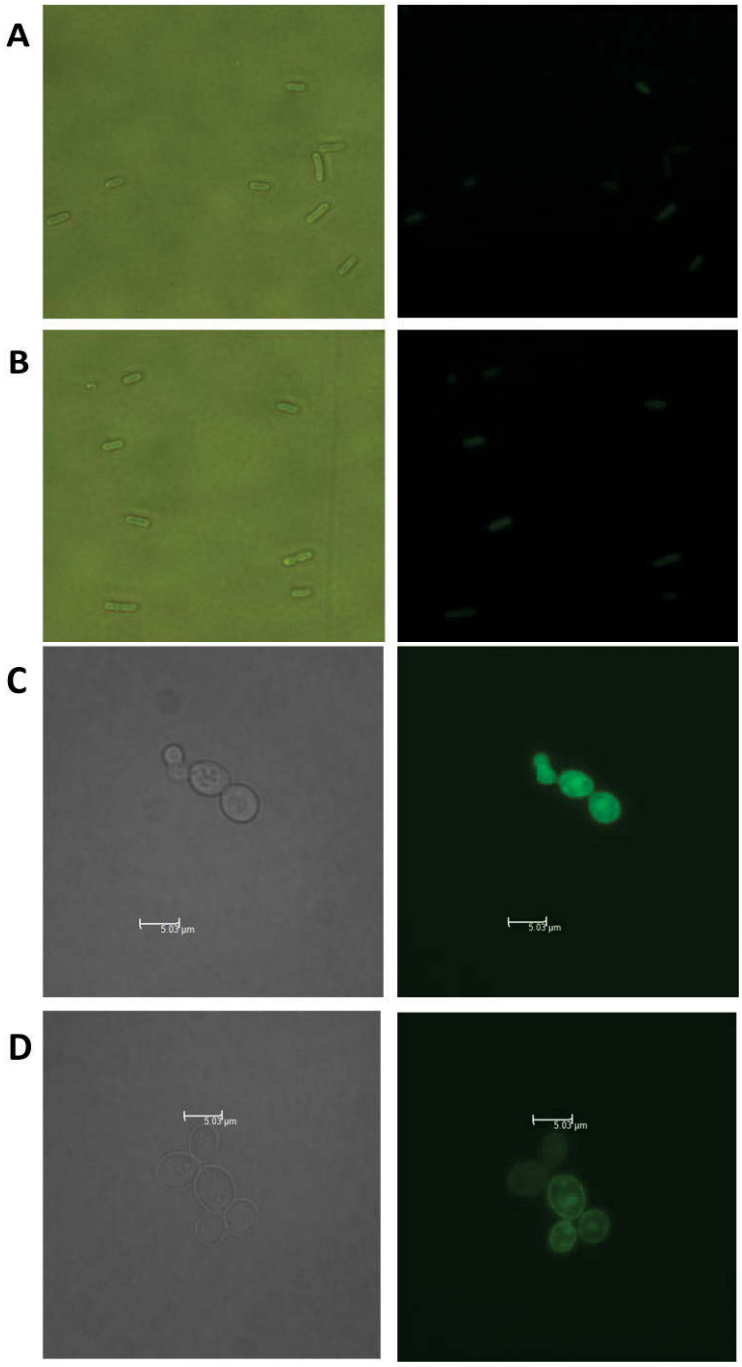

Figure A2. 8. Localization of PS *E. coli* and *C. albicans*

Fluorescent microscopy of (A) empty vector (B) GFP-Lact-C2 in *E. coli*. Fluorescence exposure = 3.5 sec and (C) *cho1ΔΔ* and (D) wild-type *C. albicans* expressing GFP-Lact-C2.

cho1ΔΔ. Because this strain produces no PS, this result was attributed to a high concentration of GFP-Lact-C2 within the cells that may show localization or accumulation as an artifact.

For *C. glabrata*, a strain bearing GFP-Lact-C2 was produced, however, efforts to produce a *cho1ΔΔ* strain were not successful and thus abandoned.

Last, for *E. coli*, we also expressed GFP-Lact-C2 in a common lab strain. However, because of the high concentration of the probe within the cells, high auto-fluorescence in our empty vector control, as well as poor resolution on microscopes available to us, no distinction or localization could be determined and this project was discontinued (Fig A2.8A and B).

Discussion

In this project, we have introduced PS specific probes, GFP-Lact-C2 and mCherry-Lact-C2 into wild-type and *cho1Δ* strains of *S. cerevisiae*. In both instances, we observed probe localization to the membrane in wild-type cells where PS is enriched. Alternatively, in *cho1Δ* strains, we saw diffuse signal as PS is not present in these strains.

After introducing the mCherry-Lact-C2 probe into *S. cerevisiae*, we decided utilize a second probe for another phospholipid, PI4,5P2, as a membrane specific probe. We hypothesized that this would allow us to monitor the movement of PS through the cell based on a separation of colors in overlapped pictures of the two probes under either red or green fluorescence.

The localization at the membrane under the green fluorescence demonstrated the localization of GFP-PH-Domain bound to the membrane, while the low signal under the red fluorescence demonstrates the diffusion of the mCherry-Lact-C2 probe into the cytoplasm. Upon the introduction of GFP-PH-domain, we found inconsistencies in the cells when viewed under red fluorescence. Most of the cells that showed clear localization around the membrane under the green fluorescence showed low or undetectable signal under the red fluorescence. The mCherry-Lact-C2 probe was diffuse in the *cho1Δ*, because PS is not being produced. Although the cells might have shown diffuse red fluorescence as predicted, the signal was bleached soon after the fluorescence was switched to the red color. This would have presented a challenge in performing time-lapse experiments with the two colors, because if the pictures are overlapped and the mCherry-Lact-C2 does not fluoresce as brightly as the PH domain-GFP, we would not be able to sufficiently observe a separation of colors. As a result, although elegant in theory, this project proved insufficient for our purposes.

We next focused efforts on controlling PS synthesis *in vivo*. We utilized the P_{GAL1} promoter which represses P_{GAL1} in the presence of glucose, suppressing the P_{GAL1}-*CHO1* gene in our construct. We expected no growth on minimal medium as a result of ethanolamine auxotrophy, but found that the strain grown in glucose (i.e. P_{GAL1}-*CHO1* repressed) was able to grow, though at a lesser degree than the strain grown in galactose (i.e. P_{GAL1}-*CHO1* expressed). This finding was further supported by thin layer chromatography where PS was

still present in the repressed strain, though at a lower degree. These findings indicated that P_{GAL1}-*CHO1* was not fully repressed in our experiments, despite what has been previously reported about P_{GAL1} providing a very tight shut off in *S. cerevisiae* (Longtine, *et al.* 1998), thus confounding our efforts to control PS production.

Despite this issue, we still wanted to determine if repressing P_{GAL1}-*CHO1* —albeit incompletely—might have an effect on PS localization intracellularly. We transformed the GFP-Lact-C2 probe into the P_{GAL1} strain, then viewed it under a fluorescent microscope. We saw an increase in mislocalization when the strain was grown in glucose (i.e. P_{GAL1}-*CHO1* repressed), showing more diffuse signal than when grown in galactose (i.e. P_{GAL1}-*CHO1* expressed). However, some frames showed cells with localized GFP-Lact-C2 signal in *cho1Δ*, while some showed more diffuse signal. In addition, there were many cells that showed partial localization, indicating that some PS was still being made within the population of cells. This inconsistency precluded our ability to fully take advantage of these tools for controlling PS production. Thus, due to the incomplete shutoff, the *cho1Δ*::P_{GAL1}-*CHO1* strain was deemed insufficient for the time-lapse experiments in monitoring the trafficking of PS and its duration at the plasma membrane.

Lyso PS Experiment

Because of the issues with *cho1Δ::P_{GAL1}-CHO1*, we decided to utilize the strains produced in this study to determine the effects of specific treatments on probe localization. First, we treated *cho1Δ* carrying pGFP-Lact-C2 with lyso-PS to monitor the movement of PS into the cells. Results of these time course experiments showed that at 30 minutes, PS localization around the plasma membrane could be observed, because the lyso PS was being converted into PS, and hence was being transported from the rough ER to the plasma membrane. Once at the plasma membrane, the PS remained there until the 180 minutes, but eventually began to diffuse back into the cytoplasm. Although this experiment showed that PS remains at the membrane for at relatively lengthy period of time, it is not representative of the biological process whereby PS is produced within cells. This experiment depends on the cell taking up extracellular lyso-PS from the medium and using it to form PS, instead of producing PS in the ER and trafficking it to the membrane. Experiments to assess PS production within the cell using fluorescent, click-tagged serine analogs are underway in collaborator Michael Best's laboratory and, if successful, will reflect a more accurate view of PS trafficking and dynamics.

Compound Experiments

Furthermore, we chose to test the effects of membrane-perturbing agents on GFP-Lact-C2 localization. In Figure A2.7, cells treated with Pap-A, the PS-

specific toxin, showed signs of cell death with PS accumulating in the cytoplasm in conjunction with loss of cell viability. Cells treated with staurosporine also had an expected accumulation of PS in punctuate dots in the cytoplasm, although cells remained viable when plated. Cells treated with SB-224289 at both 250 μM and 100 μM, showed a similar accumulation of PS in the cytoplasm with no concomitant loss of viability. Although the true mechanism of action of SB-224289 is not currently known, SB-224289 likely causes a disruption in PS trafficking by inducing large-scale endocytosis of the plasma membrane.

Last, based on the usefulness of the tools developed in this study, we wished to translate them into other relevant systems including *C. albicans*, *C. glabrata*, and *E. coli*. However, though strains containing GFP-Lact-C2 were produced in each of these studies, difficulties were encountered for each, prohibiting our ability to utilize these tools in secondary systems.

These findings, while not conclusive for our initial experimental goals, provide some evidence that PS remains at the membrane for a relatively long period (~180 minutes). In addition, although several difficulties were encountered in these studies, several strains of excellent quality and importance were produced that will be of great use in future studies on PS trafficking and membrane dynamics.

References

Achleitner G, Gaigg B, Krasser A *et al.* Association between the endoplasmic reticulum and mitochondria of yeast facilitates interorganelle transport of phospholipids through membrane contact. *Eur J Biochem* 1999;**264**: 545-53.

Andjelic CD, Planelles V, Barrows LR. Characterizing the anti-HIV activity of papuamide A. *Mar Drugs* 2008;**6**: 528-49.

Carman GM, Han GS. Regulation of phospholipid synthesis in the yeast *Saccharomyces cerevisiae*. *Annu Rev Biochem* 2011;**80**: 859-83.

Cassilly CD, Farmer AT, Montedonico AE *et al.* Role of phosphatidylserine synthase in shaping the phospholipidome of *Candida albicans*. *FEMS Yeast Res* 2017;**17**.

Cassilly CD, Maddox MM, Cherian PT *et al.* SB-224289 Antagonizes the Antifungal Mechanism of the Marine Depsipeptide Papuamide A. *PLoS One* 2016;**11**: e0154932.

Chen YL, Montedonico AE, Kauffman S *et al.* Phosphatidylserine synthase and phosphatidylserine decarboxylase are essential for cell wall integrity and virulence in *Candida albicans*. *Mol Microbiol* 2010;**75**: 1112-32.

Cho KJ, Park JH, Hancock JF. Staurosporine: A new tool for studying phosphatidylserine trafficking. *Commun Integr Biol* 2013;**6**: e24746.

Cho KJ, Park JH, Piggott AM *et al.* Staurosporines disrupt phosphatidylserine trafficking and mislocalize Ras proteins. *J Biol Chem* 2012;**287**: 43573-84.

Eckert SE, Muhlschlegel FA. Promoter regulation in *Candida albicans* and related species. *FEMS Yeast Res* 2009;**9**: 2-15.

Fairn GD, Hermansson M, Somerharju P *et al.* Phosphatidylserine is polarized and required for proper Cdc42 localization and for development of cell polarity. *Nat Cell Biol* 2011a;**13**: 1424-30.

Fairn GD, Schieber NL, Ariotti N *et al.* High-resolution mapping reveals topologically distinct cellular pools of phosphatidylserine. *J Cell Biol* 2011b;**194**: 257-75.

Gietz RD, Woods RA. Transformation of yeast by lithium acetate/single-stranded carrier DNA/polyethylene glycol method. *Methods Enzymol* 2002;**350**: 87-96.

Hanson BA, Lester RL. The extraction of inositol-containing phospholipids and phosphatidylcholine from *Saccharomyces cerevisiae* and *Neurospora crassa*. *J Lipid Res* 1980;**21**: 309-15.

Kuchler K, Daum G, Paltauf F. Subcellular and submitochondrial localization of phospholipid-synthesizing enzymes in *Saccharomyces cerevisiae*. *J Bacteriol* 1986;**165**: 901-10.

Lagace TA, Ridgway ND. The role of phospholipids in the biological activity and structure of the endoplasmic reticulum. *Biochim Biophys Acta* 2013;**1833**: 2499-510.

Lemmon MA. Pleckstrin homology (PH) domains and phosphoinositides. *Biochem Soc Symp* 2007: 81-93.

Levin DE. Cell wall integrity signaling in *Saccharomyces cerevisiae*. *Microbiol Mol Biol Rev* 2005;**69**: 262-91.

Longtine MS, McKenzie A, 3rd, Demarini DJ *et al.* Additional modules for versatile and economical PCR-based gene deletion and modification in *Saccharomyces cerevisiae*. *Yeast* 1998;**14**: 953-61.

Maeda K, Anand K, Chiapparino A *et al.* Interactome map uncovers phosphatidylserine transport by oxysterol-binding proteins. *Nature* 2013;**501**: 257-61.

Mioka T, Fujimura-Kamada K, Tanaka K. Asymmetric distribution of phosphatidylserine is generated in the absence of phospholipid flippases in *Saccharomyces cerevisiae*. *Microbiologyopen* 2014;**3**: 803-21.

Moser von Filseck J, Copic A, Delfosse V *et al.* INTRACELLULAR TRANSPORT. Phosphatidylserine transport by ORP/Osh proteins is driven by phosphatidylinositol 4-phosphate. *Science* 2015;**349**: 432-6.

Natarajan P, Wang J, Hua Z *et al.* Drs2p-coupled aminophospholipid translocase activity in yeast Golgi membranes and relationship to *in vivo* function. *Proc Natl Acad Sci U S A* 2004;**101**: 10614-9.

Nishimura K, Fukagawa T, Takisawa H *et al.* An auxin-based degron system for the rapid depletion of proteins in nonplant cells. *Nat Methods* 2009;**6**: 917-22.

Osman C, Voelker DR, Langer T. Making heads or tails of phospholipids in mitochondria. *J Cell Biol* 2011;**192**: 7-16.

Pichler H, Gaigg B, Hrastnik C *et al.* A subfraction of the yeast endoplasmic reticulum associates with the plasma membrane and has a high capacity to synthesize lipids. *Eur J Biochem* 2001;**268**: 2351-61.

Pomorski T, Lombardi R, Riezman H *et al.* Drs2p-related P-type ATPases Dnf1p and Dnf2p are required for phospholipid translocation across the yeast plasma membrane and serve a role in endocytosis. *Mol Biol Cell* 2003;**14**: 1240-54.

Selkirk JV, Scott C, Ho M *et al.* SB-224289--a novel selective (human) 5-HT1B receptor antagonist with negative intrinsic activity. *Br J Pharmacol* 1998;**125**: 202-8.

Sleight RG, Pagano RE. Rapid appearance of newly synthesized phosphatidylethanolamine at the plasma membrane. *J Biol Chem* 1983;**258**: 9050-8.

Tamura Y, Onguka O, Itoh K *et al.* Phosphatidylethanolamine biosynthesis in mitochondria: phosphatidylserine (PS) trafficking is independent of a PS decarboxylase and intermembrane space proteins UPS1P and UPS2P. *J Biol Chem* 2012;**287**: 43961-71.

Vale-Silva LA, Moeckli B, Torelli R *et al.* Upregulation of the Adhesin Gene EPA1 Mediated by PDR1 in *Candida* glabrata Leads to Enhanced Host Colonization. *mSphere* 2016;**1**.

Voelker DR. New perspectives on the regulation of intermembrane glycerophospholipid traffic. *J Lipid Res* 2003;**44**: 441-9.

Yeung T, Gilbert GE, Shi J *et al.* Membrane phosphatidylserine regulates surface charge and protein localization. *Science* 2008;**319**: 210-3.

APPENDIX III

EXTRACT FROM *SAMANEA SAMAN* LEAF EXTRACT INHIBITS THE TOXICITY OF MARINE DEPSIPEPTIDE PAPUAMIDE A

Contributing authors to this work include: Chelsi D. Cassilly,[1] John J. Bowling,[2] Marcus M. Maddox,[2] Rebecca E. Fong,[1] Sabrina V. Williamson,[1] Richard E. Lee,[2] Todd B. Reynolds[1]

1. Department of Microbiology, University of Tennessee, Knoxville, TN, USA

2. Department of Chemical Biology and Therapeutics, St. Jude Children's Research Hospital, Memphis, TN, USA

This article has not been published elsewhere at this time, nor will it be before completion of this ETD. The author contributions are as follows: Conceived and designed the experiments: CDC JJB MMM REL TBR. Performed the experiments: CDC JBJ MMM REF SVW TBR. Analyzed the data: CDC JJB MMM REL TBR. Contributed reagents/materials/analysis tools: TBR JJB REL. Wrote the paper: CDC JJB

Introduction

As reported previously (Cassilly, *et al.* 2016), a high-throughput screening approach has been developed to identify compounds that affect the PS-accessibility of a PS-binding toxin called Papuamide-A (Pap-A). Pap-A is isolated from sea sponges (Theonella *spp.*) and is known to lyse membranes containing PS (Andjelic, *et al.* 2008, Parsons, *et al.* 2006, Uzair, *et al.* 2011). Thus, Pap-A is toxic to wild-type *C. albicans*, but is non-toxic to a Cho1p mutant (*cho1*$\Delta\Delta$) (Cassilly, *et al.* 2016). Our screening approach utilized Pap-A as a filter which

would sort compounds by their ability to protect wild-type *C. albicans* from a toxic dose of Pap-A. We hypothesized that compounds which inhibit PS synthesis or PS availability at the plasma membrane, would render Pap-A unable to bind and lyse the membranes of those cells, allowing survival of the organism in the presence of Pap-A. Compounds that cause this trait would then be possible hits for antifungal drug development.

It is a well known phenomenon that plants have natural antifungal defenses (Cho, *et al*. 2013a). We thought it likely that some plants could produce compounds which might inhibit the fungal Cho1p or affect PS distribution. We screened 23,585 plant extract fractions (Natural Products Library from the University of Mississippi) for their ability to abrogate the toxic effects of Pap-A and identified one plant extract from the Rain Tree that we further characterized. The fractions of this extract did not show signs of inhibiting Cho1p, however, we identified that this extract has potent ability to inhibit the toxic effects of Pap-A.

Materials and Methods

Strains Used

All strains used in this study can be found in (Chen, *et al.* 2010). The wild-type strain from which all mutants were made is SC5314 (Gillum, *et al.* 1984). This study included both *cho1*ΔΔ (YLC337) and *cho1*ΔΔ*::CHO1* (YLC344) (Chen, *et al.* 2010). YPD (1% Bacto yeast extract, 2% Bacto peptone, and 2% dextrose (Thermo Fisher Scientific, San Jose, CA)) and minimal medium (0.67% Bacto-

yeast nitrogen base (without amino acids) 2% dextrose) were used to culture all strains as indicated (Guthrie 2002) .

Papuamide A resistance assay

This assay was performed as previously described in (Cassilly, *et al.* 2016) in a 96-well plate format. Cultures were grown overnight, shaking, at 30°C and diluted to 2 x 10^4 cells/ml in YPD. Plant extract fractions were diluted to twice the desired µg/ml concentration in a volume of 37.5 µl of YPD. Then 37.5 µl of the previously diluted cell suspension was added, diluting the final concentration of both cells and plant extract by half. Plates were incubated at 37°C for 6 hours, then 75 µl of YPD containing depsipeptide (Pap-A at 8 µg/ml) was added to each well, again diluting this concentration by half. Plates were incubated overnight at 37°C.

The next day Alamar Blue (Invitrogen, Waltham, MA) was added at a 1:10 dilution and plates were incubated at 37°C for 30 minutes to 2 hours until color change was visible. Fluorescence was then read at excitation 550 nm and emission 590 nm on a Cytation3 BioTek plate reader using Gen 5 software.

High throughput screen for Pap-A resistance

23,585 compounds from the Natural Products Library from the University of Mississippi were screened in a total of 93 384-well plates (Nunc). Using a BioMek robot with pin tools, 0.173 µl of plant extract fractions at varying concentrations were inoculated into 10 µl of YPD in each well (excluding columns

1, 2, and 13) from stock plates. Wild-type and *cho1*ΔΔ (positive control strain) were grown in liquid YPD in a 30°C shaker overnight and diluted to 10^4 cells/ml in YPD. 10 µl of wild-type were added to each well of the 384 well plates containing the test compound using a Wellmate, except column 2 where 10 µl of *cho1*ΔΔ was added. Plates were incubated for 6 hours at 37°C, and then 10 µl of YPD containing 21 µg/ml Pap-A was added to give a final concentration of 7 µg/ml in 30 µl of YPD. Plates were then incubated for another 16 hours at 37°C to allow selection for Pap-A resistance. The next day, cell survival was measured by adding 10 µl of Alamar Blue (Invitrogen, Waltham, MA) at a 1:3 dilution using a Wellmate. Plates were allowed to incubate again at 37°C for 1 hour. Plates were sealed, then fluorescence was then read at excitation 550 nm and emission 590 nm on an EnVision plate reader (Perkin Elmer, Waltham, MA). In each plate, three of the columns of wells were used as controls. Column one contained 50 µM SB-224289 as a positive control (Cassilly, *et al.* 2016). Column two contained *cho1ΔΔ* plus Pap-A, as a second positive control. Column 13 was a negative control containing wild-type cells with no compounds in the presence of Pap-A.

Phosphatidylserine Synthase Assay

This procedure was amended from (Bae-Lee and Carman 1984, Matsuo, *et al.* 2007) as described previously in (Cassilly, *et al.* 2017, Cassilly, *et al.* 2016).

Fractions of *S. saman* plant extract were added to the reaction mixture at varying concentrations to test their ability to inhibit [^{3}H]-PS production.

Ethanolamine Auxotrophy Assay

Wild-type and *cho1*ΔΔ cultures were grown in YPD overnight shaking at 30°C. The next day, cultures were washed with water and diluted to 2x10^4 cells/ml in minimal medium containing 50 mM HEPES buffer. 50 µl of cell suspensions were added to wells of a 96-well plate (Costar). Plant extract fractions were diluted into minimal medium containing 50 mM HEPES buffer either with or without 1 mM ethanolamine (one plate contained ethanolamine, the second did not), and 50 µl were added to the wells, diluting the concentration to a final of 25 µg/ml. Wild-type with no fraction added served as the negative control and *cho1*ΔΔ served as the positive control. Plates were incubated at 37°C overnight. The next day, Alamar Blue (Invitrogen) was added at a 1:10 dilution and plates were incubated for another 2 hours. Following this incubation, fluorescence was read at excitation 550 nm and emission 590 nm on a Cytation3 BioTek plate reader using Gen 5 software.

β 1,3-glucan Unmasking Microscopy

β 1,3-glucan unmasking immunofluorescence experiments were performed as described in (Davis, *et al*. 2014a). Wild-type and *cho1*ΔΔ cultures were grown in YPD overnight shaking at 30°C. The following day the cells were diluted to an

OD600 of 0.1 and Fraction 2-1 or DMSO for a negative control was added to a 100 µg/ml concentration. This was incubated at 30°C shaking for 1 hour and then cells were washed with 1X PBS. Cells were then pelleted and washed in 3% BSA rocking for 1 hour at room temperature. Cells were pelleted and then incubated with 1:800 anti-(1-3)-glucan antibody (Biosupplies Australia) and incubated on ice for 1.5 hours. Afterwards, cells were washed with 1X PBS at least 3 times before 1:600 goat anti-mouse antibody conjugated to Cy3 (Jackson ImmunoResearch) was added in 5% BSA. This was allowed to incubate for 20 minutes on ice before washing again with 1X PBS at least 3 times. Cells were resuspended in 1X PBS, added to a slide, and imaged on a fluorescent microscope at an exposure of 1 ms.

GFP-Lact-C2 Microscopy

Wild-type and *cho1*ΔΔ strains expressing GFP-Lact-C2 were grown in YPD overnight shaking at 30°C. The next day, cultures were diluted to 0.2 OD_{600} in YPD and allowed to grow shaking at 30°C for another 3 hours. Following this incubation, cultures were diluted again to 0.1 OD_{600} in 1X PBS and 100 µg/ml concentration of plant extract fraction 2-1 or DMSO negative control and incubated again shaking at 30°C for 1 hour. Cells were then pelleted, resuspended in a small volume of PBS, placed on a glass slide, and imaged via fluorescent microscopy.

Solid Phase Extraction

C18 Reverse Phase SPE was peformed to remove tannins and polyphenols, and separate the extract into three fractions. First the fraction was applied to the C18 column and deionized water was passed through to create the first fraction. Second 50% methanol was passed through to produce a second fraction. And last 100% methanol was passed through the column to create the third fraction.

Statistical analysis

Graphs were made using GraphPad Prism version 6.04. Unpaired t-tests were used to determine significance between results. RISE (Robust Investigation of Screening Experiments) software was used to analyze data from the high throughput screen and was used to calculate Z'-scores, identify 95th and 99th quantile data, and identify compounds that yielded hits of greater than 90% of positive control (*cho1*$\Delta\Delta$).

Results

We screened 23,585 plant extract fractions (Natural Products Library from the University of Mississippi) for their ability to abrogate the toxic effects of Pap-A (Fig. A3.1) (Tu, *et al.* 2010). From this screen, we identified 79 initial hits, which is a 0.3% hit rate with hits considered as fractions that allow greater that 60% of the growth of the positive control (*cho1*$\Delta\Delta$). We then performed a dose-response assay to determine both the effective concentration range of the compounds, as

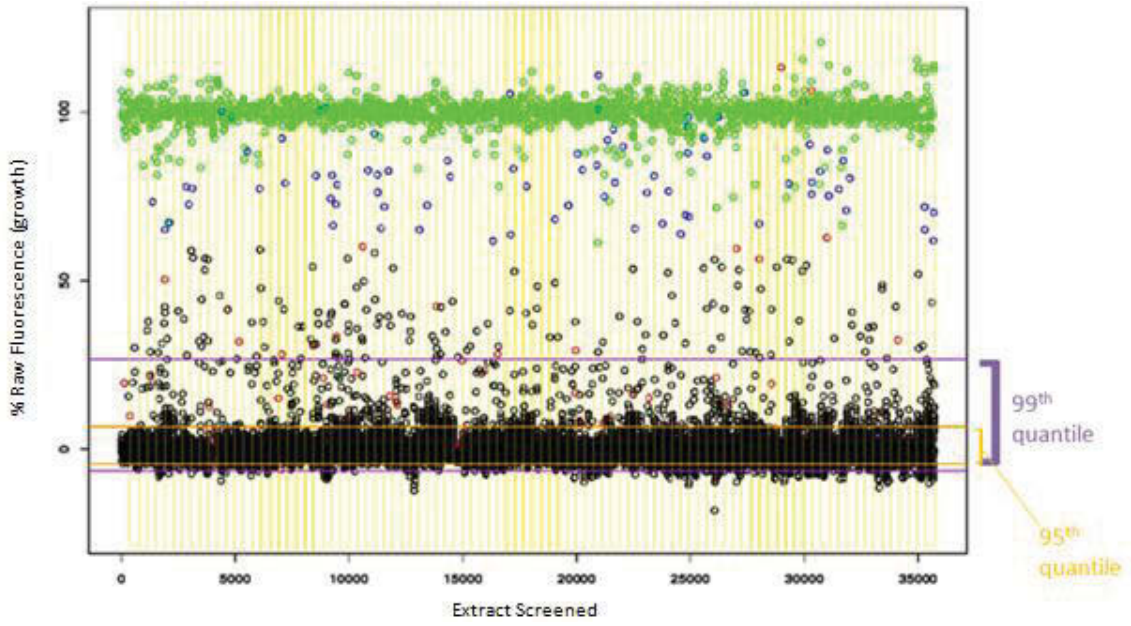

Figure A3. 1. Natural Products Library Screened Against Papuamide-A
23,585 natural product fractions were screened for their ability to protect wild-type *C. albicans* (open black circles) against 7 µg/ml Pap-A. Fluorescence was measured as a proxy of growth using Alamar Blue over approximately 1 hour at 37˚C. The untreated *cho1*ΔΔ positive control's growth in the presence of Pap-A is represented by green circles. Natural product fractions that allowed wild-type cells to display >60% (above the blue line) of the growth of *cho1*ΔΔ control are shown in blue circles. Around 95% of the tested natural products allowed growth at levels closer to the negative control wells, which contained untreated wild-type cells with Pap-A (open red circles). Horizontal lines indicate the 99th quantile (purple) where 99% of the natural product fractions fell, and the 95th quantile (yellow) where 95% of the natural product fractions lie. Vertical lines divide the natural product fractions based on the 384-well plate in which they were screened which correlate to plate numbers along the bottom. A full description of the screening method can be found in the Materials and Methods.

well as the reproducible hits (data not shown). From this dose-response, we identified two compounds that reproducibly conferred Pap-A resistance to wild-type *C. albicans*, one from the bark extract of the white oak tree *Quercus alba* and the second from leaf extract of the rain tree *Samanea saman*. The *Q. alba* extract fraction showed an average of 42.3% survival (when compared to *cho1*ΔΔ) in the presence of Pap-A at a concentration of 18.03 µg/ml (Table A3.1). The *S. saman* extract fraction showed an average of 102% survival (when compared to *cho1*ΔΔ) in the presence of Pap-A at a concentration of 41.55 µg/ml (Table A3.1).

There have been several papers published that characterized the white oak tree (Keller, *et al.* 2004, Walters, *et al.* 2001), whereas the rain tree is an understudied plant (Staples 2006). This, in addition to the fact that the rain tree extract showed higher levels of protection against Pap-A (Table A3.1), directed us to focus our studies on the rain tree extract. As plant extracts are complex mixtures of many compounds (Tu, *et al.* 2010), our goal was to identify which compound(s) within this mixture were responsible for the marked Pap-A protection.

Fractionation of *S. saman* Crude Leaf Extract

We obtained crude *S. saman* leaf extract from the University of Mississippi and performed C18 Reverse Phase SPE: hydrophobic separation to remove tannins and polyphenols, and separate the extract into three fractions. The first fraction (F1) was all compounds dissolved in deionized water, the second (F2) in

Table A3. 1. Two Natural Products Show Reproducible Resistance to Pap-A

Plate	Well	Final Conc (ug/ml)	% Growth	Source
80004	A18	41.55	111	Samanea|saman|Fabaceae|LeaF|135
80005	A18	41.55	102	Samanea|saman|Fabaceae|LeaF|135
80006	A18	41.55	96	Samanea|saman|Fabaceae|LeaF|135
80004	B09	18.03	32	Quercus|alba|Fagaceae|BarK|139.7
80005	B09	18.03	83	Quercus|alba|Fagaceae|BarK|139.7
80006	B09	18.03	12	Quercus|alba|Fagaceae|BarK|139.7

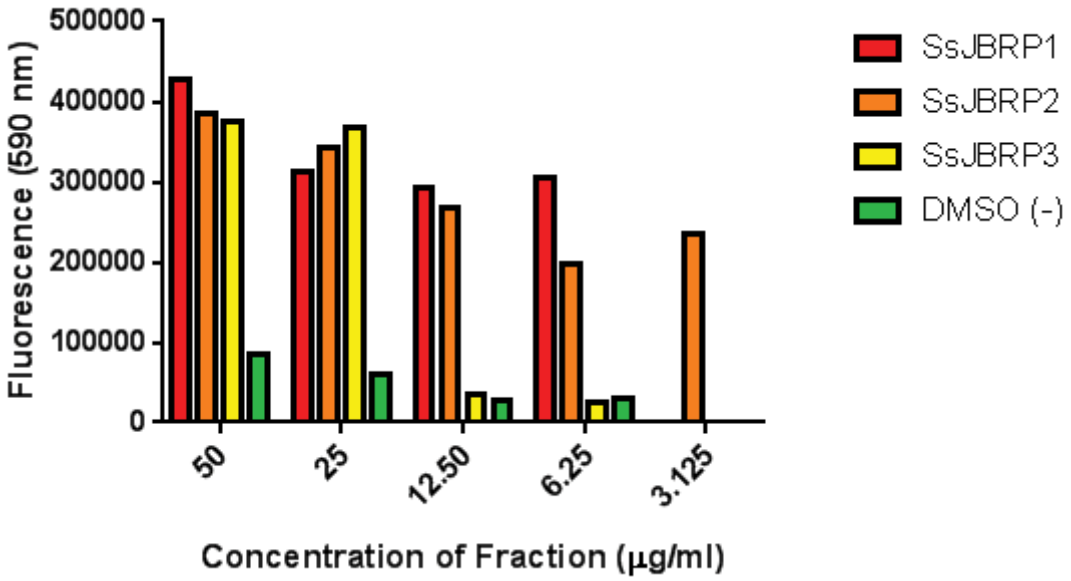

Figure A3. 2. Fraction F2 Retains the Highest Concentration of the Bioactive Component

Cells were treated with three fractions of *S. saman* plant extract for 6 hours and then treated with a lethal dose (4 µg/ml) of Pap-A. Protection is seen in all fractions at the highest concentration (50 µg/ml). However, as the concentration of the extract decreases to 3.125 µg/ml, the only fraction still able to protect wild-type cells from Pap-A is F2, indicating that the bioactive concentrates to this fraction.

50% methanol, and the third (F3) was 100% methanol. With these three fractions, we performed our Pap-A assay again to determine which fraction retained the Pap-A protective activity. This assay revealed that, while all of the fractions seem to show some Pap-A protection at high concentrations (50 µg/ml) Fraction F2 retained the Pap-A protective activity even at the lowest concentrations tested (Fig. A3.2).

Our next step was to further fractionate F2 via high-performance liquid chromatography (HPLC). For this experiment we used a C18 reverse phase column to separate the fraction based on hydrophobicity. This separated F2 into seven different portions (F2-1 through F2-7). These seven fractions were then again tested for their ability to provide Pap-A resistance in order to allow us to narrow the activity to one. Figure A3.3 shows that at the highest concentrations of the fractions tested, we see Pap-A protection in all but F2-6 and F2-7. However, as the concentration was decreased to 6.25 µg/ml, the Pap-A protection activity dropped off to include only F2-1. This indicates that the particular compound of interest was present in most fractions in residual amounts, but seemed to be most concentrated in F2-1.

S. saman Leaf Extract Fractions Do Not Inhibit Cho1p

We were interested in determining if any of the fractions generated could inhibit Cho1p in an *in vitro* PS synthase assay (Bae-Lee and Carman 1984, Cassilly, *et al.* 2016, Matsuo, *et al.* 2007). We performed this assay first with the original

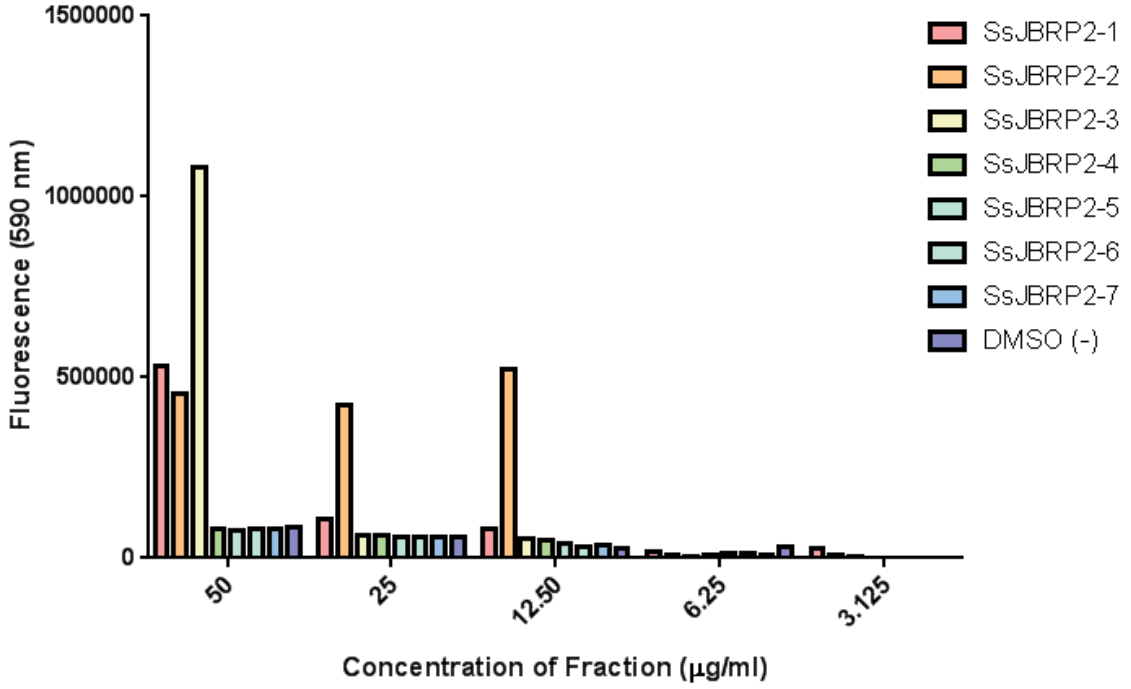

Figure A3. 3. Fraction F2-2 Retains the Highest Concentration of the Bioactive Component

Cells were treated with all fractions of *S. saman* plant extract fraction F2 for 6 hours and then treated with a lethal dose (4 µg/ml) of Pap-A. Protection is seen in all fractions of F2 aside from F2-6 and F2-7 at the highest concentration (400 µg/ml). However, as the concentration of the extract decreases to 6.25 µg/ml, the only fraction still able to protect wild-type cells from Pap-A is F2-1, indicating that the bioactive concentrates to this fraction.

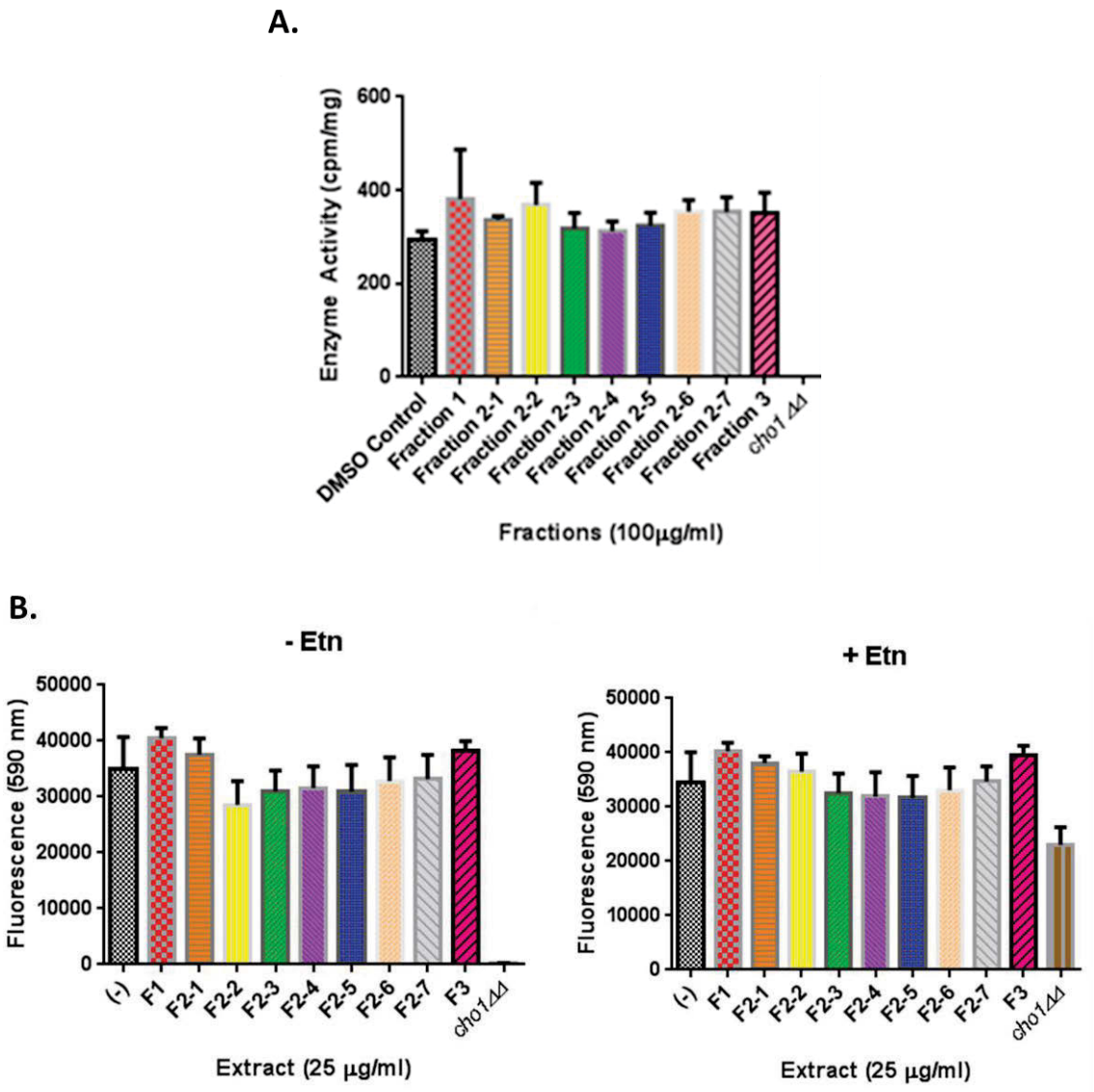

Figure A3. 4. No *S. saman* Fractions Inhibit the PS Synthase
(A) An *in vitro* PS synthase assay was performed with 100 µg/ml concentrations of each plant extract fraction. Activity is represented as counts per minute per milligram of protein, quantifying the incorporation of ^{3}H-l-serine incorporated into PS. No inhibitory activity is seen when compared with the DMSO negative control and the *cho1ΔΔ* positive control. (B) Ethanolamine auxotrophy tests were performed to assess the ability of the plant extract fraction to inhibit Cho1p *in vivo*. Cells were treated with 25 µg/ml concentration of the plant extracts and then grown in minimal medium either without or with 1 mM ethanolamine. None of the fractions produce ethanolamine auxotrophy in the wildtype when compared with the *cho1 ΔΔ* positive control.

three fractions provided by SPE (F1 and F3) and the seven fractions of F2 at a 100 µg/ml concentration of each extract fraction, well over the effective concentrations shown in our assays. We found that no fraction showed a statistically significant decrease in PS synthase activity when compared with a non-treated control (Fig. A3.4A). Additionally, we wished to determine if the fractions would inhibit Cho1p *in vivo*. To do this, we used a common trait shown by the *cho1*ΔΔ mutant, ethanolamine auxotrophy. Because PS is a precursor for the biosynthesis of phosphatidylethanolamine (PE), a vital phospholipid, when Cho1p is deleted—or as we suspect, inhibited—the organism will become an ethanolamine auxotroph and can only grow if the medium is supplemented with exogenous ethanolamine (Chen, *et al.* 2010). As a result, we used this trait to test whether any of the *S. saman* fractions caused wild-type *C. albicans* to become an ethanolamine auxotroph. We expected to see no growth in minimal medium containing no ethanolamine if the fractions inhibited Cho1p, and a return of growth in medium containing ethanolamine (indicating that the organism can uptake the ethanolamine and circumvent the need for PS to make PE). As in our *in vitro* assay, we found that no *S. saman* fractions caused the wild-type organism to become an ethanolamine auxotroph (Fig. A3.4B).

Last, we wish to determine if Fraction F2-1 produced a disruption in the cell wall organization, or PS localization, both of which might indicate a disruption in PS production or localization (Davis, *et al*. 2014a). Wild-type cells were treated with Fraction F2-1 at a 100 µg/ml concentration and tested for increased β (1,3)-

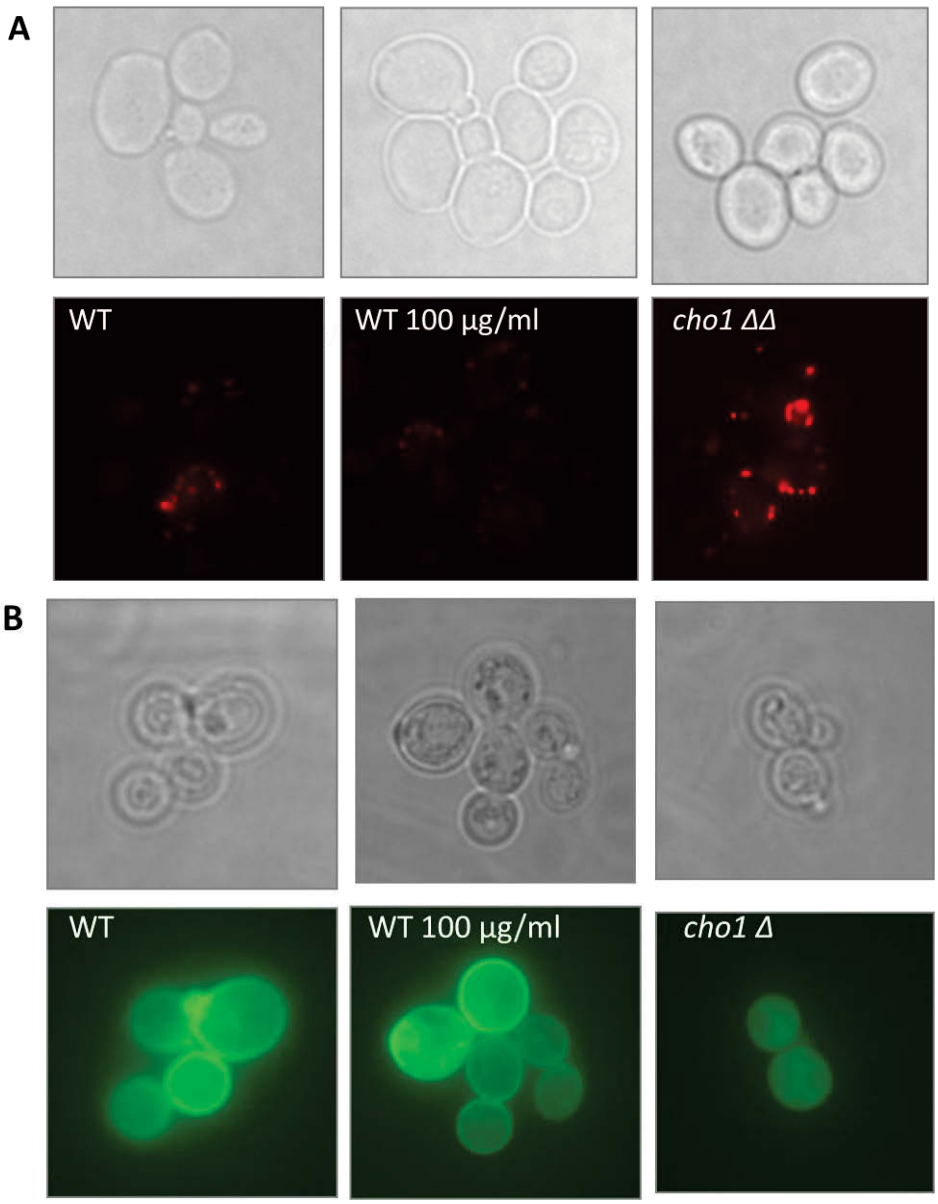

Figure A3. 5. *S. saman* Fraction 2-1 Does Not Cause B-1,3 Glucan Exposure or Disruption of PS Localization
(A) Microscopy was performed by treating wild-type and *cho1 ΔΔ* cells with DMSO or 100 µg/ml of Fraction F2-1. Cells were then washed and incubated with primary antibody for B-1,3, glucan. Then treated with secondary antibody Cy3 for imaging as an indication of disrupted cell wall structure. (B) Wild-type and *cho1 ΔΔ* cells expressing the GFP-Lact-C2 probe were treated with DMSO or 100 µg/ml of Fraction F2-1 then assessed via microscopy for mislocalization of the probe, indicating PS mislocalization.

glucan unmasking and GFP-Lact-C2 mislocalization as compared to a *cho1ΔΔ* positive control. Under no circumstances did we see increased β (1,3)-glucan unmasking or a changed in the localization of GFP-Lact-C2, indicating that Fraction F2-1 does not inhibit PS production or cause a change in cell wall organization as we originally hypothesized (Fig. A3.5). These results were unexpected based on the reproducible Pap-A protection that Fraction F2-1 provides to wild-type *C. albicans*. We expect that it is likely that Pap-A and molecules within Fraction F2-1 are interacting, causing Pap-A to be ineffective as a toxin against *C. albicans*. As we previously published for the compound SB-224289, a serotonin receptor antagonist that showed similar activity to Fraction F2-1, this could be potentially useful for applications where toxins, like Pap-A, need to be neutralized, but work should be continued to confirm these predictions.

Despite the unexpected results, we decided to continue in the fractionation of this extract in order to characterize some of the molecules that are found within the rain tree leaf. HPLC was performed by collaborators at St. Jude, however, HPLC fractionation failed to identify a discrete component responsible for the observed activity.

References

Andjelic CD, Planelles V, Barrows LR. Characterizing the anti-HIV activity of papuamide A. *Mar Drugs* 2008;**6**: 528-49.

Bae-Lee MS, Carman GM. Phosphatidylserine synthesis in *Saccharomyces cerevisiae*. Purification and characterization of membrane-associated phosphatidylserine synthase. *J Biol Chem* 1984;**259**: 10857-62.

Cassilly CD, Farmer AT, Montedonico AE *et al.* Role of phosphatidylserine synthase in shaping the phospholipidome of *Candida albicans*. *FEMS Yeast Res* 2017;**17**.

Cassilly CD, Maddox MM, Cherian PT *et al.* SB-224289 Antagonizes the Antifungal Mechanism of the Marine Depsipeptide Papuamide A. *PLoS One* 2016;**11**: e0154932.

Chen YL, Montedonico AE, Kauffman S *et al.* Phosphatidylserine synthase and phosphatidylserine decarboxylase are essential for cell wall integrity and virulence in *Candida albicans*. *Mol Microbiol* 2010;**75**: 1112-32.

Cho J, Choi H, Lee J *et al.* The antifungal activity and membrane-disruptive action of dioscin extracted from *Dioscorea nipponica*. *Biochim Biophys Acta* 2013;**1828**: 1153-8.

Davis SE, Hopke A, Minkin SC, Jr. *et al.* Masking of beta(1-3)-glucan in the cell wall of *Candida albicans* from detection by innate immune cells depends on phosphatidylserine. *Infect Immun* 2014;**82**: 4405-13.

Gillum AM, Tsay EY, Kirsch DR. Isolation of the *Candida albicans* gene for orotidine-5'-phosphate decarboxylase by complementation of *S. cerevisiae* ura3 and *E. coli* pyrF mutations. *Mol Gen Genet* 1984;**198**: 179-82.

Guthrie C, Fink, G. R. (ed.) *Methods in Enzymology* volume 350: Academic Press, 2002.

Keller HW, Skrabal M, Eliasson UH *et al.* Tree canopy biodiversity in the Great Smoky Mountains National Park: ecological and developmental observations of a new myxomycete species of Diachea. *Mycologia* 2004;**96**: 537-47.

Matsuo Y, Fisher E, Patton-Vogt J *et al.* Functional characterization of the fission yeast phosphatidylserine synthase gene, pps1, reveals novel cellular functions for phosphatidylserine. *Eukaryot Cell* 2007;**6**: 2092-101.

Parsons AB, Lopez A, Givoni IE *et al.* Exploring the mode-of-action of bioactive compounds by chemical-genetic profiling in yeast. *Cell* 2006;**126**: 611-25.

Staples GW, Elevitch, C. R. *Samanea saman* (rain tree): Fabaceae (legume family). *Species Profiles for Pacific Island Agroforestry* 2006;**Ver. 2.1**.

Tu Y, Jeffries C, Ruan H *et al.* Automated high-throughput system to fractionate plant natural products for drug discovery. *J Nat Prod* 2010;**73**: 751-4.

Uzair B, Mahmood Z, Tabassum S. Antiviral activity of natural products extracted from marine organisms. *Bioimpacts* 2011;**1**: 203-11.

Walters D, Meurer-Grimes B, Rovira I. Antifungal activity of three spermidine conjugates. *FEMS Microbiol Lett* 2001;**201**: 255-8.

APPENDIX IV

CANDIDA ALBICANS PHOSPHATIDYLSERINE SYNTHASE

PURIFICATION FOR CRYSTALLIZATION

Contributing authors to this work include: Chelsi D. Cassilly, Melinda Hauser, Brian C. Monk, Jeffrey M. Becker, Todd B. Reynolds

This article has not been published elsewhere at this time, nor will it be before completion of this ETD. The author contributions are as follows: Conceived and designed the experiments: CDC MH TBR. Performed the experiments: CDC. Analyzed the data: CDC MH TBR. Contributed reagents/materials/analysis tools: TBR MH JMB. Wrote the paper: CDC.

Introduction

We were interested in using the data obtained in Chapter 4 to inform our search for PS synthase inhibitors. We utilized the protein model produced using Molecular Operating Environment (MOE) software (Fig. 4.6), to perform a computational drug screen. The screen was performed using MOE, docking compounds within the proposed active site. From this screen of 500 National Cancer Institute diversity drug subset (https://cactus.nci.nih.gov/ncidb2.2/) defining a hit based on the highest (or more negative) free energy. Following this screen, we identified 57 possible PS synthase inhibitors. However, unfortunately because of the loose specificity of the screen, this high number of hits was unable to be screened via our complex and time-consuming PS synthase secondary screen.

The work in this appendix aimed to determine the structure of the phosphatidylserine (PS) synthase enzyme within *Candida albicans*. As described in the Introduction, there is a dire need for new antifungals as a result of rising cases of fungal infections over the last several decades. This is mostly because of the increasing number of people living in an immunocompromised state (Mishra, *et al.* 2007) due to anti-cancer chemotherapeutics, diabetes, and HIV. Nearly all the antifungal drugs used to treat life-threatening *Candida* infections target a component of plasma membrane or lipid biosynthesis. The PS synthase, Cho1p, plays an important role in this crucial process in *C. albicans* and represents a novel target.

Thus, we aimed to determine the 3-dimensional structure of this protein via protein crystallography methodology. This work is one of the first key steps towards rational drug design to inhibit Cho1p, as well as provide greater understanding of enzymes involved in phospholipid biosynthesis.

Methods and Materials

Strains

Genomic DNA was isolated from wildtype *C. albicans* SC5314 and wildtype *S. cerevisiae* Σ (TRY181). Strains were grown using YPD media.

For expression studies, *S. cerevisiae* strain BJS21 was used (Becker Lab) or for a vector control, BJ2164. These strains were grown in either YPD or Media Lacking Tryptophan (MLT) for transformation selection.

MOE Docking Computational Screen

The homology model from Chapter 4 was used in MOE. First the NCI Diversity subset of 500 compounds (https://cactus.nci.nih.gov/ncidb2.2/) was downloaded into MOE. Compounds were docked systematically based on entropy (rigidity in binding) and enthalpy (ability to make H-bonds). The parameters "S" and "LONDON" were used within MOE to assess free energy. Those compounds with the most negative free energy were selected as hits. This work was done with the assistance of the Baudry Lab on computer "Napoleon." More information about computational screens and compound docking can be found (Baudry, *et al.* 2003) and on the MOE tutorials (https://www.chemcomp.com/MOE-Molecular_Operating_Environment.htm).

.

Genetics

In order to tag CaCHO1 and ScCHO1, we utilized the plasmid pBEC2 (7.8 Kb) which contained *STE2* gene with a 3X FLAG and 6x His tag after a P_{GDP1} which is a high expressing promoter. This plasmid also contained *TRP1* for use in strains with tryptophan auxotrophy. This plasmid was digested with AatII and HpaII to release a 400 bp fragment of *STE2*. The plasmid was then CIP treated for 3 hr to remove phosphates at the end of the fragment. The fragment was then gel extracted (Qiagen) to purify the digested plasmid from the *STE2* fragment.

Next, using primer CCO74 which has 30 bp homology with P_{GDP1} and 20 bp homology with *CaCHO1* beginning, and CCO75 which has 30 bp homology

with the 3X FLAG tag and 20 bp homology with *CaCHO1* end, we amplified *CaCHO1* which was approximately 800 bp in size. This fragment and the purified plasmid (~7.5 Kb) were ligated *in vivo* when transformed together into *S. cerevisiae* strain BJS21 using the LiOAc transformation procedure described in (Gietz and Woods 2002). Transformants were selected on media lacking tryptophan (MLT) for strains capable of growing in the absence of tryptophan.

Plasmids were then isolated from 6 transformants using the ZYMO yeast plasmid extraction kit according to the manufacturer's protocol. Isolated plasmids were then transformed into DH5-α *E. coli* using ampicillin selection. Following transformation, the plasmids were miniprepped (Qiagen) and then sequenced using F1424GDP (Becker Lab) primer with homology to pBEC2. The resulting plasmid was called pCDC13.

In order to address the CTG-codon issue between *S. cerevisiae* and *C. albicans*, site-directed mutagenesis primers were produced, CCO78 and CCO79. SDM was performed as described in Chapter 4 to make the mutation L246S. Because CCO78 and CCO79 were not successful (there were repeats introduced because the sequences contained a highly repetitive sequence in the gene) new primers were made, CCO84 and CCO87. Further, a spurious mutation was identified as T162. Because of the sensitivity of the project and the importance of each amino acid, primers CCO113 and CCO114 were ordered to correct the spurious mutation to T162A (correct sequence matches to *CHO1*

allele A in the *Candida* Genome Database). The resulting plasmid, pCDC16, was transformed into BJS21 to produce CDCS43.

For tagging *ScCHO1*, we performed a PCR to amplify *ScCHO1*using primer CCO85 and CCO86 with the result of an 800 bp PCR product. *In vivo* ligation of this PCR product and the cut plasmid pBEC2 (from above) was performed in BJS21 using tryptophan auxotrophy. 6 transformants were selected and plasmids were isolated, transformed into *E. coli*, miniprepped, and then sequenced using F1424GDP (Becker Lab) primer. Mutations (particularly premature stop codons) were present and thus a new reverse primer was created, CCO98, and used. This new primer produced correct plasmids, although the selected plasmid contained a spurious mutation, L236. Because of the sensitivity of the project and the importance of each amino acid, primers CCO115 and CCO116 were ordered to correct the spurious mutation to L236F. Once successful, the plasmid became known as pCDC20 and the strain CDCS47.

Site directed mutagenesis of all spurious mutations and hypothesized phosphorylation sites was performed as described in Chapter 4. To produce the S46AS47A mutation in ScCHO1, we produced primers CCO124 and CCO125. For the S46DS47D in ScCHO1, we produced primers CCO126 and CCO127. For the S43AS44A mutation in CaCHO1, we produced primers CCO132 and CCO133. Last, for the S43DS44D mutation in CaCHO1, we produced primers CCO134 and CCO135. One plasmid was produced, pCDC26, containing ScCHO1^{S46S47D}-FLAGx3-Hisx6.

Last, a vector control strain was made containing the empty vector, p424GDP which contained Ampicillin resistance and TRP1. p424GDP was transformed into BJS21 to produce CDCS40. For primer, plasmid, and strain lists, see Tables A4.1, A4.2, and A4.3, respectively.

Western Blots

Protein was isolated from CDCS43 as described in Chapter 4 and a western blot was performed using BJS21 as a positive control and wildtype *C. albicans* as a negative control. For detection, a rat anti-FLAG primary antibody (637301 BioLegend) was used, followed by a goat anti-rat secondary antibody (926-68076 LI-COR). The western blot showed adequate expression of CaCho1p-Flagx3-Hisx6 and ScCho1p-Flagx3-Hisx6.

Phosphatase Treatment

Protein samples were treated with phosphatase as follows. 40 µg of protein was treated with 1 µl. of λ-phosphatase, 3 µl. of phosphatase buffer, 3 µl. of Mn buffer in a total volume of 30 µl. Samples were incubated at 30 C for 1 hour. Following incubation, 1 µl of Laemmli Dye was added to each tube and the entire reaction was boiled and loaded on an SDS PAGE. The western blot was then performed as described above and in Chapter 4.

Table A4. 1. Primers Used in this Study

Primer	Sequence	Source
CCO74	gtctttttttttagttttaaaacaccaagaacttagtttcgaCGGATCTAGAAC*ATGTCAGACTCATCAGCT*	This study
CDC75	GCTGCTGCCGCTGCCGCGCGGCACACCGGTCTTGTCATCGTCGTCCTTGTAGTC*TGGTTTAGGAATTTTTAAAGAT*	This study
F1424GDP	GTATATAAAGACGGTAGGTATTG	Becker Lab
CCO78	GGAATAGTTTTCCAAGATACT***TCA***TTTGAATTCCATTTGG	This study
CCO79	CCAAATGGAATTCAAA***TGA***AGTATCTTGGAAAACTATTCC	This study
CCO84	GACAACTTACCATTTGGAATAGTTTTCCAAGATACT***TCA***TTTGAATTCCATTTGGTCACAATAG	This study
CCO87	CTATTGTGACCAAATGGAATTCAAA***TGA***AGTATCTTGGAAAACTATTCCAAATGGTAAGTTGTC	This study
CCO115	GTGTCAGAAAGGGTTTCATTtTTGATAACATCCCATTCGG	This study
CCO116	CCGAATGGGATGTTATCAAaAATGAAACCCTTTCTGACAC	This study
CCO85	gtctttttttttagttttaaaacaccaagaacttagtttcgaCGGATCTAGAAC*ATGGTTGAATCAGATGAA*	This study
CCO86	GCTGCTGCCGCTGCCGCGCGGCACACCGGTCTTGTCATCGTCGTCCTTGTAGTC*GAGCTTGAAAATTCCAAAGCCA*	This study
CCO98	GCTGCTGCCGCTGCCGCGCGGCACACCGGTCTTGTCATCGTCGTCCTTGTAGTCTGGCTTTGGAATTTTCAAG	This study
CCO113	GGGTATCTCCAGCAACAATTgCCTTTGCTATTGGATTCAG	This study
CCO114	CTGAATCCAATAGCAAAGGCAATTGTTGCTGGAGATACCC	This study
CCO124	GAAGTTGGTGGCACATTAAGCAGAAGAGCCgCAgcTATATTTTCTATAAATACAACTCCATTGG	This study
CCO125	CCAATGGAGTTGTATTTATAGAAAATATAGCTGCGGCTCTTCTGCTTAATGTGCCACCAACTTC	This study
CCO126	GAAGTTGGTGGCACATTAAGCAGAAGAGCCgatgaTATATTTTCTATAAATACAACTCCATTGG	This study
CCO127	CCAATGGAGTTGTATTTATAGAAAATATATCATCGGCTCTTCTGCTTAATGTGCCACCAACTTC	This study
CCO132	GCCAACCCACCTTTATTGAGAAGATCAgCTgCATTATTCTCCTTATCCTCGAAAGATGACTTG	This study
CCO133	CAAGTCATCTTTCGAGGATAAGGAGAATAATGCAGCTGATCTTCTCAATAAAGGTGGGTTGGC	This study
CCO134	GCCAACCCACCTTTATTGAGAAGATCAgaTgatTTATTCTCCTTATCCTCGAAAGATGACTTG	This study
CCO135	CAAGTCATCTTTCGAGGATAAGGAGAATAAATCATCTGATCTTCTCAATAAAGGTGGGTTGGC	This study

Table A4. 2. Plasmids Used in this Study

Plasmid	Inserts	Source
pBEC2	Ste2p-FLAGx3-Hisx6, TRP1, Cen/Ars, Amp	Becker Lab
p424GDP	Amp, TRP1	Becker Lab
pCDC13	CaCHO1-FLAGx3-Hisx6, TRP1, Cen/Ars, Amp	This study
pCDC16	$CHO1^{L246S}$-FLAGx3-Hisx6, TRP1, Cen/Ars, Amp	This study
pCDC20	ScCHO1-FLAGx3-Hisx6, TRP1, Cen/Ars, Amp	This study
pCDC26	$ScCHO1^{S46S47D}$-FLAGx3-Hisx6, TRP1, Cen/Ars, Amp	This study

Table A4. 3. Strains Used or Produced in this Study

Strain	Organism	Genotype	Source
Σ (TRY 181)	*S. cerevisiae*	*ura3Δ his3Δ*	Lab Strain
SC5314 (Ca157)	*C. albicans*		Lab Strain
Ca159	*C. albicans*	*cho1ΔΔ*	Chen *et al.*, 2010
BJ2168	*S. cerevisiae*	*MAT***a**, *prc1-407 prb1-1122 pep4-3 leu2 trp1 ura3-52*	Becker Lab
BJS21	*S. cerevisiae*	*MAT***a**, *prc1-407 prb1-1122 pep4-3 leu2 trp1 ura3-52 ste2::Kan^R*	Becker Lab
CDCS40	*S. cerevisiae*	*MAT***a**, *prc1-407 prb1-1122 pep4-3 leu2 trp1 ura3-52 ste2::Kan^R* p424GDP	This Study
CDCS43	*S. cerevisiae*	pCDC16	This Study
CDCS47	*S. cerevisiae*	pCDC20	This Study

Results

The preliminary steps involved in this project involved generating a “tagged” version of Cho1p that can be expressed at high volumes and isolated via affinity chromatography for further purification and characterization. 6xHis tags are ideal for this because they are easily bound to Nickel columns for high quality purification (Monk, *et al.* 2014). In order to do this, we utilized the plasmid pBEC2 which contained *STE2* gene with a triple FLAG tag and 6 His tag after a P_{GDP1} which is a high expressing promoter. The resulting plasmid, pCDC16, contained CaCHO1-Flagx3-Hisx6 under the P_{GDP1} promoter. This plasmid was transformed into BJS21 *S. cerevisiae* to produce CDCS43. Expression of CaCHO1-Flagx3-Hisx6 was confirmed via western blot (Fig. A4.1).

In addition to *CaCHO1*, we were interested in tagging *ScCHO1* as well to perform the crystallization of both proteins in tandem. This, we hypothesized, would provide us with higher chances of success. Thus, we produced the plasmid pCDC20 which contained ScCHO1-Flagx3-Hisx6 under the P_{GDP1} promoter. This was transformed into BJs21 to produce the strain CDCS47. Following this, protein from CDCS47 was isolated and a western blot was performed to confirm expression using the same parameters as for CDCS43 (Fig. A4.1).

Interestingly, we saw the presence of a doublet band around 34 and 36 KDa in both CaCHO1-Flagx3-Hisx6 and ScCHO1-Flagx3-Hisx6. Previous work (as described in Chapter 4) demonstrated that Cho1p in *S. cerevisiae* is

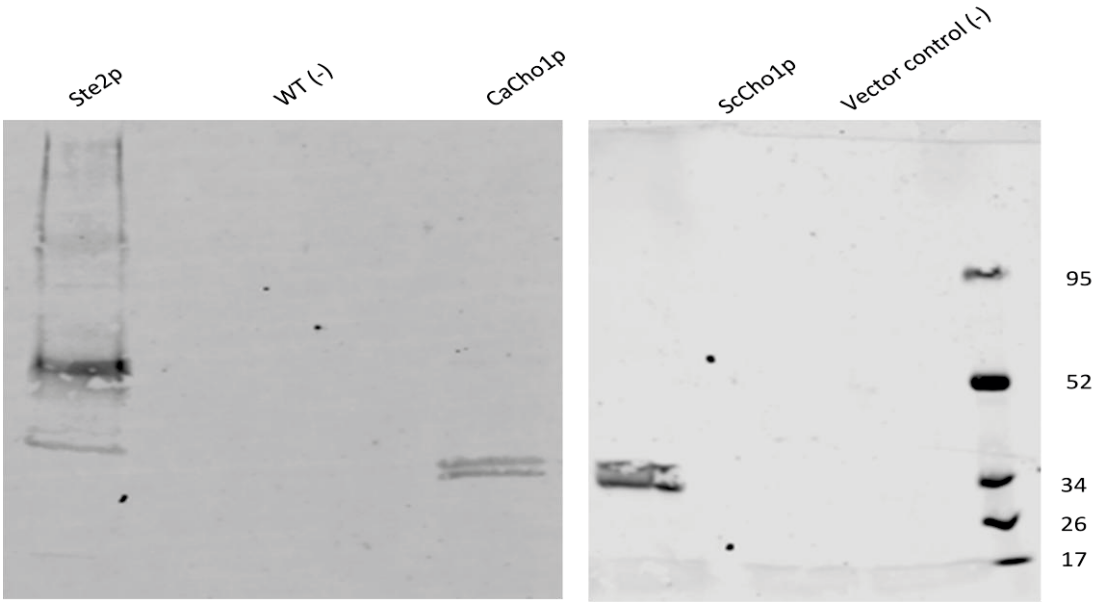

Figure A4. 1. Expression of CaCho1p-Flagx3-Hisx6 and ScCho1p-Flagx3-Hisx6

Western blot analysis using an anti-FLAG antibody shows bands for CaCho1p-Flagx3-Hisx6 and ScCho1p-Flagx3-Hisx6 around ~34 KDa. Ste2p-Flagx3-Hisx6 is shown as a positive control and either wild-type *C. albicans* or a BJS21 strain carrying a vector control plasmid as negative controls. The ladder along the right side shows the band sizes in KDa.

phosphorylated by protein kinase C (Choi, *et al.* 2010, Kinney and Carman 1988). In order to determine if this was the reason for the doublet band we observed, we treated protein samples with λ-phosphatase. Indeed, we saw a disappearance of the doublet band in ScCho1p-Flagx3-Hisx6 when treated with λ-phosphatase (Fig. A4.2A). Unfortunately, these results were inconsistent for CaCho1p-Flagx3-Hisx6 which showed only a slight disappearance of the band sometimes and other times protein samples of CaCho1p-Flagx3-Hisx6 untreated with λ-phosphatase, but incubated at 30°C for 1 hour showed a loss of the doublet band. This variability may indicate that the phosphorylation of CaCho1p-Flagx3-Hisx6 could be very transient (Fig. A4.2B).

Because having a mixed population of phosphorylated and unphosphorylated protein could cause serious issues with a crystallization procedure, we made an effort to identify possible phosphorylation sites in both *CaCHO1* and *ScCHO1*. Based on previous studies in *S. cerevisiae* (Choi, *et al.* 2010), two serine residues were identified as phosphorylation sites, S46 and S47. Homologous serine residues were identified in *CaCHO1*, S43 and S44. Thus, we decided to mutate these residues to alanine and aspartic acid. Alanine would served to completely abolish the phosphorylation site, while aspartic acid would be a mimic of a phosphate group. Although SDM procedures were carried out for all primer combinations in pCDC14 and pCDC20 respectively, due to time constraint, the project was never completed.

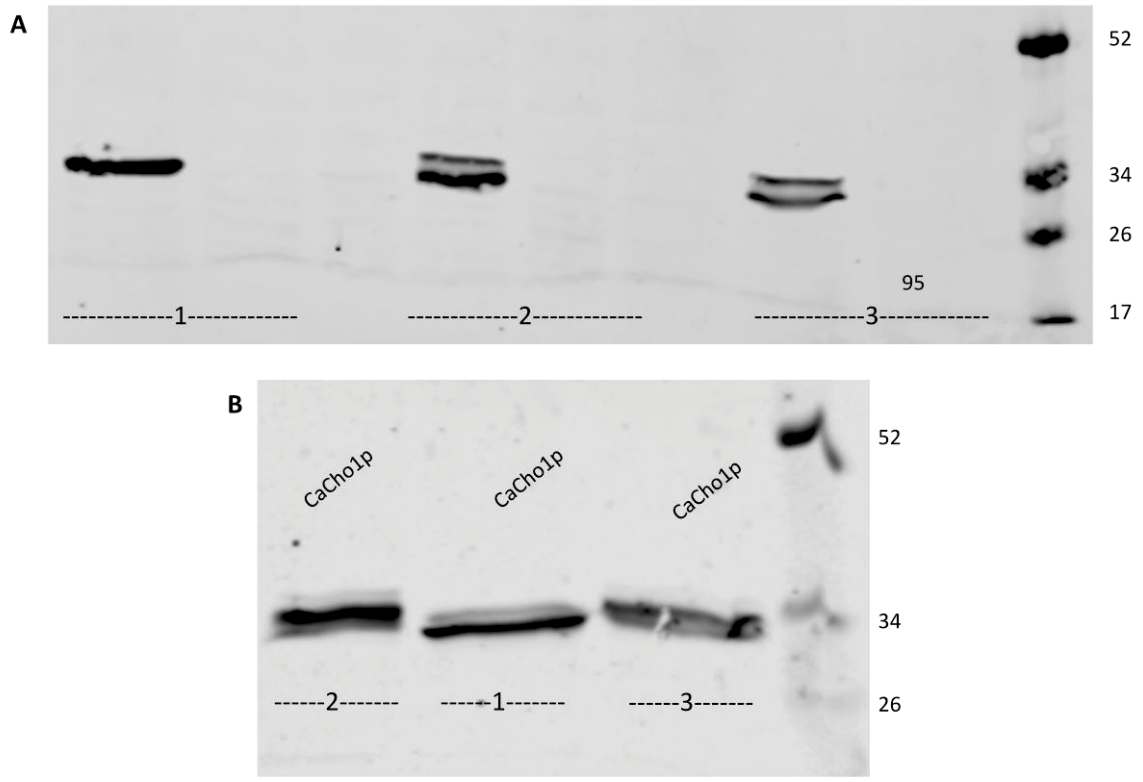

Figure A4. 2. Phosphatase Treatment of ScCho1p-Flagx3-Hisx6 and CaCho1p-Flagx3-Hisx6

Protein samples were either 1) treated with λ-phosphatase for 30 minutes at 30°C, 2) incubated without the enzyme for 30 minutes at 30°C, or 3) untreated, then analyzed via western blot using an anti-FLAG antibody. (A) ScCho1p-Flagx3-Hisx6 and (B) CaCho1p-Flagx3-Hisx6. In A) the ~36 KDa band disappears, leaving only the dephosphorylated 34 KDa band. In B) there is a slight disappearance of the 36KDa band, but it is not as stark as the difference in ScCho1p-Flagx3-Hisx6. The ladder along the right side shows the band sizes in KDa.

References

Baudry J, Li W, Pan L *et al.* Molecular docking of substrates and inhibitors in the catalytic site of CYP6B1, an insect cytochrome p450 monooxygenase. *Protein Eng* 2003;**16**: 577-87.

Choi HS, Han GS, Carman GM. Phosphorylation of yeast phosphatidylserine synthase by protein kinase A: identification of Ser46 and Ser47 as major sites of phosphorylation. *J Biol Chem* 2010;**285**: 11526-36.

Gietz RD, Woods RA. Transformation of yeast by lithium acetate/single-stranded carrier DNA/polyethylene glycol method. *Methods Enzymol* 2002;**350**: 87-96.

Kinney AJ, Carman GM. Phosphorylation of yeast phosphatidylserine synthase *in vivo* and *in vitro* by cyclic AMP-dependent protein kinase. *Proc Natl Acad Sci U S A* 1988;**85**: 7962-6.

Mishra NN, Prasad T, Sharma N *et al.* Pathogenicity and drug resistance in *Candida albicans* and other yeast species. A review. *Acta Microbiol Immunol Hung* 2007;**54**: 201-35.

Monk BC, Tomasiak TM, Keniya MV *et al.* Architecture of a single membrane spanning cytochrome P450 suggests constraints that orient the catalytic domain relative to a bilayer. *Proc Natl Acad Sci U S A* 2014;**111**: 3865-70.

VITA

Chelsi Danielle Cassilly was born in Florence, AL on 21 June 1990. She attended Eisenhower High School in Shelby Township, MI and graduated from Independence High School in Thompson's Station, TN in 2008. She earned a B.S. in Molecular Biology with minors in Chemistry and English from Lipscomb University in May 2012. She worked as a term technical intern at Vanderbilt University under the direction of Dr. Robert Carnahan during the summer of 2012 before joining the Department of Microbiology at the University of Tennessee in August of 2012. She worked in the lab of Dr. Todd Reynolds and wrote this dissertation in 2017.